Investigation of Factors Controlling Cutaneous Circulation in Flaps

Clare Josephine Tollan BSc (Med Sci) MB ChB MRCS

Submitted in fulfilment of the requirements for the degree of Doctor of Medicine (M.D.)

Faculty of Medicine

College of Medical, Veterinary and Life Sciences

University of Glasgow

2011

Abstract

The aim of this research was to investigate the blood supply to the lower abdomen. This is a commonly used donor site for autologous reconstruction following breast cancer and the flap of tissue used is based on the deep inferior epigastric circulation (DIEP flap) or the superficial inferior epigastric circulation (SIEA flap).

A pilot study investigated the feasibility of assessing the vascular territory of multiple blood vessels in the lower abdomen, and also observed the timing of changes in skin blood supply after free flap transfer. Further studies included sampling using microdialysis catheters, from different areas of the flap, around the theoretical time of opening of choke vessels between angiosomes. Manipulation of skin blood flow was initially investigated using capillary malformations as a model, observing current clinical use of EMLA and AMETOP topical anaesthetic pre-laser treatment.

Table of Contents

Abstract 2
List of Tables 6
List of Figures 8
Acknowledgement 11
Author's Declaration 12
Definitions 13
1 Investigation of factors controlling cutaneous flap circulation 14
1.1 Introduction 14
1.2 Free Tissue Transfer 17
1.3 Breast reconstruction 18
1.4 Blood supply of the skin 21
2 Materials 23
2.1 Materials for Chapter 3 23
2.1.1 Videomicroscope 23
2.1.2 Confocal Microscope 24
2.2 Materials for Chapters 3, 4, 5, 6. 26
2.2.1 Laser Doppler imaging 26
2.3 Materials for chapter 7 28
2.3.1 Microdialysis Catheters 28
2.3.2 Microdialysis and Flap Monitoring 29
3 Microcirculatory changes following application of topical anaesthetics 31
3.1 Background 31
3.2 Introduction 31
3.2.1 Topical anaesthetic 34
3.3 Methods 36
3.3.1 Subjects & protocol 36
3.4 Results 37
3.4.1 Data description 45
3.4.2 Statistical modelling 48
3.4.3 Random effects 51
3.4.4 Homogeneity of variance 51
3.4.5 Checking model assumptions: Normality 52
3.4.6 Comparison with additional observer 53
3.5 Conclusion 56
3.6 Discussion 56
3.6.1 Capillary malformations and laser treatment 64
3.6.2 Use of confocal microscope in assessment of capillary malformations 65
4 Pilot study to assess skin blood flow in the lower abdomen 68
4.1 Introduction 68
4.2 Methods 69
4.2.1 Use of descriptive statistics in studies using laser Doppler (Chapters 4, 5 & 6) 73
4.3 Results 75
4.3.1 Intra operative scans – Clamp time versus scan time 75
4.3.1.1 Data Description and test of interaction between Scan Time and Clamp Time 80
4.3.1.2 The effect of Scan Time 81
4.3.1.3 The effect of clamp time 83
4.3.2 Comparison of areas of 'good' blood supply with areas of 'poor' blood supply 83

4.4 Conclusion....86
4.5 Discussion....86
5 Laser Doppler assessment of post-operative perfusion....97
5.1 Introduction....97
5.2 Method....98
5.2.1 Analysis of data and descriptive statistics....99
5.3 Results....100
5.3.1 Data description....101
5.3.1.1 Perfusion by time point....102
5.3.1.2 Perfusion by zone....103
5.3.1.3 Perfusion by angle....104
5.3.2 Statistical modelling of the data....105
5.3.2.1 Model of data....107
5.3.2.2 Predicted means for timepoint....108
5.3.2.3 Predicted means for zone....109
5.3.2.4 Predicted means for angle....109
5.3.3 Data separated by Angle, above or side....110
5.3.3.1 Data description from above, including normalised data....110
5.3.3.2 Statistical modelling, image data from above....115
5.3.3.3 Data description from the side, including normalized data....116
5.3.3.4 Statistical modelling, image data from the side....120
5.4 Conclusion....122
5.5 Discussion....123
6 A comparison of the perfusion territory of the Deep versus Superficial Inferior Epigastric system....126
6.1 Introduction....126
6.1.1 Background....126
6.1.2 Angiosomes and zones of the lower abdomen....129
6.1.3 Objective....132
6.2 Methods....133
6.2.1 Data processing and statistical analysis....134
6.3 Results....135
6.3.1 Descriptive Statistics....136
6.3.2 Analysis of variance....142
6.3.3 Analysis by Vessel, by Zone, and by Vessel and Zone....146
6.4 Conclusion....149
6.5 Discussion....149
6.5.1 Donor site....150
6.5.2 Blood supply to the lower abdomen....152
6.5.3 Perforator topography....154
6.5.4 Pre-operative imaging....157
6.5.5 Flap perfusion....158
6.5.5.1 Number of perforators and row of perforators....159
6.5.5.2 Venous congestion....161
6.5.5.3 Venous congestion versus arterial inflow....163
6.5.6 Fat necrosis and partial necrosis....164
6.5.7 Zones & experimental studies....168
6.5.7.1 Experimental DIEP studies....170
6.5.7.2 Experimental SIEA studies....178
7 Microdialysis analysis of DIEP flaps....185
7.1 Introduction....185
7.2 Method....187
7.3 Results....189
7.3.1 Interleukin-6 (IL-6)....190

7.3.1.1 Data description of IL-6 190
7.3.1.2 Statistical modelling, IL-6 194
7.3.1.2.1 Predicted means of IL-6 concentrations 195
7.3.1.3 Test of linear trend with hours post-operatively, IL-6 196
7.3.2 Fibroblast Growth Factor basic (FGFß) 197
7.3.2.1 Statistical modelling & tests of linear trend, FGFß 200
7.3.2.1.1 Predicted means of FGFß concentrations 201
7.3.3 Tumour Necrosis Factor alpha (TNFα) 202
7.3.3.1 Statistical modelling & tests of linear trend, TNFα 206
7.3.3.1.1 Predicted means of TNFα concentrations 207
7.4 Conclusion 208
7.5 Discussion 209
7.5.1 Mechanism of delay 209
7.5.2 Molecular mechanisms 212
7.5.2.1 IL-6, FGFß and TNFα 214
7.5.2.2 Manipulation of flap survival & factors improving flap survival 218
8 Summary 221
Appendix 224
List of References 265

List of Tables

Table 3-1 - Patient number and number of laser treatments received. 37
Table 3-2 - Number of vessels with diameter measurements. 46
Table 3-3 - Summary statistics of vessel diameter in micrometers (micron). 46
Table 3-4 - Mean diameter measurements, (SD in brackets), & number of measurements. Grouped by patient, anaesthetic, microscope and time-point. 47
Table 3-5 - Mean diameter measurements, by treatment group, time-point, and microscope type. 47
Table 3-6 - Approximate F-tests of main effects and interactions. 50
Table 3-7 - Predicted mean log-diameters 51
Table 3-8 - Anti-logged predicted mean log-diameters 51
Table 3-9 - Approximate F-tests of main effects and interactions (weighted analysis). 52
Table 3-10 - Joint effect of topical anaesthetic, microscope type, and timepoint. 53
Table 3-11 - Mean diameter by timepoint, microscope type and anaesthetic type. Primary observer. 53
Table 3-12 - Predicted mean diameters (log scale, base 10) by anaesthetic and timepoint. 54
Table 3-13 - Second observer re-analysis of videomicroscope pictures patients 4 - 11. 54
Table 3-14 - Second observer mean vessel measurements pre- and post-application of topical anaesthetic, per patient. 55
Table 3-15 - Summary data for second observer; mean, standard deviation and number of measurements for vessel diameter. 55
Table 3-16 - Mean, standard deviation and number of measurements* for log vessel diameter (base 10). 56
Table 4-1 - Intraoperative clamp and scan times. 73
Table 4-2 - Median flux for each Laser Doppler scan. 77
Table 4-3 - Summary statistics for flux by clamp time and scan time. 80
Table 4-4 - Clamp time 5 minutes v 20 minutes. 81
Table 4-5 - Differences in flow (5 min scan time minus 10 min scan time) by clamp time. Rows - clamp time. 81
Table 4-6 - Two-way ANOVA: Median flow versus Patient, Scan Time. 82
Table 4-7 - Mean flow (averaged over scan time), by clamp time. 83
Table 4-8 - Raw data: median perfusion, by Patient, Clamp time (minutes), and quality of perfusion. 84
Table 4-9 - Flux by clamp time and 'good' or 'poor' perfusion. 84
Table 4-10 - Two-independent samples t-test, 'good' v 'poor'. 85
Table 5-1 - Frequency distribution of number of zone and base line measurements 101
Table 5-2 - Summary statistics of perfusion (flux) by time point. 102
Table 5-3 - Summary statistics of perfusion by zone. 103
Table 5-4 - Summary statistics of perfusion by angle. 104
Table 5-5 - Wald tests of main effects and interactions. 106
Table 5-6 - Wald tests and approximate F-tests for model with no interactions between fixed-effect factors. 107
Table 5-7 - Predicted mean perfusion (log scale base 10) by timepoint. 108
Table 5-8 - Anti-logged predicted mean perfusion by timepoint. 108
Table 5-9 - Predicted mean perfusion (log scale base 10) by zone 109
Table 5-10 - Anti-logged predicted mean perfusion by zone. 109

Table 5-11 - Predicted mean perfusion (log scale base 10) by angle..... 109
Table 5-12 - Anti-logged predicted means by angle. 110
Table 5-13 - Median perfusion by zone and time point, from above. 113
Table 5-14 - Median perfusion (number of measurements) by zone and time point, from above. Normalized against baseline. 114
Table 5-15 - Approximate F-tests to two main effects and their interaction. Imaging from above. 115
Table 5-16 - Approximate F-tests for model with no interaction between zone and timepoint. 115
Table 5-17 - Anti-logged predicted mean perfusion by time point, from above. 116
Table 5-18 - Anti-logged predicted mean perfusion by zone, from above. 116
Table 5-19 - Median perfusion by zone and time point from side. 119
Table 5-20 - Median perfusion by zone and time point from side. Normalized against baseline. 120
Table 5-21 - Approximate F-tests of main effects and interactions..... 121
Table 5-22 - Approximate F-test for model with only the main effect of zone. 121
Table 5-23 - Anti-logged predicted mean perfusion by zone (side). 122
Table 6-1 - Intraoperative LDI scanning order for vessels supplying lower abdominal skin. 134
Table 6-2 - Flux results per vessel. For whole flap per vessel, and also divided by zone. Number of perforators and position in medial or lateral row marked for DIEP vessels. † denotes vessel chosen clinically by surgeon for reconstruction. 139
Table 6-3 - Mean flow, standard deviation and number of observations, by vessel type, side and zone..... 141
Table 6-4 - Three factor interaction..... 142
Table 6-5 - ANOVA. Analysis of variance of median flow..... 145
Table 6-6 - Comparison of ANOVA test results with non-parametric test results. 146
Table 6-7 - Predicted means by zone (both SIEA and DIEP). Standard error of a difference between two of these means is 3.95 on 27 degrees of freedom. ... 147
Table 6-8 - Predicted means by vessel and zone. Standard error of a difference between two means for the same vessel is 4.81 on 48.02 degrees of freedom. The standard error of a difference for two means in the same column is4.90, on 25.24 degrees of freedom. 147
Table 6-9- Significance of difference between zones 1 - 4 for DIEP and SIEA vessels. 148
Table 7-1- Approximate F-tests of main effects and interactions, IL-6..... 194
Table 7-2 - Predicted mean concentrations by time point..... 195
Table 7-3- Approximate F-tests of main effects and interactions (time fitted first)..... 196
Table 7-4 - Approximate F-tests of main effects and interactions (catheter fitted first)..... 196
Table 7-5 - Approximate F-tests of main effects and interactions, FGFβ. Time fitted first..... 201
Table 7-6 - Approximate F-tests of main effects and interactions, FGFβ. Catheter fitted first. 201
Table 7-7 - Predicted means by time point (square root scale). FGFβ..... 202
Table 7-8 - Approximate F-tests of main effects and interactions, TNFα. Time fitted first..... 206
Table 7-9 - Approximate F-tests of main effects and interactions. TNFα. Catheter fitted first. 207
Table 7-10 - Predicted mean concentrations by time point. TNFα. 208

List of Figures

Figure 2-1 - Vivascope 1500, MAVIG. 24
Figure 2-2 - Vivascope 1500 attaching to skin surface to be examined. 25
Figure 2-3 - Moor LDI2 laser Doppler scanner 27
Figure 2-4 - Microdialysis catheter with semi-permeable membrane at tip. 28
Figure 3-1 - Absorption spectrum for oxyhaemoglobin and melanin chromophores. 32
Figure 3-2 - Number of previous laser treatments received. 37
Figure 3-3 - Patient 6 videomicroscope image pre-application of EMLA. 38
Figure 3-4 - Patient 6 videomicroscope image post-application of EMLA. 39
Figure 3-5 - Patient 8 videomicroscope image pre-application of ametop. 39
Figure 3-6 - Patient 8 videomicroscope image post-application of ametop. 40
Figure 3-7 - Patient 6 confocal microscope image pre-application of EMLA. 41
Figure 3-8 - Patient 6 confocal microscope image pre-application of EMLA with red line to illustrate vessel position. 41
Figure 3-9 - Patient 6 confocal microscope image post-application of EMLA. 42
Figure 3-10 - Patient 6 confocal microscope image post-application of EMLA with red line to illustrate vessel position. 43
Figure 3-11 - Patient 1 confocal microscope image pre-application of ametop. 44
Figure 3-12 - Patient 1 confocal microscope image as above (Figure 3-11) illustrating vessel. 44
Figure 3-13 - Patient 1, additional example of confocal microscope image pre-application of ametop. 45
Figure 3-14 - Patient 1 additional image as above (Figure 3-14), illustrating vessel. 45
Figure 3-15 - Diameter by topical anaesthetic, microscope and time point. Mean diameters in blue. 46
Figure 3-16 - Ametop group pre- and post- application of topical anaesthetic. 48
Figure 3-17 - EMLA group pre- and post- application of topical anaesthetic. 48
Figure 3-18 - Diameter by microscope, anaesthetic and timepoint 49
Figure 3-19 - Log diameter (base 10) by microscope, anaesthetic and timepoint 49
Figure 4-1 - Moor Laser Doppler Scanner LD12-IR & its use intraoperatively. 71
Figure 4-2 - DIEP lower abdominal flap raised on perforating vessels. 72
Figure 4-3 -Patient No 5. Plot of pixel colours within polygon outline of DIEP flap. 74
Figure 4-4 - Patient 8; 5 minute clamp time, 5 minute scan. 76
Figure 4-5 - Patient 8; 5 minute clamp time, 10 minute scan. 76
Figure 4-6 - Patient 8; 5 minute clamp time, 15 minute scan. 76
Figure 4-7 - Patient 8; 5 minute clamp, 20 minute scan. 77
Figure 4-8 - Colour representation of 'flux' and numerical flux value. 77
Figure 4-9 - Patients 1 - 4. 78
Figure 4-10 - Patients 5 - 8. 78
Figure 4-11 - Line scan patient 8 with scanning line across DIEP flap marked. 5 minute clamp time, scan between 0 and 5 minutes. 79
Figure 4-12 - Line scan patient 3, 20 minute clamp time, between 0 and 5 minutes following clamp release. 79
Figure 4-13 - 5 minute clamp time. 82
Figure 4-14 - Patient 7 DIEP flap with rectangle 1 representing are of 'good' flow, and rectangle 2 representing area of 'poor' flow. 84
Figure 4-15 - Areas of Good versus Poor flux. 85

Figure 5-1 - Hartrampf's zones of lower abdomen. 97
Figure 5-2 - Laser Doppler image of patient 4 from above. 99
Figure 5-3 - Laser Doppler imaging of patient 4 from the side. 100
Figure 5-4 - Patient 8, bruising laterally. 101
Figure 5-5 - Boxplots of perfusion by time point. 102
Figure 5-6 - Boxplots of perfusion by zone. 103
Figure 5-7 - Boxplots of perfusion by angle. 104
Figure 5-8 - Perfusion by time point and zone, from above. 111
Figure 5-9 - Perfusion as a percentage of 'base', by time point and by zone, from above. 112
Figure 5-10 - Median perfusion by time point and zone, image from above. ... 113
Figure 5-11 - Median perfusion by time point and zone, image from above. Normalized against baseline. 114
Figure 5-12 - Perfusion by time point and zone, from side. 117
Figure 5-13 - Perfusion as a percentage of 'base', by time point and by zone, from side. 118
Figure 5-14 - Median perfusion by time point and zone, image from side. 119
Figure 5-15 - Median perfusion by time point and zone, image from side. Normalized against baseline. 120
Figure 5-16 - Median perfusion by time point and zone, normalized against baseline and image from above. 123
Figure 6-1 - Hartrampf's zones. 130
Figure 6-2 - Dinner's zones. 131
Figure 6-3 - Division of flux image into zones. 135
Figure 6-4 - Hartrampf's zones 137
Figure 6-5 - Patient 1, scan 1. Left SIEA vessel supplying flap. 137
Figure 6-6 - Patient 1, scan 2. Right DIEP vessel supplying flap. 138
Figure 6-7 - Patient 1, scan 3. Right SIEA vessel supplying flap. 138
Figure 6-8 - Patient 1, scan 4. Left DIEP vessel supplying flap. 138
Figure 6-9 - Plot of individual values of median flow per laser Doppler scan. . 140
Figure 6-10 - Residual plots from ANOVA; Histogram of residuals, Fitted-value plot, Normal plot and Half-Normal plot. 143
Figure 6-11 - Predicted means by Vessel and Zone. 147
Figure 6-12 - Patient 4 left DIEP laser Doppler scan. Supplied by two medial perforators. Hartrampf zone 3 appears to be better perfused than zone 2.... 172
Figure 6-13 - Patient 10, right DIEP laser Doppler scan. Supplied by one medial perforator. Hartrampf zone 3 appears to be better perfused than zone 2..... 172
Figure 6-14 - Patient 10, left DIEP laser Doppler scan. Supplied by 3 small medial perforators. Hartrampf zone 3 appears to be better perfused than zone 2. 173
Figure 6-15 - Patient 5, laser Doppler scan of left DIEP with one medial perforator. Hartrampf zone 2 appears to be better perfused than zone 3, and the perfusion area of the flap is centralised. 175
Figure 6-16 - Patient 5, laser Doppler scan of right DIEP with one lateral perforator. Hartrampt zone 3 is better perfused than zone 2, and the perfusion of the flap appears to be hemiabdominal. 175
Figure 6-17 - Patient 2, laser Doppler scan of right SIEA. 179
Figure 6-18 - Patient 2. Laser Doppler scan of left SIEA. 179
Figure 6-19 - Patient 4. Laser Doppler scan of right SIEA. 180
Figure 6-20 - Patient 4. Laser Doppler scan of left SIEA. 180
Figure 6-21 - Patient 6. Laser Doppler scan of left SIEA. 181
Figure 6-22 - Patient 5. Laser Doppler scan of right SIEA. 182
Figure 6-23 - Patient 5. Laser Dopper scan of left SIEA. 182
Figure 7-1 - Zones of lower abdomen. 186

Figure 7-2 - CMA 71 High Cut-Off catheter and accessories. 188
Figure 7-3 - Microdialysis catheter tip showing molecule collection through dialysing membrane. 189
Figure 7-4 - Patient 1. Concentration versus time by catheter. 190
Figure 7-5 - Patient 2. Concentration versus time by catheter. 191
Figure 7-6 - Patient 3. Concentration versus time by catheter. 191
Figure 7-7 - Patient 4. Concentration versus time by catheter. 192
Figure 7-8 - Patient 5. Concentration versus time by catheter. 192
Figure 7-9 - Patient 6. Concentration versus time by catheter. 193
Figure 7-10 - Mean concentration averaged over 6 patients versus time, by catheter. 194
Figure 7-11 - Predicted concentrations by time, IL-6. 195
Figure 7-12 - Patient 1. Concentration versus time by catheter. FGFβ. 197
Figure 7-13 - Patient 2. Concentration versus time by catheter. FGFβ. 198
Figure 7-14 - Patient 3. Concentration versus time by catheter. FGFβ. 198
Figure 7-15 - Patient 5. Concentration versus time by catheter. FGFβ. 199
Figure 7-16 - Patient 6. Concentration versus time by catheter. FGFβ. 199
Figure 7-17 - Mean concentration averaged over 5 patients versus time, by catheter. 200
Figure 7-18 - Predicted back-transformed concentrations by time. FGFβ. 202
Figure 7-19 - Patient 1. Concentration versus time by catheter. TNFα. 203
Figure 7-20 - Patient 2. Concentration versus time by catheter. TNFα. 203
Figure 7-21 - Patient 3. Concentration versus time by catheter. TNFα. 204
Figure 7-22 - Patient 4. Concentration versus time by catheter. TNFα. 204
Figure 7-23 - Patient 5. Concentration versus time by catheter. TNFα. 205
Figure 7-24 - Patient 6. Concentration versus time by catheter. TNFα. 205
Figure 7-25 - Mean concentration averaged over 6 patients versus time, by catheter. TNFα. 206
Figure 7-26 - Predicted concentrations by time point. TNFα. 208
Figure 7-27 - Anti-logged predicted natural log perfusion by zone and time point, Chapter 5. 212

Acknowledgement

I would like to acknowledge and thank those who have helped me, especially the patients generous enough to volunteer to be part of these studies.

I would like to thank those at Moor, Dr Rodney Gush and colleagues, for offering their experience of work with laser Doppler imaging. Mavig and Mike Mc Farland at Schuco very kindly organised for us to have use of the Vivascope confocal microscope.

I would especially like to thank Dr William MacLaren for the statistical modelling for each of the studies in this thesis, and for his patience and willingness to incorporate the clinical complexity of the studies. Gen Stat and Minitab statistical packages were used thoughout the thesis. Professor Bill Ferrell at Glasgow University offered his experience in the data description of laser Doppler imaging which was very helpful at the outset of analysis.

I would like to thank my supervisors Mr Mackay, Mr Soutar and Dr MacFarlane for their guidance. Dr MacFarlane advised on the possibilities in looking for molecular markers in the very small microdialysis samples, and performed the immunoassays in Chapter 7. Without Mr Mackay's ongoing involvement and ambition in clinical research, these studies would not have been possible, and I would like to thank him for all his help.

I would like to thank my husband Vivek for his patience, and also in his capacity as a previous laser fellow for providing a second blinded observer's analysis of vessel diameters in Chapter 3. My parents have always supported and encouraged me throughout my studies, and I would especially like to thank them.

Author's Declaration

I hereby declare that all of the work presented in this thesis is my own and the work described in this thesis has been carried out by myself unless otherwise stated or acknowledged.

This thesis is of my own composition and has not, in whole or in part, been submitted for consideration for any other degree.

Definitions

CM	Capillary malformation
CLSM	Confocal Laser Scanning Microscopy
CT	Computed tomography
CTA	Computed tomography angiography
d.f.	Degrees of freedom
DIEA	Deep Inferior Epigastric Artery
DIEP	Deep Inferior Epigastric Artery perforator, occasionally referred to as DIEAP
EMLA	Topical anaesthetic - Eutectic Mixture of Local Anaesthetics
FGFβ	Basic Fibroblast Growth Factor also known as bFGF, FGF2.
Fluence	Energy per unit area e.g. Joules per centimetre squared (J/cm^2) Used to describe laser outputs.
flux	In relation to laser Doppler output this is proportional to blood flow.
IL-6	Interleukin-6. Cytokine.
LD	Latissimus Dorsi (muscle). Usually used to describe the flap.
MDCTA	Multidetector-row computed tomographic angiography
PDL	Pulsed dye laser
s.e.	Standard error
SIEA	Superficial Inferior Epigastric Artery. SIEA flap.
TNFα	Tumour Necrosis Factor alpha. Cytokine.
TRAM	Transverse Rectus Abdominis Muscle. Describes the flap using this muscle.

1 Investigation of factors controlling cutaneous flap circulation

1.1 Introduction

Reconstructive surgery aims to restore the form and function of deformed, damaged or lost body parts. Defects may have resulted from a wide variety of pathologies including congenital structural loss, traumatic injury, following surgical debridement and tumour resections. When undertaking a reconstruction, the primary goal is safety, with preservation of life and limb. Restoration of function and form improves the patient's quality of life, and may require increasingly complex reconstructions. In planning a reconstruction various factors must be taken into consideration, including the patient's medical status and their lifestyle expectations, and a balanced decision made on the level of reconstruction that would best benefit the patient.

Blood supply is the most important factor governing the movement of tissues in the body. The two main methods by which tissue is transferred are grafts and flaps. Grafts and flaps differ fundamentally in the way that their blood supply is obtained. A graft is a piece of tissue that is moved without its blood supply. In order to survive it has to become reattached and obtain a fresh blood supply from its new habitat. This process, referred to as 'take' of the graft, occurs over a period of days with an outgrowth of capillaries from the recipient site uniting with those on the deep surface of the graft. In contrast a flap is a piece of tissue that is moved maintaining its blood supply and is not reliant on the recipient site for its vascularity. A flap contains a network of blood vessels, arterial, venous and capillary. It is this set of blood vessels that ultimately determine the flaps total or partial survival during and after its transfer from donor to recipient site.

Flaps are classified in a number of ways, and may be local, regional or distant flaps. Local flaps were initially limited to random pattern flaps, in the first half of the century. These are based on 'safe' length to breadth ratios for example 2:1. This rectangular skin flap can be elevated and rotated to close an adjacent wound. Restrictions of this kind of flap other than the set dimensions include the arc of rotation, and the proximity to the wound and the associated zone of

injury. The clinical relevance of the anatomy of the cutaneous vasculature led to the description of axial pattern flaps[1]. Axial flaps contain a named artery running along the axis of the flap in the subcutaneous tissue. This anatomical understanding changed the course of flap surgery.

For larger defects flaps can be regional and pedicled from known adjacent vasculature. The tissue is moved to close the defect with the vessels left intact. An example would be a Latissimus dorsi muscle breast cancer reconstruction, where muscle and skin from the back are pedicled through the axilla to cover the chest defect. The tissue is supplied by the thoracodorsal artery and vein. In contrast, a free flap involves disconnecting the main artery and vein supplying the tissue of the flap, and then reconnecting the artery and vein to vessels near the recipient site, which may be any distance from the donor site. The ability to perform this anastomosis of vessels with external lumen diameters of 0.5mm to 2mm became increasingly possible and reliable in the 1970s with the development of high-quality operating microscopes, microsurgical instruments and swaged microsutures. Free flap transfer has allowed greater flexibility in reconstructing defects with the design of customised flaps and without the restraints of loco-regional flap transfers. Free flaps can be composite, including bone and nerve in addition to muscle, fat, fascia and skin. Often these flaps are named according to composition for example fasciocutaneous or musculocutaneous, in addition to the vascular basis of their classification.

Difficulties with these flaps include total and partial flap failure. Total flap failure is less than 5% for most free tissue transfers. If a flap appears to be failing upon regular post-operative monitoring, the patient is rapidly returned to theatre and the microvascular anastomosis inspected. The flap can often be salvaged. Partial flap failure occurs due to problems within the vasculature of the flap itself. Part of the flap may have inadequate blood supply and become necrotic over a period of days. This cannot be salvaged by further surgery. In flaps undergoing partial failure, it is often the area of the flap furthest from the main artery and vein, the ‘pedicle’, supplying the flap that fails. The risk of partial failure can limit the amount of tissue that is safely taken as part of the free flap, and this is unhelpful when large volumes of tissue are required to reconstruct a defect. In many cases it is the tissue furthest from the pedicle that is the most valuable for the reconstruction, for example in lower limb

trauma. The anastomosis of the pedicle to recipient vessels should be as far from the zone of injury as possible, and it is therefore the most distal area of tissue that will cover the defect. The vascular territory that can reliably be taken as part of a flap can be understood by anatomical concept of 'angiosomes'.

An angiosome is a composite block of tissue supplied by a source artery and its accompanying vein. These three dimensional territories are linked to their neighbouring angiosomes by anastomotic vessels[2]. Implications for free flap transfer are that an angiosome can safely be taken as a block of tissue, and that the flap design can also safely incorporate the adjacent angiosome. The angiosomes are linked by simple anastomotic vessels and also by reduced-calibre 'choke' vessels. These choke vessels may play an important role in skin flap survival.

To examine the changes in cutaneous circulation which occur during and following flap transfer, this research will use blood supply to the lower abdomen as a model. This is a commonly used donor site for autologous reconstruction following breast cancer. The flap of tissue used is based on the deep inferior epigastric circulation (DIEP, deep inferior epigastric perforator) or the superficial inferior epigastric circulation (SIEA, superficial inferior epigastric artery). These flaps span four adjacent angiosomes. The angiosome with the vascular pedicle entering it is the most vascularly robust, followed by the two adjacent angiosomes. A fourth angiosome is prone to partial failure and for this reason is not included in the flap by some surgeons. For the patient, this can led to a less symmetrical breast reconstruction as less tissue is available. If this fourth angiosome or 'zone' is included, and succumbs to partial failure, the result is similarly a poorer cosmetic outcome, a longer stay in hospital and a predilection to infection. By observing the timing of blood flow changes to this fourth zone, the intra-operative predictability of blood supply to this zone, the biochemical changes in the flap in the immediate period after transfer, and the possibility of manipulating and improving the blood supply in this last angiosome, it is hoped that this research can further detail the anatomy and physiology of cutaneous flap circulation. This research may aid future investigation looking at ways of manipulating and improving flap circulation, improving the success of

flaps and ultimately improving the safety and cosmetic result of free flap transfer for patients.

1.2 Free Tissue Transfer

Free tissue transfer has evolved dramatically in the last 30 years with the anatomical revolution, the realisation that arterial anatomy was more important than simple length-breadth ratios[3]. Axial pattern flaps[4;5], muscle and musculocutanous flaps[6] and fasciocutaneous flaps[7] were described. Alongside further mapping of the cutaneous circulation[2;8] and improved knowledge of the anatomy, the last few decades have seen increasing refinements of the original microvascular transfers performed. The most recent phylum of transfers, perforator flaps[9], have continued to supply large robust flaps with long pedicles, although have improved donor site morbidity.

In 1975 the deltopectoral flap[10], based on the intercostal vessels, and the groin flap[5], based on the superficial circumflex iliac vessels, were the only known free flap donor sites[11;12]. The development of free microvascular tissue transfer allowed an increasing number of known axial flaps to be utilised as free flaps. Today, the free deltopectoral flap has fallen from favour due to its donor site morbidity and short pedicle, although the groin flap is still in occasional first-line use as a cutaneous free flap[13].

Free flaps became popular in the 1970s and 1980s with multiple new reports of musculocutaneous and fasciocutaneous flaps. The versatility and high success rate of free tissue transfer led to widespread adoption. The terminology ‘perforator flap’ was used for the first time in a clinical setting by Koshima and Soeda in 1989[14]. The concept of a perforator flap is a flap consisting of skin and subcutaneous fat, supplied by a vessel that perforates the muscle without significantly contributing to the muscle’s vascularity, and therefore not requiring the muscle carrier to be harvested as part of the flap as had previously been the case. Perforator flaps are a significant improvement of musculocutaneous flaps. In situations where only skin is required for a specific reconstruction, perforator flaps reduce the donor site morbidity by leaving the muscle intact. As about eighty percent of free flaps are required for resurfacing purposes, a more ‘ideal’ reconstruction is achieved with a perforator flap, replacing like with like.

The classification of perforator flaps has caused confusion in the literature[9;15-18]. They have been categorized according to their location, arterial supply or muscle of origin. The Gent consensus reached at the Fifth International Course on Perforator Flaps in 2001 attempted to represent the opinions of pioneers in the field of perforator flap surgery[15]. Perforator flaps were to be named according to the pedicle of the underlying muscle as a foundation for further refinements in the future. The range of donor sites is currently extensive. One of the most versatile flaps over time and currently in use, has been the latissimus dorsi flap, having all the attributes of size, reliability, long and large diameter pedicles, and therefore a range of applications[19;20]. For reconstructions requiring skin, a perforator flap however can provide significant advantages over even a latissimus dorsi musculocutaneous flap. For example, in breast reconstruction, a DIEP perforator flap provides more skin and has less donor site morbidity than a latissimus dorsi flap as no muscle is taken. A DIEP flap itself is an evolution of the musculocutaneous TRAM flap (transverse rectus abdominis muscle) for breast reconstruction again decreasing donor site morbidity and the risk of abdominal hernias[21].

Perforator flaps, whilst sharing the benefits of a reliable blood supply with their predecessors, musculocutaneous flaps, represent a significant improvement over musculocutaneous flaps by permitting muscle to be spared for reasons of donor site functional morbidity[22], or recipient site contour. They are also an improvement over 'axial' pattern flaps in three ways. Firstly, skin match can be enhanced and donor sites concealed as perforator flaps have an increased number of donor sites. Cosmesis at times has taken a second place to safety, but with the advent of perforator flaps this is no longer the case. Secondly, the direct route which the perforator takes to the subdermal plexus permits radical thinning[23]. This cannot be matched in axial flaps with deep course vessels and multiple dermal feeders. Thirdly, perforator flaps have longer large calibre pedicles in comparison to their muscular counterparts due to release of additional intramuscular pedicle length in their dissection.

1.3 Breast reconstruction

Breast reconstruction following mastectomy for breast cancer is becoming more common. Women are now routinely offered the opportunity for reconstruction, which can be carried out either using their own tissue, which is called

autologous reconstruction, or using implants. There are advantages to using the patients' own tissue in terms of the ability to tolerate radiotherapy, which is important with the great increase in immediate reconstruction, and also the reduction of long term problems including reoperation particularly for a type of scarring called capsule formation around implants. There are also psychological advantages to some women of not having a reconstruction with foreign material particularly given past media scares about silicone implants. A large amount of skin can be transferred with autologous reconstructions which gives a better reconstruction cosmetically.

Autologous reconstruction is performed by moving some of the patients own tissue with its blood supply which is called a flap. The two common flaps used to reconstruct a breast are the latissimus dorsi flap from the back and flaps based on the blood supply of the rectus abdominis muscle from the lower abdomen. These flaps contain the named muscle and the overlying skin, a musculocutaneous flap. The blood supply to the skin passes through the muscle in perforating arteries and veins.

Flaps from the lower abdomen have evolved over the years to minimise morbidity from the donor site. Originally the flaps were pedicled on one entire rectus abdominis muscle and its contained arteries and veins which was called a pedicled Transverse Rectus Abdominis Musculocutaneous (TRAM) flap. Then the TRAM flap was moved as a free flap or free tissue transfer from the abdomen when the tissue was completely detached with only a small segment of rectus abdominis muscle and the supplying artery and the draining vein (the deep inferior epigastric artery and vein). These vessels were joined up to a recipient artery and vein either in the axilla or to the internal mammary vessels behind the ribs beside the sternum using microvascular techniques. Now all of the rectus abdominis muscle is usually left behind to minimise donor site morbidity and the skin and fat are transferred as a free flap on the perforating vessels which pass through the muscle. This called a Deep Inferior Epigastric artery Perforator (DIEP) flap.

The blood supply to the lower abdominal skin also comes from a Superficial Inferior Epigastric Artery (SIEA) as well as the Deep Inferior Epigastric artery Perforators(DIEP) on each side[2]. The tissue (free flap) from the abdomen can be

based on any of these vessels and a flap based on the superficial inferior epigastric artery has an even lower risk of causing abdominal weakness or herniation than the more commonly used Deep Inferior Epigastric Artery flap (DIEP) since it does not require the tough rectus sheath to be divided[24]. Many surgeons dissect and expose the deep inferior and superficial inferior epigastric arteries on both sides of the abdomen before choosing the most suitable artery and vein(s) on which to base the microvascular free flap anastomoses. This is decided by assessment of vessels size compared with the proposed recipient vessel and the skin perfusion clinically. The chosen artery and vein will provide the blood supply to this area of skin and fat, the 'free flap', when it is transferred to its new site as a reconstructed breast.

From cadaveric studies the blood supply of the skin is divided into angiosomes. An Angiosome is the area perfused by an individual artery and its draining veins. Angiosomes are separated by choke vessels. It is generally agreed that a flap based on a specific artery and its draining vein can safely include an immediately adjacent angiosome but the blood supply into any further angiosomes is less reliable and may result in partial loss of the flap. Animal studies have suggested that choke vessels may open up 2-3 days after a flap is raised. Flaps may also fail because of blockage of the main supplying artery or draining vein either due to twisting or external pressure or clotting at the site of the microvascular anastomosis, this may result in total loss of the flap.

Typical failure rates for free flap transfers are 3-4%. Partial loss of the DIEP flap is not uncommon with tissue loss in the angiosomes furthest from the supplying vessels often called zone IV of a DIEP flap. The SIEA system appears to be less consistent in terms of its arterial size and frequency than the deep system[25;26]. The area supplied by a SIEA flap is harder to predict and the overall failure rate appears higher than with DIEP flaps (Canniesburn Free Flap Audit). It is hoped that this and subsequent studies can better map the blood supply to the lower abdominal skin in vivo. The benefit of this would be improved safety of the operation particularly in terms of partial flap loss by better patient selection for DIEP and SIEA flaps. A better understanding of the in vivo perfusion of flaps would also allow study of the mechanisms which cause choke vessels to open and potentially allow for their pharmacological manipulation.

1.4 Blood supply of the skin

Detailed studies of the anatomy of cutaneous vasculature has been performed by many anatomists including Manchot (1889), Esser (1927) and Salmon (1936). Advances in the 20th century began to give clinical significance to this work. Tansini described the latissimus dorsi flap supplied by the thoracodorsal artery in 1906, Shaw and Payne describe direct flaps for hand reconstruction, and Bakamjian described perforators of the internal thoracic system published in 1969. The anatomical revolution in the 1970s, with the development of dependable microvascular anastomoses, led the way for pioneers like Daniel and Taylor[27], Harii[10], Cobbett[28] and Acland[12] to perform and rapidly advance free tissue transfer. The ability to perform these transfers has encouraged surgeons and anatomists to return to dissection, dissecting and researching for increasingly precise vascular anatomy. This knowledge of the anatomy of the Cutaneous arteries and veins is fundamental to the design of flaps and the skin incisions chosen.

In 1987 Taylor and Palmer[2] performed a study using dye injections and radiographic investigations in over 50 cadavers showing the blood supply to be a three dimensional network of vessels in all tissue layers, giving rise to the 'angiosome' concept. An angiosome is the composite block of tissue, comprised of the skin and underlying structures, supplied by a named source artery being one part of the three dimensional jigsaw making up the body[29]. The angiosomes are connected by true anastomoses or reduced calibre 'choke' vessels. These choke vessels are like resistors in an electrical circuit. When a flap is raised they provide initial resistance to the flow of blood from the tip of the flap to the base. These choke vessels later open, and this is shown experimentally in rabbits to be between 48 and 72 hours[30]. It is thought that the opening of these choke vessels is a permanent and irreversible event, and is an active process associated with hyperplasia and hypertrophy of cells in all layers of the choke artery wall[31].

Increases is choke vessel calibre have been observed mainly during the 'delay phenomenon'. Delay is any pre-operative manoeuvre that results in increased flap survival. These have been used since Taliacozzi in the 16th century and involve procedures such as elevating the flap maintaining its blood supply in the donor site, before transferring it to the recipient site after a time period,

typically about 1 week. The mechanism of delay is incompletely understood and there are a number of theories based around 'training' the flap to rely on the vessel(s) that will supply the flap when moved to the recipient site. The improvement in blood supply is likely to be related to the opening of choke vessels[32-34].

The mechanisms surrounding the opening and increase in calibre in choke vessels are yet to be elucidated. Better understanding of the timing of this mechanism in humans, and the factors controlling the opening of choke vessels may allow future pharmacological manipulation of their opening, decreasing partial flap failure and increasing the amount of tissue that can safely be transferred in a range of reconstructions.

2 Materials

Each individual chapter has details of the Method used.

2.1 Materials for Chapter 3

2.1.1 Videomicroscope

Videomicroscopy describes a technique of visualising the dermis through the use of a microscope coupled to a video camera system. The technique was originally used by Fagrell[35;36] to investigate normal skin circulation and later by Motley et al[37] and Eubanks[38] to investigate capillary malformation skin. Sivarajan and Mackay studied the use of the videomicroscope for examining the capillary structure of capillary malformations before and after laser treatment[39;40]. They also validated the technique by measuring the pressure applied to the skin surface when using the videomicroscope and demonstrated that this was less than was required to blanch the capillaries within the malformation[41]. The videomicroscope is calibrated on the skin surface and then by altering the focus the capillaries become clear, and the degree of focusing gives a value for the depth.

The videomicroscope used in this thesis is the Cyscope Compact Videomicroscope (PW Allen, Tewkesbury, UK) fitted with a 200x lens and coupled to a colour photo printer (Mitsubishi Colour Video Copy Processor). This allowed the capture of images which were later analysed using the image of a 1mm graticule to measure capillary diameters.

2.1.2 Confocal Microscope

In Chapter 3 the technique of Confocal Laser Scanning Microscopy (CLSM) is used for imaging vascular malformations. Confocal microscopy describes a technique used to increase the optical resolution of an image to be obtained by focussing individually on small points within the object and eliminating the out-of focus incident light. This prevents the blurring of images that would occur with wide field microscopy. Confocal Laser Scanning Microscopy uses a laser to illuminate the target object, and this use of coherent laser light further reduces noise from the object in comparison to incoherent light found in normal microscopes. The scanning process produces a raster or grid pattern of the object which can gradually focus deeper within the object to produce a three dimensional image.

Figure 2-1 - Vivascope 1500, MAVIG.

The confocal microscope used in the thesis is the Vivascope 1500 (Mavig GmbH, Munich, Germany, Figure 2-1). This is a portable confocal microscope connected to a computer and takes real time images, 500µm by 500µm, of the skin. The Vivascope 1500 uses a laser beam in the near infrared range (830nm), directed through a series of lenses and a beam splitter.

The skin is imaged by firstly applying a steel ring with adhesive to the area of skin to be viewed, and a small amount of clear gel is applied. The laser tube is then positioned over the ring and a magnet attaches them to keep the area to be viewed in place.

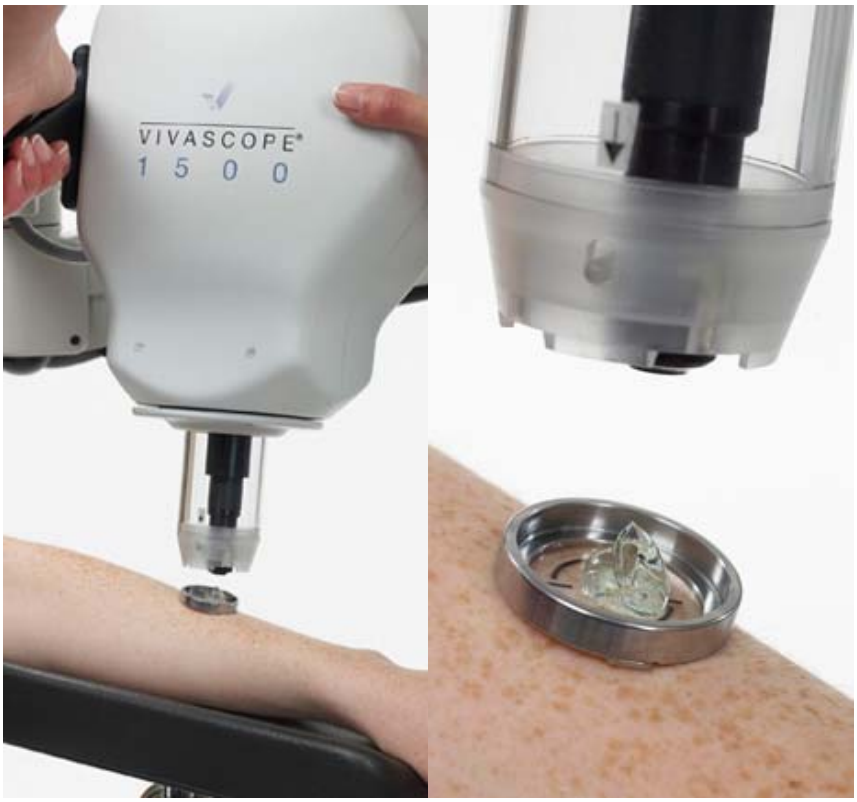

Figure 2-2 - Vivascope 1500 attaching to skin surface to be examined. Steel ring attaches to skin with adhesive.

The scanning controls operate from the computer which allows stacked imaged from the skin surface increasing in depth to be rapidly acquired. Images are in black and white unlike the videomicroscope, and this can make vessels more challenging to identify without the video function. The digital storage of a vast number of images makes this a valuable research tool.

The confocal microscope has been used clinically for many dermatological applications including the imaging of pigmented skin lesions[42;43], non-malignant skin lesions and their response to treatment[44], malignant skin lesions[45;46] and melanoma[47].

2.2 Materials for Chapters 3, 4, 5, 6.

2.2.1 Laser Doppler imaging

Laser Doppler flowmetry is a non-invasive technique used to measure skin blood flow using a probe attached to the skin. The device uses a laser beam directed at the skin surface, which then reflected back to a photo-diode within the device. Laser light incident upon moving cells, for example red blood cells within dermal capillaries, undergoes a Doppler shift. Backscattered light is detected by a photodetector and recorded by the processor within the unit as 'flux' which is linearly proportional to the velocity of blood flow within the vessel[48] and the concentration of red blood cells. Laser Doppler imaging works using the same principle but it can detect flux across a region, rather than at a single point, by scanning the laser beam over this area. It also has the advantage of being non-contact[49].

The laser Doppler device used in this thesis is the Moor LDI2 laser Doppler imager (Moor Industries, Axminster, UK) coupled to Moor Research software. There are two laser light sources within the scanner, a 660nm visible red laser diode aiming beam and a 780nm near infra-red laser diode used for the laser Doppler measurements. A coaxial beam is produced and the laser is a Class 3R laser device.

Figure 2-3 - Moor LDI2 laser Doppler scanner

The use of laser Doppler to evaluate the skin microcirculation was first published by Stern in the journal Nature in 1975[48].

Since then laser Doppler imaging and flowmetry have been used in numerous studies examining the skin microcirculation[50-53], examining changes after the administration of vasoactive substances[54;55] and for free flap monitoring[56-59].

Clinically one of the most frequent uses of laser Doppler imaging is in burn depth assessment[60-62]. The provide an estimate of healing time base on whether the burn is likely to take less than 14 days to heal (high blood flow), between 14 and 21 days to heal (medium blood flow), or more than 21 days to heal and thus benefit from early excision and grafting.

2.3 Materials for chapter 7

2.3.1 Microdialysis Catheters

Microdialysis is a technique for measuring the concentrations of substances in the extracellular fluid in a tissue. The technique involves using a semipermeable membrane through which a physiological salt solution is constantly pumped, and the solution equilibrates with the surrounding tissue fluid.

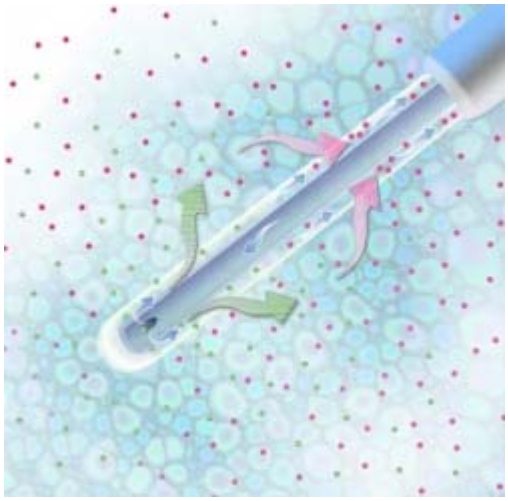

Figure 2-4 - Microdialysis catheter with semi-permeable membrane at tip. (Pictures courtesy of CMA Stockholm / Dipylon Medical AB)

Perfusion fluid enters through an inner tube and exits this tube at the distal end (Figure 2-4). It then flows in the space between the inner tube and the outer dialysis membrane. The dialysis takes place at this point as molecules from the surrounding tissue can diffuse into the perfusion fluid. The microdialysis membrane used for monitoring for flap ischaemia has a 'cut-off' of molecule size 20 kiloDaltons. This will allow small molecules such as glucose, pyruvate and lactate to diffuse. The concentration should be relative to the concentration in the extracellular fluid. In our study in Chapter 7 we have used the specialized CMA 71 high cut-off microdialysis catheter which allows molecules as large as 100 kiloDaltons to pass though the pores in the outer dialysis membrane. In addition to the pore or cut-off size of the membrane, the length of the dialysing membrane in the catheter is different with different products, and the speed at which the perfusion fluid is pumped can also be varied. All of these factors will alter the rate of collection of extracellular molecules.

The microdialysate returning from the microdialysis catheter is collected in a microdialysis vial, which in flap monitoring can be removed at set times to be analysed by a bedside analyser. Our samples were stored immediately at minus eighty degrees Celsius for later analysis at Glasgow University once the collection part of our study protocol in Chapter 7 was complete.

The use of microdialysis allows the concentrations of substances, be they cytokines, hormones, drugs or sugars to be measured in near-real time within the tissue. The microdialysis equipment used in this thesis was produced by CMA Microdialysis, Stockholm, Sweden.

The technique of microdialysis has a number of features[63;64];

- Its specifically measures concentrations within the extracellular matrix
- It can be placed within a wide range of tissues including fat, brain and cardiac muscle
- It can be used for continuous monitoring for days
- The dialysate is held distinct from the tissue so as not to contaminate the tissue

By varying the permeability of the semi permeable membrane, the speed of the dialysate flow and length of the catheter different volumes and sizes of molecules can be measured.

2.3.2 Microdialysis and Flap Monitoring

The microdialysis technique was first used clinically in neurointensive monitoring following studies in the 1980s using it as a tool in brain research[65-67]. Rojdmark and Ungerstedt et al first used microdialysis as a technique for studying myocutaneous flaps in 1998[68]. They examined 10 women having breast reconstruction using either a TRAM or Latissimus dorsi flap reconstruction. They looked at three specific compounds and compared the concentration of these derived from a microdialysis catheter within the flap and compared this to values obtained from a control located in the tissue overlying the hip area. The compounds studied were glucose, glycerol and lactate levels. In flaps which had

no problems it was found that the glucose level initially showed a transient increase, before returning to its baseline. Glycerol again showed an increase for approximately 12 hours before returning to baseline and lactate showed a slight prolonged increase. When there was vascular compromise to the flap the glucose levels fell rapidly, followed by an increase in lactate and glycerol levels.

Setala et al further evaluated the use of microdialysis in monitoring flaps post operatively[69-72]. They used pyruvate as well as glucose and lactate levels to show the onset of ischaemia and demonstrated the chemical profiles occurring in arterial and venous related flap compromise[72]. They demonstrated both in an animal study and in humans that ischaemia led to a decrease in glucose and an increase in lactate levels, as found with Ungerstedt's study but also that the lactate to pyruvate ratio remained normal during arterial occlusion, but increased in venous occlusion[70;72]. A 77% successful take back rate was demonstrated, with a 95% overall success rate. No flap was lost to due to delay in diagnosis secondary ischaemia in microdialysis monitored free flaps[69]. Microdialysis has been increasingly used in monitoring flaps[69-78] as well as a research tool[63;64;68;79-82].

3 Microcirculatory changes following application of topical anaesthetics

3.1 Background

This study was used to illustrate and evaluate changes in skin vascularity following a pharmacological agent. The model of capillary malformations and topical anaesthetics was chosen as a common example of a pharmacological agent applied to skin in clinical practice.

3.2 Introduction

Capillary malformations (CMs) or 'port-wine stains' are a type of vascular lesion consisting of ectatic dermal capillaries present at birth. The pathogenesis is though to be related to a deficiency or absence of regulating neurons surrounding the ectatic blood vessels[83-85]. There are two main subtypes of vascular lesions, as defined by Mulliken and Glowacki in 1982[86]; haemangiomas and vascular malformations (including capillary vascular malformations, CMs). Haemangiomas are absent at birth, appear in the first few weeks of life, and grow at a much faster rate than the rest of the body within the first year. There is marked hypercellularity of their endothelial cells during the proliferative phase. After this period they undergo a slow involution and fibrosis. Haemangiomas are more common in females. Vascular malformations in contrast to haemangiomas are present at birth, grow proportionately with the rest of the body, and do not resolve, persisting through out life and often developing nodularity in adulthood. Vascular malformations can be subdivided into arterial, arteriovenous, venous, capillary (CMs or port-wine stains) or lymphatic malformations. Capillary malformations are equally predominant in males and females, occurring in 1 - 3 per thousand live births[87]. Vascular malformations may also occur as part of a syndromal illness such as Sturge-Weber syndrome where there is involvement of the meningeal vessels which can lead to seizures and mental retardation[88].

Laser treatment is currently the most successful treatment for capillary malformations. Laser ('light amplification by stimulated emission of radiation') light is monochromatic, coherent, and nondivergent, delivering a high power density[89]. Following the publication of the theoretical foundation for laser in

Einstein's paper on the quantum theory of radiation in 1917, it was not until 1960 that the first practical results of laser technology were published. Maiman introduced a ruby rod laser emitting a wavelength of 694 nm[90], and the effects of a ruby laser on skin was reported in a preliminary paper by Goldman[91]. Other lasers were developed during this period including the Nd:Yag (1961), the argon laser (1962), and the carbon dioxide laser (1964). Unfortunately laser treatment of capillary malformations lead to scarring and pigment change in many cases[92].

In 1983 Anderson and Parish published the theory of selective photothermolysis which lead to a new understanding of laser-tissue interactions[93]. They realised that to improve the effects of laser light on a target, the laser wavelength should be matched to the absorption spectrum of the target or 'chromophore', thus imparting selective damage. Additionally the pulse duration of the laser should be equal to or shorter than the thermal relaxation time of the target to minimise damage to surrounding tissues. This allowed treatment parameters to be optimised allowing more precise targeting of the intended structure with minimal collateral damage. The target chromophore in the treatment of vascular lesions is oxyhaemoglobin and therefore the laser light should meet a peak in the absorption spectrum of oxyhaemoglobin (Figure 3-1).

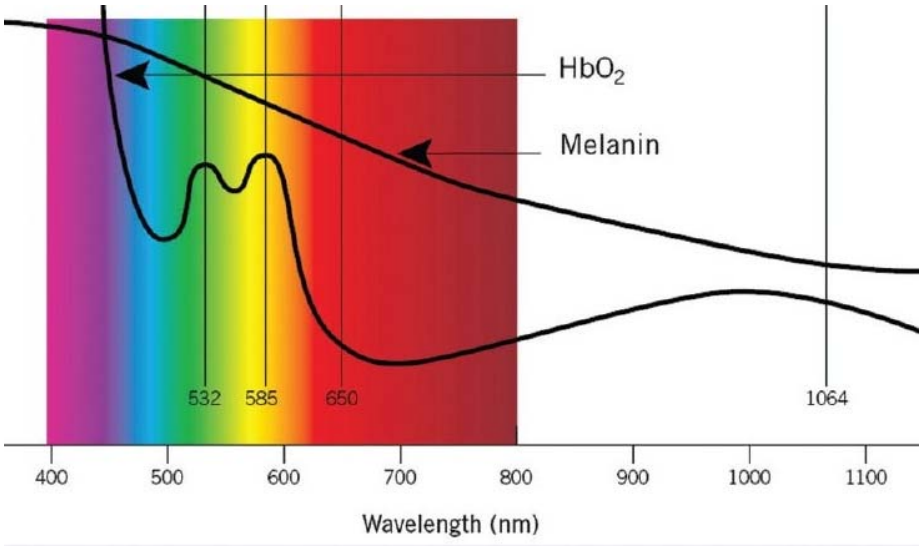

Figure 3-1 - Absorption spectrum for oxyhaemoglobin and melanin chromophores.

The thermal relaxation time of the vessels in capillary malformations is related to the vessel diameter (e.g. 30 - 150 μm) and is between 1 - 10 milliseconds[94], and the pulse duration should not be longer than this. To cause thermal damage

to a CM vessel it must be heated to 70°celsius via the heating of oxyhaemoglobin by laser light[95].

Despite knowledge of the theory of Selective photothermolysis and the advances in laser technology, only a minority of patients will achieve full clearance of their capillary malformations[96-98]. The majority of capillary malformations lighten with pulsed dye laser treatments with an average of 50% lightening at 2.5 treatments[99], and most improvement occurs within the first five treatments. Further treatments may lead to a smaller percentage improvement in some patients[96;100]. After ten treatments complete disappearance of CMs occurs in only 10% of patients[101]. Prognostic factors include site of the capillary malformation with those on the lower limb and midface performing poorly in comparison with laser treatment for CMs on the lateral face and trunk[98]. Eubanks et al attributed this to different vessel structures, as observed by videomicroscopy, at these sites[38;97]. A biopsy study by Fiskerstrand et al in 1996 demonstrated that the vessels responding better to pulsed dye laser treatment had larger diameters and were more superficially located in the dermis than the vessels poorly responding CMs[102]. Similarly a study by Sivarajan and MacKay in 2004 found that vessels with a diameter greater than 50 micrometers were adequately treated (PDL 585nm, 0.45msec pulse duration), whereas those less than 50 micrometers appeared resistant to treatment[40].

Smaller vessels may be inadequately treated due to the thermal relaxation time being significantly shorter than the pulse durations, as initially proposed by Anderson and Parrish[93], and demonstrated through Monte Carlo modelling[103]. Reducing laser pulse durations as low as 0.02 msec (20 μseconds) may lead to photomechanical damage with microvessel rupture[104] which can cause pigment change and scarring, rather than the desired selective photothermal damage that results in the vessel wall denaturation. Suggestions to improve the outcome of laser treatment of capillary malformations other than reducing the pulse duration, include altering the wavelength, spot size and fluence (energy, Joules/cm^2). Deeper vessels require a longer wavelength to ensure adequate tissue penetration[105]. Larger spot sizes also increase the depth of penetration as shown histologically[106] and this is explained by the scattering of light in modelling studies[107]. Increasing the fluence (J/cm^2) can lead to further improvement of capillary malformations up to a maximum limited by

complications such as scarring and pigment change[100]. Smaller vessels require higher fluences because the energy required to heat the vessel wall is a greater fraction of the absorbed energy[108]. The use of epidermal cooling can improve the results of pulsed dye laser treatment by protecting the epidermis, allowing higher fluences to be used[109;110]. Epidermal cooling devices commonly used include contact methods (e.g. Sapphire Chill Tip, Lumenis, Santa Clara, USA), cool air jets (Cryo 5, Zimmer Medical Systems, Irvine USA), and cryogen sprays (Dynamic Cooling Device, Candela Corp, Wayland, USA).

Alternatively altering vessel diameters rather than laser parameters has been investigated. A study by Svaasand et al demonstrated that an occlusive blood pressure cuff inflated to 100mmHg on the upper arm reduced the incident laser light require to produce purpura by 40%[111]. This is relevant when treating small CM vessels of less than 20μmetres. Suggestions when employed for CMs on the body include employing the Trendelenberg position. A further study by this group reported the use of suction cups attached to the laser hand pieces to produce hypobaric pressure for 5 - 15 seconds at laser treatment[108]. Hypobaric pressure of 17kPa to 51kPa resulted in more intense purpura in response to laser treatment, and 35% less fluence was required to produce the same level of purpura. Clinically there was a statistically significant difference in blanching for the CMs with local hypobaric pressure than those without, seven months post laser treatment. It has also been reported that hypobaric pressures allow higher temperatures to be achieved in small diameter vessels[112]. Temperature has also been demonstrated, by McGill and Mackay in 2006, as a factor causing capillary dilatation in both untreated and laser treated skin[113]. Although the effects of temperature on laser treatment outcome have not been demonstrated, increased temperature has been shown to cause vasodilatation in both head and neck CMs and limb CMs, but increased capillary blood flow only in the head and neck CMs. It has been postulated that this difference in blood flow between head and neck CMs and limb CMs, may explain the poorer response of limb CMs to laser treatment[114].

3.2.1 Topical anaesthetic

The use of topical anaesthetic is commonplace in non-ablative laser treatments. Although not painful, laser treatment causes discomfort often likened to an elastic rubber band hitting the skin. Younger children undergoing treatment for

capillary malformations are given general anaesthetics, and older children and adults are offered topical anaesthetic. This can reduce anxiety before treatment, which is important given that multiple laser treatments will be required. Topical anaesthetics are applied directly to the skin and left for the recommended period of time (minutes to hours depending upon the preparation). The stratum corneum is the main barrier to penetration in skin with an intact epidermis. Covering the topical anaesthetic with an occlusive plastic dressing (e.g. tegaderm) enhances penetration to the dermis. Once the anaesthetic is through the epidermis, it acts locally on nerve endings inhibiting sodium channels and blocking impulse conduction.

Commonly used topical anaesthetics include EMLA and Ametop. EMLA, the most widely used anaesthetic[115], is a 5% eutectic mixture of lidocaine and prilocaine, which are both from the amide group of anaesthetics. EMLA is an abbreviation for Eutectic Mixture of Local Anaesthetics. Eutectic mixtures result in liquids that melt at lower temperatures than their single components[116]. This allows higher concentrations of the anaesthetics which results in better dermal anaesthesia. The efficacy of EMLA has been shown in several clinical trials including venepuncture, split skin grafting and in laser treatment[117-128]. Ametop, which has a faster onset of action than EMLA, contains 4% tetracaine (maximum safe dose is 5 grams) and is an ester anaesthetic which have comparatively short half-lives in the body. It has proven efficacy[129;130], and similar reported adverse events as EMLA[131]. Side effects can include pruritis and oedema.

Application of EMLA can lead to a noticeable pallor of the skin in patients and this has been noted by many authors[124;125;132]. Conversely tetracaine (ametop) can be associated with local erythema[132]. As laser treatment for capillary malformations targets haemoglobin as the chromophore in selective photothermolysis, changes in the colour of the skin could effect the efficacy of laser treatment. This study was designed to investigate the vessel diameter in capillary malformations before and after application of EMLA or ametop local anaesthetic, which may have implications for laser treatment of vascular lesions. Additionally, following free flap reconstructive surgery where topical agents such as nitrate patches (GTN) are anecdotally applied to the skin to open choke vessels, it provides a model for the potential assessment of vessels in response to vasoactive agents using videomicroscopy or confocal microscopy.

3.3 Methods

3.3.1 Subjects & protocol

Eleven patients with capillary vascular malformations were recruited for investigation of vessel size before and after elective application of a topical anaesthetic prior to laser treatment. Patients were allocated to having either EMLA or ametop topical anaesthetic applied to the skin requiring pulsed dye laser treatment.

EMLA (AstraZeneca) contains 2.5% lidocaine and 2.5% prilocaine and was applied for a minimum of 90 minutes with a duration of anaesthesia of 2 hours. Ametop (S&N Health) gel contains 4% tetracaine and is applied for 30 minutes with anaesthesia lasting for 4 - 6 hours. The topical anaesthetics were applied and covered with an occlusive dressing, being removed after their respective duration of action prior to laser treatment (90 minutes for EMLA, 30 minutes for ametop). Patients were advised not to consume caffeine or smoke 24 hours before their appointment, and they were acclimatised in a temperature controlled room before measurements of vessel size were taken. Details of the number of previous laser treatments to their capillary malformation were also noted. Munsell colour chart were used to note the colour of the capillary malformation before and after application of topical anaesthetic.

All eleven patients' capillary malformations were assessed using confocal laser scanning microscopy (CLSM) before application of topical anaesthetic and after the removal of topical anaesthetic. The confocal microscope used in this study was the Vivascope 1500 Mavig GmbH, Munich (Materials 2.1.2, page 24). This uses an 830nm infra-red laser to image the skin. Digital images and videos are produced by the attached imaging computer. A total of 421 diameters were measured.

A videomicroscope (PW Allen, Tewksbury, UK, connected to a 200x magnification Cy-Scope lens with image capture via a Mitsubishi Colour Video Copy Processor) was used in eight patients in addition to the confocal microscope to confirm findings. The videomicroscope measures capillary diameter and depth in a technique developed[39] and used in many studies performed in Canniesburn Plastic Surgery Unit[40;41;114;133;134]. The diameter of capillaries from the video-

captured images were measured using a 1mm hand held graticule. There were nine pre- and nine post-local anaesthetic videocaptured images, and three measurements were taken from each of these, totalling 27 pre- and 27 post-anaesthetic diameters. Statistical calculations were made using Gen Stat and Minitab 16 statistical software, and the data were modelled by Dr William MacLaren, Statistician (Acknowledgments).

A laser Doppler scanner was additionally used to image the capillary malformations pre- and post-application of topical anaesthetics.

3.4 Results

Of the 11 patients recruited, 6 patients had EMLA topical anaesthetic and 5 patients had ametop. Previous laser treatments undergone by each patient are displayed below (Table 3-1 & Figure 3-2) to exclude this as a confounding factor or explanation for initial differences in diameter.

Patient no. (ametop)	no. treatments	Patient no. (emla)	no. treatments
4	0	5	27
9	37	7	17
10	21	11	20
1	14	2	2
8	13	3	4
		6	0

Table 3-1 - Patient number and number of laser treatments received.

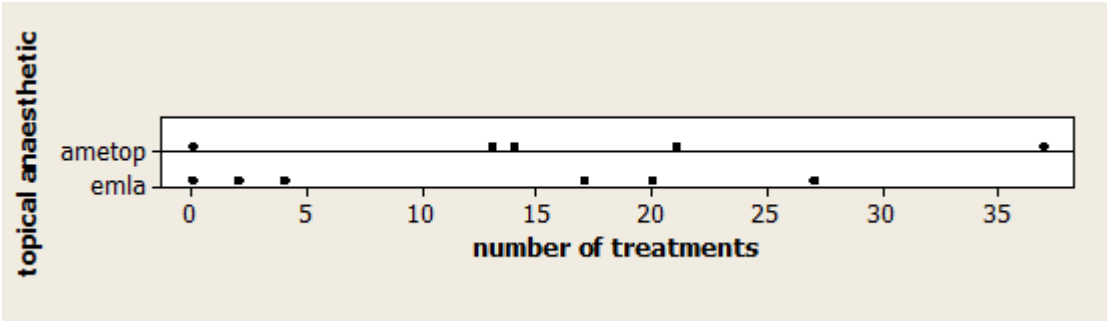

Figure 3-2 - Number of previous laser treatments received.

The ametop group of patients had an average of 17 (median 14) laser treatments, whereas the EMLA group had an average of 11.67 (median 10.5) laser treatments. The Mann Whitney test was applied to the null hypothesis that the two distributions have the same median and this was not rejected,

P=0.7144. There is no significant difference between the number of laser treatments in the EMLA and ametop groups.

Patients had Fitzpatrick skin types 1 and 2. Munsell colour chart readings were taken before and after topical anaesthetic although little colour change was observed.

A laser Doppler scanner (LDI2, Moor, as per Materials 2.2.1) was used to image the initial 3 patients, although unfortunately due to a technical error no further patients could be analysed using laser Doppler. The data from the laser Doppler are therefore not included in the results.

All 11 patients' vessel diameter measurements were made using the confocal microscope pre- and post application of topical anaesthetic.

The videomicroscope was additionally used in 8 patients (in place of the laser Doppler), 4 of whom had EMLA and 4 had ametop.

A total of 565 vessel diameter measurements were made. Examples of the videomicroscope images are shown in Figure 3-3, Figure 3-4, Figure 3-5 & Figure 3-6 below.

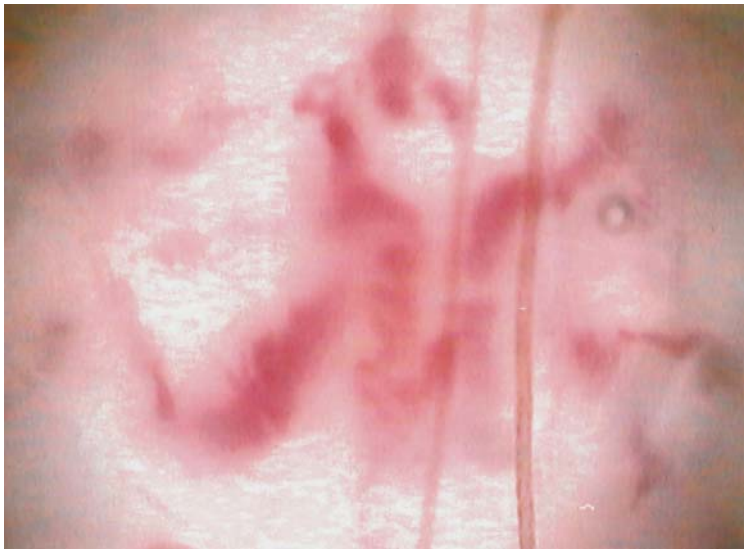

Figure 3-3 - Patient 6 videomicroscope image pre-application of EMLA.

There are large vessels centrally in this micrograph (two hairs can also be seen in this picture), Figure 3-3.

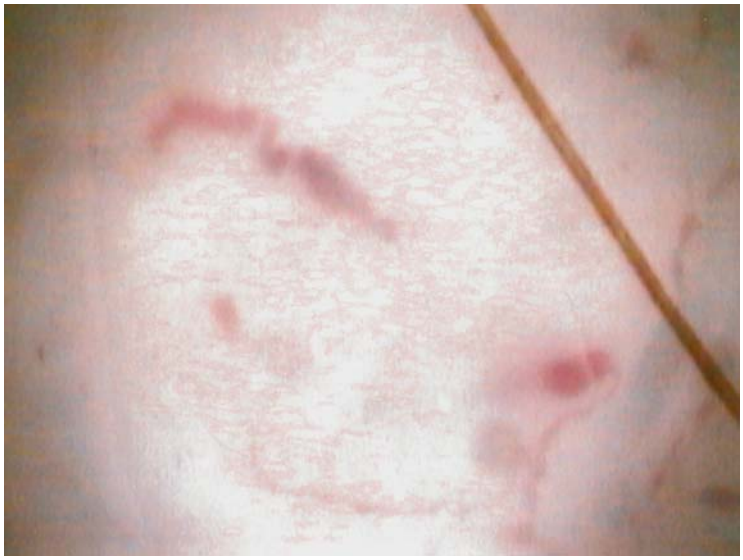

Figure 3-4 - Patient 6 videomicroscope image post-application of EMLA.

This, Figure 3-4, is the same patient as Figure 3-3 following application of EMLA. No two images can represent exactly the same area of skin.

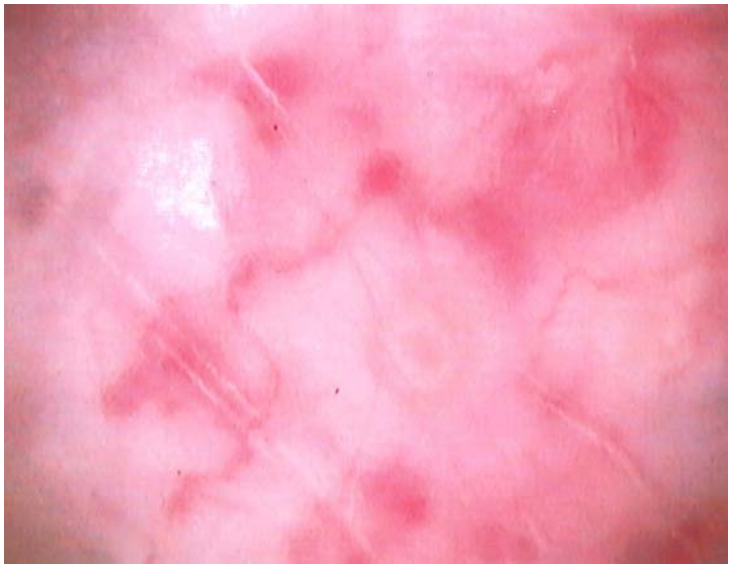

Figure 3-5 - Patient 8 videomicroscope image pre-application of ametop.

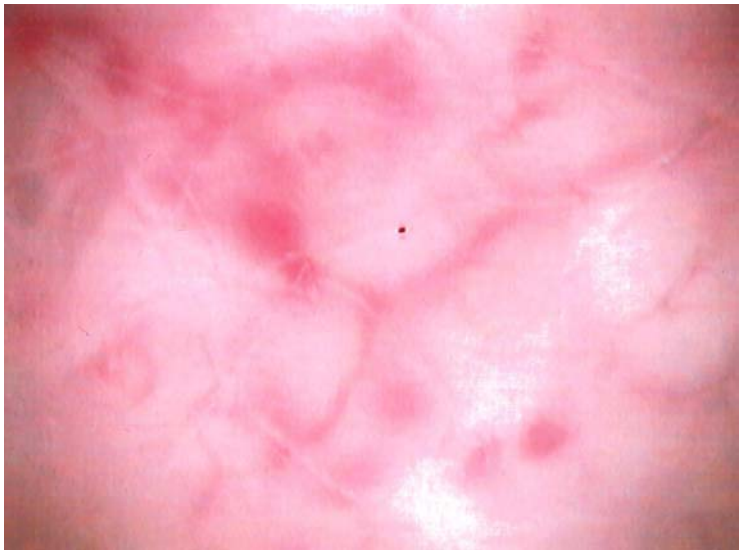

Figure 3-6 - Patient 8 videomicroscope image post-application of ametop.

The images shown below are from the confocal microscope and, as they are imaged using a laser, they are in black and white (Figure 3-7, Figure 3-9, Figure 3-11, Figure 3-12, Figure 3-13 & Figure 3-14). This makes vessels more difficult to identify from still images in comparison with videomicroscopy. Figure 3-7 & Figure 3-8, and Figure 3-9 & Figure 3-10 below show a particularly clear vessel, pre- and post-application of EMLA.

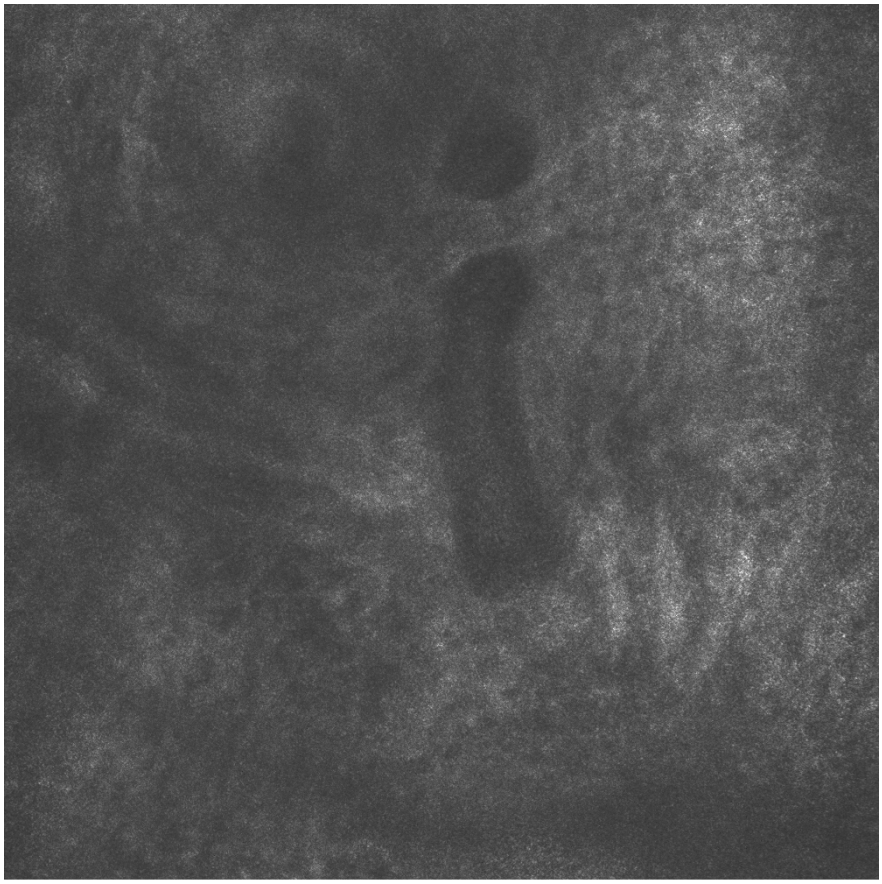

Figure 3-7 - Patient 6 confocal microscope image pre-application of EMLA.

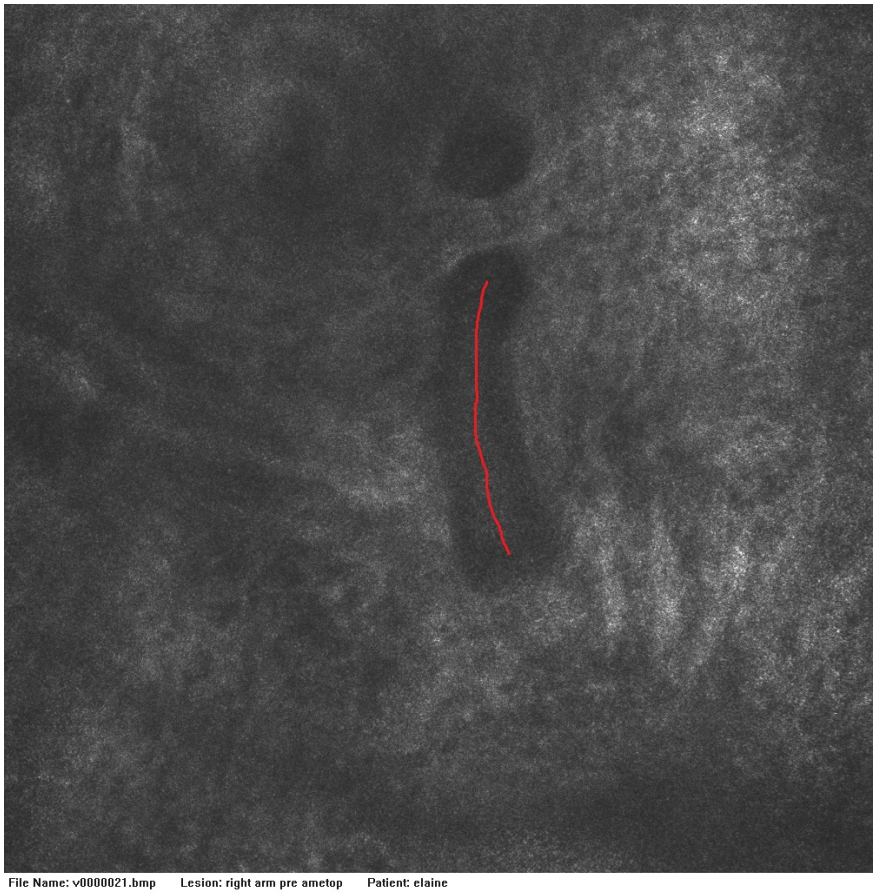

Figure 3-8 - Patient 6 confocal microscope image pre-application of EMLA with red line to illustrate vessel position.

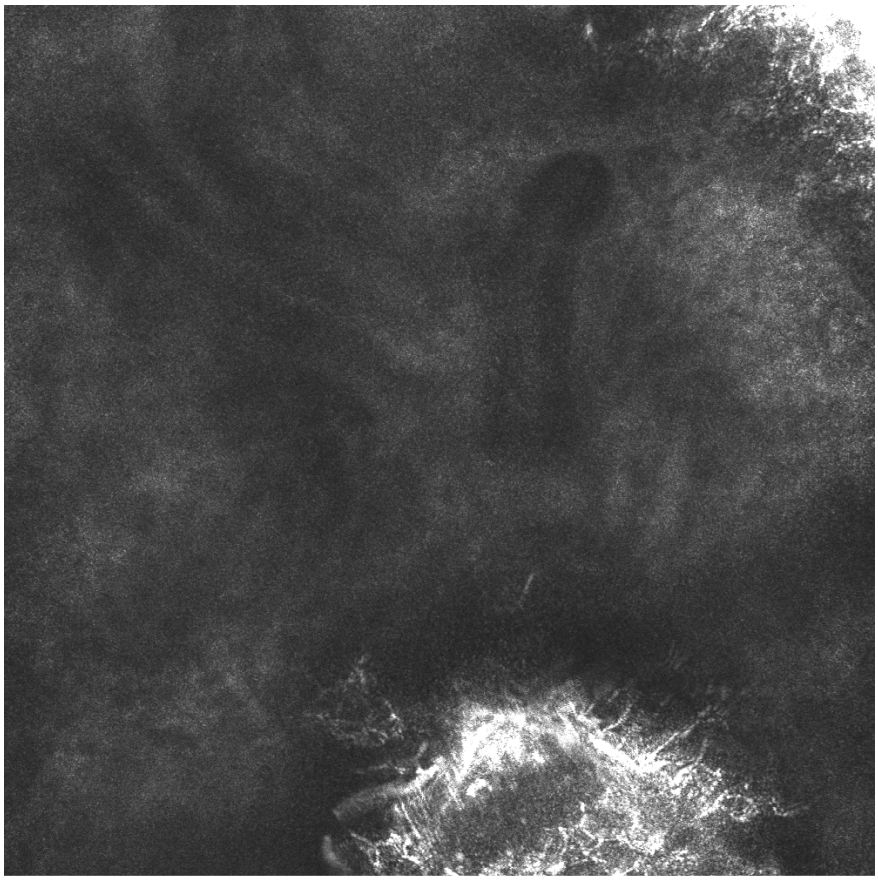

Figure 3-9 - Patient 6 confocal microscope image post-application of EMLA.

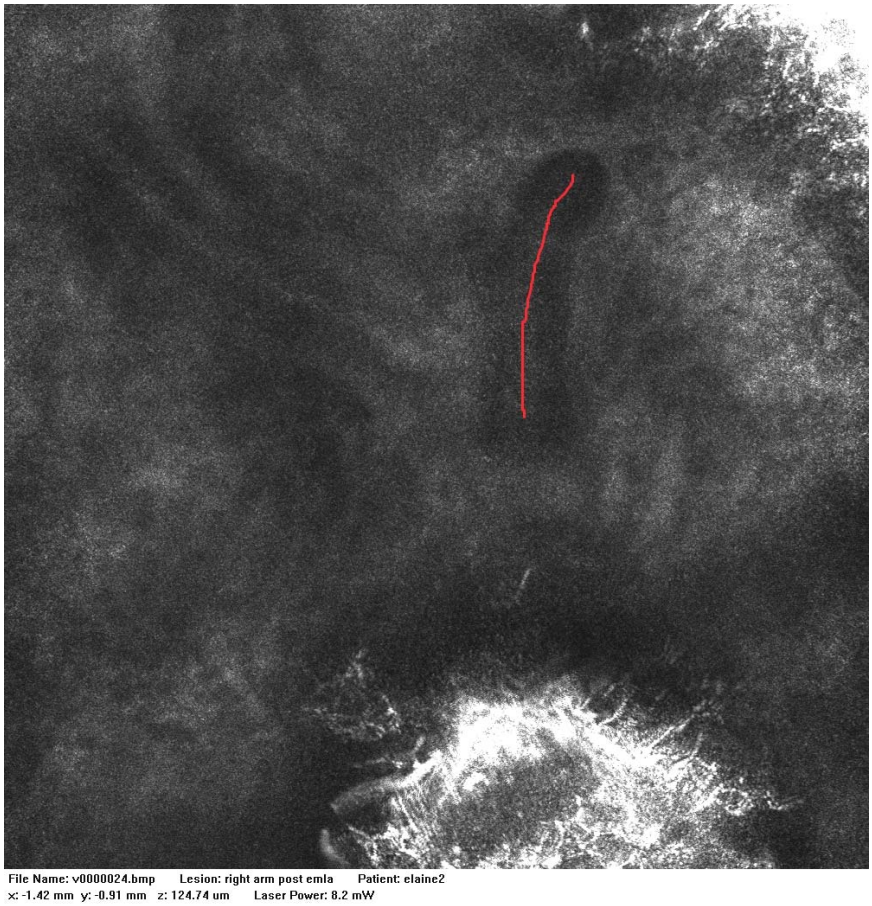

Figure 3-10 - Patient 6 confocal microscope image post-application of EMLA with red line to illustrate vessel position.

The confocal microscope pictures below have vessels which are more easily identifiable using the real-time 'movie' function (Figure 3-11, Figure 3-12, Figure 3-13 & Figure 3-14). The vessels, which are difficult to see, are highlighted in subsequent figures (Figure 3-12 & Figure 3-14).

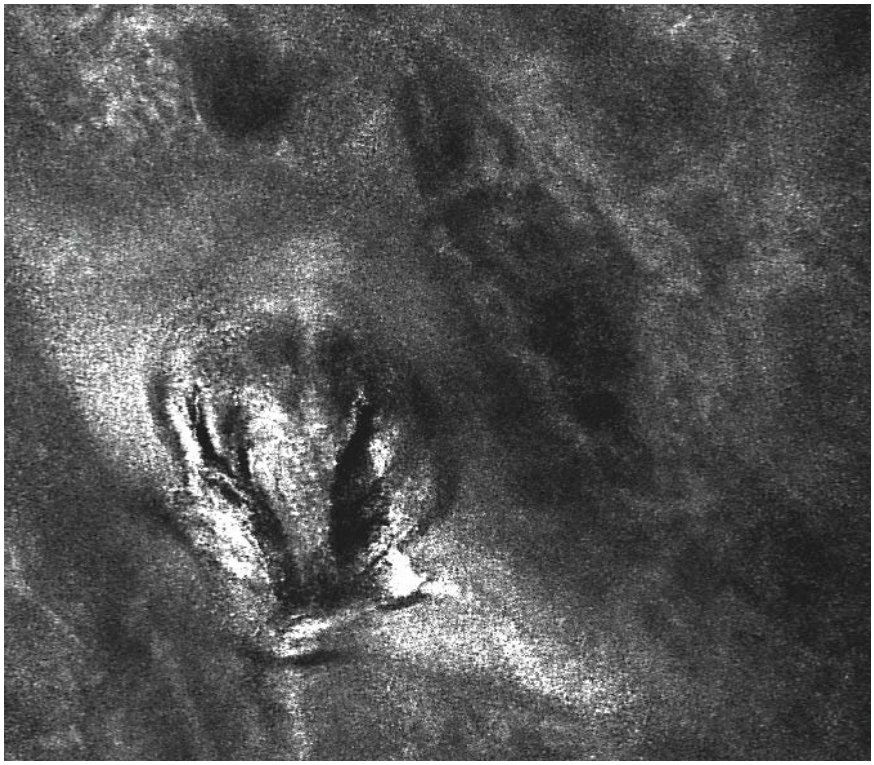

Figure 3-11 - Patient 1 confocal microscope image pre-application of ametop.

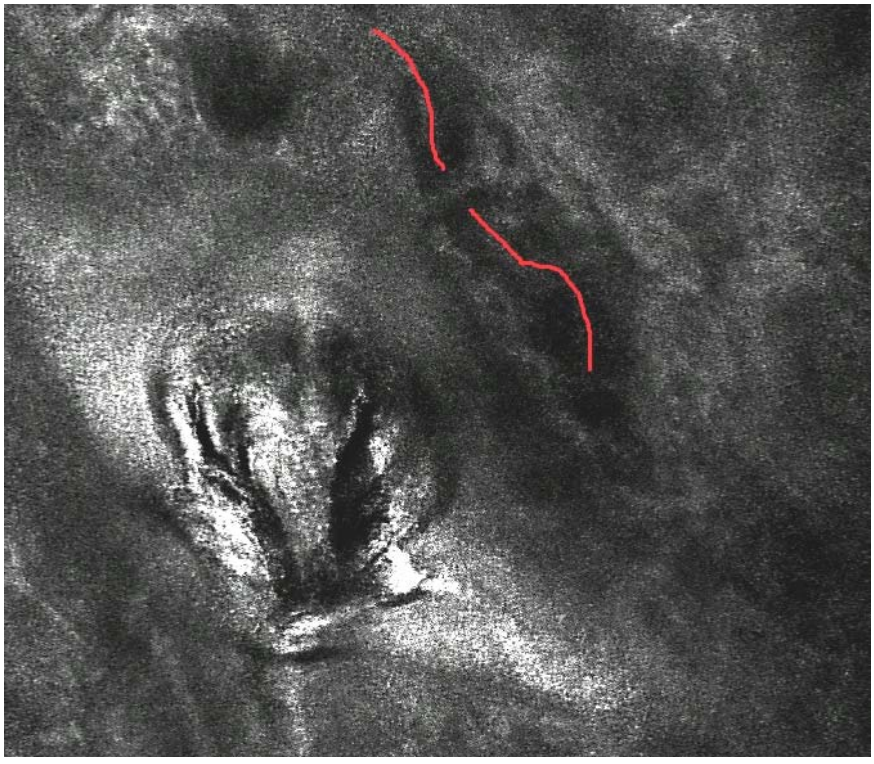

Figure 3-12 - Patient 1 confocal microscope image as above (Figure 3-11) illustrating vessel.

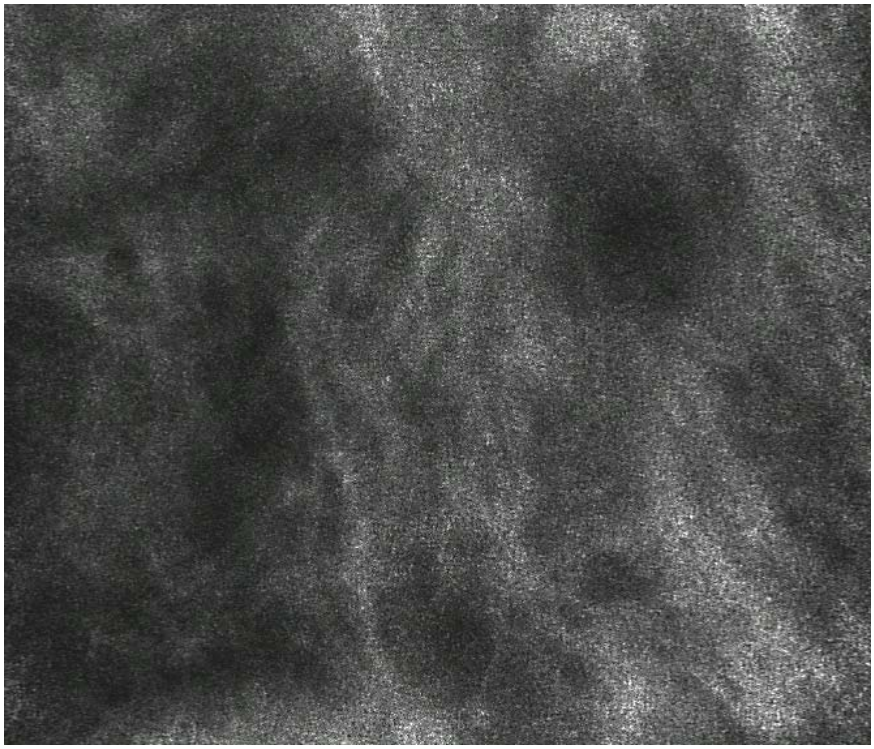

Figure 3-13 - Patient 1, additional example of confocal microscope image pre-application of ametop.

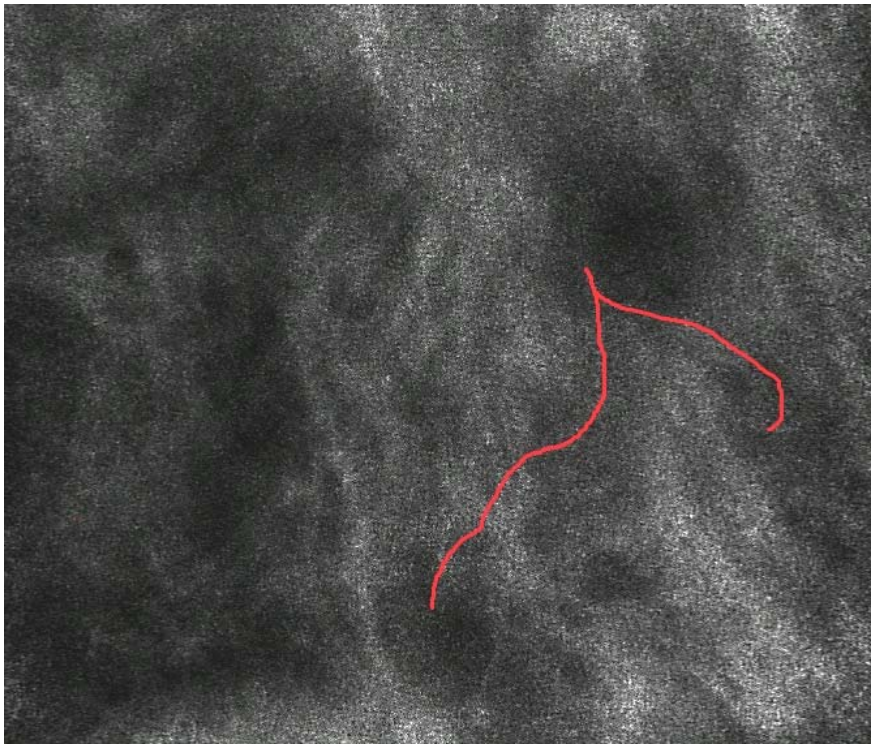

Figure 3-14 - Patient 1 additional image as above (Figure 3-14), illustrating vessel.

3.4.1 Data description

The number for measurements for each patient and the anaesthetic used are shown in Table 3-2 and the summary statistics for diameter are shown in Table 3-3.

	Timepoint	Pre		Post	
	Micro	Confocal	Vidmic	Confocal	Vidmic
Anaesthetic	Patient				
Ametop	1	21	0	12	0
EMLA	2	33	0	18	0
EMLA	3	12	0	9	0
Ametop	4	15	9	18	9
EMLA	5	30	9	12	9
EMLA	6	34	9	24	9
EMLA	7	18	9	8	9
Ametop	8	19	9	25	9
Ametop	9	26	9	22	9
Ametop	10	15	9	15	9
EMLA	11	18	9	17	9

Table 3-2 - Number of vessels with diameter measurements.

Number	Mean	SD	Min	Q1	Median	Q3	Max
565	50.87	30.96	10	35.75	43.7	54	325.2

Table 3-3 - Summary statistics of vessel diameter in micrometers (micron).

The distribution of the diameters for vessels for each topical anaesthetic before and after application, and for each microscope type are shown in Figure 3-15 below, and each individual's results in Table 3-4 below.

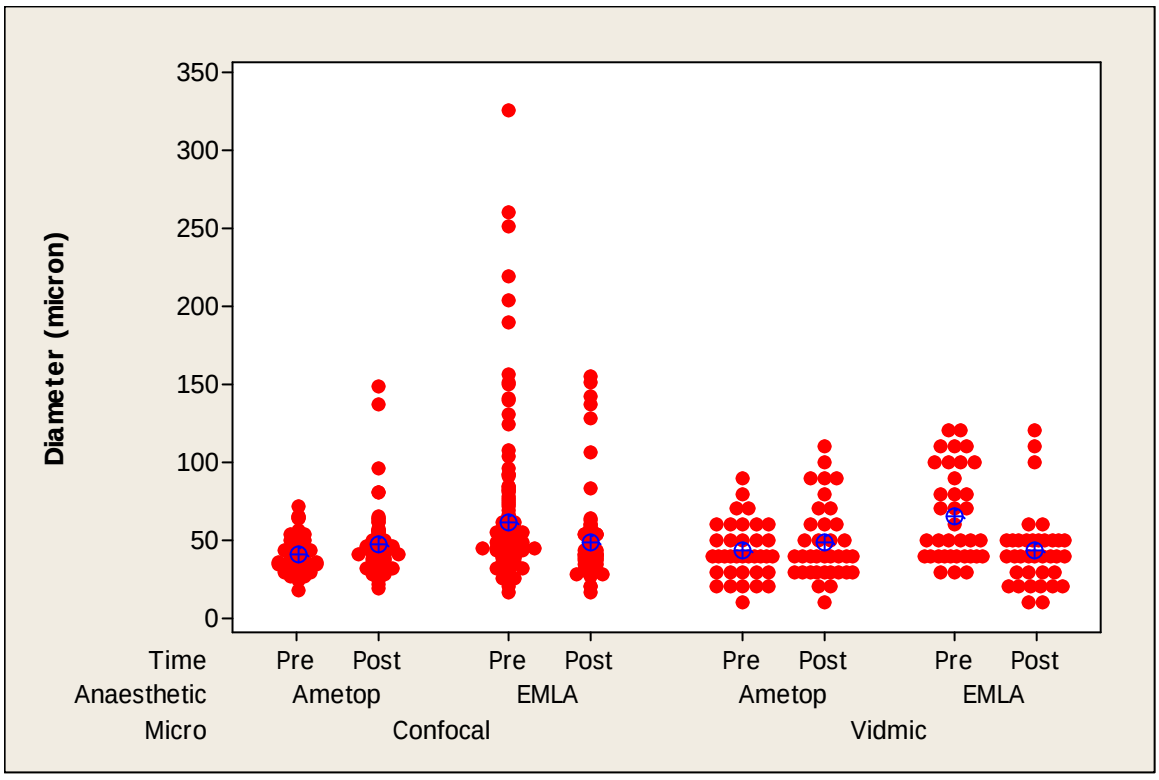

Figure 3-15 - Diameter by topical anaesthetic, microscope and time point. Mean diameters in blue.

Anaesthetic	Patient	Microscope			
		Confocal		Video microscope	
		Time-point		Time-point	
		Pre-	Post-	Pre-	Post-
Ametop	**1**	35.1 (6.0) 21	36.2 (7.3) 12	0	0
EMLA	**2**	52.4 (12.8) 33	42.4 (11.7) 18	0	0
EMLA	**3**	48.6 (10.3) 12	43.0 (10.9) 9	0	0
Ametop	**4**	45.0 (10.3) 15	42.3 (10.6) 18	44.4 (8.8) 9	41.1 (10.5) 9
EMLA	**5**	47.1 (25.6) 30	37.1 (10.2) 12	57.8 (25.4) 9	37.8 (9.7) 9
EMLA	**6**	73.5 (39.2) 34	57.7 (31.3) 24	74.4 (28.8) 9	47.8 (23.9) 9
EMLA	**7**	31.4 (8.9) 18	32.5 (7.8) 8	50.0 (24.0) 9	33.3 (18.0) 9
Ametop	**8**	39.9 (12.3) 19	51.5 (30.6) 25	52.2 (21.1) 9	72.2 (26.4) 9
Ametop	**9**	46.6 (8.2) 26	50.3 (12.4) 22	27.8 (14.8) 9	41.1 (10.5) 9
Ametop	**10**	34.0 (8.0) 15	48.7 (11.4) 15	48.9 (16.9) 9	41.1 (29.3) 9
EMLA	**11**	122.0 (89.6) 18	61.9 (39.3) 17	80.0 (31.6) 9	55.6 (35.7) 9

Table 3-4 - Mean diameter measurements, (SD in brackets), & number of measurements. Grouped by patient, anaesthetic, microscope and time-point.

The distribution of diameters is skewed to the right, especially for the confocal microscope. The diameters plotted show the variability of diameters in individual patients as well as between patients.

The effects of factors on mean diameter can be seen in Table 3-5. Post-treatment with ametop there was a small increase in the overall diameter of the vessels measured (6.4 microns and 5.6 microns difference using the confocal and videomicroscopes respectively)(Figure 3-16). Post-treatment with EMLA there was a decrease in diameter (13.3 microns and 22 microns difference using the confocal and videomicroscopes respectively)(Figure 3-17). Additionally, comparison of the confocal microscope and videomicroscope suggests little difference in observed mean diameters, although the numbers of patients are small.

Confocal			Video		
Group	**Pre**	**Post**	**Group**	**Pre**	**Post**
Ametop (n=5)	40.6 (10.3) 96	47.0 (18.9) 92	**Ametop (n=4)**	43.3 (18.0) 36	48.9 (24.4) 36
EMLA (n=6)	62.0 (46.5) 145	48.7 (26.6) 88	**EMLA (n=4)**	65.6 (29.1) 36	43.6 (24.4) 36

Table 3-5 - Mean diameter measurements, by treatment group, time-point, and microscope type.

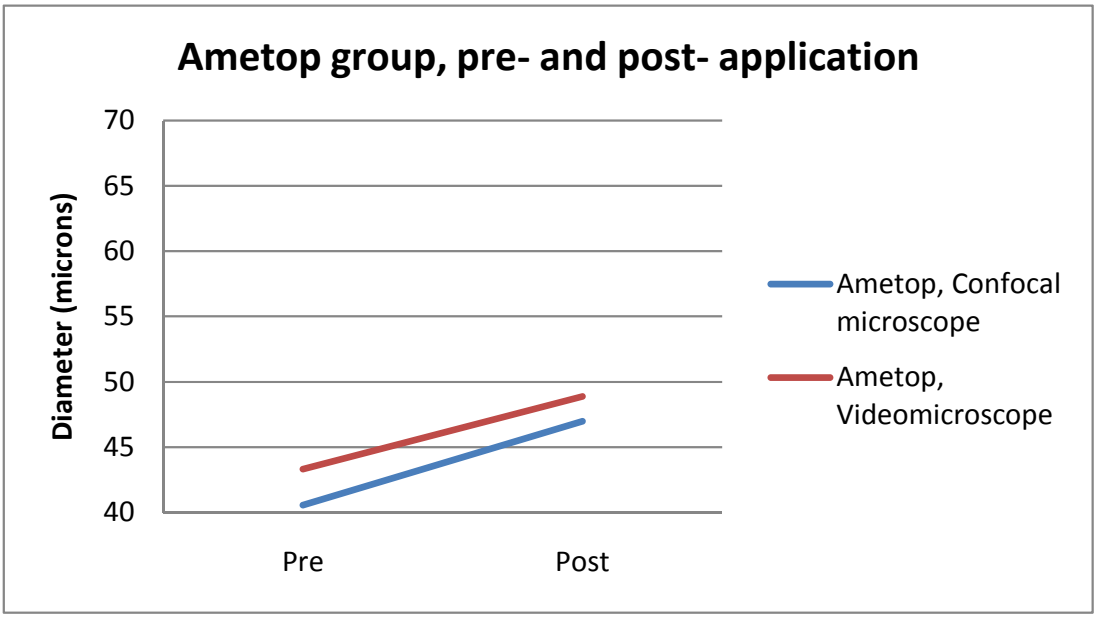

Figure 3-16 - Ametop group pre- and post- application of topical anaesthetic.

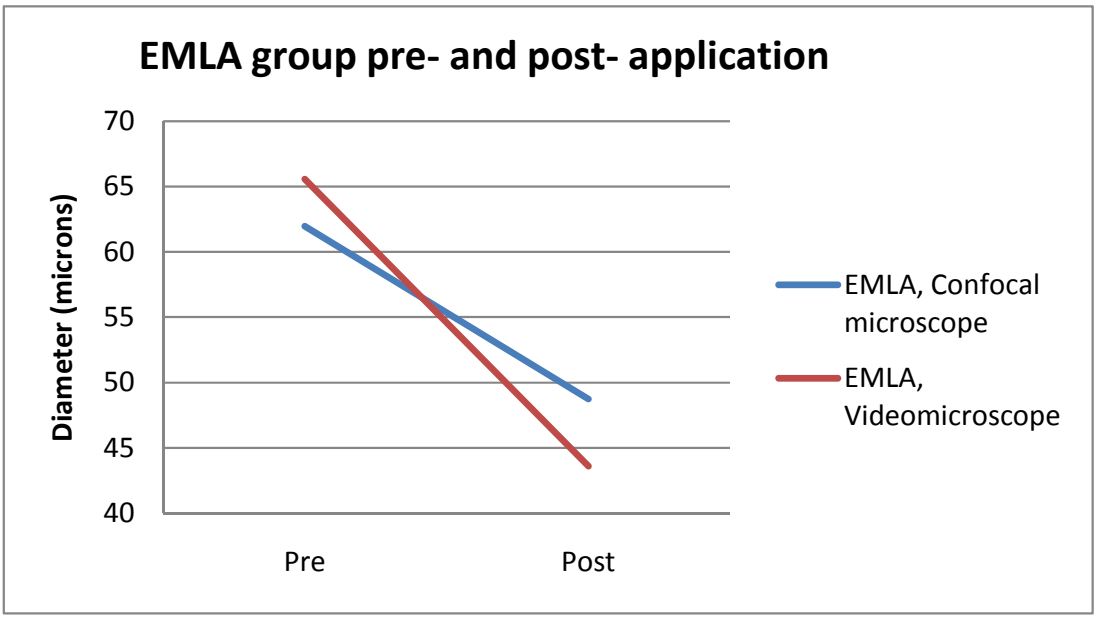

Figure 3-17 - EMLA group pre- and post- application of topical anaesthetic.

3.4.2 Statistical modelling

The method of Residual Maximum Likelihood (REML) was used as there were two sources of random variation (patients and vessels), different numbers of vessels measured per patient, and also no videomicroscope measurements for three patients. REML is a technique for estimating variance components in unbalanced data[135;136]. It provides unbiased estimates of variance components.

As the observations of diameter are skewed to the right (Figure 3-15 & Figure 3-18), the REML analysis was carried out on the log transformation (base 10) of the diameters. The skew has been lessened to some degree, Figure 3-19.

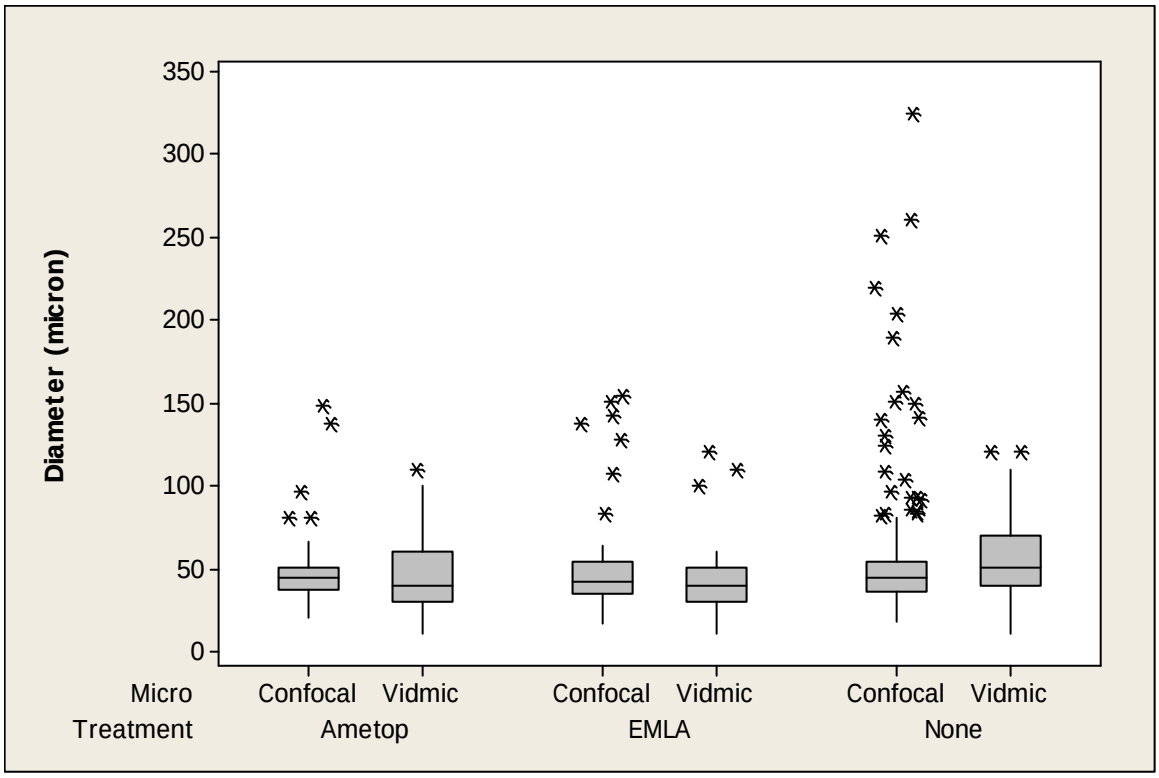

Figure 3-18 - Diameter by microscope, anaesthetic and timepoint

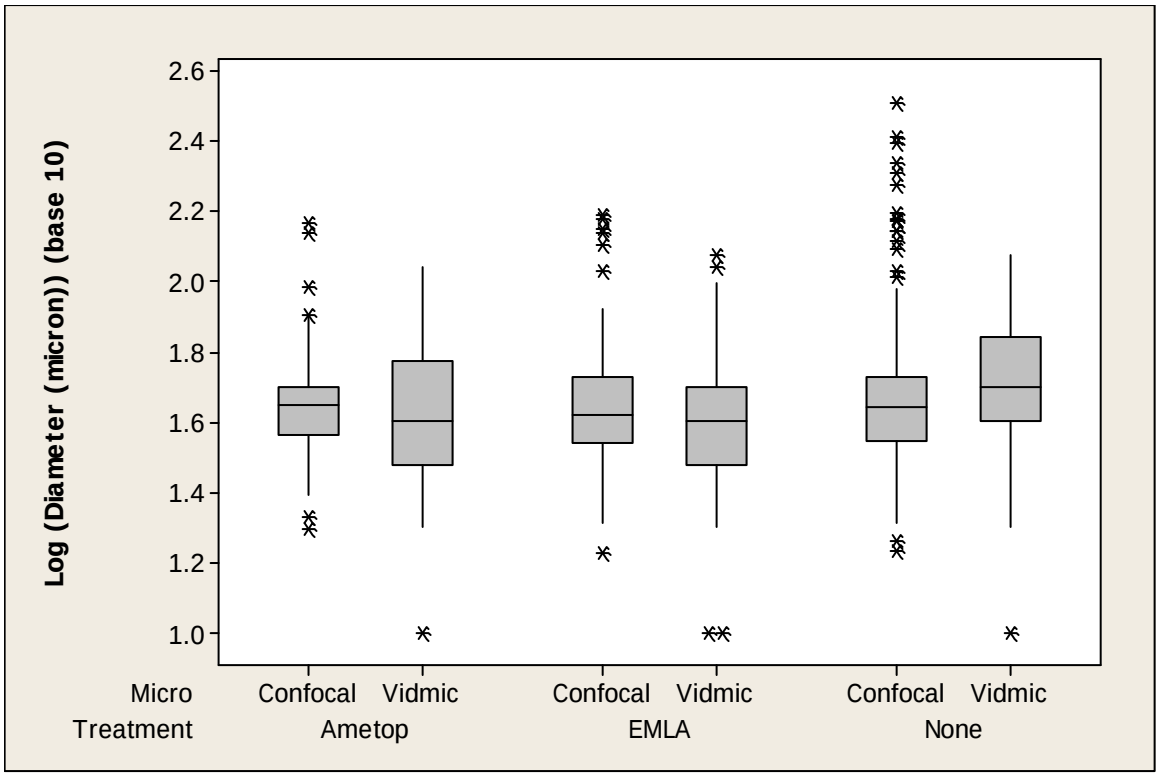

Figure 3-19 - Log diameter (base 10) by microscope, anaesthetic and timepoint

In the REML model analysis (fitter to log diameter), the following factors were 'fixed effects'; treatment at three levels (EMLA, ametop and none) and Microscope type at two levels (confocal microscope and videomicroscope). Four random effects were included; the main effect of patient, a two-factor interaction between patient and microscope, a two-factor interaction between patient and treatment, and one three-factor interaction between patient, microscope type and treatment. Within-patient variation is estimated by the residual error variance. The REML method provides unbiased estimates of fixed effects, and of variance components corresponding to random effects. The statistical significance of fixed effects was assessed using approximate F-tests, Figure 3-19.

	Test statistic (Approximate F)	Numerator df	Denominator df	P-value
Microscope type (M)	0.05	1	7.6	0.835
M|Treatment (T)*	0.02	1	7.6	0.892
T	11.20	2	8.6	0.004
T|M	11.19	2	8.6	0.004
M.T|M+T**	0.92	2	13.2	0.424

Table 3-6 - Approximate F-tests of main effects and interactions.

***M□T indicates the effect of microscope type adjusted for the effect of treatment.**
****M.T indicates the interaction between M and T.**

The main effect of microscope type was tested alone and allowing for the effect of treatment. Similarly the main effect of treatment was tested alone and allowing for the effect of microscope type. The two-factor interaction between microscope type and treatment was tested allowing for both main effects.

Microscope type has no significant effect whether treatment is included or not (p=0.835, p=0.892 including treatment). The interaction between microscope type and treatment is also not statistically significant (p=0.424).

The main effect of treatment is statistically significant, regardless of whether microscope is included in the model, p=0.004. Treatment is the only factor to have an effect upon mean diameter. The predicted mean log-diameters for treatment are shown in Table 3-7 below.

Pre-treatment	Post Ametop	Post EMLA
1.671	1.702	1.536

Table 3-7 - Predicted mean log-diameters

To assess changes in vessel diameter following application of topical anaesthetic, t-tests were performed. The difference in the predicted means (log) post-treatment for ametop is -0.031. The standard error is 0.029 and on 8.6 degrees of freedom the P-values is 0.361. There is therefore no evidence that Ametop affects the mean diameter.

Similarly, the difference in pre- and post-application of EMLA is 0.135. This gives a P-value of 0.002 (standard error 0.029, 8.6 degrees of freedom). It is concluded that EMLA reduces the mean diameter of vessels.

Anti-logging these values of predicted means gives the diameters in Table 3-8 below, which may be interpreted as geometric mean diameters.

Pre-treatment	Post Ametop	Post EMLA
46.9	50.4	34.4

Table 3-8 - Anti-logged predicted mean log-diameters

There is a 27% reduction in post-EMLA diameter, and the 95 % confidence interval for the reduction in geometric mean diameter is between 15% and 37% reduction (lower and upper points of logged 95% confidence interval are 0.068 and 0.202).

3.4.3 Random effects

Most of the random variation in the data are between measurement of different vessels for a given patient, rather than between patients (details in Appendix).

3.4.4 Homogeneity of variance

The residual variation is greater for the videomicroscope than for the confocal microscope (0.0360 v 0.02124). The within-patient variability is greater for the videomicroscope although there are more outlying values.

To check whether this apparent difference between residual variables had any effect on the results, the REML analysis was repeated including a weighting variable. Observations were inversely weighted by their residual variance, with

measurements from the videomicroscope given weight 1, and with the confocal microscope weight 1.7. The results of this analysis, Table 3-9, were very similar to the unweighted analysis Table 3-6, and the predicted means and standard errors only varied from the unweighted analysis by 0.001.

	Test statistic (Approximate F)	Numerator df	Denominator df	P-value
Microscope type (M)	0.05	1	7.7	0.837
M|Treatment (T)*	0.02	1	7.7	0.890
T	10.69	2	8.8	0.004
T|M	10.68	2	8.8	0.004
M.T|M+T**	0.81	2	16.4	0.462

Table 3-9 - Approximate F-tests of main effects and interactions (weighted analysis).

The greater variability of the of the videomicroscope has minimal effect on the results of the REML analysis and the same conclusions are drawn.

3.4.5 Checking model assumptions: Normality

There is evidence of non-Normality of the residual errors as the Anderson-Darling test gives a p value of <0.05. There is no evidence of non-Normality for random effects (p=0.144, Anderson-Darling test), nor any evidence of patient-treatment interactions (p=0.551), nor patient microscope interactions (p=0.989), nor patient-microscope-treatment interactions (p=0.096).

Due to the evidence of non-Normality of residual errors, the effects of anaesthetic and the difference between types of microscope were tested using non-parametric tests. Interaction between treatment and microscope type was tested, and the null hypothesis that interaction can be described by a single parameter was not rejected (p=0.471) nor was the null hypothesis that the interaction parameter is zero (p=0.363). Assuming no interaction, the mean effect of microscope was tested and this was not statistically significant (p=0.834). The null hypothesis that the effects of the two anaesthetics are identical was tested and this was statistically significant, p=0.0304.

The non-parametric tests and the REML analysis therefore give the same findings as regards the statistical significance of experimental factors.

3.4.6 Comparison with additional observer

Although the anaesthetic timepoint were divided into three groups, none, post-EMLA and post-ametop, it is apparent from Table 3-2 & Figure 3-19 that there is a difference between the pre-EMLA group and the pre-ametop group.

Time		1(Pre)		2(Post)	
Micro		Confocal	Vidmic	Confocal	Vidmic
top_anaesthetic					
Ametop	Xbar	40.55	43.33	46.97	48.89
	SD	10.27	18.05	18.94	24.35
	Freq	96	36	92	36
EMLA	Xbar	61.97	65.56	48.74	43.61
	SD	46.55	29.12	26.62	24.40
	Freq	145	36	88	36

Table 3-10 - Joint effect of topical anaesthetic, microscope type, and timepoint.

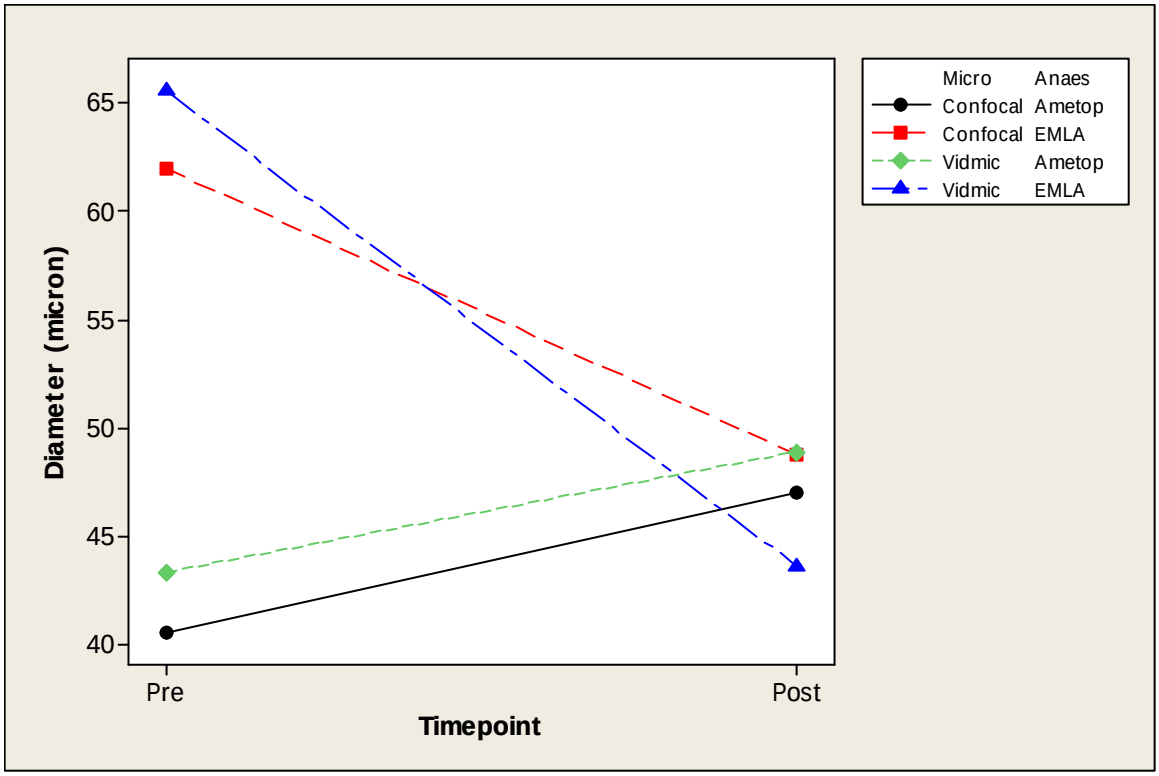

Table 3-11 - Mean diameter by timepoint, microscope type and anaesthetic type. Primary observer.

The mean diameters pre-application of topical anaesthetic were 40.55 and 43.33 (confocal microscope and videomicroscope respectively) for the ametop group, and 61.97 and 65.56 for the EMLA group. The predicted mean diameters (log base 10 scale) are shown in Table 3-12 below (degrees of freedom 8.2, standard error of difference 0.029 for pre- and post- application with the same anaesthetic (i.e. rows), and standard error of 0.059 for comparison of anaesthetics at the same time point (i.e. columns)).

Anaesthetic	Timepoint	
	Pre	Post
Ametop	1.588	1.635
EMLA	1.745	1.596

Table 3-12 - Predicted mean diameters (log scale, base 10) by anaesthetic and timepoint.

Comparing the pre-application of EMLA group with the pre-application of ametop group (s.e. 0.059), the p-value is 0.029 which is significant. Between anaesthetic groups post application there is no significant difference (p=0.528). Between ametop pre- and post- application there is no significant difference in vessel diameter (p=0.144). The application of EMLA however reduced the diameter of vessels post application (p=0.001), as in the initial statistical analysis.

The results following division of the 'pre-' group into pre-EMLA and pre-ametop result in the same conclusions as the original statistical analysis, that EMLA reduces vessel diameter and ametop has no significant effect. In view of the difference between pre-treatment groups, a further blinded observer re-measured pictures from the videomicroscope pictures to ensure the accuracy of the findings.

Nine vessels were chosen for each timepoint for each patient (to keep data balanced) as shown in below;

Replicate		1	2	3	4	5	6	7	8	9
Patient_number	Time point									
(Ametop) 4	Pre	30	30	50	20	40	30	20	10	10
	Post	20	20	20	20	20	40	20	20	10
(EMLA) 5	Pre	50	40	20	10	50	100	60	40	10
	Post	10	10	30	10	20	20	40	40	20
(EMLA) 6	Pre	120	70	20	170	60	30	50	20	40
	Post	110	30	40	80	40	20	10	60	40
(EMLA) 7	Pre	10	20	60	60	20	50	20	20	10
	Post	10	10	20	10	10	20	10	20	10
(Ametop) 8	Pre	130	90	30	60	50	80	50	10	20
	Post	140	30	90	60	90	30	70	140	60
(Ametop) 9	Pre	10	30	20	10	10	20	10	10	20
	Post	40	30	20	20	30	20	30	20	20
(Ametop) 10	Pre	70	60	10	110	30	30	80	40	30
	Post	110	30	80	30	20	10	60	40	10
(EMLA) 11	Pre	140	40	50	60	40	80	100	60	90
	Post	60	70	60	80	40	60	40	60	20

Table 3-13 - Second observer re-analysis of videomicroscope pictures patients 4 - 11.

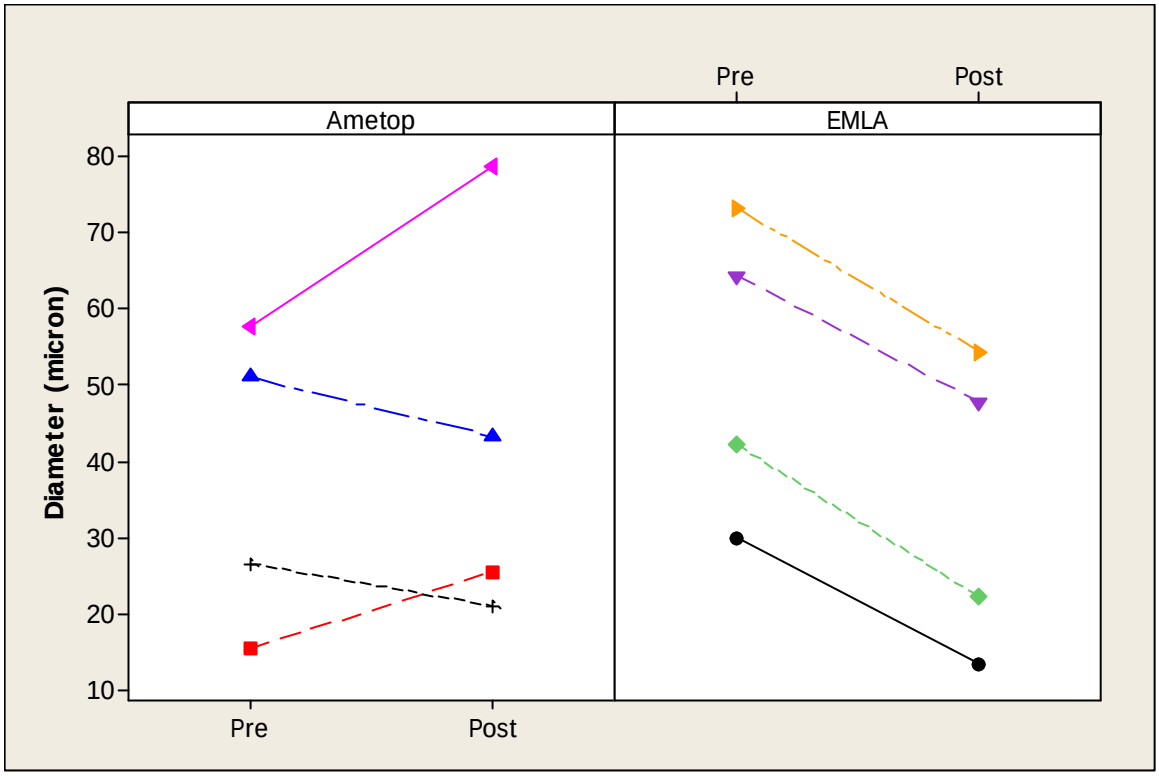

Table 3-14 - Second observer mean vessel measurements pre- and post-application of topical anaesthetic, per patient.

Time_pt		Pre	Post	Margin
Topical_Anaesthetic				
Ametop	Mean	37.78	42.22	40.00
	StDev	30.15	34.65	32.33
	Freq	36	36	72
EMLA	Mean	52.50	34.44	43.47
	StDev	37.52	25.24	33.02
	Freq	36	36	72
Margin	Mean	45.14	38.33	41.74
	StDev	34.60	30.35	32.61
	Freq	72	72	144

*The 36 measurements are of nine vessels on each of four patients

Table 3-15 - Summary data for second observer; mean, standard deviation and number of measurements for vessel diameter.

The mean pre-treatment value for the EMLA group is higher again than that for the pre-treatment value of the ametop group, 52.2 microns v 27.8 microns.

The diameters were logged (base 10). Normality tests (Anderson-Darling) were not significant for the untransformed or transformed data. The transformed data are shown in Table 3-16 below.

Time_pt		Pre	Post	Margin
Topical_Anaesthetic				
Ametop	Mean	1.4511	1.5107	1.4809
	StDev	0.3389	0.3094	0.3236
	Freq	36	36	72
EMLA	Mean	1.6088	1.4211	1.5150

	StDev	0.3312	0.3291	0.3412
	Freq	36	36	72
Margin	Mean	1.5300	1.4659	1.4979
	StDev	0.3421	0.3203	0.3318
	Freq	72	72	144

*The 36 measurements are of nine vessels on each of four patients

Table 3-16 - Mean, standard deviation and number of measurements* for log vessel diameter (base 10).

Firstly F-test of equal variances was carried out and showed no difference between the pre-ametop and pre-EMLA groups (p=0.77). Equal variance was then assumed when carrying out two-sample t-tests. There was no statistical difference between mean vessels diameter of the pre-ametop and pre-EMLA groups (p=0.344, s.e.0.154, d.f. 6), despite the mean EMLA vessel diameter being larger (52.5 v 37.8).

There was no statistically significant effect of ametop (p=0.424, s.e.0.069, d.f. 6) on vessel diameter. EMLA however had a significant effect, p=0.035, reducing vessel diameter by an average of 35.1%.

3.5 Conclusion

In conclusion, the topical anaesthetic EMLA reduces the vessel diameter within capillary malformations ($p<0.05$). Ametop has no statistically significant effect (p=0.361). These results were confirmed by a second observer's measurements of the videomicroscope vessel diameter. In addition, no significant differences were found between the videomicroscope and newer clinical confocal microscope.

3.6 Discussion

The use of topical anaesthesia continues to grow in both surgical and laser practice, with increasing numbers of formulations available including EMLA (5% eutectic mixture of lidocaine and prilocaine)[137], Ametop (4% tetracaine)[138], Rapydan (lidocaine plasters), and ELA-Max (4% liposomal lidocaine)[138] and S-caine peels (7% eutectic mixture of lidocaine and tetracaine)[139-142] out with the United Kingdom. Improving the time to onset[139;141], the quality of the anaesthesia[137;140;142], the duration of the anaesthesia and absorption through the skin, have been studied, in addition to comparisons of the quality of analgesia[138;142;143]. The rate of onset of anaesthesia is determined by many factors including the concentration and potency, the amount of binding to

plasma proteins and local tissues, the rate of metabolism and the degree of vascularity at the site of application. EMLA has provided anaesthesia for minor surgical procedures such as the shaving of skin lesions, skin grafting[124-126], and non-ablative laser treatments, as well as its more commonly known use in venepuncture[119;120;129;137;144]. EMLA has a low risk of side effects[145]. Reported and known side effects of topical anaesthetics include local erythema, pruritus and oedema[131], the risk of systemic toxicity when maximum doses are not observed[146], and individual case reports including methaemoglobinaemia in a 3 month old who had EMLA applied for 5 hours[115], and an EMLA chemical injury to the eye during erbium laser resurfacing[147]. All have effective reports of their use in laser surgery.

The effects of topical anaesthetics on the microcirculation however, are less well understood, with many conflicting studies. For example, there is disagreement as to whether EMLA causes an increase or decrease or no change in blood flow[148-150]. Similarly Ametop is though to have vasodilatory properties[150] although this has not been confirmed by our own study. The mechanism of action of changes in blood flow is also unclear. Once the topical anaesthetic has been absorbed the skin, it acts on nerves by preventing the influx of sodium and thus the propagation of action potentials. B-fibres, (myelinated preganglionic fibres) and C-fibres (pain, temperature and mechanoreceptors) have the smallest diameter and are the first blocked by anaesthetic, followed by delta (pain and cold), gamma (motor to muscle spindles), beta (touch and pressure), and finally the alpha fibres (proprioception and somatic motor) of the myelinated A fibre group[151]. Despite knowledge of the nerve fibres blocked factors confounding effects on vascularity may include the concentration (lidocaine has vasodilatory and vasoconstrictive effects depending upon concentration) and duration of application of anaesthetic (EMLA has a biphasic response), myogenic effects on pre-capillary sphincters, oedema and alterations in skin thickness, the presence of diabetes mellitus or hypertension and other unknown interactions.

In 1989 Bjerring et al published a paper, shortly after the introduction of EMLA, studying the vascular response of skin following EMLA[149]. This paper was the first to outline the biphasic response vascular reaction to EMLA, explaining some of the disagreements of earlier authors. Both lidocaine and prilocaine have

concentration dependent vasodilator and vasoconstrictor properties[152;153]. Nine healthy volunteers' forearms had EMLA, an EMLA placebo, and a moisturising cream applied followed by an occlusive dressing. The three creams were in contact with the skin at different sites for 0.5, 1, 1.5, 2, 3, 4, 5 and 6 hours. Measurements were made using reflectance spectroscopy which was then used to calculate an 'erythema index' from the absorbance of light by haemoglobin in the upper dermal vascular plexus. Skin blood flow was also measured by laser Doppler flowmetry. Bjerring et al discovered a biphasic response to EMLA with a reduction in the erythema index (i.e. blanching) $p<0.02$, and a reduction in flow (62.3% of pre-treatment value) maximal at 1.5 hours of application. After more than 3 hours of application of EMLA, erythema appeared in the few hours after removal of EMLA, and was present immediately after EMLA removal in all applications longer than 4 hours. At 6 hours the blood flow was 148% of the pre-treatment value. There were similar reductions in the erythema index of the EMLA placebo and moisturising cream but no biphasic increase in blood flow with longer periods of application. The reduction in the erythema index and blood flow at 1.5 hours is in agreement with our findings regarding EMLA, with reduction in vessel diameter within capillary malformations during this time period.

Larkin et al in 1993, investigating the reactive hyperaemia response, found a decrease in the reactive hyperaemia response in 8 volunteers following the application of EMLA to their forearms. Reactive hyperaemia is an increase in blood flow when circulation is re-established after a period of occlusion[151]. There was no alteration in the basal skin blood flow-flux rate following 60 minutes of EMLA application as measured by laser Doppler flowmetry. Following basal flow measurements, the hyperaemic response after 90, 180 and 360 second intervals of forearm blood occlusion was recorded and was found to be reduced in the EMLA treated sites. Capsacin was then applied topically to selectively activate the peripheral endings of sensory C fibres (pain), and vasodilation by this mechanism was not altered in the EMLA sites. Similarly, the effect of injecting Calcitonin Gene-Related Peptide (CGRP), a potent vasodilator, did not appear to be altered by EMLA. Larkin et al concluded that EMLA has little effect on resting blood vessel tone and did not alter postsynaptic mechanisms of vasodilation, although does reduce the magnitude and duration of reactive hyperaemia. They also thought that the mechanism of reactive hyperaemia was

likely to be mediated by a local reflex involving sensory nerves and a cyclooxygenase product.

Arildsson et al investigated the response of capillaries to heat following EMLA application of different durations[148]. The 12 healthy volunteers had EMLA applied for 20 minutes, 40 minutes, 1 hour, 2 hours and 3 hours, and after the appropriate application time a 45 degrees Celsius probe was applied and the response measured using laser Doppler perfusion imaging. The capillary density was also measured using capillary microscopy. They found a persisting perfusion increase after heat provocation associated with an increasing application time of EMLA from 40 minutes. In normal skin the blood flow is expected to return to normal baseline values within 30 seconds[154]. Following the 3 hour application of EMLA, this time had increased to at least 14 minutes. There was a lower number of active capillaries after a longer application time, although there was no significant relationship between the capillary density and the changes in skin perfusion. The decrease in capillary density was less after the application of a placebo cream and was therefore not though to be due to oedema. The perfusion increase in response to heat as measured by laser Doppler was postulated to originate in a deeper vessel plexus due to the decreased capillary density despite the heat stimulus.

Haggblad et al[155] further investigated the response of analgesized skin (EMLA) to heat, questioning whether increased perfusion originated in the superficial capillaries or in the deeper lying vessels as previously suggested by Arildsson[148], one of the co-authors. Reflection spectroscopy was used to assess the changes in the chromophores oxyhaemoglobin and deoxyhaemoglobin, and comparing the to changes in perfusion as measured by laser Doppler flowmetry. They were in 80% agreement in the EMLA and heat provocation model. The increase in perfusion in response to heat appeared to be mainly due to oxyhaemoglobin, with the deoxyhaemoglobin being sixfold less, rather than a mixture of both. The authors concluded that this was due to an increase in perfusion in a deeper lying plexus, as without a significant increase in the deoxyhaemoglobin, the increase in flow cannot be in capillaries due to an increased metabolic rate. This would not conflict with our study results as the capillary diameters measured were the most superficial capillaries in each of the CMs, which may

not relate to the same plexus both due to the abnormal anatomy and the number of laser treatments.

Hafner et al in 2003 looked at the effects of EMLA on the microcirculation using laser Doppler flowmetry (red 780nm and green 543nm), videocapillaroscopy and temperature, in the nailfold of the fourth finger in 12 volunteers[156], stating that the red laser (780nm) measures blood in the thermoregulatory plexus, and the green laser (543nm) measures blood in the nutrititive plexus. EMLA was applied for 60 minutes (under an occlusive dressing) and following this there was a minimal change in red blood cell velocity, no significant change in arterial capillary diameter, a drop in temperature (-10.1%, $p<0.02$), and a rise in laser Doppler flux with the green 543nm laser(13%, $p=0.9$) and a drop in flux with the red laser, 780nm (-13.9%, $p=0.79$). Of note using a placebo cream there was a significant decrease in mean capillary red blood cell velocity ($p<0.01$), a drop in temperature (-16.7%, $p<0.001$) and a drop in laser Doppler flux with the green 543nm laser(-41.9%, $p<0.03$) and red 780nm laser (-51.8%, $p<0.04$). The authors concluded that there was a relative increase in capillary red blood cell velocity with EMLA due to the fact that there was a decrease in velocity with placebo and no change with EMLA.

By using two wavelengths of laser Hafner et al have investigated the laser Doppler flux or flow at two different depths, although fail to suggest the likely depth measurement. The flux dropped for both the red and green lasers in the placebo, and both were significant. The flux only dropped using the red laser (780nm), -13.9%, and increased with the green laser (543nm), +13%, in the EMLA sample, although neither were significant. The authors stated that the green laser at 543nm measures at the depth of the 'nutritive plexus', and that EMLA causes an increase in skin perfusion in the nutritive plexus. The 'nutritive plexus' as described by the authors, presumably refers to the more superficial papillary dermis as the green laser will have the more superficial penetration. There was no note of how the papillary dermis was identified, no reference for the depth of the papillary dermis the nailfold, and no explanation as to whether the deeper reticular dermis may have been included in this measurement. The referenced paper on the laser type pilots the use of this green 543nm laser in brain tissue where it penetrates to a depth of 0.25mm (250μm), but penetration in skin is likely to be more superficial with increased scattering and reflectance.

Similarly the red laser (780nm) light measuring the 'thermoregulatory plexus', (presumably meaning reticular dermis) would penetrated more deeply, up to 1mm. As both the EMLA and placebo flux values decrease using the red laser, and have decreases in temperature, no effects on the thermoregulatory plexus were attributed to EMLA. The authors conclusion may not be entirely accurate as the thermoregulatory plexus should describe the more superficial plexus (papillary), and the nutritive plexus describes the deeper reticular plexus. Despite this it is clear that they have shown different vascular reactions at different depths which is worthy of explanation.

EMLA has been used in physiological studies as an adjunct to investigate vascular and neural mechanisms in the cutaneous microcirculation, which can also serve to provide information about abnormal behaviour in disease states. In 2002, Berghoff et al in a complex study investigated the vascular and neural mechanisms of acetylcholine (ACh) mediated vasodilation in the forearm cutaneous microcirculation[157]. EMLA, applied for 2 hours, was used as part of the protocol to block cutaneous nerve function, before iontophoresing ACh or sodium chloride to this site and to a control site. EMLA was found not to alter the basal cutaneous blood flow as measured by laser Doppler flowmetry. EMLA significantly reduced the response to ACh-mediated vasodilation ($p<0.001$), with a smaller percentage increase in flow in comparison to the control site, suggesting that EMLA causes an incomplete neural blockade. Other similar studies have found that local anaesthesia significantly reduces axon reflex-related vasodilation while has no effect on the total ACh-related vasodilation[158]. No change in basal flow in response to EMLA in Berghoff's study does not directly relate to the capillary vasoconstriction and blanching that we observed, although as suggested by Hafner[156] and Haggblad[155] there may be different responses in the vascular beds observed. Caselli et al in a similar study with the iontophoresis of sodium nitroprusside (SNP, vasodilatory), and heating, observed that EMLA (1-2 hour application time) resulted in a reduction in the direct response of vasodilation to SNP ($p<0.05$), although no significant change in the axon mediated indirect reflex-related response[159]. The heat-related vasodilatory response was also reduced following dermal anaesthesia, between 40 and 42 degrees Celsius ($p<0.01$). The reduction in response to SNP was hypothesised to be a direct action of lidocaine (constituent of EMLA) on the vascular smooth muscle cells.

The idea that EMLA can act directly on the vascular smooth muscle cells would appear to be in contrast to a paper by Hseih et al in 2006 demonstrating that EMLA caused vasodilation and no skin wrinkling in replanted fingers. This implies that intact sympathetic nerve function is required for the vasoconstrictive effect of EMLA[160]. A laser Doppler imager was used to detect perfusion changes in 14 replanted finger pulps approximately 16 months after replantation, following 30 minutes of 40 degrees Celsius water immersion or 30 minutes of EMLA application. Control fingers demonstrated wrinkling and a decrease in perfusion after both water immersion and EMLA application ($p<0.001$). Vasoconstriction is though to be the mechanism of wrinkling. In the replanted finger tips there was a statistically significant vasodilatory response after both water immersion and EMLA application ($p<0.001$), and no wrinkling. There was no statistical difference between the effects of water immersion and EMLA in the control or replant groups. EMLA in summary has been suggested to have neuronal blocking effects on sensory and motor neurons through voltage-gated sodium and potassium channels, and may also cause vasoconstriction though effects on post-ganglionic neurons and smooth muscle cells[157], and additionally may have an effect on autonomic nerve function[160].

Ametop is a newer topical anaesthetic and other than studies on its efficacy, studies of Ametop's effect on the microcirculation are limited in comparison with EMLA. Ametop (tetracaine 4%) is though to be more likely than the amide anaesthetic EMLA to cause allergic reactions, as it is from the ester rather than amide group of anaesthetics. The recommended application time is 30 minutes which is shorter than that for EMLA. In a study by Friedman et al in 1999 comparing four topical anaesthetics, EMLA, Tetracaine, ELA-Max and Betacaine, using a 1064nm laser as the pain stimulus, EMLA provided better analgesia at both 30 minutes and 60 minutes than tetracaine ($p<0.01$)[138]. This was the first published trial of the efficacy of tetracaine in 12 volunteers, and there were no comments made regarding erythema or changes in vascularity.

In 2008 Wiles et al performed a comparative study using EMLA and Ametop, to assess the vascular reactivity of the skin following topical anaesthesia[150]. The hypothesis was that Ametop but not EMLA would increase forearm skin blood flow-flux and reduce the hyperaemic response to transient ischaemia by an alteration in vascular tone. Twenty healthy volunteers were recruited and a

control cream, and EMLA or Ametop applied to each forearm for 60 minutes under an occlusive dressing. Blood flow (flux), and hyperaemic response following 20 seconds of brachial artery occlusion, were recorded using laser Doppler flowmetry. Measurements were made 30, 60, 90, and 120 minutes after application of topical anaesthetic. Ametop significantly increased the blood flow-flux over the control than EMLA (95 units of flux versus 2, $p<0.001$). EMLA had no significant effect on blood flow. Both Ametop and EMLA caused a reduction in the Transient Hyperaemic Response Ratio (THRR) which is calculated as the increase in flow-flux after occlusion release (hyperaemia), divided by the decrease in flow-flux on occlusion. This represents a reduction in vascular reactivity. THRR significantly decreased with Ametop at 60 minutes, whereas was only significant for EMLA at 120 minutes. The authors concluded that the differences between Ametop and EMLA were not likely to be a local anaesthetic class effect and that EMLA possessed vasoconstrictive properties that counteracted the vasodilatory effect of the local anaesthetic. Similarly Ametop's vasodilatory effects may relate to properties of Ametop itself rather than those of local anaesthetics. Additionally the data do not support earlier authors'[161] suggestion that hyperaemia is mediated by a local sensory reflex, as EMLA does not inhibit the THRR as much as the control. Wiles et al performed a further similar study, again with 20 healthy volunteers, comparing EMLA, Ametop and Rapydan, a medicated heated plaster containing the anaesthetics lidocaine and tetracaine[162]. Ametop and Rapydan application lead to an increase in skin blood flow that was not seen with EMLA. The respective vasoconstriction and no change in diameter with EMLA and Ametop demonstrated in our study, in comparison to no change in flow and increase in flow observed by Wiles et al[162], may be agreeable and represent different vascular beds (CMs versus normal skin) rather than a difference in anaesthetic effect.

Our study is in support of EMLA having vasoconstrictive properties as suggested by Wiles[162] et al, as we have demonstrated a reduction in vessel diameter ($p<0.05$). We did not observe a significant vasodilatory response with Ametop as there was no significant change in vessel diameter. A consideration less noted that may affect the use of local anaesthetics especially in laser treatment is the reported increase in skin thickness (0.1mm after 2 hours application of EMLA) by Tahir et al[163], as this may alter the relative depths of the target chromophores.

3.6.1 Capillary malformations and laser treatment

As discussed in the introduction (3.2), laser treatment of lesions involves, as described by the theory of Selective Photothermolysis, matching the wavelength of the laser with the absorption spectrum of the target chromophore, matching the pulse duration with the thermal relaxation time of the target, and providing enough energy to heat the target and cause destruction without unduly damaging surrounding tissues and causing scarring. Altering vessel diameters in capillary malformations therefore alters the laser-tissue interaction which may affect the efficacy of treatment.

Following laser treatment, remaining viable capillary malformation blood vessels were found to be small with a median diameter of 14μm in a biopsy study by Fiskerstrand et al[102], and less than 50μm using in vivo measurements by Sivarajan et al[40].

For effective treatment of CM vessels it is necessary to match the thermal relaxation of the vessel to the pulse duration of the laser. In a cylindrical vessel model the thermal relaxation time can be calculated from the following equation, based on a Gaussian temperature distribution[93];

$Tr=D^2/16_k$

Where Tr = Thermal Relaxation time

D = Diameter of the vessel

k = Thermal diffusivity of blood ($1.3x10^{-3}$ cm^2 sec^{-1})

This equation predicts that the thermal relaxation time for the remaining vessels in a non-responsive CM to be too short to be adequately treated using the pulse durations of commonly available lasers[94]. Reducing vessel diameter, for example by the use of EMLA, may therefore be detrimental by reducing the thermal relaxation time further from the pulse duration of the laser.

In addition to vessel diameter, flow may be another confounding factor in the successful laser ablation of vessels[114]. Arildsson et al noted that 3 hour EMLA treatment did not change basal skin perfusion[154], and in their later study noted a

decrease in capillary density with EMLA[148]. A heat stimulus increased the flow as measured by laser Doppler, but with no changes in capillary density, the laser Doppler was postulated to be recording changes in a deeper plexus. In our study we examined the most superficial of the capillaries in the capillary malformations, as these are the capillaries most susceptible to laser treatment (mean depth 124.6μm, range 25 - 210μm). Unfortunately we were not able to have simultaneous laser Doppler images due to a technical error with our laser Doppler, as it would be interesting to have assessed whether the decreased capillary diameter with EMLA, that we recorded using videomicroscopy and confocal microscopy, equated to a hypothesised decreased flow rate or an increased flow rate as per Arildsson in normal skin. Additionally flow rates subjectively determined using the videomicroscope and confocal microscope may have helped determine if the laser Doppler readings were primarily generated by the superficial capillaries or deeper vessels in the first couple of millimeters of skin. Jernberk et al increased the flow, as measured by laser Doppler, by infusing calcitonin gene-related peptide in 10 patients with CMs[84]. There was an improvement in the cosmetic result of laser treatment although it was not known whether this was due to presumed vessel dilatation or regulation blood flow by means of connected arterioles. There was no measurements of diameter. Flow is a further parameter that has relevance in the treatment of capillary malformations as high flow rates dissipate the heat absorbed by the target chromophore haemoglobin before there is sufficient heating and damage to the vessel wall.

The use of EMLA and Ametop in this setting could influence the response of CM vessels to laser treatment by directly affecting the vessel sizes within the malformation. We have shown that EMLA causes a statistically significant reduction in the sizes of these vessels and may therefore affect the response. Ametop has been referenced in other studies as more likely to increase vessel size and if this or another treatment were found to increase vessel diameter without excessive flow, it may be advantageous in treating these patients.

3.6.2 Use of confocal microscope in assessment of capillary malformations

Confocal microscopy is a tool that has been developed used to study microcirculation and skin over the last 20 years. One of the first in vivo studies

examined the microcirculation of the rat brain[164]. Clinically, the nerve density in capillary malformations has been investigated using confocal microscopy and histological specimens by Selim et al in 2004, and it was found that nerve density is decreased in capillary malformations perhaps as part of the pathogenesis[165]. A further study in 2010 of benign vascular lesions examined criteria for diagnosis using the confocal microscope in 7 patients, one of whom had a capillary malformation. The CM using confocal microscopy was described as a collection of large dilated vessels in the mid- to superficial dermis, with vessel diameters of 75 - 100 μm, with fibrous septae around the ectatic vasculature[166]. Melanocytic lesions have been imaged with confocal microscopy and compared with dermatoscopy and histopathological diagnosis of lesions[167;168]. In a study by Pellacani et al, 2005, thirty six out of thirty seven malignant melanomas were correctly identified and forty seven out of sixty five benign lesions (difficulties in the diagnosis of spitz naevi)[167]. Confocal microscope was found to be a useful tool in the diagnosis of melanocytic lesions, limited only by a depth of 200μm to 300μm. Langley et al in 2007 compared 125 melanocytic lesions preoperatively with both confocal microscopy and dermatoscopy, finding that the sensitivity of the confocal microscope was greater than with dermatoscopy (97.3% versus 89.2%), although the specificities were similar (83.0% versus 84.1%)[168].

The confocal microscope (see Chapter 2, materials) as a tool for assessing capillary malformations has been compared in this study with the videomicroscope. There was no statistical difference in the diameters measured ($p=0.835$ pre-anaesthetic, $p=0.892$ post anaesthetic). Advantages of the confocal microscope include the ability to digitally store both images and video footage, and record the depths at which these were recorded. As the images are created using a near infrared laser beam, 830nm, they are displayed in black and white, which makes the video application a necessity for identifying vessels. Once the confocal microscope magnetically attaches to a metal ring which adheres to the skin, the focussing depth and movements in two dimensions are controlled via the attached computer. This is in contrast to the videomicroscope, which as a hand held device may be more prone to inadvertent pressure from the operator, and may therefore have operator variability in the measurement of depth. The residual variation for the videomicroscope was slightly greater than the confocal microscope (0.0360 v 0.02124). The

videomicroscope however displays the skin in colour and vessels containing red blood cells are clearly visible and quickly identified. Laser Doppler imaging gives an impression of flow within a capillary malformation, but cannot determine vessel depth and diameter, and therefore cannot provide enough information to predict response to treatment.

It has been suggested in modelling studies by Lakmaker et al that capillaries deeper than 0.8 - 0.9mm in the skin do not affect the colour of the skin due to the optical properties of light[169]. Studies have also shown that pulsed dye lasers with a wavelength of 585nm are unlikely to penetrate the skin more than 0.65nm[170] and that the depth of the vessels predicts the response to laser treatment[37]. Longer wavelengths will penetrate slightly more deeply and 595nm pulsed dye lasers are often used in previously treated capillary malformations, and occasionally 1064nm Nd:YAG lasers[171]. Newer technologies being investigated to address the problem of depth in resistant capillary malformations include the use of the Cynergy laser which combines an initial pulse of a 585nm wavelength to change the oxyhaemoglobin to methaemoglobin, and then a second more deeply penetrating laser pulse of 1064nm targeting the methaemoglobin.

It was thought that the colour of an untreated capillary malformation could predict the response to laser treatment, some authors reporting the best response in pink lesions[172], and others in red lesions[173]. Pink lesions are thought to contain superficial, small diameter vessels, red lesions relatively superficial vessels and purple lesions the deepest vessels[102]. Unfortunately in a study of 261 CM patients over a 5 year period the colour was found not to be of prognostic value[97], and in a study of 55 CMs, the colour did not relate to capillary diameter or depth[133]. Imaging of the depth and diameter of vessels is therefore necessary to make any attempt at treatment predictions, perhaps in combination with flow[174], and to help determine alterations in laser parameters and manipulations of resistant capillary malformations that can improve the response to laser treatment.

4 Pilot study to assess skin blood flow in the lower abdomen

4.1 Introduction

This study was designed to examine the feasibility of predicting blood supply to adjacent angiosomes of the lower abdomen in vivo. A moor laser Doppler scanner was used intraoperatively to assess the validity of scanning the territory of a vessel within operative clinical time constraints. This study functioned as a pilot study with the aim of designing a further study to scan multiple vessels' territories intraoperatively, during DIEP flap transfer. Validating this methodology would allow laser Doppler scanning to be undertaken in other free flap transfers.

To assess differences in perfusion between individual vessels supplying a flap intraoperatively it is necessary to temporarily clamp and unclamp the vessels being investigated. To perform free tissue transfer (or pedicled tissue transfer) the flap is raised on the blood vessel that will be supplying the flap, and all other tissue (skin, fat, fascia, muscle etc) divided. At this point in the operation the flap is only being supplied by a particular vessel or vessels, receiving no other blood supply. It is at this time that an impression can be gained of how well a particular vessel supplies a flap. The further most angiosomes may appear 'dusky' or 'pale' with less sufficient venous or arterial blood supplies respectively. We wished to assess whether an investigative method could be used once the flap is raised to compare multiple vessels without being biased by; the sequence in which the vessels are assessed, reactive hyperaemia following microvascular clamping, and the microvascular clamp time, and in addition whether there was a significant difference between areas of 'good' and 'bad' flow within a flap. For example if the blood supply of the Superficial Inferior Epigastric Artery (SIEA) were to be compared with a Deep Inferior Epigastric Perforator artery (DIEP), it would be necessary to apply a microvascular clamp to the DIEP vessel(s) whilst the SIEA vessel(s) are investigated, and then apply a clamp to the SIEA vessel(s) and unclamp the DIEP vessels(s). Before investigating the DIEP vessels a sufficient period would have to elapse to allow the blood supply to become stable following reactive hyperaemia.

Further studies to examine the blood supply of the lower abdomen would ideally involve clamping each of the four supplying arteries (left and right DIEP and SIEA vessels) and their accompanying veins and sequentially releasing the clamps to see the area of skin supplied by each of these vascular pedicles. So as not to unduly prolong the operation a study to look at the area perfused by each of the four arterial pedicles supplying the lower abdomen would involve clamping all the pedicles and then sequentially releasing each one and performing a laser Doppler scan five minutes after clamp release. This would give varying clamp times of 5 to 25 minutes during an approximate 30 – 35 minute intraoperative window, before the tissue flap is transferred to the recipient site. Although the order of clamp release could be randomised, the effect of clamping duration as well as the timing of blood flow measurements with laser Doppler scans after clamp release may affect any results. This pilot study was designed to evaluate any effects of differing clamp and scanning times.

The aim of this pilot study was to evaluate effect on laser Doppler scan results of differing ischaemic times due to clamping, and clarify scanning times that would avoid the period of reactive hyperaemia. A secondary aim was to assess whether it was possible to visually differentiate areas that had statistically significant differences in flux. Knowledge of these parameters would allow the design of further intraoperative studies and maximise the information gathered within operative time constraints.

4.2 Methods

Between May 2007 and October 2007 eight female patients were recruited for an intraoperative laser Doppler study whilst undergoing delayed breast reconstruction following mastectomy, with DIEP free flaps, in Canniesburn Plastic Surgery Unit, Glasgow Royal Infirmary. This pilot study included eight patients undergoing delayed breast reconstruction with DIEP (Deep Inferior Epigastric Perforator) free flaps. Patients undergoing delayed rather than immediate reconstruction were chosen as they require a skin paddle on the flap amenable to laser Doppler scanning postoperatively (as per Chapter 5). Patients undergoing immediate reconstruction and skin sparing mastectomies have the DIEP flap almost entirely buried and therefore impossible to observe using laser Doppler scanning. Ethical approval was granted by Glasgow Royal Infirmary Ethics Committee, and no changes were made to the reconstructive procedure.

The patients had an average age of 49yrs (40 – 52 years old) and average BMI of 27 (21 to 30). All patients were non-smokers or ex-smokers at the time of surgery. A Laser Doppler Scanner was used to non-invasively measure blood supply to the skin of the DIEP flap intra- and postoperatively.

The Laser Doppler Scanner is a device designed and routinely used to assess blood supply to the skin as described in Chapter 2, for example in burns patients, and does not require direct patient contact (see Figure 4-1). The Laser Doppler scanner LDI2-IR (Moor Instruments, Axminster, Devon, UK) incorporates a class IIIB laser. There are two laser light sources with a single coaxial laser output; the visible red laser diode aiming beam (wavelength 660nm, 0.25mW), and the near infra-red laser diode (wavelength 780nm, 2.25mW, Class IIIR) used for the laser Doppler measurements. Research software, Moor V5.3, was used to carry out the patient scans; Large scan setting, 4 msec/pixel, 70cm from patient, and scanner at a 15 degree angle. The Laser Doppler records an image of the area scanned on the 'scan' setting. Each pixel recorded represents a number which is a unit of flux. The unit of flux recorded by the Doppler principal is proportional to blood flow. As the flux data are positively skewed, the median value of flux rather than mean was used following a review of the literature (see statistics section below, 4.2.1). In the 'line scan' setting the LDI repeatedly scans the same line and graphically displays the flux as a function of position and time (see Results Figure 4-11).

Figure 4-1 - Moor Laser Doppler Scanner LD12-IR & its use intraoperatively.

Intraoperatively the DIEP flap was raised on perforating vessels chosen by the surgeon (see Figure 4-2). There was no deviation from standard operative procedure. The intraoperative sequence of scans took a maximum of 35 minutes, and were performed once the flap was raised, prior to being transferred, when the surgical team commonly have a short lunch break. It was therefore felt that these scans would not prolong the operation. In addition, ischaemic preconditioning has been shown to be beneficial for flap survival[31;175;176], so clamping should not have an adverse effect on flap outcome.

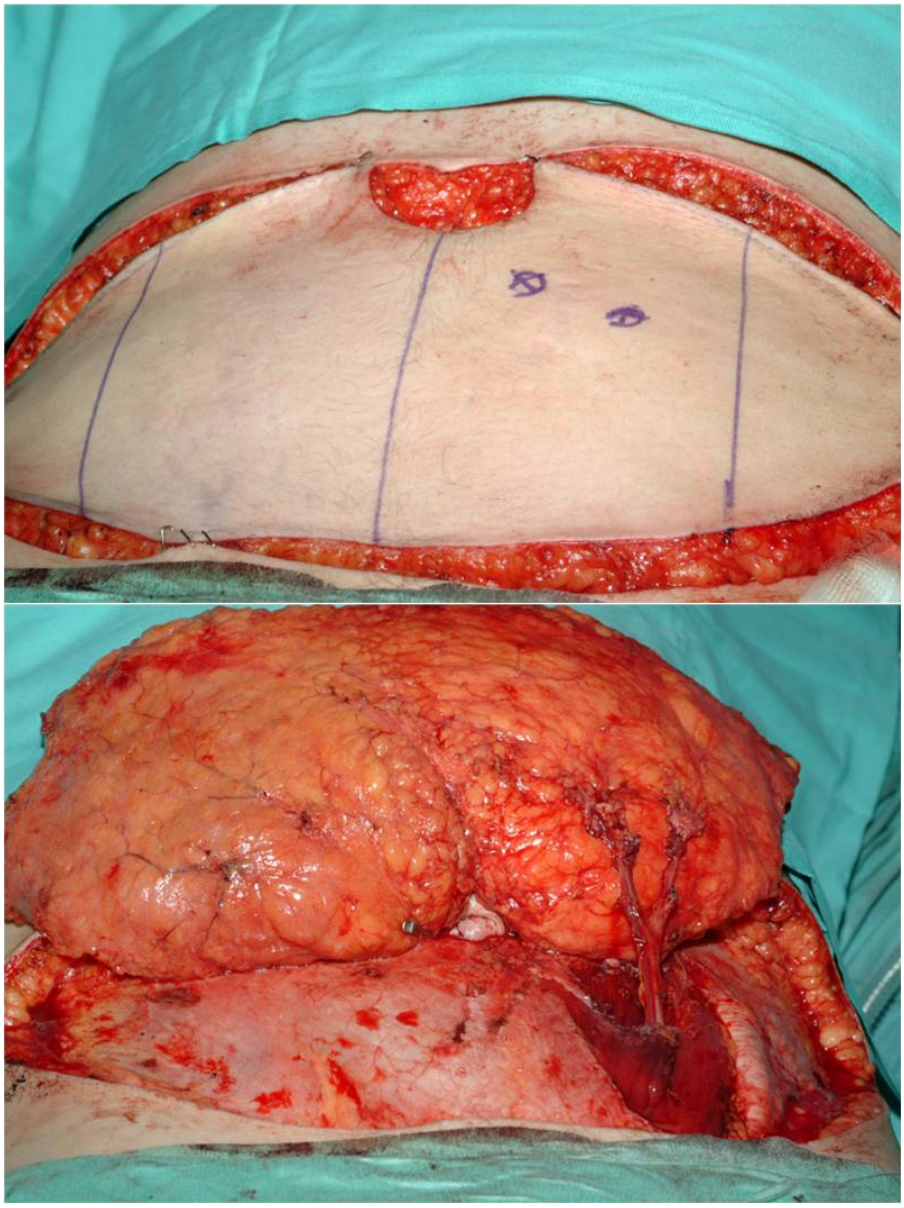

Figure 4-2 - DIEP lower abdominal flap raised on perforating vessels. Pictures show both surface (zones and likely position of perforators marked) and under surface, prior to application of microvascular clamp and scanning (Patient 8).

Once the flap was raised a vascular clamp was placed on the deep inferior epigastric pedicle. During this period the flap was not perfused. The patients were split into two groups; four patients had a clamp time of five minutes, and the other four patients had a clamp time of twenty minutes. These clamp times were chosen as they were the extremes of clamp time that could be used in the allotted time without unduly prolonging the operation. Also, as scans can take up to 5 minutes depending upon the area to be scanned, a clamp time of less then 5 minutes would not be of practical use when waiting for the initial scan taking 5 minutes to be completed in future studies. Following clamp release after five minutes or twenty minutes, the flap was reperfused for five minutes to allow for reactive hyperaemia (during which period a simple laser Doppler line

scan was taken to chart the reactive hyperaemia), and laser Doppler image scans were then performed every 5 minutes. Each scan took less than five minutes, the exact time depending upon the size of the flap. The four patients who had a clamp time of 5 minutes then had scans 5 minutes, 10 minutes, 15 minutes and 20 minutes after clamp release and reperfusion of the DIEP flap. Patients with a clamp time of 20 minutes similarly had laser Doppler scans 5 minutes and 10 minutes after clamp release (see Table 4-1).

	Clamp time	Scan times			
Patient 1	20 minutes	5 minutes	10 minutes		
Patient 2	20 minutes	5 minutes	10 minutes		
Patient 3	20 minutes	5 minutes	10 minutes		
Patient 4	20 minutes	5 minutes	10 minutes		
Patient 5	5 minutes	5 minutes	10 minutes	15 minutes	20 minutes
Patient 6	5 minutes	5 minutes	10 minutes	15 minutes	20 minutes
Patient 7	5 minutes	5 minutes	10 minutes	15 minutes	20 minutes
Patient 8	5 minutes	5 minutes	10 minutes	15 minutes	20 minutes

Table 4-1 - Intraoperative clamp and scan times.

Following laser Doppler scanning, the DIEP vessels were divided and anastomosed to the recipient internal mammary vessels in the chest. The flap was then inset and the abdominal donor site closed. Post operative laser Doppler scans were taken as part of a separate study in recovery, and at 4 hours, 16 hours, 24 hours, 48 hours and 72 hours after vessel anastomosis. This postoperative study is described in Chapter 5.

4.2.1 Use of descriptive statistics in studies using laser Doppler (Chapters 4, 5 & 6)

The scans were analysed using the Moor Laser Doppler Imager research software, Version 5.3. Areas within the scan can be identified by drawing polygons to trace the outline of the abdominal flap or zones of the flap. Shapes can be duplicated within scans or across sequential scans. Descriptive statistics including the mean and median flux are then requested for the outlined area from the Moor software. All subsequent statistical analysis of laser Doppler images in chapters 4, 5 and 6 has been performed using the medians calculated Moor Research software descriptive statistics.

There is little in the literature regarding the choice of medians versus means when analysing laser Doppler image scans and many papers are unclear as to which was used. Baker et al 2009[177] reviewed laser Doppler imaging data from

five burns centres, and commented that flux and mean flux data were the best statistical predictor of healing time, rather than clinical judgement. There was no reference to the possibility of using median flux. Jeng et al Previous study using median flux when using LDI to determine need for excision and grafting Jeng at al 2003[60]. Newton et al 2001[178] used median flux in a study looking at microvascular endothelial function in human skin. Doses of acetylcholine, methacholine, bradykinin and substance P were iontophoretically administered to the skin of healthy volunteers. The Moor laser Doppler was used, and dedicated imaging software. No explanation was given for using median.

Advice for this study was taken from both Professor William Ferrell, Glasgow University, who has performed iontophoretic and rheumatological studies[179] using the Moor Laser Doppler imaging equipment, and Dr William MacLaren, Statistician at Glasgow Caledonian University. Both advised the use of medians rather than means as the distribution of flux is clearly positively skewed (see Figure 4-3). We compared the results of this study using both means and medians and the same conclusions were drawn with the same confidence intervals.

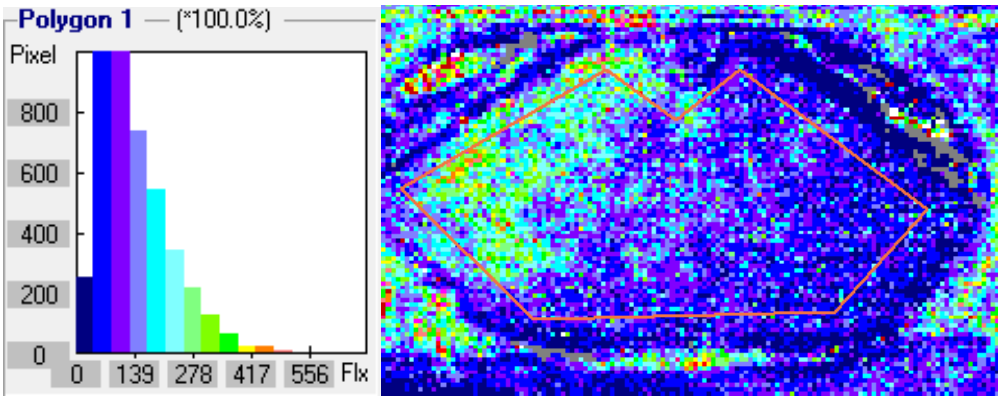

Figure 4-3 -Patient No 5. Plot of pixel colours within polygon outline of DIEP flap. Positive skew of flux demonstrated.

Within an individual Laser Doppler scan, areas of 'good' and 'poor' blood supply can be subjectively identified. Intraoperatively, being able to differentiate between well perfused and poorly perfused areas, may have clinical relevance. It suggests the physiological territories of the DIEP vessel scanned, which may help select a vessel in situations where there is a choice of vessel (Chapter 6 comparative study SIEA v DIEP). The territory of the flap intraoperatively may be related to areas which later undergo partial necrosis, and have relevance in

safer flap dimensions and design (see chapter 5, LDI scanning for 3 days post-operatively). For these reasons we assessed whether there was a statistical difference in flux between areas subjectively chosen to be areas of comparatively good and poor flow within a flap.

Two identical rectangles were placed within each 5 minute scan, chosen to represent areas of good and poor blood supply. The median flux for these areas was used to calculate whether there was a statistical difference. Absolute values for flux for areas of flap are less relevant than the difference between areas of flux as the perfusion of a flap is always relative to the patients overall perfusion and the perforating vessel(s) supplying the flap.

4.3 Results

Eight patients had delayed DIEP breast reconstruction following mastectomies for breast cancer. The mean operative time was 7 hours 40 minutes (5 hours 25 minutes to 8 hours 30 minutes) and there were no flap failures. The intraoperative scanning period took less than 35 minutes, followed by a mean flap ischaemia time of 113 minutes (65 minutes to 155 minutes) during free flap transfer and anastomosis. Post operative scans were performed in recovery, and at 4 hours, 16 hours, 24 hours, 48 hours and 72 hours after vessel anastomosis (discussed in chapter 5).

4.3.1 Intra operative scans – Clamp time versus scan time

The objective of these scans was to try and establish reproducible scanning times, beyond a period of reactive hyperaemia, with variation in clamp times within a limited intraoperative time period.

24 scans were performed in eight patients, with clamp times of 5 minutes or 20 minutes, and scanning times of 5 and 10 minutes (all eight patients), and 15 and 20 minutes for the four patients with the shorter (5 minute) clamp times, as described in the methods. The scans are represented pictorially as shown for patient 8 in Figure 4-4, Figure 4-5, Figure 4-6, & Figure 4-7. Flux is represented by the colour of the pixel, and is an arbitrary value calculated by the Moor Laser Doppler Scanner which is proportional to flow (see Figure 4-8). All Laser Doppler scans are in the Appendix.

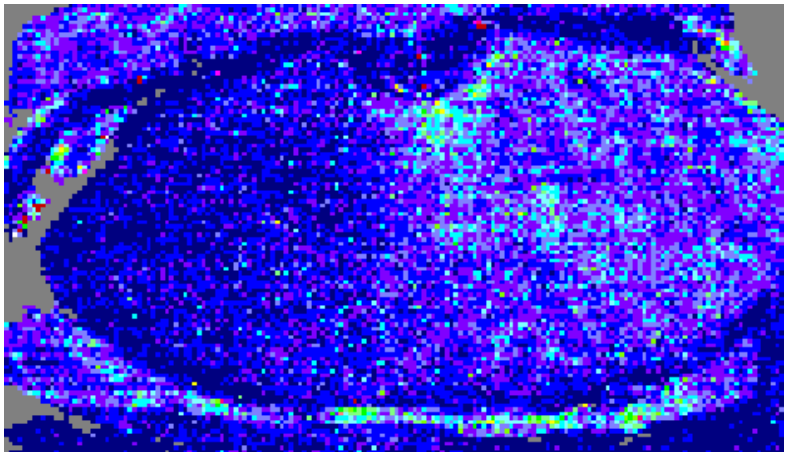

Figure 4-4 - Patient 8; 5 minute clamp time, 5 minute scan.

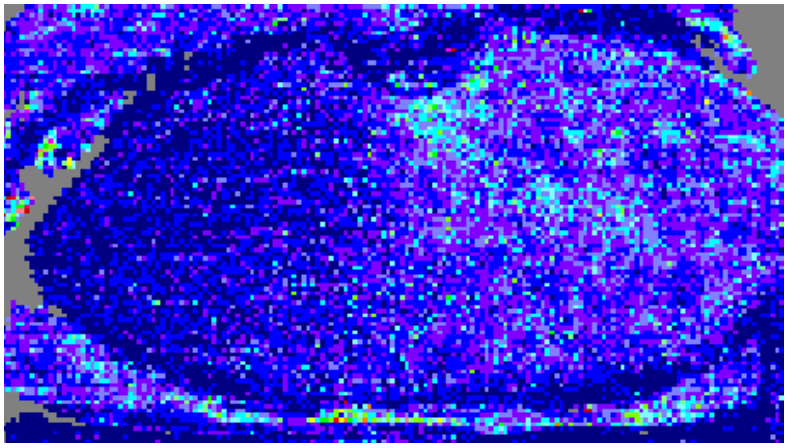

Figure 4-5 - Patient 8; 5 minute clamp time, 10 minute scan.

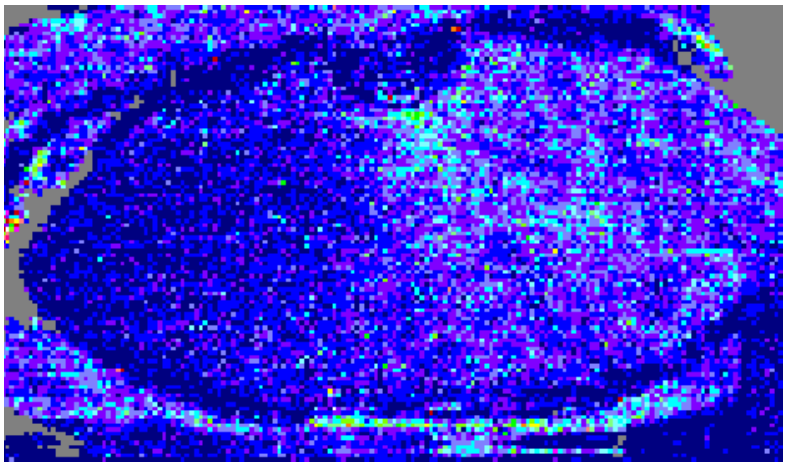

Figure 4-6 - Patient 8; 5 minute clamp time, 15 minute scan.

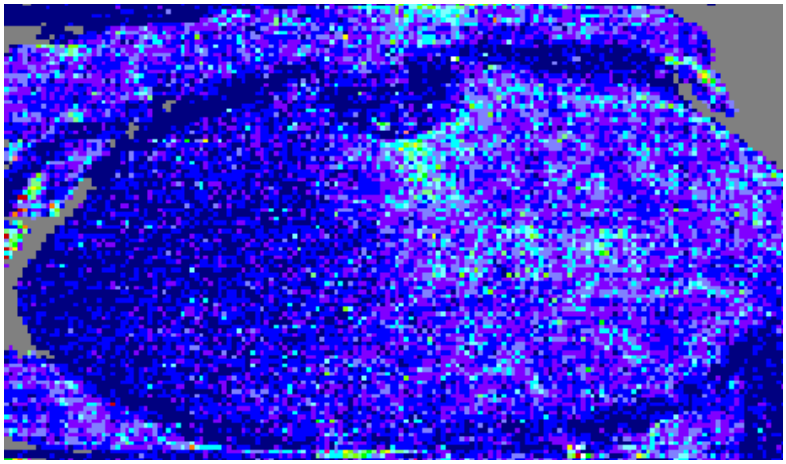

Figure 4-7 - Patient 8; 5 minute clamp, 20 minute scan.

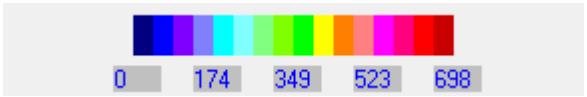

Figure 4-8 - Colour representation of 'flux' and numerical flux value. Flux is proportional to blood flow.

The median flux rather than mean flux was used in the statistical analysis as the units of flux were positively skewed (see section 4.2.1). The median flux was calculated using the moor laser Doppler software, and the raw data are shown in Table 4-2, and graphically in Figure 4-9 & Figure 4-10.

Patient	Clamp time	Scan Time	Median
1	20	5	59
1	20	10	63
2	20	5	91
2	20	10	91
3	20	5	138
3	20	10	131
4	20	5	125
4	20	10	125
5	5	5	123
5	5	10	124
5	5	15	123
5	5	20	124
6	5	5	77
6	5	10	79
6	5	15	81
6	5	20	82
7	5	5	100
7	5	10	100
7	5	15	98
7	5	20	100
8	5	5	88
8	5	10	88
8	5	15	88
8	5	20	88

Table 4-2 - Median flux for each Laser Doppler scan.

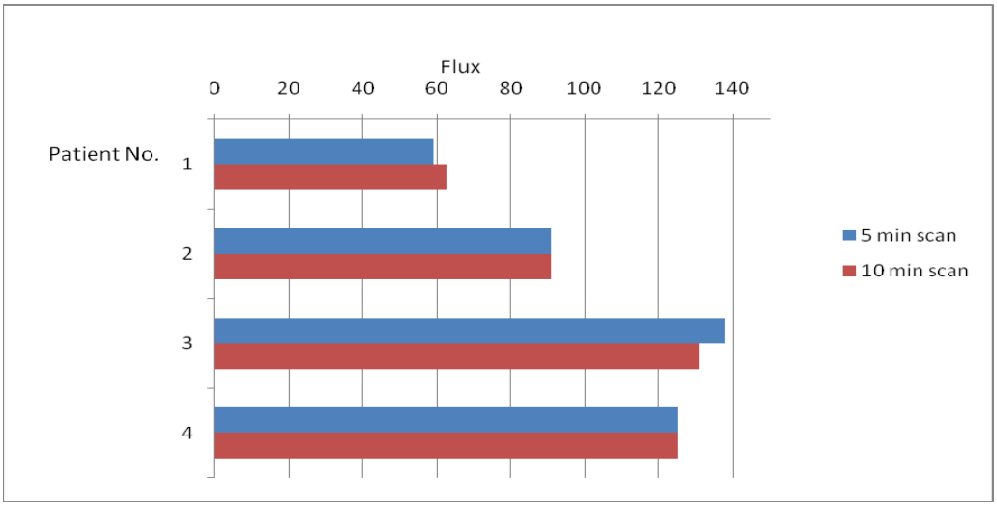

Figure 4-9 - Patients 1 - 4.
20 minute clamp time. 5 & 10 minute scan times.

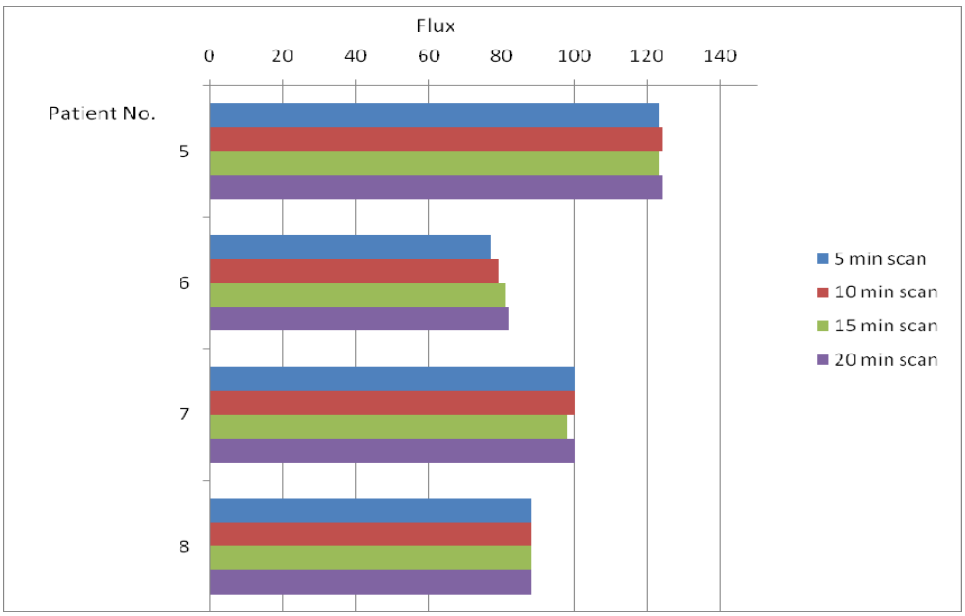

Figure 4-10 - Patients 5 - 8.
5 minute clamp time. 5, 10, 15 and 20 minute scan times.

It can be noted that for each patient the median flux does not appear to change significantly with time (Table 4-2, Figure 4-9 & Figure 4-10), in keeping with the hypothesis that the reactive hyperaemia is complete by the first scan at five minutes after clamp release. In addition, descriptive information on the period of reactive hyperaemia was provided by a line scan during the first five minutes after clamp release, before scanning of the DIEP commenced (illustration 4.2). A line scan is a one-dimensional scan where the scanner continuously scans backwards and forwards along the horizontal axis of the flap to produce a graph

with the y-axis being time, and the x-axis representing points along the horizontal axis of the flap (see Figure 4-11).

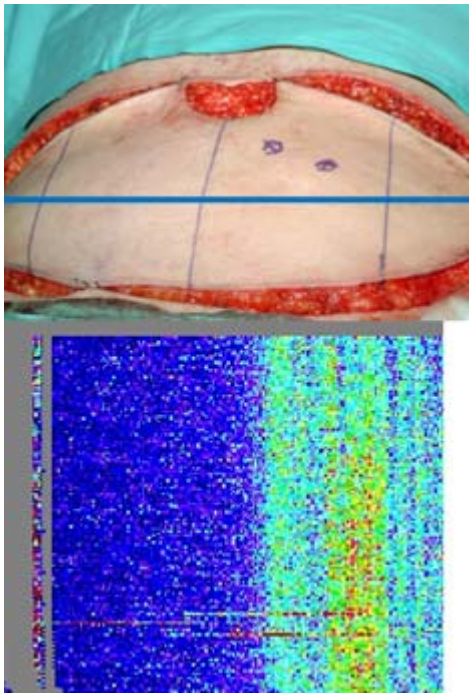

Figure 4-11 - Line scan patient 8 with scanning line across DIEP flap marked. 5 minute clamp time, scan between 0 and 5 minutes.

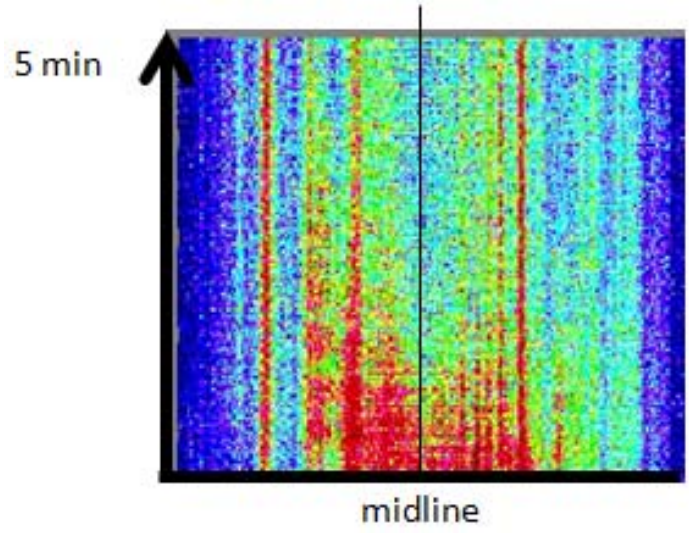

Figure 4-12 - Line scan patient 3, 20 minute clamp time, between 0 and 5 minutes following clamp release.

As preliminary illustrations, these would suggest that reactive hyperaemia is complete before the 5 minute scan time.

All subsequent patient scans were image scans, 4 patients having two intraoperative scans (clamp time 20 minutes, scans at 5 minutes and 10 minutes), and 4 patients having four intraoperative scans (clamp time 5 minutes, scans at 5 minutes, 10 minutes, 15 minutes and 20 minutes), totalling 24 scans

(see Table 4-1 & Table 4-2). The mean flux for these scans was 99.42 units, s.d. 22.17.

4.3.1.1 Data Description and test of interaction between Scan Time and Clamp Time

The summary statistics for flux, by clamp time and by scan time are shown in Table 4-3 below.

Rows: Clamp time Columns: Scan Time

	5	10	15	20	All
5	97.00	97.75	97.50	98.50	97.69
	19.71	19.50	18.38	18.57	17.05
	4	4	4	4	16
20	103.25	102.50	*	*	102.88
	35.54	31.68	*	*	31.17
	4	4	4	4	16
All	100.13	100.13	97.50	98.50	99.42
	26.81	24.49	18.38	18.57	22.17
	8	8	8	8	32

Table 4-3 - Summary statistics for flux by clamp time and scan time. Rows - clamp time, columns - scan time (mean, SD, n).

Due to the design of the study there are no scan times of 15 minutes and 20 minutes from the four patients with clamp time 20 minutes. Analysis of the data are therefore performed in two overlapping groups. Firstly, data for scan times 5 minutes and 10 minutes from all 8 patients were analysed, and secondly data from the 4 patients with scan times 5, 10, 15 and 20 minutes were analysed.

To examine the effect of clamp time (5 minutes versus 20 minutes), the scan times of 5 minutes and 10 minutes were analysed, as these were measured for all 8 patients. Table 4-4 shows these data.

	5	10	All
5	97.0	97.8	97.4
	19.71	19.50	18.16
	4	4	8
20	103.3	102.5	102.9
	35.54	31.68	31.17
	4	4	8
All	100.1	100.1	100.1
	26.81	24.49	24.81

	8	8	16

Table 4-4 - Clamp time 5 minutes v 20 minutes.
Rows - clamp time, columns - scan time.

For the four patients with a clamp time 5 minutes, flow at scan time 5 minutes is slightly less than at scan time 10 minutes (97.0 versus 97.8). For four patients with clamp time 20 minutes the effect of clamp time is in the opposite direction (103.3 versus 102.5) and again small. When averaged over clamp times the difference in flow between scan times 5 minutes and 10 minutes is zero (100.1 = means), and the effect of scan times shall be analysed further in the following section. When averaged over scan times, flow at clamp time 20 minutes is slightly greater than at clamp time 5 minutes (102.9 versus 97.4).

To assess whether this difference in flow was significant, the difference in flow between individual patients was calculated, see Table 4-5.

	Mean	StDev	Count
5	-0.75	0.957	4
20	0.75	4.573	4
All	0.00	3.162	8

Table 4-5 - Differences in flow (5 min scan time minus 10 min scan time) by clamp time.
Rows - clamp time.

The mean differences were compared between the two clamp groups using a two-independent-samples-t-test. As the sample standard deviations are different Levene's test of equality of variances[180] was performed and was not statistically significant (p=0.289). The two-independent –samples t-test was performed on presumption that the population variances were equal giving a p-value of 0.545. There is therefore insufficient evidence that the effect of scan time (5 minutes versus 10 minutes) depends on clamp time.

4.3.1.2 The effect of Scan Time

The effect of scan time was assumed not to vary with clamp time on the basis of the test results in the section above (p=0.545).

As above (Table 4-5), the mean of eight differences in flow (scan time 5 minutes minus scan time 10 minutes, 100.1 – 100.1) is exactly zero, and hence the main effect of scan time is not statistically significant (p= 1.000).

Looking at the four patients with clamp time of 5 minutes (Table 4-3,), it can be seen that there is little change in mean flow (97.00, 97.75, 97.50 & 98.50).

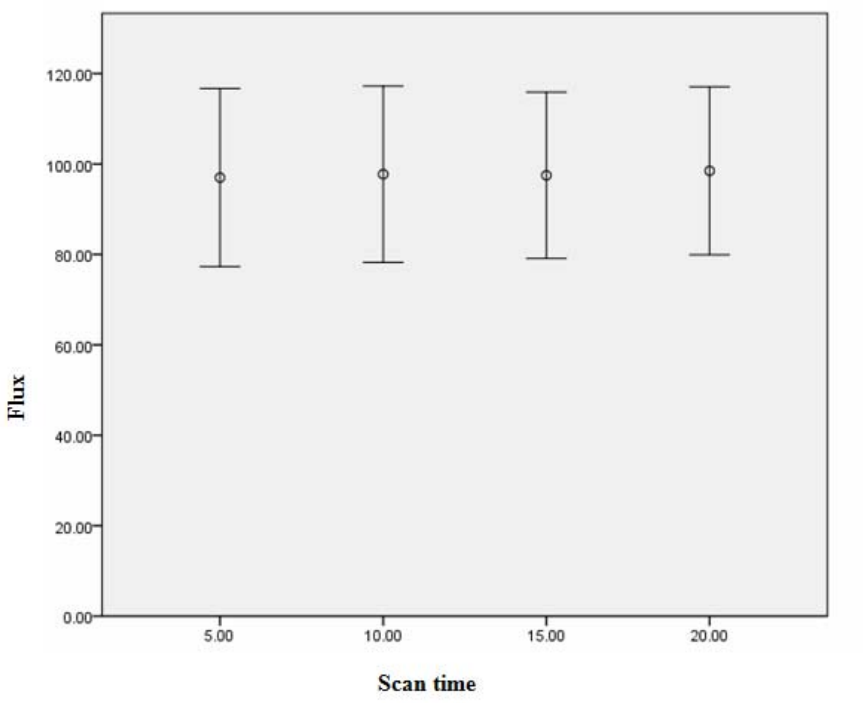

Figure 4-13 - 5 minute clamp time.
Scans at 5, 10, 15 and 20 minutes, 1 s.d. error bar.

A repeated measures analysis of variance was carried out, with patients as "subjects factor" and scan times (5,10,15 and 20) as the "timepoint factor" as shown below (Table 4-6);

Source	DF	SS	MS	F	P
Patient	3	4340.69	1446.90	926.01	
ScanTime	3	4.69	1.56	1.00	0.436
Error	9	14.06	1.56		
Total	15	4359.44			

Table 4-6 - Two-way ANOVA: Median flow versus Patient, Scan Time.

The F-statistic to test differences in mean flow between the four scan times is not statistically significant (F=1.00 on 3 and 9 d.f., P=0.436). This test assumes compound symmetry when the variances of flow at the different scan times are equal and the six covariances between the scan times are also equal. If compound symmetry is not assumed, the Greenhouse-Geisser correction factor reduces the degrees of freedom. The F-statistic of 1.00 is unchanged, and the p value is 0.399 rather than 0.436. This does not change the conclusion of no significant difference in flow between the four scan times.

4.3.1.3The effect of clamp time

Again assuming that there is no interaction between clamp time and scan time (see 4.3.1.1), the two clamp times were compared with respect to the mean perfusion averaged over scan time (Table 4-7).

	Mean	StDev	Count
5	97.4	19.60	4
20	102.9	33.59	4
All	100.1	25.63	8

Table 4-7 - Mean flow (averaged over scan time), by clamp time.

A two-sample t-test was carried out comparing the two Clamp Time groups with respect to mean flow. There was insufficient evidence of a difference in mean flow between the two clamp groups (P= 0.787). The 95% confidence interval for the main effect (clamp time 5 minutes minus clamp time 20 minutes) was (-53.1, 42.1).

4.3.2 Comparison of areas of 'good' blood supply with areas of 'poor' blood supply

Areas of 'good' blood supply and 'poor' blood supply were chosen visually by placing a rectangle over each area within the Moor research software v5.3 for each of the 5 minute scans (Figure 4-14).

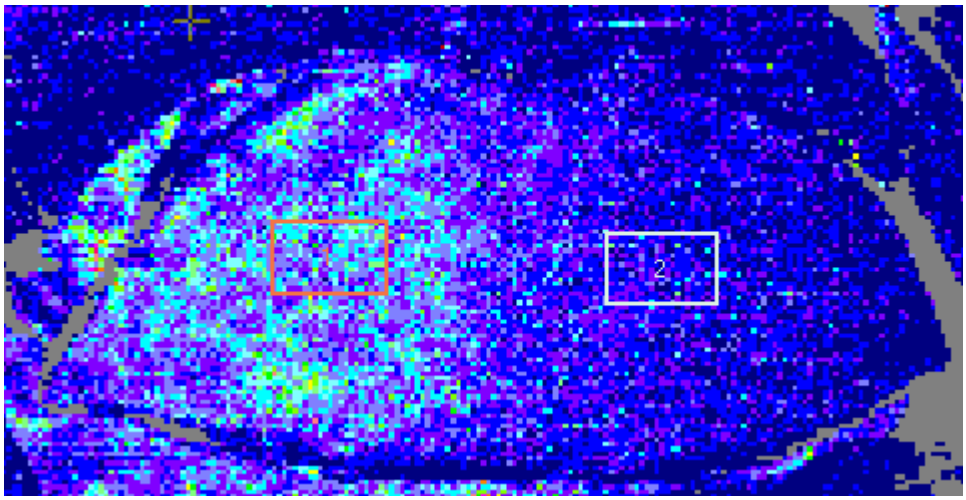

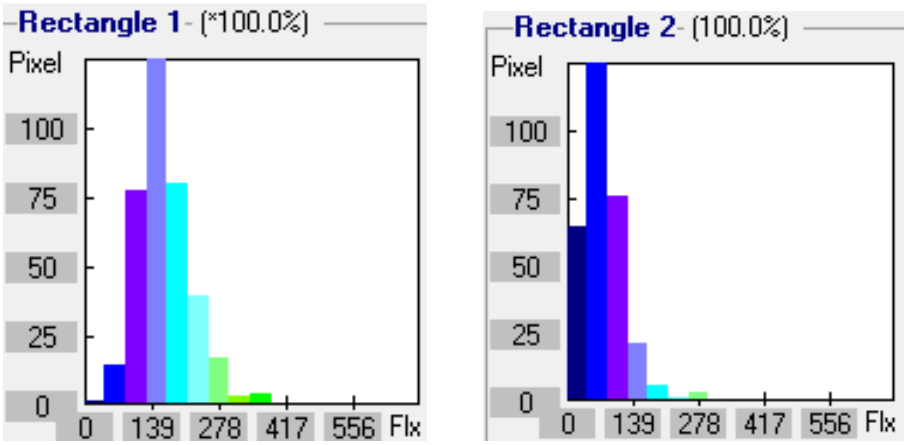

Figure 4-14 - Patient 7 DIEP flap with rectangle 1 representing are of 'good' flow, and rectangle 2 representing area of 'poor' flow.
Histogram of flux v number of pixels shown below.

The raw data for each of these areas is shown below, Table 4-8.

Patient	Clamp Time	Perfusion Good	Perfusion Poor
1	20	98	47
2	20	125	41
3	20	148	99
4	20	154	76
5	5	188	82
6	5	115	43
7	5	158	53
8	5	125	44

Table 4-8 - Raw data: median perfusion, by Patient, Clamp time (minutes), and quality of perfusion.

The summary statistics for eight patients, each with a rectangle of ‘good’ perfusion and ‘poor’ perfusion, were then compared (Table 4-9, Figure 4-15). Averaged over clamp time, flow is lower in areas of poor perfusion. Averaged over perfusion (good and poor), flow varies little with clamp time.

Rows: Clamp Time Columns: Perfusion

	Good	Poor	All
5	146.50	55.50	101.00
	33.21	18.23	54.60
	4	4	8
20	131.25	65.75	98.50
	25.45	26.92	42.59
	4	4	8
All	138.88	60.62	99.75
	28.58	21.98	47.32
	8	8	16

Table 4-9 - Flux by clamp time and 'good' or 'poor' perfusion.
Key: mean, SD, number of observations.

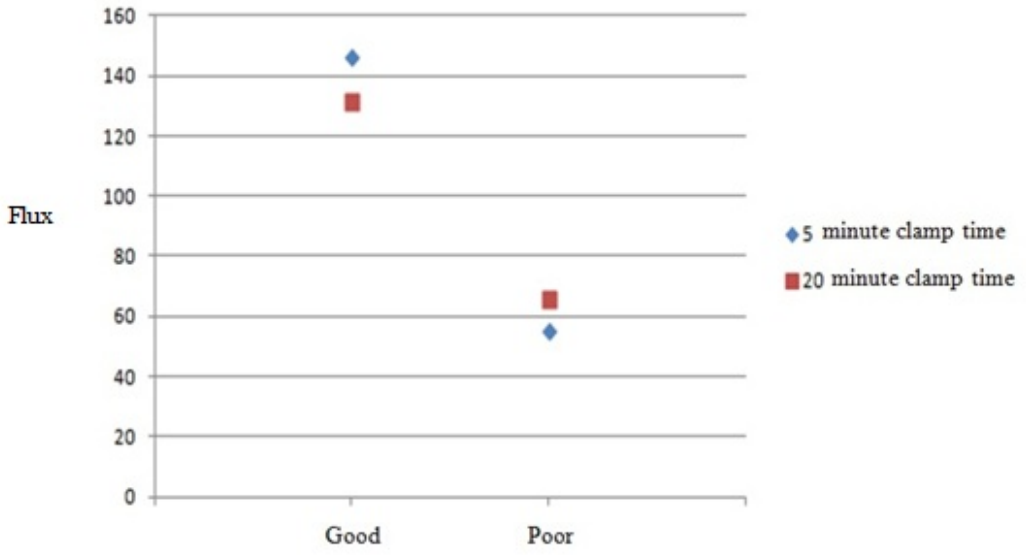

Figure 4-15 - Areas of Good versus Poor flux.
5 minute scan time, n = 8 patients and two sites per patient.

The differences in flow (good flow minus poor flow) were compared between the two clamp time groups to see if clamp time had an effect. This was done using a two-independent-samples t-test, yielding a t-statistic of 2.05 (P=0.087), Table 4-10.

```
Clamp  N  Mean  StDev  SE Mean
 5     4  91.0   17.1      8.6
20     4  65.5   18.1      9.0


Difference = mu ( 5) - mu (20)
Estimate for difference:  25.5
95% CI for difference:  (-5.0, 56.0)
T-Test of difference = 0 (vs not =): T-Value = 2.05  P-Value = 0.087  DF = 6
Both use Pooled StDev = 17.6210
```

Table 4-10 - Two-independent samples t-test, 'good' v 'poor'.

There is therefore insufficient evidence that the difference in flow between well- and poorly perfused areas differs according to clamp time.

To assess whether there is a difference in perfusion between well perfused and poorly perfused areas, a paired t-test was carried out. The mean difference in flow between well perfused and poorly perfused areas over all eight patients is 78.25. The standard deviation of the differences, 17.621 on 6 d.f., was used as calculated above. The standard error of the mean is 6.23 giving a t-statistic of 12.56 (P<0.001).

The conclusion is that the mean flow in well-perfused areas is higher than in poorly-perfused areas.

4.4 Conclusion

In summary, laser Doppler imaging, with clearly defined clamp and scan times to allow repetition of scanning within one surgical procedure, allows an impression physiological territory of individual vessels to be ascertained. Knowledge of this physiological territory aids where there is a choice of vessel, a decision that would otherwise be made by clinical inspection of the calibre vessel, and aids by highlighting the area of skin that is least well perfused when the flap requires to be reduced in size to fit the recipient site. For example it is hoped that this will allow better selection of patients for DIEP and SIEA flaps for breast reconstruction as well as better planning of individual flaps by improved ability to predict partial flap loss.

The protocol and methodology of clamp and scan times also allows maximal information to be gained in the intraoperative period when planning further research studies.

4.5 Discussion

Since its introduction in the 1970s, the use of laser Doppler for post-operative monitoring of the blood flow in free flaps has become well established[181-190]. Post-operative monitoring with laser Doppler includes implantable laser Doppler probes, laser Doppler flowmetry and laser Doppler scanning. Intraoperative methods of assessing free flaps are less well established and have been performed experimentally using laser Doppler[191;192] and other methods such as indocyanine green videoangiography (ICGA)[193;194], O2C spectroscopy[192] & near-infrared reflection spectroscopy[195], investigating factors such as anastomotic patency[193], the overall flow within the flap, the area of skin perfused by a vessel and differences between zones[195;196], intrinsic transit times[197], and the predictive value of intraoperative findings postoperatively[193]. These studies have not influenced the intra-operative choice of vessel which has been chosen clinically.

This study was designed to establish reproducible scanning times following vessel occlusion. Establishing a time after reperfusion at which the blood flow stabilises would allow design of future studies, using laser Doppler or other

methods of analysis, to intraoperatively compare vessels in as short a time window as possible. The increase in blood flow following a period of occlusion of blood flow to a tissue is known as 'reactive hyperaemia'. Reactive hyperaemia is a metabolic mechanism for local blood flow control, and usually increases the blood flow to the tissue by four to seven times normal[198] following reperfusion. When blood supply to tissue is occluded, the arterioles dilate beyond the occlusion in response to hypoxia so that when blood flow is re-established increased blood flow occurs (reactive hyperaemia). This increased flow repays the oxygen deficit[151] and washes out vasoactive metabolites. The longer the period of occlusion, the greater the metabolic stimulus, and the greater the total cumulative blood flow afterwards[199;200].

Studies that have used laser Doppler during tissue transfer have waited varying lengths of time, between 3 and 20 minutes, following any interventions, before scanning[188;191;201;202]. It would seem to be presumed that this is a reasonable amount of time to wait for the blood supply to stabilise. In an experimental animal study, Hallock 1992, divided three to six day old pedicled epigastric flaps in rats, allowing ten minutes after pedicle division for 'equilibration' before taking flow recordings with a laser Doppler probe[201]. Yoshino et al, 1997, monitored thirty seven intraoral free flaps using a laser Doppler flowmeter. Measurements were taken before and after flap elevation, after reconstruction, and at one two and three post operative days. Intraoperatively it was noted that the 'value of the blood flow stabilised within 3 minutes'[188]. In a case report, Khan 2004, laser Doppler was used to assess neovascularisation of a cross leg flap before division[202]. The flap was inset for 3 weeks and clamped daily in the 10 days prior to pedicle division. Laser Doppler readings were taken during clamping to assess neovascularisation, and 20 minutes post clamping. As this study involves assessment of a pedicled flap in the 3 week time period before division rather than an intraoperative assessment, there is less pressure to scan in the shortest interval perhaps explaining why a 20 minute scan time post clamping was chosen.

In an intraoperative study with similarities to this pilot study, Ulusal et al[191] (Taiwan 2006) examined the abdominal vessels of 43 patients undergoing breast reconstruction with abdominal flaps, with six patients having vessels compared by laser Doppler. Abdominal free tissue transfer was performed using SIEA

vessels (Superficial Inferior Epigastric Artery) in preference to the DIEP (Deep Inferior Epigastric Artery Perforator) vessels where possible, according to the study protocol. Suitable SIEA vessels were 'pulsatile' with a 'diameter greater than or equal to 1mm', and these were then compared with the ipsilateral DIEP vessel using four laser Doppler probes in each of the four zones. Readings were obtained preclamping, for 10 minutes for the DIEP vessels (SIEA vessels clamped), and for 10 minutes for the SIEA vessels (DIEP vessels clamped) consecutively, and the data were 'gathered after a stabilisation period of 10 minutes' for each vessel. The times chosen are not referenced and there is little in the literature regarding the choice of timings. The contralateral SIEA and DIEP vessels were not included in scanning. The method of using laser Doppler in this study is likely to have taken a minimum of 50 minutes (3 ten minute scans with 2 ten minute stabilisation periods in between) to observe two vessels (SIEA & DIEP), with the SIEA being the only vessel clamped and having a clamp time of 20 minutes. This total time of 50 minutes for the use of the laser Doppler is not specifically discussed. In our study scan time, and clamp time, in a short intraoperative window (around 30 minutes) have been investigated. We have proposed a period of 5 minutes rather than 10 minutes, between scans to allow for reactive hyperaemia or 'stabilisation', maximising the number of vessels that could be scanned in future comparative studies.

Following ischaemia, as caused by applying a microvascular clamp to a vessel supplying a flap, reactive hyperaemia occurs and the blood flow will stabilise after reactive hyperaemia. The duration and magnitude of the reactive hyperaemia are related to, amongst other factors, the duration of the ischaemia. A small animal study, Kinnunen et al 2000, effectively looking at reactive hyperaemia in the context of microvascular / flap surgery was performed on 6 rats, with the aim of looking at vascular responsiveness before, immediately after and 90 minutes after performing a microvascular anastomosis of an epigastric flap[203]. The study compared the immediate response to five clamp times, 15, 30, 60,120 and 180 seconds, before, after and 90 minutes after anastomosis using a laser Doppler probe. The duration of the 'overshoot' increased with clamp time in the pre-anastomosis group and the 90 minutes after anastomosis group in response to clamp time, from between 20 to 30 seconds at 15 seconds clamp time to around 70 seconds at 180 seconds clamp time. The increased overshoot in blood flow was less pronounced in the directly

after anastomosis group, thought to be due to a temporary decrease in autoregulatory capacity. In this study the magnitude of the overshoot did not show a clear difference. Further rat studies by Kinnunen conclude that the duration and amplitude of post-occlusive reactive hyperaemia are reduced in hypothermia[204], are increased following ischaemic pre-conditioning[205] and during hypovolaemia[206]. Although the clamp times are short in these studies, all being within 3 minutes, the over shoot or reactive hyperaemia lasts no longer than 160 seconds in the control groups[203;204] in keeping with the results of our study, albeit with longer clamp times, with stabilisation of blood flow in under 5 minutes. Our study compares clamp times and demonstrates no significant difference between clamp times of 5 minutes and 20 minutes ($p=0.787$) in flow scanned at 5 and 10 minutes post-occlusion, suggesting that the over-shoot of reactive hyperaemia has occurred by 5 minutes.

Studies investigating reactive hyperaemia, out with the realm of microvascular and flap surgery as discussed, confirm a recovery frequently within 5 minutes. Post occlusive reactive hyperaemia is used as a provocation test to investigate vascular reactivity, the ability of the endothelium to release factors causing smooth muscle relaxation and therefore vessel dilatation, in different scenarios. This assessment of endothelial function using post-occlusive reactive hyperaemia is not standardised, and can be assessed with venous plethysmography[207;208] or less invasively using laser Doppler[209]. As in Kinnunen's rat studies where external factors such as hypothermia, hypovolaemia and ischaemic pre-conditioning affect the duration and amplitude of reactive hyperaemia, factors such as anatomical site[210;211], age[212], fitness level[212-214], the menstrual cycle, smoking[215;216], drugs including anti-hypertensives[217] and local anaesthesia[159] and diseases such as cardiovascular disease[210], HIV[218;219] and scleroderma[219] also affect reactive hyperaemia. Most studies using post-occlusive reactive hyperaemia to investigate endothelial function choose occlusive pressure in the forearm or finger, although the thigh is also used. Laser Doppler measurements are made in the arm and thigh, or more distally in the fingers or foot, with some authors choosing sites to avoid thermoregulatory arteriovenous (AV) shunts. Outcome measures include time to resting flux[210] (immediately following occlusion before peak flux is reached), time to peak flux[210;213;218;220-223], peak flux amplitude[200;210;215;218-223], time to half recovery[210;221], and time to recovery following reactive hyperaemia[213;215;218;220-222]. The studies using time to recovery

following post-occlusive reactive hyperaemia have particular relevance to our proposed method of intraoperative clamping and scanning although they use a variety of anatomical sites and occlusion times as will be discussed.

Monsuez et al in 2000[218] investigated the reduced hyperaemic response in HIV-infected individuals by inflating a suprasystolic cuff on the upper arm for 210 seconds and measuring the response using a laser Doppler probe on a finger. Forty eight individuals were enrolled in the study; nineteen symptomatic HIV-1 patients, nineteen asymptomatic HIV-1 patients and nineteen healthy volunteers. The duration of the hyperaemic response in the control group was 80 seconds which is consistent with the time for reactive hyperaemia in our study although having a different anatomical site and a shorter ischaemic time. The amplitude and duration of the hyperaemic response were significantly reduced in HIV-infected patients lasting only 23 seconds and 33 seconds in symptomatic and asymptomatic patients respectively.

Tur et al[215] investigated post-occlusive reactive hyperaemia in twenty smokers and eighteen non-smokers using laser Doppler flowmetry. A pneumatic cuff on the upper arm was inflated to 300mmHg for four minutes and laser Doppler flowmetry recordings were taken from the volar forearms. The recovery time in the non-smoking group was 7.0±2.1 minutes and 10.0±3.9 in the smoking group, with a lower peak flow in the smokers. This impaired capillary recruitment in smoking was also found in a study by Ijzerman et al[216]. Tur concluded that the abnormal response in smokers was worrying given that reactive hyperaemia is protective for tissue damage following a period of ischaemia. The recovery period of the control group in this study is significantly longer than previous studies quoted relating to reactive hyperaemia, and is in conflict with the recovery period of less than 5 minutes found in our intra-operative study. This increased recovery time is likely to be due to a number of factors including a different anatomical site with muscle being more metabolically active than the mainly adipose tissue that we were assessing[224], and also a longer ischaemia (4 minutes) than many studies in the literature.

A similarly designed study of thirty-nine individuals by Hansell et al[220] measured microcirculatory changes related reactive hyperaemia and iontophoretically administered acetylcholine. A pneumatic cuff on the wrist at 200mmHg

occluded flow for four minutes after which a laser Doppler probe measured flux in the dorsal skin of the left hand. Hansell's group of subjects aged between 17 and 56 (median 27) includes two smokers (smoking reduces the duration of reactive hyperaemia[215]), and seven taking oral contraceptives or oestrogen replacement or low dose steroids which may all have a degree of influence on the duration and magnitude of reactive hyperaemia. Tur's[215] subjects did not take any medication in the month prior to testing, were also normotensive and were aged between 20 and 40 years with an average age of 28.8 in the non-smokers. The time to peak hyperaemia in Hansell's study was 9.7 seconds and the hyperaemia duration 95 seconds (8.5 – 222 seconds) after which perfusion returned to pre-occlusive values. This study by Hansell has an ischaemia time of four minutes as in Tur's study, although correlates with the findings of our study with a hyperaemia duration of less than 5 minutes.

Lenasi et al[213] investigated the effect of regular physical training on cutaneous microvascular activity using laser Doppler flowmetry in 39 patients; 19 trained competitive cyclists and 20 age-matched controls. Reactive hyperaemia was one of the comparisons between the groups, and was measured with a laser Doppler probe attached to the third finger following 8 minutes of occlusion with a suprasystolic cuff on the finger. The recovery time in the control group was 154.6±4.6 seconds and 241.5±21.6 seconds in the athlete group. This finding among others led the authors to conclude that physical conditioning leads to increased endothelium-dependent vasodilation. This increased vasodilator capacity of endothelium in trained individuals in other studies with greater areas under the reactive hyperaemia curve[212;214]. Wollersheim et al[221] compared post-occlusive reactive hyperaemia in 29 patients with primary Raynaud's phenomenon, 30 patients with secondary Raynaud's phenomenon (additionally suffering from either connective tissue diseases, rheumatoid arthritis, sjogren syndrome, scleroderma or severe arterial obstructive disease) and 24 healthy volunteers without cardiovascular disease. Measurements were made with a laser Doppler probe attached to a finger, and a pneumatic finger cuff inflated to 200mmHg for 5 minutes. The duration of reactive hyperaemia was 143.4±74.1 seconds in the normal controls, 105.2±79.6 seconds in those with primary Raynaud's and, 92.2±61.1 seconds, 67.7±57.4seconds and 216.8±57.1 seconds in those with secondary Raynaud's in the connective tissue disease, scleroderma and arterial occlusive disease subsets respectively. A final study using recovery

time as an outcome measure was performed by Bungum et al[222] in 1996 comparing reactive hyperaemia in forearm skin in fifteen healthy women during the menstrual cycle. Laser Doppler was used to monitor the blood flow changes following 3 minutes of arterial occlusion with a pneumatic cuff at 300mmHg. The time to recovery after 3 minutes of ischaemia was 77 seconds in the follicular phase and 51.3 seconds in the luteal phase. Interestingly a similar method using finger pulp was performed in which the recovery time was around 18 – 22 seconds but this did not reach statistical significance between the two groups. The postulated reason for differences between the two sites was the presence of AV shunts in the finger pulp and thought to therefore give values that were more related to 'central body heat excess' than reflecting hyperaemic response. All three studies have reactive hyperaemia times in all subset groups of under five minutes.

Other studies, not using 'time to recovery' following reactive hyperaemia as an outcome measure, often prefer 'time to maximum flux' or 'time to half recovery', and frequently graphically represent the results giving an indication of the time to recovery. Morales et al[210] in 2004 attempted to standardise laser Doppler perfusion monitoring and a reproducible analysis method for post-occlusive reactive hyperaemia in 24 patients with peripheral arterial obstructive disease and 30 healthy controls. They proposed a protocol including laser Doppler calibration and subject preparation and manoeuvres. A pneumatic cuff was used on the thigh for 3 minutes occlusion, 30mmHg above systolic pressure, and the probe was on the dorsum of the foot to reduce the thermoregulatory blood flow and number of AV anastomoses. Statistical analysis of results confirmed that the time paramaters measured (time to resting flux, time to maximum flux and time to half recovery) were superior to flux values (resting flux and maximum flux) in discriminating between groups. Although time to recovery was not measured, a graphical control example within the paper suggests a time of around 200 seconds (occlusion time 210 seconds), with statistical values for time to resting flux, time to maximum flux and time to half recovery as 2 seconds, 19 seconds and 68 seconds respectively in control patients. Also, a paper by Maggi et al[219] investigating microcirculation in HIV-positive patients found that patients had increased perfusion in capillaries, perhaps due to neuropathy. The time for recovery from reactive hyperaemia following 200mmHg occlusion for 10 minutes in the arm (laser Doppler probe

placed on finger) appears to be less than 5 minutes in the 23 patient control group. Finally a study of 10 healthy patients by Agarwal et al[223] graphically represent recovery of one patient from 5 minutes are pressure cuff occlusion within 2 – 3 minutes. Albeit lower levels of evidence, in different sites and in different patient populations, these studies' control patients further support our finding that reactive hyperaemia in our study is complete within 5 minutes.

Of relevance to our protocol, and its use in future studies involving a period of vessel occlusion intraoperatively, is the reproducibility of post-occlusive reactive hyperaemia. Thijssen et al[211] investigated reproducibility in different anatomical sites; the forearm, calf and thigh. Measurements were made in eight healthy males using venous occlusion plethysmography, a technique of measuring the volume of the limb or part of a limb by occluding to give a measure of perfusion or blood flow and other physiological parameters[207;208]. Thijssen concluded that measurements had 'acceptable-to-good' short (3 hours) and medium term (6 – 10 days) reproducibility in measuring post-occlusive reactive hyperaemia with a suprasystolic cuff pressure of 220mmHg for 13 minutes. Tee et al[200] investigated the influence of occlusion time on postocclusive forearm skin reactive hyperaemia using laser Doppler flowmetry in 20 healthy volunteers. Occlusion of the upper arm with suprasystolic pressure was randomised to one, two or three minutes. Increase in flux was the outcome measure and they concluded that although there were significant differences in flux between each of the three occlusion times, occlusions of less than 3 minutes produced submaximal reactive hyperaemia. Three minutes occlusion time was suggested as a good compromise in future studies to produce sufficient changes in flux without being too uncomfortable in awake patients. In our study, clamp times are a minimum of 5 minutes and are therefore not within the less than 3 minute time frame of 'submaximal' reactive hyperaemia as suggested by Tee, although for the purposes of our study a reduced hyperaemia period is not problematic. The reproducibility that Thijssen refers to, both short-term (hours) and long-term (days), does not affect our intraoperative protocol complete in less than one hour. There are no repeat measurements planned on the vessels following free flap transfer, and the purpose of the protocol is to identify times for clamping and scanning that provide reproducible and reliable results within a short intraoperative time window, with the aim being to compare vessels within one patient rather than between patients, again minimising possible variables.

Patient factors as described above that may have an influence on the time taken for reactive hyperaemia were not exclusion criteria for our pilot study. The ladies recruited were undergoing delayed breast reconstruction with a DIEP free flap and were therefore deemed to be relatively healthy, and in addition we wished that this protocol could be used in any patient undergoing free flap transfer which would have no specific exclusion criteria other than perhaps smoking. There were no outliers in our data. All ladies claimed to be non-smokers or ex-smokers immediately pre-operatively, none had significant cardiovascular disease, scleroderma or HIV or other known systemic disease, there were no extremes of age (40-52 years old) or fitness, and one patient was taking anti-hypertensive medication (possibly reducing reactive hyperaemia[217]). Intra-operatively comparisons were between laser Doppler scans during a thirty minute time window during which the patients were haemodynamically stable. Factors altering vascular reactivity and therefore the reactive hyperaemia time should be contemplated, but would not preclude the use of laser Doppler or other methods to assess flap perfusion providing an adequate period for resolution reactive hyperaemia has been left. Although in this pilot study we have successfully allowed five minutes for the completion of reactive hyperaemia, if there were suspicion that reactive hyperaemia may last longer due to external factors, or factors requiring a bigger oxygen deficit to be repaid for example a dramatically increased clamp time or a more metabolically active flap (e.g. perhaps musculocutaneous), laser Doppler line scanning would allow temporal resolution to confirm stability of flow prior to image scanning. Laser Doppler image scanning gives a two dimensional pictorial image, as would other techniques like indocyanine green videoangiography, whereas a laser Doppler probe or laser Doppler line scanning will give one dimensional flux information only, continuous in time. These continuous one-dimensional flux values could be used, where necessary, to confirm stability before a method of image scanning is commenced.

In future studies based on this scanning and clamping methodology, it would be necessary to be able to visually distinguish differences in perfusion across the area of a flap, to gain information about both the vascular territory of individual vessels and in comparison of vessels when there is a choice of vessel. For this reason two small rectangles were subjectively visually placed on each flap using the Moor laser Doppler research software, one representing an area of ‘good’

flux and the other representing an area of 'poor' flux. Statistical analysis confirmed that flux was higher in areas visually chosen as well-perfused than in areas chosen as poorly-perfused ($p<0.01$). Studies to compare perfusion across flaps, using both laser Doppler flowmetry[191;225;226] and laser Doppler imaging and also other techniques such as laser fluorescence angiography (indocyanine green)[196;227;228] or near-infrared reflection spectroscopy[195], statistically analyse the results post-operatively to quantify the differences between zones once the perforating vessel(s) have been chosen. Our studies can be used in a similar way in multiple vessels per patient with the use of appropriate clamping and scanning times, and additionally may also be used in the intraoperative decision of which vessel to base the flap on and which sections of the flap are best kept when a reduction in flap size is required for the recipient site. The difference in flux, between zone 1 as a baseline and any other area, is more important than the absolute flux value. To provide information that is valuable in making these choices, differences in flow must be visually rather than just statistically apparent.

Baker et al[177] assessed the performance of laser Doppler predictions of burn healing time, an accepted method of increasing the accuracy of predictions[60-62]. It was noted that it was not yet practical to use a 'mean flux-based methodology' for wound predictions as there is a 'distribution of flux values' and the spatial distribution of these is important. Burns software gives the tissue that has a distribution of flux additional colours to represent overlap areas, areas that do not fall into a clear predictive burn healing time groups. This wide distribution of flux values can also be seen in flap images, especially as the standard or research software used displays a coloured pixel per flux value without grouping areas like burns software. Interpretation of areas with wide ranging values of flux, which may not be outlined within zones, and their relation to the well-perfused and poorly-perfused areas of a flap, may firstly help in deciding which areas of a flap should preferentially be discarded before transfer to the recipient site. Possible relations of perfusion and flux to postoperative partial necrosis have been investigated and discussed in Chapter 5. Laser Doppler images may secondly be of benefit when deciding between vessels intraoperatively in an individual patient by providing an impression of the area of the flap that has good perfusion and also whether there seems to be any obvious difference in the baseline flow or flux in zone 1 between vessels.

In summary, laser Doppler imaging, with clearly defined clamp and scan times to allow repetition of scanning within one surgical procedure, allows an impression physiological territory of individual vessels to be ascertained. Knowledge of this physiological territory aids where there is a choice of vessel, a decision that would otherwise by made by clinical inspection of the calibre vessel, and the area of skin least well perfused when the flap requires to be reduced in size to fit the recipient site. The protocol and methodology of clamp and scan times also allows maximal information to be gained in the intraoperative period when planning further research studies. Chapter 5 investigates the postoperative perfusion of the DIEP flaps studied in this chapter, and chapter 6 intraoperatively compares SIEA and DIEP vessels using the methodology delineated by this pilot study.

5 Laser Doppler assessment of post-operative perfusion

5.1 Introduction

In addition to investigating the intraoperative effects of clamping and scanning times on laser Doppler scan results in Chapter 4, laser Doppler scans were performed postoperatively for up to 72 hours after free flap transfer on these patients. This was to observe changes in perfusion in the first 72 hours post-operatively when choke vessels are thought to dilate between angiosomes. The angiosomes of the lower abdomen with regards to deep inferior epigastric perforator (DIEP) flaps and transverse rectus abdominis are commonly referred to as 'zones'. The most commonly used terminology are Hartrampf's zones, Figure 5-1 below, with zone 1 representing the midline zone where the pedicle enters the flap, zone 2 is the contralateral midline zone, zone 3 is the ipsilateral lateral zone, and zone 4 the contralateral lateral zone. The significance and debate over these zones is explained in more detail in Chapter 6.

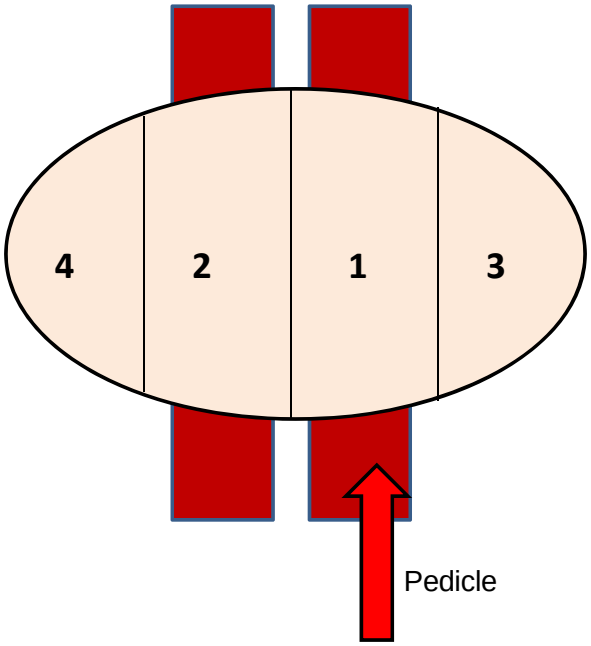

Figure 5-1 - Hartrampf's zones of lower abdomen.

Laser Doppler imaging has been used as both a research tool and for flap monitoring in the post-operative period (mainly in the form of laser Doppler flowmetry with attachable probes). In designing a further study using microdialysis catheters to assess tissue chemistry over a 72 hour period (Chapter

7), we wished to observe whether haemodynamic changes within a DIEP flap could be detected non-invasively using laser Doppler imaging, and if so, to observe changes in perfusion between angiosomes during this period of choke vessel dilation.

5.2 Method

The eight patients recruited for the intra-operative pilot study described in Chapter 4, were included in this 72 hour laser Doppler post-operative study.

As described previously (Chapter 4), eight female patients undergoing delayed breast reconstruction with DIEP flaps following mastectomy were recruited for the intra-operative and post-operative pilot studies. Only delayed flaps were included as the flaps needed a skin paddle that could be scanned post-operatively. The DIEP (Deep Inferior Epigastric Artery Perforator) flap is a lower abdominal perforator flap consisting of skin and fat, that is commonly used in autologous breast reconstructions. The DIEP vessels in this study were anastomosed to the internal mammary vessels, adjacent to the sternum, and the skin and fat inset to form an aesthetically acceptable breast reconstruction.

Laser Doppler image scans were performed post-operatively once the patient had returned to the recovery ward, and at 4 hours, 16 hours, 24 hours, 48 hours and 72 hours post-operatively. As before the laser Doppler scanner used was the LDI2-IR from Moor Instruments, Axminster, Devon, UK. There are two laser light sources with a single coaxial laser output; the visible red laser diode aiming beam (wavelength 660nm, 0.25mW), and the near infra-red laser diode (wavelength 780nm, 2.25mW, Class IIIR) used for the laser Doppler measurements. Research software, Moor V5.3, was used to carry out the patient scans; Large scan setting, 4 msec/pixel, 70cm from patient, and scanner at a 15 degree angle. Each pixel recorded represents a number which is a unit of flux. The unit of flux recorded by the Doppler principle is proportional to blood flow. Scans were performed from above the patient and from the side of the patient to account for the curvature of the reconstructed breast and the angle of incidence of the laser light. Patients were always scanned in the same supine position when warm and haemodynamically stable. As it was not possible to control for medications, temperature and fluid balance, a baseline measurement

of normal skin was taken as a reference point for the effect of any confounding factors.

Ethical approval was granted by Glasgow Royal Infirmary Ethics Committee. No changes were made to the operative procedure or to the post-operative care and routine clinical flap monitoring.

5.2.1 Analysis of data and descriptive statistics

Details of the data analysis from the laser Doppler scans for chapters 4, 5 and 6 are given in Section 4.2.1, page 73.

The scans were analysed using the Moor Laser Doppler Imager research software, Version 5.3. The area of perfusion in each zone to be analysed was marked by a circle using the Moor research software (Figure 5-2 & Figure 5-3). As there were dressings over the wounds and curvature of the skin surface, the central areas of each zone were chosen to try and minimise any artefactual error.

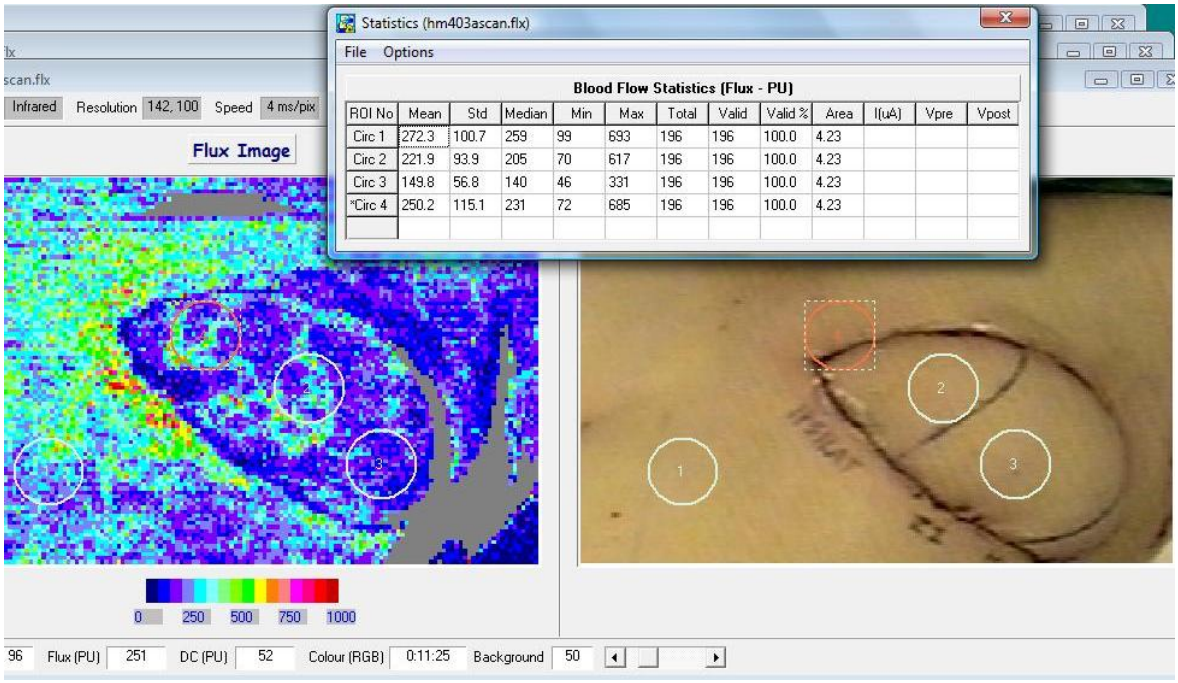

Figure 5-2 - Laser Doppler image of patient 4 from above.
Laser Doppler flux image on left, video image on right. Placement of circles over zones 3, 1 and 2 from left to right. Baseline measurement on patients abdomen. Statistical output form Moor research software version 5.3 displayed. (NB. Alignment of flux image and video image do not match due to convergence error of the detector and camera within the Moor LDI2 laser Doppler. This has no practical significance for the flux image and results are not affected).

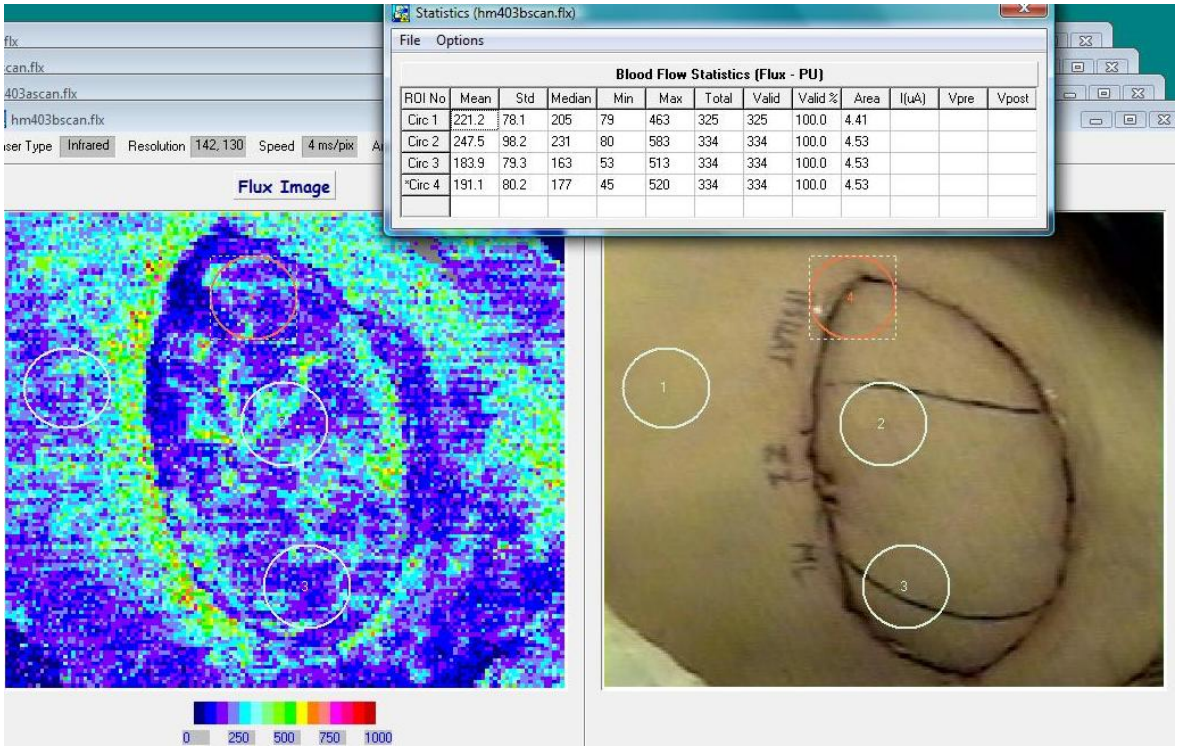

Figure 5-3 - Laser Doppler imaging of patient 4 from the side.
Placement of circles over zones (see flux image on left only), and baseline from patients abdomen.

The medians calculated for each of these areas were used in the subsequent statistical analysis of the data. Statistical packages used were GenStat and Minitab version 16.

5.3 Results

The patients had an average age of 49yrs (40 – 52 years old) and average BMI of 27 (21 to 30). The average operative time was 7 hours and 40 minutes and the average ischaemic time was 113 minutes (range 68 minutes - 155 minutes). Three patients had zone 4 of the DIEP flap remaining in the tissue for reconstruction at flap transfer. Patient 8 suffered from distal flap necrosis in zone 4 which was later debrided (Figure 5-4). There were no flap failures.

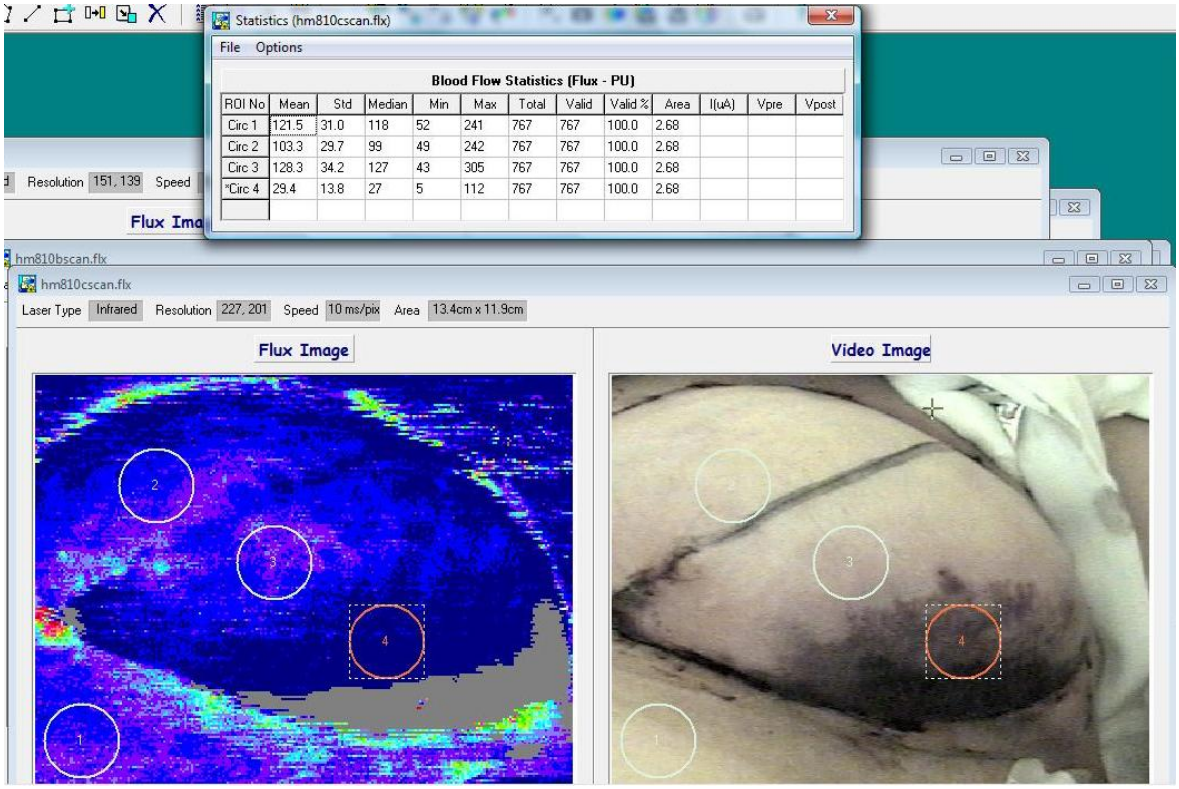

**Figure 5-4 - Patient 8, bruising laterally.
Scan at 72 hours post-operative.**

5.3.1 Data description

The number of measurements for each patient for each timepoint and angle of scanner (from above or from the side) are shown in the frequency distribution in Table 5-1. The number of measurements include a baseline measurement from the patients own skin plus up to four additional measurements for zones 1 - 4 of the inset DIEP flap.

Timepoint	Angle	Patient 1	2	3	4	5	6	7	8
Post-op	Above	4	4	4	4	4	0	4	3
	Side	0	0	0	4	5	3	0	0
Four hours	Above	4	4	4	3	4	3	4	4
	Side	0	0	4	3	4	3	0	4
Sixteen hours	Above	4	4	3	3	4	3	4	4
	Side	4	0	3	4	5	3	0	4
Twenty-four hours	Above	4	4	3	3	4	3	4	3
	Side	3	0	0	3	4	3	0	3
Forty-eight hours	Above	4	4	3	4	5	3	4	3
	Side	3	0	0	4	4	3	0	4
Seventy-two hours	Above	4	4	3	4	4	3	4	3
	Side	3	0	4	4	5	3	0	4

Table 5-1 - Frequency distribution of number of zone and base line measurements by patient, time-point and angle.

5.3.1.1 Perfusion by time point

The perfusion by time point is shown in Figure 5-5 and the summary statistics in Table 5-2.

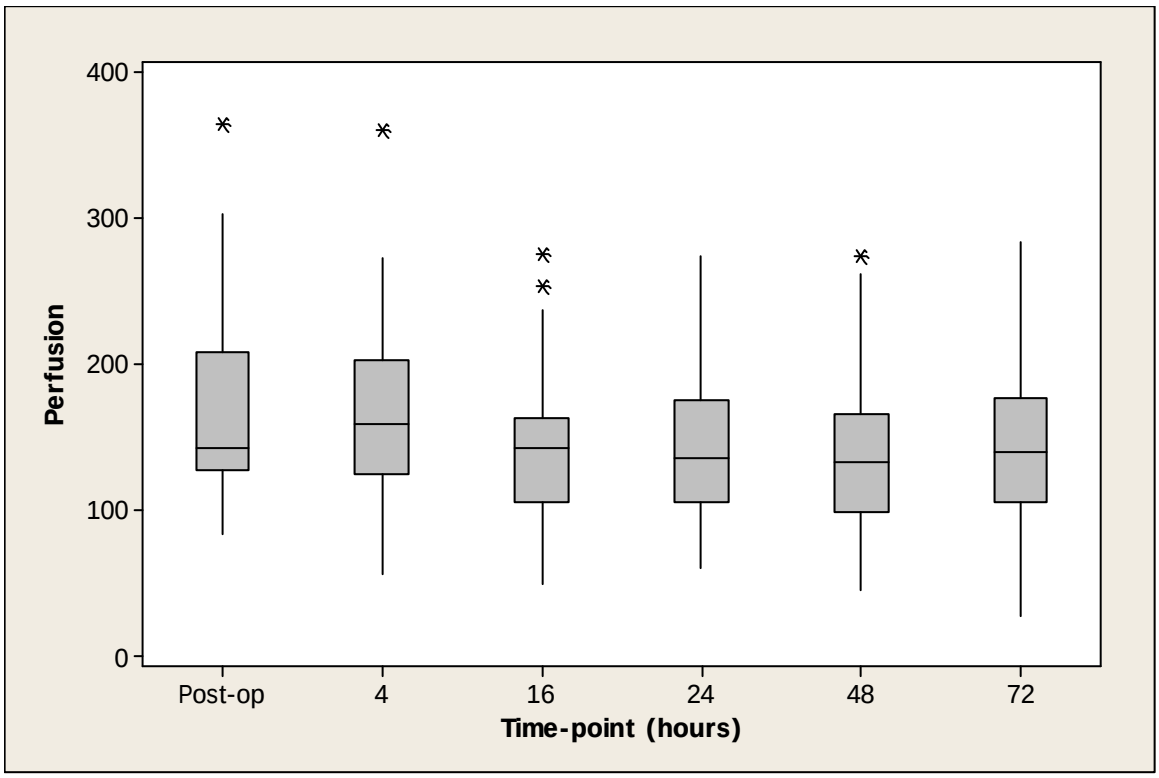

Figure 5-5 - Boxplots of perfusion by time point.

Variable	Time-point	N	N*	Mean	SE Mean	StDev	Minimum	Q1
Median	Post-op	39	0	169.3	10.1	62.8	84.0	128.0
	Four hours	48	0	164.88	8.55	59.21	56.00	124.50
	Sixteen hours	52	0	140.58	6.96	50.16	49.00	106.00
	Twenty-four hours	44	0	142.55	6.93	45.96	61.00	105.50
	Forty-eight hours	48	0	136.98	7.53	52.15	45.00	98.50
	Seventy-two hours	52	0	144.98	7.54	54.36	27.00	105.50

Variable	Time-point	Median	Q3	Maximum
Median	Post-op	143.0	208.0	364.0
	Four hours	158.50	202.75	360.00
	Sixteen hours	142.00	163.50	275.00
	Twenty-four hours	136.00	175.00	274.00
	Forty-eight hours	133.50	165.75	274.00
	Seventy-two hours	139.50	177.25	284.00

Table 5-2 - Summary statistics of perfusion (flux) by time point.

The mean perfusion decreases slightly from post operative values (169.3 units of flux) until 4 hours (164.9). At 16 hours the mean perfusion is lower (140.6), and remains at approximately this level at further time points. The mean exceeds the median at all time points which is consistent with the right skew of the distribution.

5.3.1.2Perfusion by zone

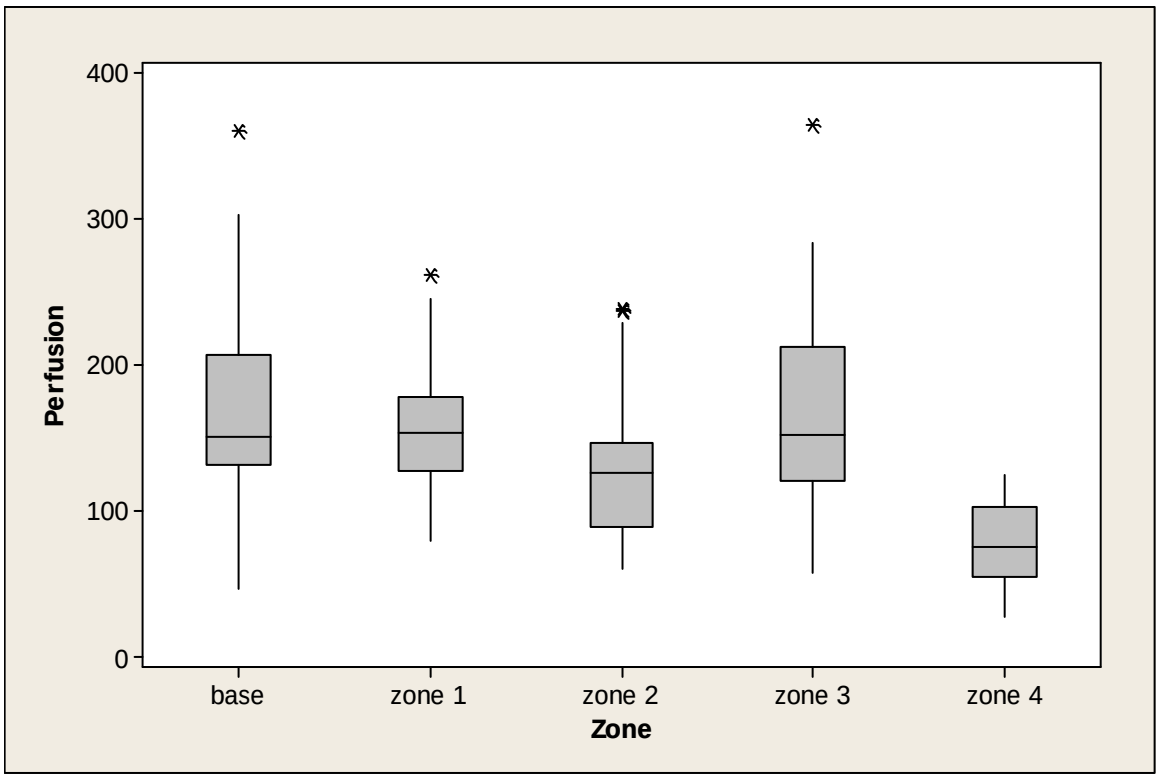

Figure 5-6 - Boxplots of perfusion by zone.

Variable	Zone	N	N*	Mean	SE Mean	StDev	Minimum	Q1	Median
Median	base	77	0	169.29	6.39	56.05	46.00	132.00	151.00
	zone 1	73	0	156.47	4.97	42.45	79.00	127.50	154.00
	zone 2	73	0	124.56	4.61	39.39	61.00	89.50	126.00
	zone 3	44	0	168.52	9.87	65.50	58.00	121.25	151.50
	zone 4	16	0	78.06	7.21	28.85	27.00	55.25	75.50

Variable	Zone	Q3	Maximum
Median	base	206.50	360.00
	zone 1	178.00	261.00
	zone 2	147.00	239.00
	zone 3	213.00	364.00
	zone 4	103.25	125.00

Table 5-3 - Summary statistics of perfusion by zone.

It can been seen from Figure 5-6 that zone 4 is the least well perfused. Zones 1 & 3 have the highest perfusion values and appear similarly well perfused.

5.3.1.3Perfusion by angle

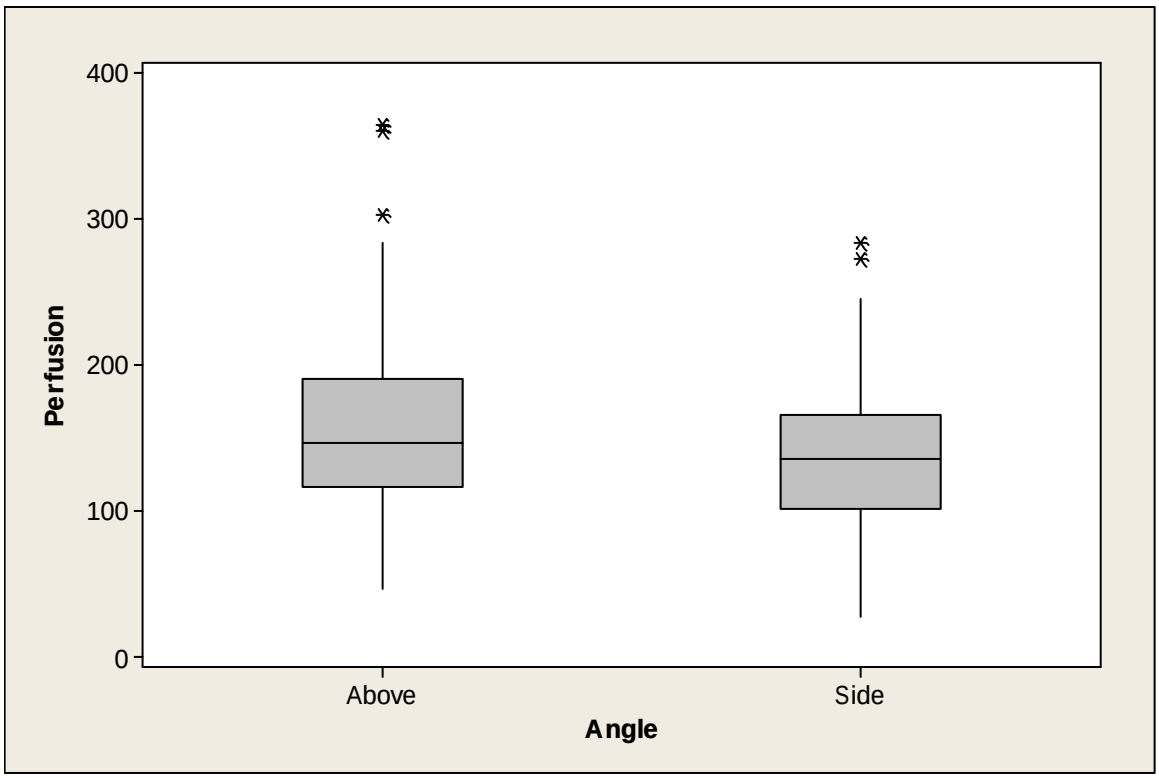

Figure 5-7 - Boxplots of perfusion by angle.

Variable	Angle	N	N*	Mean	SE Mean	StDev	Minimum	Q1	Median
Median	Above	169	0	157.42	4.45	57.79	46.00	116.50	147.00
	Side	114	0	136.93	4.53	48.35	27.00	101.75	135.50

Variable	Angle	Q3	Maximum
Median	Above	190.50	364.00
	Side	165.25	284.00

Table 5-4 - Summary statistics of perfusion by angle.

Figure 5-7 & Table 5-4 show the boxplots of perfusion by angle. 'Above' representing the laser Doppler scanner being placed above the patient, and 'Side' representing the laser Doppler positioned at 90 degrees from the above angle. Side measurements were included to incorporate the curvature of the breast reconstruction as not all of the flap skin could be imaged from above.

The perfusion observed from Above is higher, which is in keeping with zone 1 of the DIEP generally being the most medial area of the flap as the vessels are anastomosed to the internal mammary vessels.

It is also of note as per Table 5-1, there are not equal numbers of measurements for the side and above, nor at the different time points.

5.3.2 Statistical modelling of the data

To test the statistical significance of the effects of the factors timepoint, zone and angle, a linear model was fitted to the data. The method of residual maximum likelihood (REML) was used to fit the model[229]. The REML analysis was carried out on the log transformation (base 10) of the perfusion measure as examination of residual plots from a fit of the model to the perfusion measure showed that residual variability tended to increase with mean perfusion. Statistical significance of effects was assessed using approximate Wald tests provided by GenStat.

The model contains the following fixed effects; the main effects of timepoint (T), zone (Z), and angle (A); the two-factor interactions T.Z, T.A and Z.A; the three-factor interaction T.Z.A. A random factor 'patient' (P) was also included in the model to allow for correlations made on the same patient.

	Wald Test statistic (Approximate Chi-squared)	d.f.	P-value
Angle (A)	190.28	1	<0.001
A|Time-point (T)	193.96	1	<0.001
A|Zone (Z)	107.74	1	<0.001
A|Z+T	112.23	1	<0.001
A|Z+T+Z.T	70.78	1	<0.001
Z	115.63	4	<0.001
Z|A	33.09	4	<0.001
Z|T	113.18	4	<0.001
Z|A+T	31.44	4	<0.001
Z|A+T+A.T	31.15	4	<0.001
T	12.33	5	0.030
T|A	16.02	5	0.007
T|Z	9.88	5	0.079
T|A+Z	14.37	5	0.013
T|A+Z+A.Z	14.38	5	0.013
T.A|T+A	7.81	5	0.167
T.A|Z+A+T	7.52	5	0.185
T.A|Z+A+T+A.Z	7.30	5	0.199
T.A|Z+A+T+T.Z	7.33	5	0.197
T.A|Z+A+T+Z.T+Z.A	7.19	5	0.207
A.Z|A+Z	3.30	4	0.509
A.Z |A+Z+T	3.31	4	0.508
A.Z |A+Z+T+A.T	3.09	4	0.542
A.Z |A+Z+T+Z.T	2.87	4	0.580
A.Z |A+Z+T+A.T+Z.T	2.73	4	0.604
T.Z|T+Z	62.23	20	<0.001
T.Z|T+A+Z	20.77	20	0.410
T.Z|T+A+Z+Z.A	20.34	20	0.437
T.Z|T+A+Z+A.T	20.59	20	0.422
T.Z|T+A+Z+Z.A+A.T	20.23	20	0.444
T.A.Z|T+A+Z+Z.A+Z.T+A.T	27.54	17	0.051

Table 5-5 - Wald tests of main effects and interactions.

The main effect of angle (A) is statistically significant ($p<0.001$) regardless of which other terms are present. The main effect of zone (Z) is also statistically significant ($p<0.001$) regardless of which other terms are used.

The main effect of timepoint (T) is statistically significant except when allowance is made for the effect of zone only ($p=0.079$). However, when angle is also allowed for, the main effect of timepoint regains its significance.

Neither of the two-factor interactions T.A, A.Z were statistically significant.

The interaction T.Z was statistically significant ($p<0.001$) allowing for the sum of the main effects only (T+Z). If the allowance is additionally made for the angle, the interaction loses its significance.

The thee-factor interaction T.A.Z just fails to reach statistical significance ($p=0.051$).

5.3.2.1Model of data

Wald and F-tests for the model are shown in Table 5-6.

The first set of p-values is for sequential tests i.e. zone without adjustment for angle or timepoint, timepoint allowing for zone, & angle allowing for zone and timepoint.

The second set of p-values are for tests of individual terms, adjusted for both of the other two terms. The difference between zones in mean perfusion (log scale base 10) are statistically significant ($p<0.001$), adjusted for the effects of timepoint and angle. Similarly the difference between time points is significant ($p=0.032$) and the difference between angle is significant ($p=0.045$).

Sequentially adding terms to fixed model

Fixed term	Wald statistic	n.d.f.*	F statistic	d.d.f.*	F pr
Zone	40.69	4	10.17	21.8	<0.001
Time_point	13.14	5	2.63	34.1	0.041
Angle	12.01	1	12.01	2.8	0.045

Dropping individual terms from full fixed model

Fixed term	Wald statistic	n.d.f.	F statistic	d.d.f.	F pr
Zone	31.97	4	7.99	21.8	<0.001
Time_point	13.96	5	2.79	34.1	0.032
Angle	12.01	1	12.01	2.8	0.045

Table 5-6 - Wald tests and approximate F-tests for model with no interactions between fixed-effect factors.

5.3.2.2 Predicted means for timepoint

A table for the predicted mean perfusion log scale (base 10) by timepoint is shown in Table 5-7. The standard errors of differences between pairs are shown in the lower triangular matrix.

Time_point	
Post-op	2.129
Four hours	2.139
Sixteen hours	2.077
Twenty-four hours	2.070
Forty-eight hours	2.050
Seventy-two hours	2.082

Standard errors of differences between pairs

Time_point Post-op	1	*				
Time_point Four hours	2	0.030	*			
Time_point Sixteen hours	3	0.030	0.029	*		
Time_point Twenty-four hours	4	0.030	0.030	0.029	*	
Time_point Forty-eight hours	5	0.030	0.029	0.029	0.029	*
Time_point Seventy-two hours	6	0.029	0.029	0.029	0.029	0.029
		1	2	3	4	5

Time_point Seventy-two hours	6	*	
		6	

Table 5-7 - Predicted mean perfusion (log scale base 10) by timepoint.

Comparing each of the time differences gives a significant drop in perfusion between 4 hours and 16 hours post-operatively (p=0.046). None of the other sequential time differences are significant (post-op to 4 hours, p=0.74, 16 hours to 24 hours p=0.82, 24 hours to 48 hours p=0.50, 48 hours to 72 hours p=0.28). There is no significance between the post-operative perfusion and the perfusion at 72 hours (p=0.11).

The anti-logged predicted mean perfusion by timepoint is shown below, Table 5-8.

Post-op	4 hours	16 hours	24 hours	48 hours	72 hours
134.586	137.721	119.399	117.490	112.202	120.781

Table 5-8 - Anti-logged predicted mean perfusion by timepoint.

5.3.2.3Predicted means for zone

Table 5-9 below shows the predicted mean perfusion on the log scale (base 10) by zone. These predictions are adjusted for the effects of timepoint and angle. The standard errors of differences between pairs are in the lower triangular matrix.

Zonebase	zone 1	zone 2	zone 3	zone 4
2.197	2.158	2.077	2.127	1.896

Standard errors of differences between pairs

Zone base	1	*				
Zone zone 1	2	0.038	*			
Zone zone 2	3	0.038	0.038	*		
Zone zone 3	4	0.043	0.044	0.043	*	
Zone zone 4	5	0.057	0.057	0.057	0.061	*
		1	2	3	4	5

Table 5-9 - Predicted mean perfusion (log scale base 10) by zone

There is a significant difference in perfusion between zone 1 and zone 2 ($p=0.045$), and between zones 1 and 4 ($p<0.001$), 2 and 4 ($p=0.004$), and 3 and 4 ($p=0.001$).

The anti-logged predicted mean perfusion by zone is shown in Table 5-10 below.

Base	1	2	3	4
157.398	143.880	119.399	133.968	78.7046

Table 5-10 - Anti-logged predicted mean perfusion by zone.

5.3.2.4Predicted means for angle

AngleAbove	Side
2.112	2.070

Standard errors of differences between pairs

Angle Above	1	*	
Angle Side	2	0.012	*
		1	2

Table 5-11 - Predicted mean perfusion (log scale base 10) by angle.

The difference between above and side angles is significant (p=0.046) as expected from the approximate F-test in Table 5-6. The anti-logged predicted mean perfusion by angle is shown in Table 5-12 below.

Above	Side
129.419	117.489

Table 5-12 - Anti-logged predicted means by angle.

5.3.3 Data separated by Angle, above or side

As the Angle was significant, the data were separated into data obtained from above and from the side. Two separate analyses were carried out, one for each angle, and the effects of time point and zone investigated.

The effects of angle are significant as shown by the F-test in Table 5-6 and the t-test (p=0.046), and cannot be further examined by carrying out separate analyses. Further analyses are to compare the interaction between time point and zone from the different angles.

Additionally the perfusion was normalised against the 'base' perfusion, with each of the perfusions for zones 1 to 4 being expressed as a percentage of the base perfusion at the same time point. This was to determine whether the perfusion of the DIEP flap was varying from the patients' own perfusion (base measurements taken from patients' in situ skin rather than flap skin, as described previously), as an attempt to control for factors such as the effects of anaesthetic agents wearing off, hydration, temperature and analgesia of the patient at a particular time point.

5.3.3.1Data description from above, including normalised data

The boxplots in Figure 5-8 and Figure 5-9 (normalized data) display the data by time point and zone. Perfusion for the base appears on average to be greater than that in zone 1, and zone 1 perfusion appears greater than zone 2. The perfusion in zone 3 appears to be similar to the base, but the variability is greater. There were fewer measurements for zone 4 and these appeared to be lower than the other zones and the baseline skin perfusion. In the normalised boxplot similarly, the perfusion in zones 1 & 3 are higher than zone 2, which in turn is higher than zone 4.

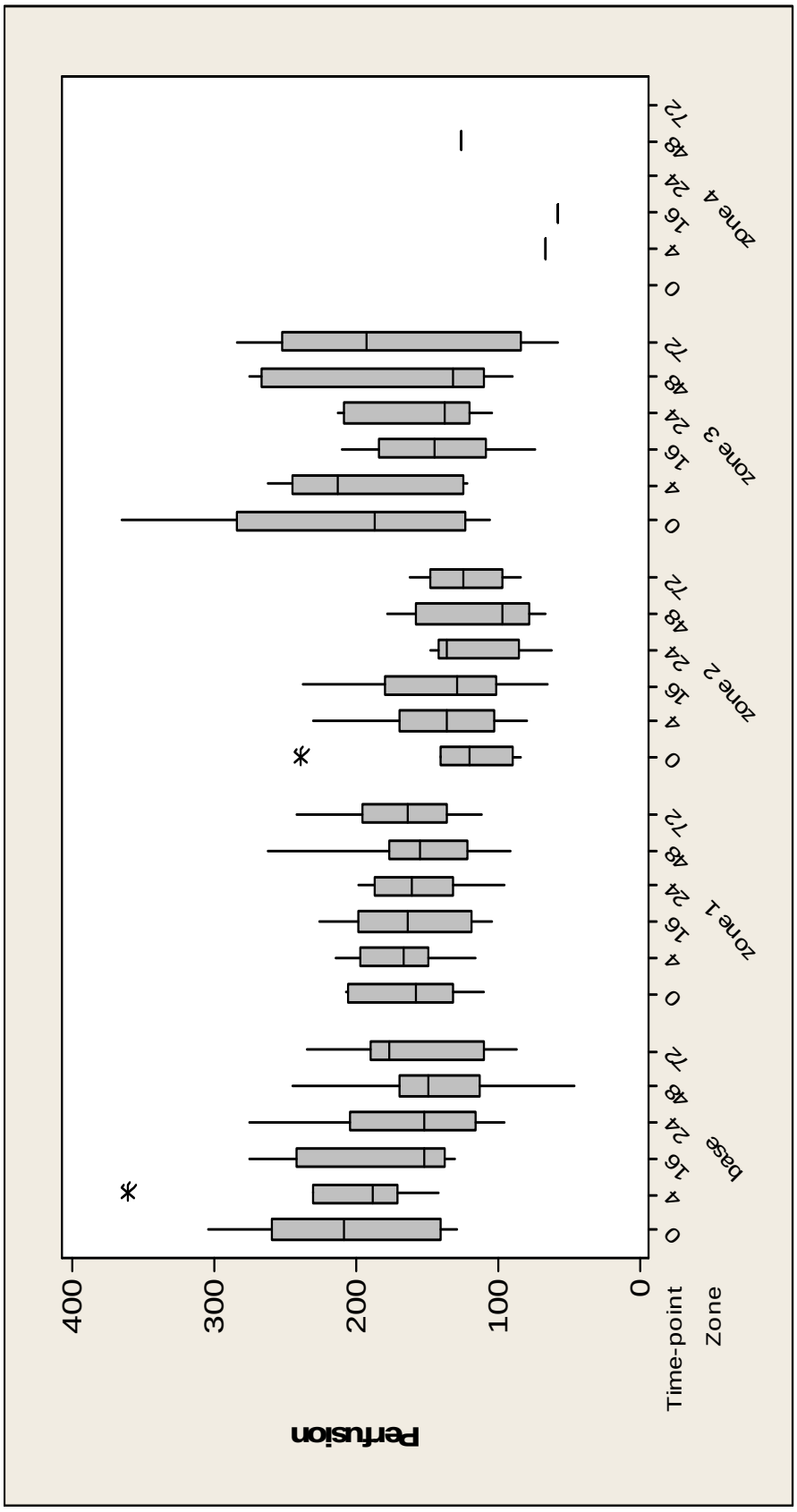

Figure 5-8 - Perfusion by time point and zone, from above.

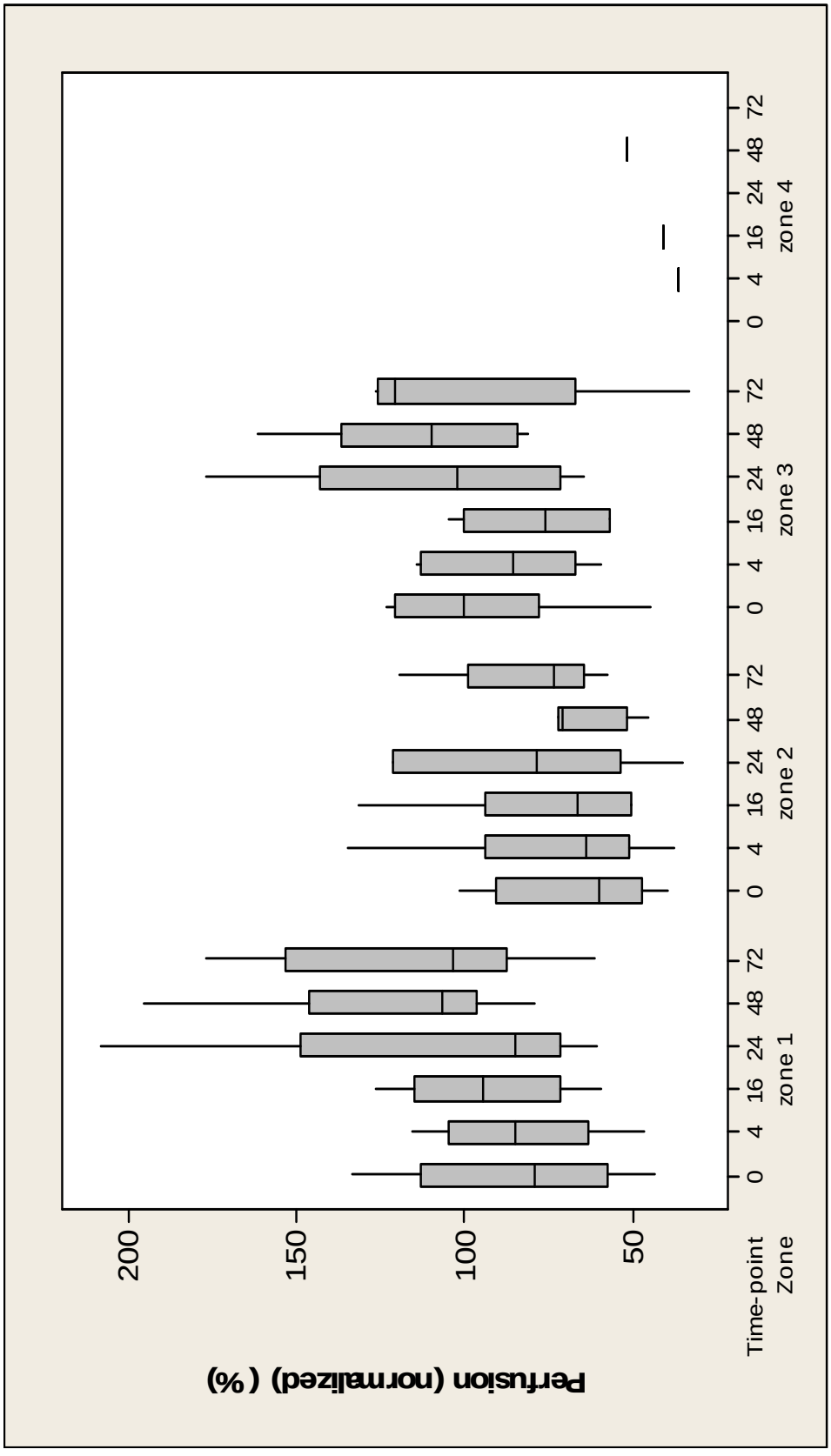

Figure 5-9 - Perfusion as a percentage of 'base', by time point and by zone, from above. (Single outlier, zone 2, 48 hours, 387% not shown.)

The median perfusions, Figure 5-10 & Table 5-13, shown below show that for the base measurement (i.e. the patients' own skin and state of perfusion) the

perfusion declines between post-operatively and 16 hours post-operatively, and then remains flat until 48 hours, returning at 72 hours to a value between the 16 hour value and the four hour value. Zones 1 & 2 show a flatter time profile than the base measurement, apart from a dip at 48 hours in the zone 2 perfusion. Zone 3 perfusion does not differ greatly from the base and there is a peak at four hours.

	Post-op	Four hours	Sixteen hours	Twenty-four hours	Forty-eight hours	Seventy-two hours	All
base	208.0 7	187.0 7	151.5 8	151.5 8	149.0 8	176.5 8	172.5 46
zone 1	158.0 7	166.0 7	163.0 8	159.5 8	155.0 8	163.0 8	163.0 46
zone 2	119.0 7	135.0 6	128.0 7	135.0 7	96.0 8	123.5 8	119.0 43
zone 3	186.0 6	213.0 5	144.0 5	137.0 5	131.0 5	192.0 5	144.0 31
zone 4	* 0	66.0 1	58.0 1	* 0	125.0 1	* 0	66.0 3
All	141.0 27	168.0 26	151.0 29	138.5 28	132.5 30	150.0 29	147.0 169

Table 5-13 - Median perfusion by zone and time point, from above.

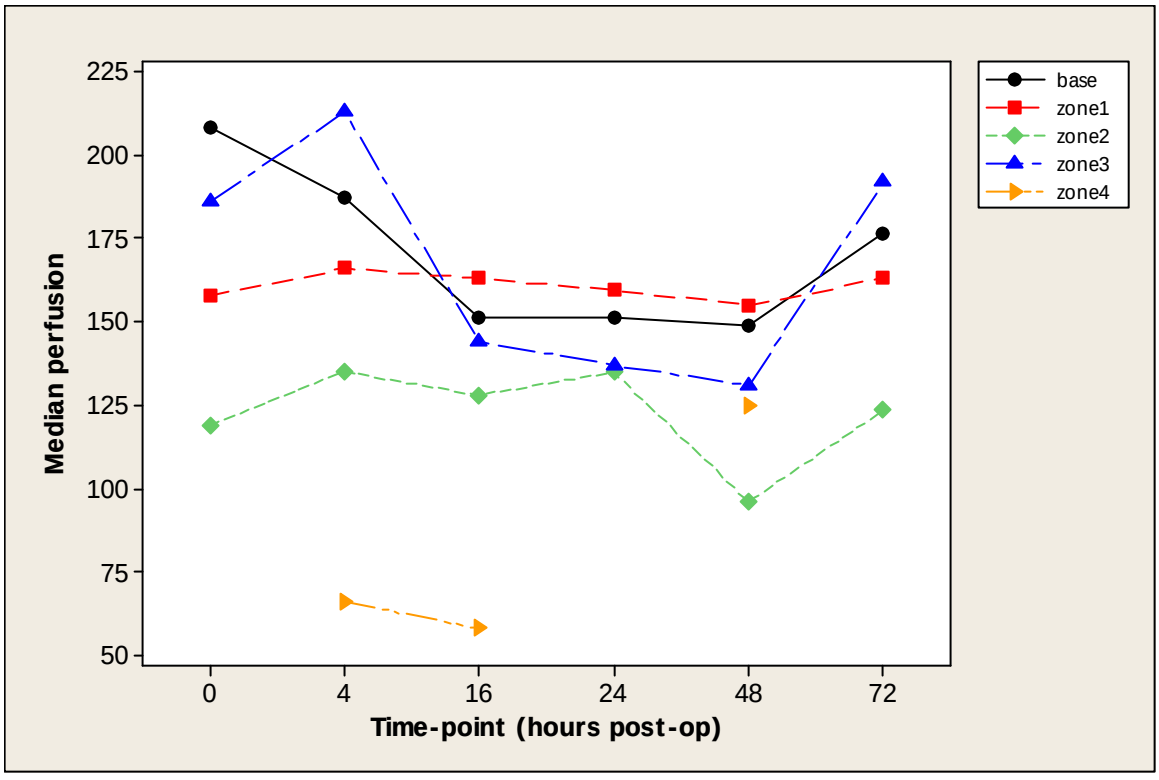

Figure 5-10 - Median perfusion by time point and zone, image from above.

Table 5-14 and Figure 5-11 below display the data relative to the patients baseline as before. In comparison with Figure 5-10 above it can be noted that zone 1 has a relative increase in perfusion at 16 hours, and zone 3 has a dip at this time. Zone 2 appears to peak at 24 hours. Overall the perfusion at 72 hours is greater than immediately post-operatively.

	Post-op	Four hours	Sixteen hours	Twenty-four hours	Forty-eight hours	Seventy-two hours	All
zone 1	79.157	84.657	94.608	85.088	106.318	103.338	96.5446
zone 2	60.007	63.726	66.457	78.497	70.558	73.468	68.0643
zone 3	100.366	85.215	76.005	102.295	110.085	120.945	100.5231
Zone 4	* 0	36.071	40.851	* 0	51.231	* 0	40.853
All	84.1720	79.6819	76.0021	85.0820	90.4022	100.5221	85.21123

Table 5-14 - Median perfusion (number of measurements) by zone and time point, from above. Normalized against baseline.

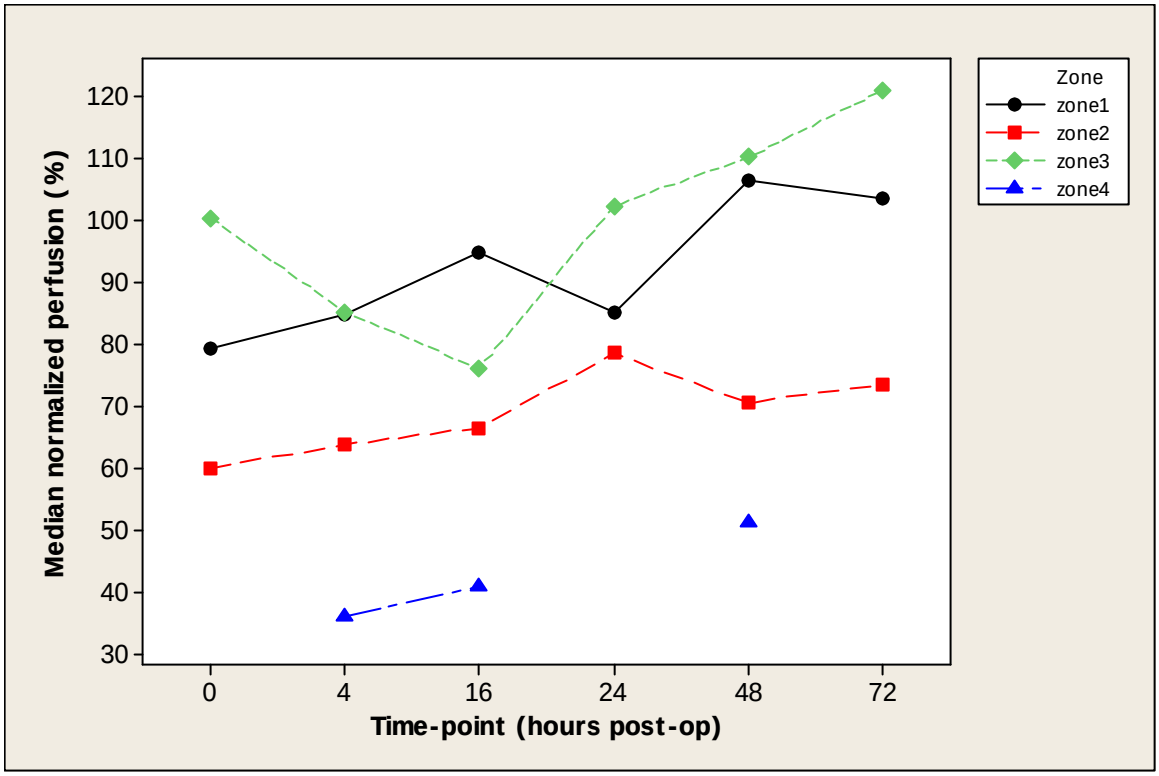

Figure 5-11 - Median perfusion by time point and zone, image from above. Normalized against baseline.

5.3.3.2Statistical modelling, image data from above

A REML model was fitted to log base 10, and the fixed effects were zone, time point, and their interaction. The results of fixed effects are shown in Table 5-15 below.

	F-test statistic	Numerator d.f.	Denominator d.f.	P-value
Zone (Z)	5.10	4	22.3	0.005
Z|Timepoint (T)	4.99	4	22.3	0.005
T	2.91	5	31.4	0.028
T|Z	2.82	5	31.4	0.032
T.Z|T+Z	0.95	17	89.9	0.520

Table 5-15 - Approximate F-tests to two main effects and their interaction. Imaging from above.

The interaction between zone and time point (T.Z) is not statistically significant (p=0.520). This implies that the differences between the zones and the base are not statistically significant, and that the time profiles run in parallel.

A model is including the only two main effects is shown in Table 5-16 below. The p-value for the effect of time point adjusted for zone (p=0.038) and the effect of zone adjusted for time point (p=0.004), are both significant.

Sequentially adding terms to fixed model

Fixed term	Wald statistic	n.d.f.	F statistic	d.d.f.	F pr
Timepoint	13.96	5	2.79	32.4	0.033
Zone	20.95	4	5.23	23.4	0.004

Dropping individual terms from full fixed model

Fixed term	Wald statistic	n.d.f.	F statistic	d.d.f.	F pr
Timepoint	13.54	5	2.71	32.4	0.038
Zone	20.95	4	5.23	23.4	0.004

Table 5-16 - Approximate F-tests for model with no interaction between zone and timepoint.

The predicted mean perfusions (log base 10 scale) by zone and by time point, when imaged from above has been used to calculate significance levels between zones and between time points.

The using predicted mean perfusions on 32.4 d.f. there is no significant difference between sequential post-operative time points, but there is a significant decrease from the immediate post-operative period to 24 hours

(p=0.03), which further decreases to 48 hours (p=0.006, from post-op value). This increases again to 72 hours when there is no difference between this time point and the perfusion immediately post-operatively, as previously with the entire data set.

The anti-logged predicted mean perfusion by time point (from above) are in Table 5-17 below.

Post-op	4	16	24	48	72
143.5	142.2	128.8	120.8	114.8	126.6

Table 5-17 - Anti-logged predicted mean perfusion by time point, from above.

The predicted mean perfusions for the zones (log base 10 scale, d.f.=23.4) show that perfusion is greatest in the base, followed by zone 1, zone 3, zone 2 and zone 4 sequentially. There is no significant difference between the base and zone 1, nor between zone 1 and 3, nor between zones 2 & 3, nor between zones 2 and 4. The difference in perfusion between zones 1 & 2 is significant (p=0.014) and between zones 3 & 4 (p=0.010). The anti-logged predicted mean perfusions per zone are shown below.

Base	Zone 1	Zone 2	Zone 3	Zone 4
165.6	158.1	118.6	147.9	77.8

Table 5-18 - Anti-logged predicted mean perfusion by zone, from above.

5.3.3.3 Data description from the side, including normalized data

The boxplots in Figure 5-12 and Figure 5-13 (normalized data) display the data by time point and zone. Perfusion for the base appears to be not very dissimilar from that in zone 1. Perfusion in zone 1 and base appears greater than the perfusion in zone 2. Zone 3 has some large fluctuations. There are few measurements for zone 4. In the normalized data the perfusion in zone 1 looks greater than in zone 2, zone 3 is again very variable and zone 4 has the lowest perfusion but few measurements.

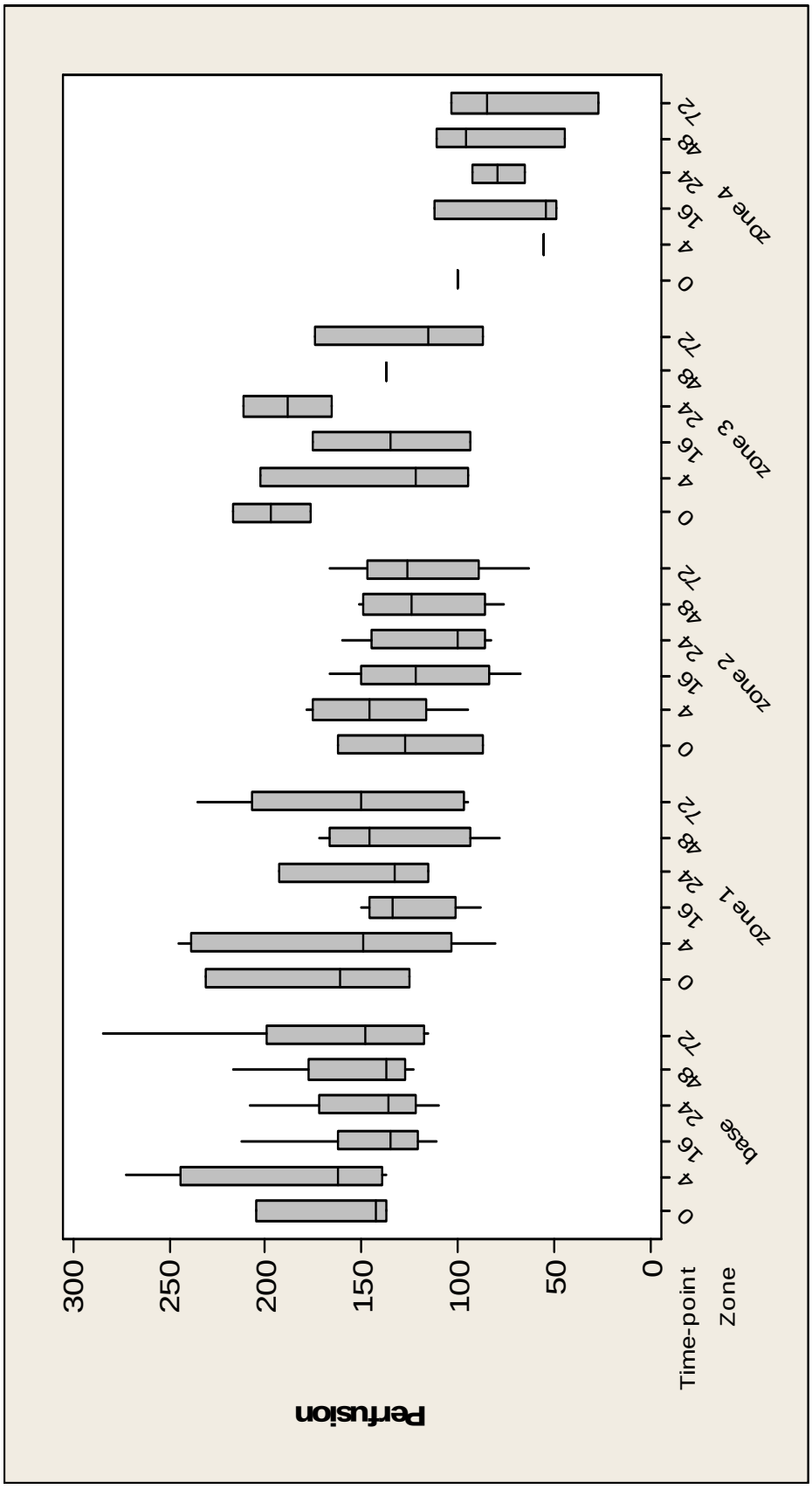

Figure 5-12 - Perfusion by time point and zone, from side.

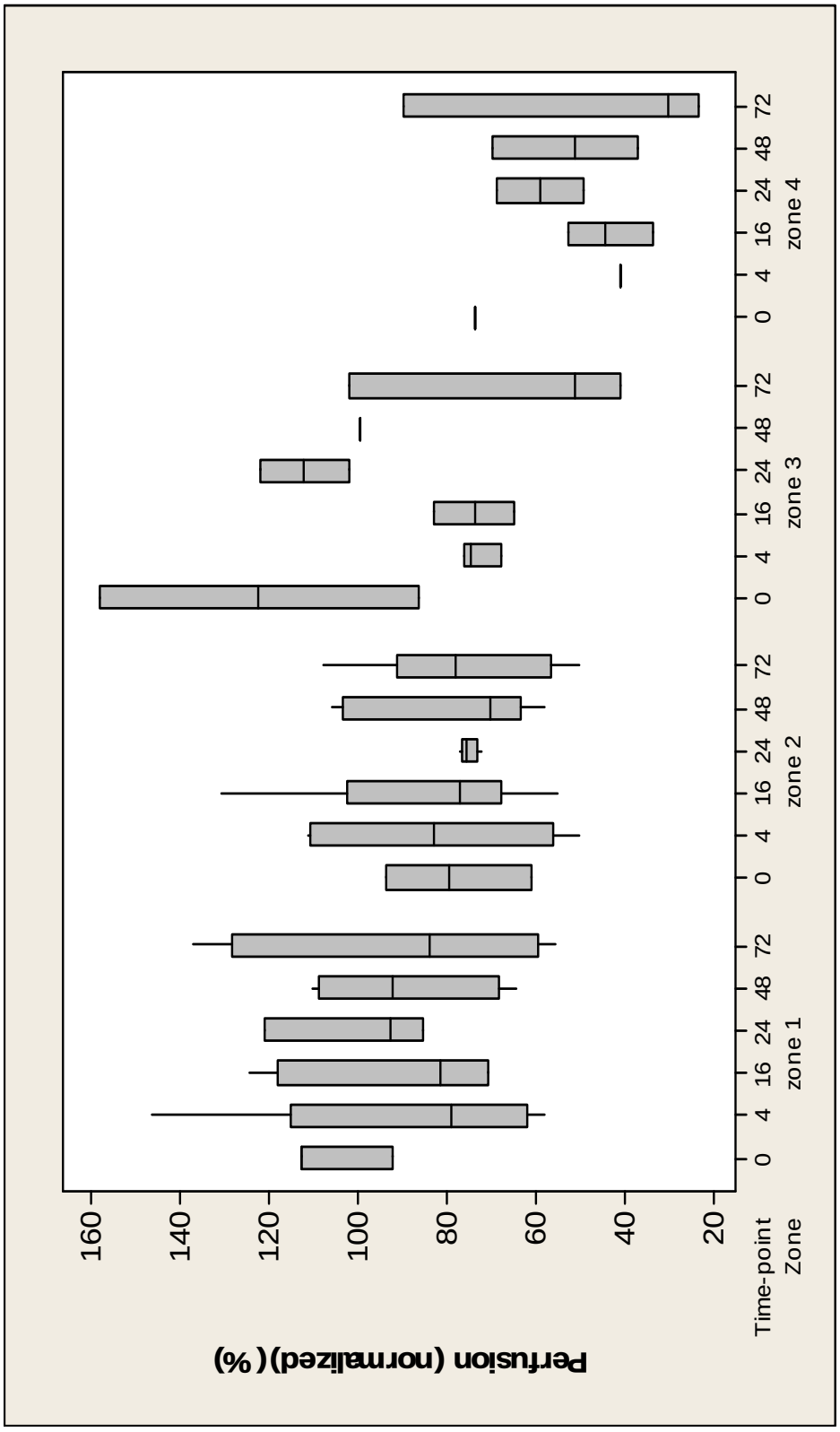

Figure 5-13 - Perfusion as a percentage of 'base', by time point and by zone, from side.

Table 5-19 and Figure 5-14 display the median perfusion by zone and time point (from the side). The baseline measurement increases between post-operatively and 4 hours, then decreases at 16 hours to a point slightly less than the immediate post-operative value, and then remains relatively constant until it is at a value slightly above the post-operative value at 72 hours. The perfusion in

zone 1 follows that of the base, and in zone 2 the perfusion is slightly lower with a peak at 4 hours and a dip at 24 hours. Zone 3 is very variable between time points, and zone 4 appears lower than the other zones.

	Post-op	Four hours	Sixteen hours	Twenty-four hours	Forty-eight hours	Seventy-two hours	All
base	143.0 3	163.0 6	135.0 6	136.0 5	138.0 5	148.5 6	139.0 31
zone 1	161.0 3	149.5 6	134.0 6	133.0 3	146.5 4	151.0 5	140.0 27
zone 2	128.0 3	146.0 6	122.5 6	100.0 4	124.0 5	126.5 6	126.5 30
zone 3	197.0 2	122.0 3	135.0 2	189.0 2	138.0 1	116.0 3	166.0 13
zone 4	101.0 1	56.0 1	55.0 3	79.5 2	96.0 3	85.0 3	85.0 13
All	152.0 12	147.5 22	125.0 23	134.0 16	135.5 18	126.0 23	135.5 114

Table 5-19 - Median perfusion by zone and time point from side.

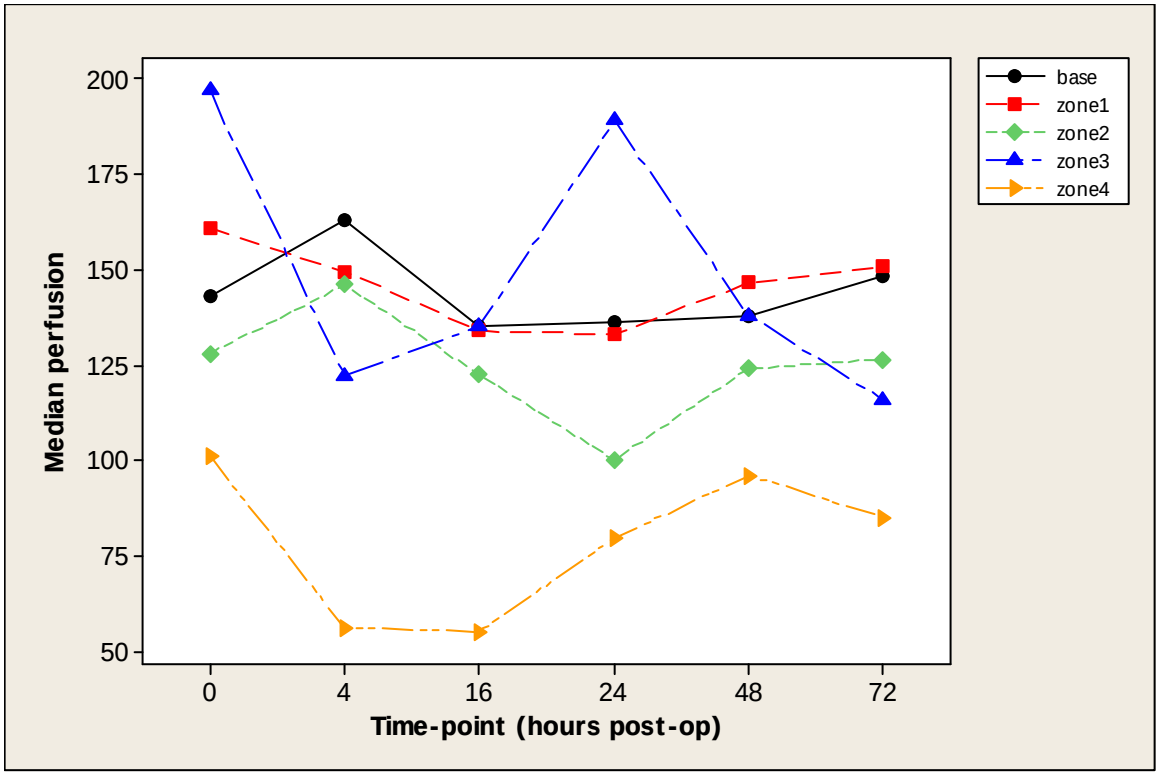

Figure 5-14 - Median perfusion by time point and zone, image from side.

Table 5-20 and Figure 5-15 below display the data relative to the patients baseline. In comparison with Figure 5-14 zones 1, 2 and 4 follow a relatively

similar time course with an initial, a plateau, an increase to 24 hours and then a further decrease. The perfusion in zone 2 is comparatively flat.

	Post-op	Four hours	Sixteen hours	Twenty-four hours	Forty-eight hours	Seventy-two hours	All
Zone 1	112.59 3	78.69 6	81.13 6	92.79 3	92.26 4	83.90 5	89.66 27
Zone 2	79.51 3	82.65 6	76.79 6	75.51 4	70.05 5	77.86 6	75.51 30
Zone 3	122.37 2	74.36 3	73.73 2	111.99 2	99.28 1	50.88 3	82.63 13
Zone 4	73.72 1	40.88 1	44.00 3	58.64 2	51.15 3	29.93 3	48.89 13
All	91.97 9	75.28 16	72.60 17	76.92 11	70.05 13	73.26 17	75.78 83

Table 5-20 - Median perfusion by zone and time point from side. Normalized against baseline.

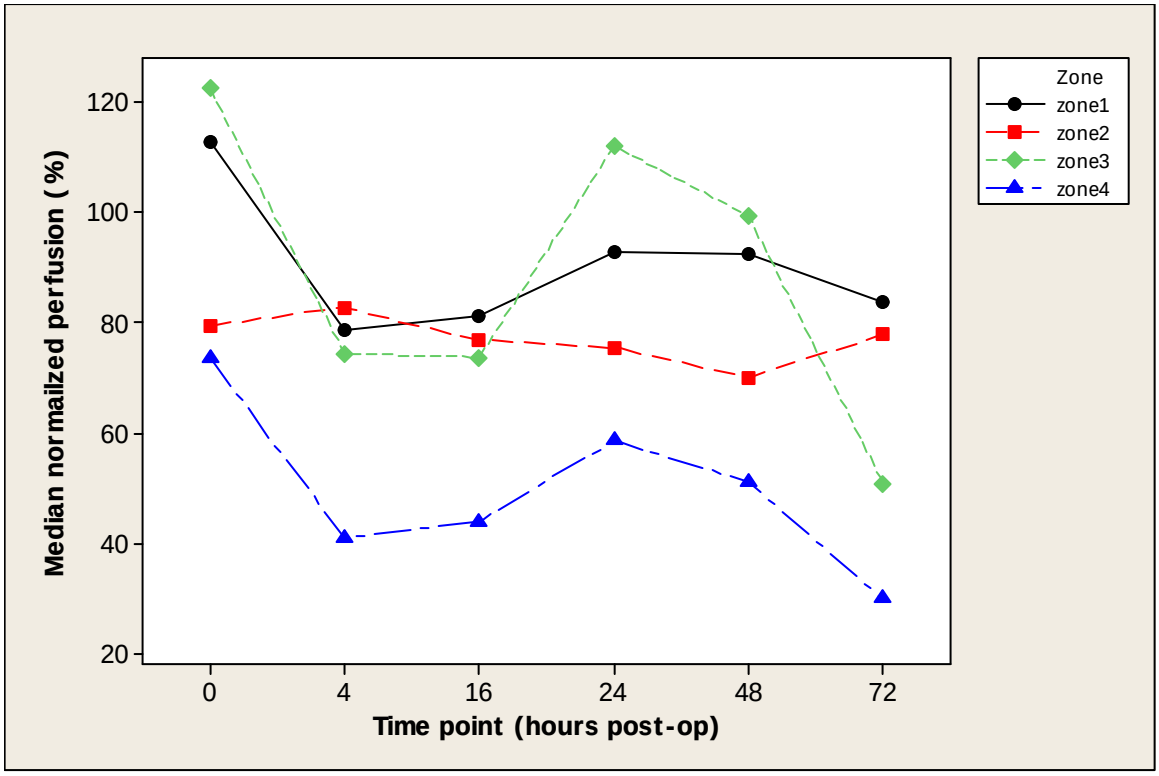

Figure 5-15 - Median perfusion by time point and zone, image from side. Normalized against baseline.

5.3.3.4 Statistical modelling, image data from the side

As for the data imaged from above, two separate REML models were fitted to the log base 10 model. The fixed effects were zone, time point and their interaction. The results of the fixed effects are in Table 5-21 below.

	F-test statistic	Numerator d.f.	Denominator d.f.	P-value
Zone (Z)	6.30	4	15.5	0.003
Z|Timepoint (T)	6.13	4	15.5	0.004
T	2.04	5	18.3	0.120
T|Z	1.91	5	18.3	0.141
T.Z|T+Z	0.78	20	49.8	0.720

Table 5-21 - Approximate F-tests of main effects and interactions

The interaction between zone and time point is not statistically significant (p=0.720). This implies that differences in the shape of the time profiles of log (base 10) perfusion between zones, and importantly between zones and the base, are not statistically significant.

Differences between mean log-perfusion at the various time points are not statistically significant.

Differences between mean log-perfusion at the various zones are statistically significant regardless of whether time points are allowed for (p=0.003, p=0.004).

A model is obtained therefore including only the main effects of zone. Table 5-22 shows the results of an approximate F-test for this model.

Tests for fixed effects

Sequentially adding terms to fixed model

Fixed term	Wald statistic	n.d.f.	F statistic	d.d.f.	F pr
Zone	25.40	4	6.35	16.6	0.003

Dropping individual terms from full fixed model

Fixed term	Wald statistic	n.d.f.	F statistic	d.d.f.	F pr
Zone	25.40	4	6.35	16.6	0.003

Table 5-22 - Approximate F-test for model with only the main effect of zone.

Using predicted mean perfusions and 16.6 d.f., there is no difference between the base and zone 1, zone 1 and zone 2, zone 1 and 3,and zone 2 and zone 3. There is a significant difference decrease between zone 3 and 4 (p=0.01). The anti-logged predicted mean perfusions per zone (from the side) are shown in Table 5-23 below.

Base	Zone 1	Zone 2	Zone 3	Zone 4
149.6	129.4	121.9	118.9	74.1

Table 5-23 - Anti-logged predicted mean perfusion by zone (side).

5.4 Conclusion

The original analysis using the whole data set shows that angle, time and zone are all independently significant.

The interaction between time and zone was statistically significant ($p<0.001$) allowing for the sum of main effects only (T+Z). This loses significance if an allowance is made for the angle.

The three-factor interaction T.A.Z. just fails to reach statistical significance ($p=0.051$).

There is therefore no evidence that there is a difference between the zones with time - it would appear that the zones and baseline move in parallel.

When the data are divided by whether the laser Doppler images were recorded from above the patient or from the side of the patient, the interaction between zone and time point is again not statistically significant from above ($p=0.52$) or from the side ($p=0.72$), although the power has been reduced. Normalizing the data against the baseline however reveals in the image recordings from above, a departure from a parallel course in zone 3 (see Figure 5-11 & below). Zones 1, 2 and 4 have increasing trend in perfusion post-operatively, where as zone 3 decreases to 16 hours followed by an increase. This contradicts the non-significant results in the original analysis ($p=0.051$), and it should therefore be noted that the results approach significance.

As a pilot study for designing the microdialysis study in DIEP flaps (see Chapter 7), this study has revealed changes in perfusion across the zones over a 72 hour time period, but has not identified a specific time period where changes take place nor statistical significance of these changes.

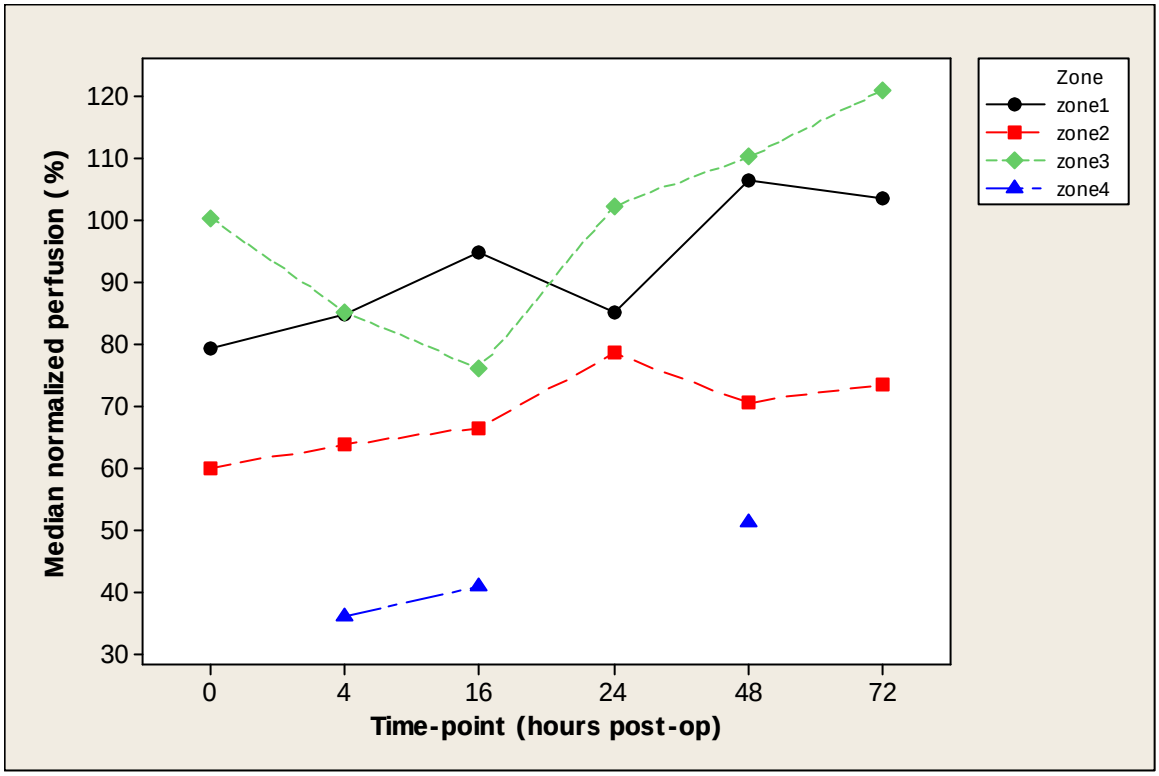

Figure 5-16 - Median perfusion by time point and zone, normalized against baseline and image from above.
As before, Figure 5-11.

5.5 Discussion

Laser Doppler flowmetry has been used in the study of the microcirculation since its first application in 1975[50;230]. Laser Doppler flowmetry and laser Doppler imaging both work by the Doppler effect with a frequency shift in the backscattered light, following illumination of the tissue by laser light. The flux value calculated is a linear function of the average velocity of moving cells. Flowmetry, where a probe is attached to the skin, has been widely used in flap monitoring[181;183;185;186;192;231-239], with the technique being to observe the trends in flux rather than the absolute flux . It continuously records the state of perfusion. Laser Doppler imaging or scanning provides a two-dimensional image which is built by the laser beam scanning a set area. This is more useful in comparing areas at a point in time, for example the zones of a flap, and this application of laser Doppler is a valuable adjunct in the early assessment of burns[240-242].

This study was designed to look at the pattern in perfusion across the flap in the first 72 hours post-operatively, during the period when choke vessels between

angiosomes are believed to dilate[2;31]. There was a trend towards significance with the interaction between zone, time point and angle just failing to reach significance (p=0.051). The pattern in zone 3 appears to decrease to a point 16 hours post-operatively before beginning to increase in perfusion. Zones 1, 2 and 4 show a more gradual increase in perfusion. Due to the uncontrollable confounding factors such as the post-operative effects of anaesthetic, fluid balance, medication, nutrition, anxiety and pain, and the patient's position and activity, the values for each zone were normalized against a baseline of the patient's abdominal skin away from the wound sites, to take into account the patient's overall state of perfusion at the time of measurement.

A study in 2006 by Figus et al monitored the laser Doppler flowmetry readings and light reflectance spectrophotometry (LRS) readings for a post-operative period of 48 hours[189]. Laser Doppler readings showed an increase in flow post-operatively, with variable readings. An overall difference in trend was noticed, with an increased flux in the group with no complications (n=10) compared with patients who later suffered from fat necrosis or required surgical re-exploration (n=6). Light reflectance spectrophotometry transmits a light into the skin and the backscattered light spectrum depends upon the haemoglobin absorption. There was an initial fall in oxygenation for the first hour post-operatively followed by a steady rise, reaching pre-operative values at around 12 to 16 hours post-operatively. The pattern of light reflectance spectrophotometry follows the laser Doppler perfusion pattern seen in zone 3 in our study, with an initial decrease in perfusion before a steady increase after 16 hours(Figure 5-11, zones Figure 5-1). It is not clear why zone 2 in our study followed the increasing perfusion pattern of zone 1, yet zone 3 had an initial decline, especially as many authors believe zone 3 to have better perfusion than zone 2[227;243-246], as discussed in Chapter 6.

A study of 16 DIEP flaps and 4 SIEA (superficial Inferior Epigastric Artery) flaps by de Weerd et al in 2008 used dynamic infrared thermography (DIRT)[247]. DIRT is a non-invasive technique based on infra-red imaging that the authors report has a good correlation with laser Doppler. Measurements were taken on the first, third and sixth post-operative days, revealing a hyperaemia on day 1, especially in zone 1. This hyperaemia subsided between days 3 and 6. The authors also noted that Hartrampf zone 3 was better perfused than zone 2, and this is

discussed further in Chapter 6. The pattern of perfusion described by these authors with an initial hyperaemia is that seen in our post operative study in zones 1, 2 and 4, and is also the overall pattern of zone 3, despite the initial decrease, in the first day. The authors discuss Dhar's study of delay phenomenon[31], and the most dramatic time of opening of choke vessels as being between 48 hours and 72 hours, but they do not offer thoughts on the timing of this in relation to their own findings, other than illustrating choke vessel opening and concluding that there is a stepwise progression of perfusion during the first post-operative week.

Studies have also shown a long term increase in perfusion from the immediate post-operative period. A study in 2008 by Figus et al compared three time points of perfusion in 26 DIEP patients, pre-operatively (6 hours of monitoring), the first 48 hours post-operatively, and at 3 months (3 hours)[248]. There was a statistically significant increase in perfusion between each of the three time points, although the value for each time point was an average over the time monitored and therefore is not comparable with our study. Similarly Heitland et al found that DIEP flap perfusion had increased by 13%, using Doppler ultrasound, at 18 months post-operatively[249].

Our study has shown increasing perfusion in the first 72 hours post-operatively. Between 16 and 48 hours there are multiple changes in the gradient of the perfusion in each of the zones. This may or may not be related to dilatation of vessels and opening of choke vessels. As a pilot study prior to the use of research microdialysis catheters this study has clarified that there are changes in perfusion during the first 3 days, and changes between individual zones. Chapter 7 uses the method of high cut-off microdialysis catheters in DIEP flaps over the same period to investigate possible changes in tissue cytokines.

6 A comparison of the perfusion territory of the Deep versus Superficial Inferior Epigastric system

6.1 Introduction

6.1.1 Background

Flaps taken from the lower abdomen for reconstruction have evolved over the years to minimise morbidity from the donor site. Flaps using the rectus abdominis muscle, supplied by the superior and inferior epigastric arteries (dominant pedicles) have been described increasingly since the 1970s[250-255].

Early anatomical studies of the blood supply to skin (Manchot 1889, Salmon 1936) contributed to the knowledge of areas of skin supplied by single vessels, and the clinical significance of this work only began to be realised decades later. During the second world war Shaw and Payne developed tubed abdominal flaps based on the inferior epigastric and circumflex iliac arteries[256]. Tai in 1974 described and successfully made use of a transverse rectus abdominis (TRAM) flap based on the superior epigastric vessels to cover chest wall defects in five patients who required radical resections for breast cancer[250]. Similarly, Mathes and Bostwick in 1977 presented a case report reconstructing the abdominal wall following a gunshot wound by rotating a myocutaneous flap based on the superior epigastric artery[252]. In 1979 Drever described the intramuscular course of the superior epigastric artery and described the operative technique of a myocutaneous flap based on this vessel, with a vertical skin island (VRAM), to release a burns scar contracture in a 12 year old, stating that 'the possible uses of this flap warrant future investigation'[254].

With the simultaneous advent of microsurgery in the early 1970s and the ability to perform microvascular anastomoses, and increasing number of flaps were transferred as free flaps. Holmstrom in 1979 used the 'abdominoplasty flap' based on the inferior epigastric vessels as a free flap to reconstruct a breast after radical mastectomy[253]. Pennington et al (1980) used free a rectus abdominis myocutaneous flap based on the inferior epigastric vessels to reconstruct an infraclavicular shotgun wound, and in his paper stressed the

advantage of this flap as having large vessels, a long vascular pedicle and aesthetic and functional acceptibility[251]. Perhaps more importantly the disadvantages of the TRAM flap noted included the need to reconstruct the anterior rectus sheath to prevent hernia formation and potential problems with abdominal wall support. Hartrampf, Scheflan & Black in 1982 clarified multiple surgical techniques of using the rectus abdominis muscle including the 'vertical rectus abdominis musculocutaneous flap' (VRAM), the 'horizontal upper rectus abdominis flap', and the 'horizontal lower rectus abdominis flap' (TRAM) with an 'easy-to-conceal suprapubic linear donor site'[257;258]. This TRAM flap description is still the commonly used donor site in free TRAM flap breast reconstruction cases. In 1983 and 1984 Taylor, Boyd & Corlett published a clinical and anatomical study, further delineating the anatomy of the deep inferior epigastric artery stating that it is the dominant blood supply to the skin of the anterior abdomen, the average diameter of the deep inferior epigastric perforator vessels were 3.4 millimeters, and that the largest perforating vessels were in the paraumbilical area and therefore some part of a skin island should be over this area[259;260].

A major modification of the TRAM flap was published by Koshima and Soeda in 1989 in their paper entitled 'Inferior epigastric artery skin flaps without rectus abdominis muscle'[14]. They describe raising the lower abdominal skin, finding a perforating vessel and dissecting it through the muscle, firstly as an island flap for a patient with malignant lymphoma in his groin, and secondly as a free flap for a patient with a squamous cell carcinoma on the lateral aspect of his tongue. The flap described based on a Deep Inferior Epigastric artery Perforator, is known as the DIEP flap. They noted that this flap may almost have the same skin territory of the TRAM flap, that they thought the risk of abdominal herniation to be eliminated, and that a disadvantage was the variable size and location of the perforator and the technical difficulty of dissecting the perforator within the muscle.

An early series of 15 DIEP flaps was published by Allen in 1994, who commented that the ideal material for breast reconstruction is fat and skin, and that the DIEP flap allowed large volumes of tissue transfer, with the example a 1443 gram flap in the series[21]. Several large series of DIEP flap reconstructions have been published subsequently with favourable results and a general agreement that in suitable patients the DIEP flap leaves less donor site morbidity than the TRAM

flap for breast reconstruction. Blondeel published his experience of 100 DIEP flap reconstructions in 1999 with a 2% flap failure rate and 1% with a unilateral abdominal bulge[261]. Similarly Hamdi et al in a series of 50 DIEPs had a 2% failure rate and 5% of patients with an abdominal bulge but no hernia[262]. Nahabedian et al compared 118 TRAM flaps with 20 DIEP flaps and concluded that the incidence of abdominal bulge was significantly less in DIEP flaps although the ability to perform a sit-up post operatively was not related to the type of flap[263]. The muscle-sparing TRAM flap is a technique modification of the TRAM to damage the least amount of muscle and fascia attempting to give more comparable donor site results to the DIEP flap, and one series which separately classifies this type of TRAM flap reports an incidence of 5% abdominal bulge versus 2% in the DIEPs, and an ability to perform sit-ups of 97% versus 100% in the DIEPs, although these numbers were not of statistical significance[264]. A systematic review by Salion in 2009 of eight papers comparing 329 TRAM flaps and 161 DIEP flaps, with comparison of the flaps being an inclusion criteria, concluded that whilst the total necrosis or flap failure rate in DIEPs was higher (4.15% v 1.59%), as was the fat necrosis rate (25.5% v 11.3%), there was no significant difference in the partial necrosis rate 3.54% v 1.60%) or abdominal bulge (8.07% v 11.25%)[265].

Although the donor site morbidity in the DIEP flap is arguably an improvement on the TRAM flap, a lower abdominal flap which does not cut rectus sheath is the Superficial Inferior Epigastric Artery (SIEA) flap which also utilises the lower abdominal skin and fat and can have a hidden suprapubic linear scar. The SIEA flap was first reported as a free flap in 1971 by Antia and Buch who used a de-epithelialised SIEA flap to correct a contour defect, secondary to a hemi-maxillectomy, in a 35 year old lady. The SIEA artery had a diameter of only one millimetre and to overcome this difficulty the vessels were harvested at their origin with a cuff of femoral artery and saphenous vein, before being anastomosed to the external carotid artery and internal jugular veins respectively[266]. Boeckx et al presented a series of 10 lower abdominal free flaps, 3 being SIEA flaps, and used a technique of exposing the origin of the superficial inferior epigastric artery and taking this vessel and the superficial circumflex iliac artery (SCIA) from the common femoral artery, if they shared the same trunk, to increase the size of the anastomosis[267]. Taylor and Daniel's anatomical study in 1975, 'The anatomy of several free flap donor sites', reports the mean calibre of the SIEA was 1.4mm in 100 cadaver dissections[26]. They also

noted that the SIEA had a common origin with the SCIA in 48% of cases, and was completely absent in 35% of cases. In 1992, Stern and Nahai published their retrospective series of 31 patients, again noting the unsuitability or absence of the SIEA in 4 patients (13%)[268]. They commented that the patients made a rapid recovery from 'a procedure which only invades the body's cutaneous envelope'. Although the vascular anatomy may not be as reliable as other flaps, the SIEA flap has a very favourable donor site.

The SIEA flap has been used for various kinds of reconstruction, from the abdominal wall[269], vaginal[270] and penile[271] reconstructions to upper limb[268;272], hand[268;272],facial[266;268] and breast reconstructions[273]. Arnez et al emphasised the benefits of the use of the SIEA flap in breast reconstruction in particular, where the lower abdominal skin and fat are a good match for breast tissue[274]. The SIEA in his view is the logical next step, ahead of the TRAM and DIEP flaps, when the lower abdomen is being considered as the donor site for breast reconstruction, and many authors share a similar view[273;275].

6.1.2 Angiosomes and zones of the lower abdomen

As discussed in the Introduction Chapter 1, the blood supply to the skin is made up of 'angiosomes'. Angiosomes were defines by Taylor and Palmer as composite blocks of tissue supplied by named source vessels[2]. The body is though to be made up of a jigsaw of angiosomes interlinked by reduced calibre 'choke vessels' (Chapters 1, 5 & 7). When a flap is based on an angiosome it is thought that the adjacent angiosomes to this angiosome can be included in the flap with a safe blood supply[2]. Partial necrosis and fat necrosis result from insufficient blood supply within a flap and are not uncommon with tissue loss in the angiosomes furthest from the supplying vessels. Flaps may also fail because of blockage of the main supplying artery or draining vein either due to twisting or external pressure or clotting at the site of the microvascular anastomosis, and this may result in total loss of the flap.

Angiosomes in the lower abdomen with regards to the TRAM and DIEP flaps are commonly referred to as 'zones' following the works of Scheflan[244;257;276;277], Dinner[244;276-278] and Hartrampf[257]. Scheflan[276;277] divided the ellipse into four equal parts numbering them in descending order of his clinical impression of perfusion in the first sixteen patients[279] undergoing pedicled TRAM flap breast

reconstruction, based on the superior epigastric artery. Zone 1 is the zone over the perforating vessel, zone two is the zone immediately across the midline, zone 3 is the ipsilateral lateral zone, and zone 4 the contralateral lateral zone. This order was changed by Dinner following further observation of the vascularity of the flap, with zones 2 and 3 being swapped so that zone 2 was now on the side ipsilateral to the perforator. Dinner divided these zones over the edges of the rectus sheath[226;244]. The nomenclature that has remained in the literature when discussing zones is Scheflan's original description and numbering, although is known as 'Hartrampf's zones'.

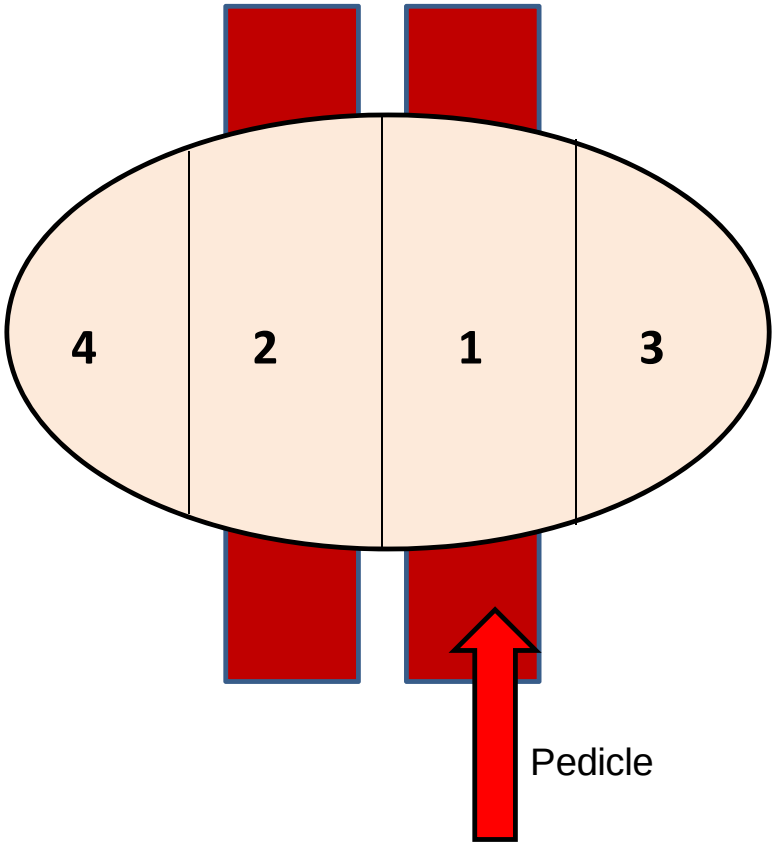

Figure 6-1 - Hartrampf's zones.

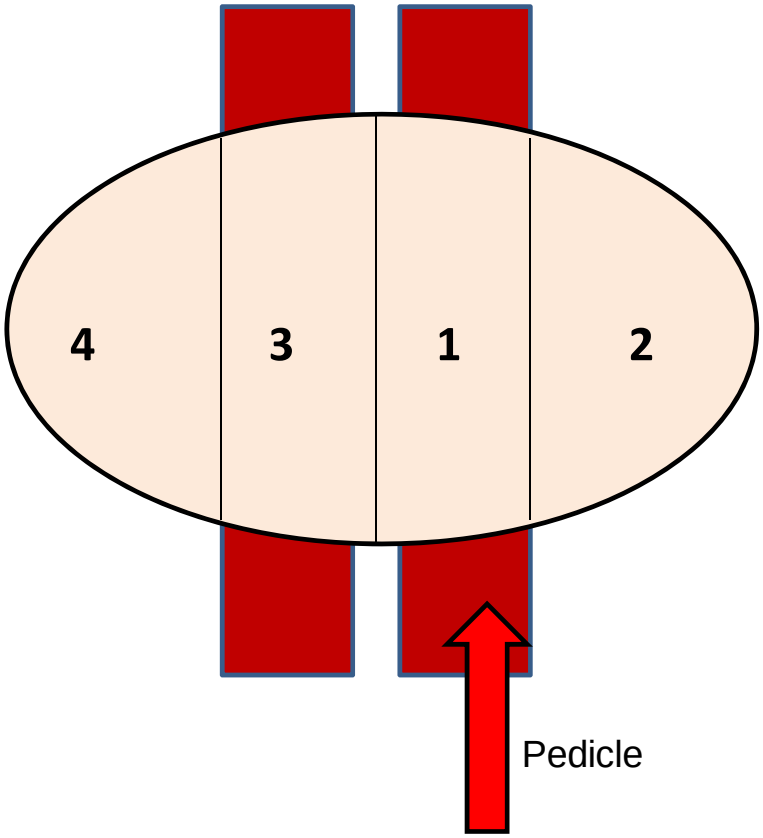

Figure 6-2 - Dinner's zones.

Breast reconstruction from the lower abdomen now largely relies on the deep inferior epigastric artery perforators (DIEP flaps and inferiorly based free TRAM flaps) as the dominant blood supply, rather than the superior epigastric artery with a move away from superiorly based pedicled TRAM flaps. The nomenclature for the zones has remained as Hartrampf's zones for both the DIEP and TRAM free flap reconstructions, although the order of zones for the SIEA (Superficial Inferior Epigastric Artery) flap is less clear. There is increasing evidence in the literature to suggest that zone 3 and zone 2 should exchange numbers reverting to Dinner's original description (Figure 6-2)[227]. Clinically zone 4 (i.e. the contralateral lateral zone in either nomenclature) has undoubtedly the poorest blood supply and highest incidence of venous congestion[280], and is usually excised and discarded before transfer to the breast for this reason, reducing the incidence of fat necrosis and partial necrosis. If the flap needs to be further reduced in size to produce a better aesthetic match, it is relevant whether zone 2 or zone 3 is the better perfused. The need to understand the area of perfusion equally applies to SIEA flaps, as the anatomy and diameter of the vessel is not constant[24-26;268;281].

6.1.3 Objective

The objective of this study is to delineate the blood supply to abdominal skin flaps commonly used for breast reconstruction by;

1) comparing blood supply of flaps based on the Deep Inferior Epigastric Perforator arteries (DIEP flap) with those based on the Superficial Inferior Epigastric Artery (SIEA flap) in terms of their area of perfusion and dominance.

2) comparing the zones of the DIEP and SIEA vessels, with reference to the Hartrampf perfusion zones.

Intra-operative non-invasive laser Doppler scanning will be used to image the skin perfusion for each vessel in turn, having established reliable scanning and clamp times in the pilot study.

Scanning intra-operatively may provide adequate information to guide the choice of vessel, the choice of vessel being determined firstly by perfusion to the flap and flap volume required, and secondly to minimise donor site morbidity. Clinically, perfusion of a vessel is not assessed until the vessel is chosen, and the choice of vessel depends to a large extent on vessel diameters observed during the dissection and the difficulty of the dissection if a DIEP vessel is thought to have a tortuous course through the muscle. The additional intraoperative information supplied by the laser Doppler scanner may also help in the choice of vessel for other free flap donor sites in the body.

Flap design may also be made more reliable by intraoperative scanning as the choice of areas to discard be based on a more objective assessment of skin perfusion, rather surgeon's clinical impression of skin perfusion, thus allowing one to more accurately predict perfusion after free flap transfer when choosing vessels and designing flaps.

It is hoped that this and subsequent studies can better map the blood supply to the lower abdominal skin in vivo. The benefit of this would be improved safety of the operation, reduce partial necrosis due to poor perfusion, and allow the surgeon to more reliably decide intra-operatively between SIEA and DIEP flaps.

6.2 Methods

This study was performed on ten patients undergoing immediate or delayed Deep Inferior Epigastric Perforator flap breast reconstruction following mastectomy for breast cancer. The study was performed between October 2007 and October 2008 in Canniesburn Plastic Surgery Unit, Glasgow Royal Infirmary. Ethical approval was granted by Glasgow Royal Infirmary Ethics Committee, and no changes were made to the reconstructive procedure. A laser Doppler scanner was used intraoperatively to assess the blood supply to the skin of the lower abdomen from each of the four supplying vessels (right and left DIEP vessels and right and left SIEA vessels).

The Laser Doppler scanner LDI2-IR (Moor Instruments, Axminster, Devon, UK) (Figure 2-3) was used non-invasively to assess the patients intraoperatively with the timing of scanning and clamping based on the pilot study results in Chapter 4. The laser Doppler scanner is discussed in more detail in Chapter 2, Materials. As in Chapter 4, research software Moor V5.3, was used to carry out the patient scans with the large scan setting, 4 msec/pixel speed, and the scanner head 70cm from patient and at a 15 degree angle.

This study follows the pilot study used to evaluate clamping and scanning times intraoperatively in Chapter 4 (Results, page 75). Clearly defined scan and clamp times allow repetition of scanning within one surgical procedure. To avoid scanning during the period of reactive hyperaemia of a vessel following clamp release it was concluded that scanning 5 minutes after clamp release provided a stable value for the flux, which is proportional to blood flow. Based upon the results of the pilot study for lower abdominal blood flow in Chapter 4 the method for this study was designed allowing the assessment of 4 vessels during a 35 minute intraoperative window.

Intraoperatively the lower abdominal flap was raised on four source vessels; perforators from the right DIEP vessels, perforators from the left DIEP vessels, the right SIEA vessels and the left SIEA vessels. Laser Doppler scanning was carried out immediately prior to division of the vessels and transfer of the flap to the recipient site for breast reconstruction. All vessels were clamped for an ischaemic time of five minutes, and then each vessel, in turn, was unclamped and allowed to supply the flap for five minutes before the flap was scanned by

the laser Doppler. Only one of the four vessels was supplying the flap at a time so that the laser Doppler scan could record the area that this vessel supplies. Each scan took 2 - 3 minutes and the overall intraoperative scanning period was around 35 minutes. The order in which the vessels were scanned for each patient was allocated randomly using random number tables and the orders are shown in Table 6-1 below.

	1st LDI scan	2nd LDI scan	3rd LDI scan	4th LDI scan
Patient 1	Left SIEA	Right DIEP	Right SIEA	Left DIEP
Patient 2	Left SIEA	Right SIEA	Right DIEP	Left DIEP
Patient 3	Right DIEP	Right SIEA	Left SIEA	Left DIEP
Patient 4	Right SIEA	Right DIEP	Left SIEA	Left DIEP
Patient 5	Left DIEP	Right DIEP	Right SIEA	Left SIEA
Patient 6	Right SIEA	Left DIEP	Right DIEP	Left SIEA
Patient 7	Left DIEP	Right DIEP	Right SIEA	Left SIEA
Patient 8	Right SIEA	Right DIEP	Left SIEA	Left DIEP
Patient 9	Left SIEA	Right SIEA	Right DIEP	Left DIEP
Patient 10	Right DIEP	Left DIEP	Left SIEA	Right SIEA

Table 6-1 - Intraoperative LDI scanning order for vessels supplying lower abdominal skin. The vessels were all clamped for a 5 minute period, followed by unclamping of the first vessel for 5 minutes before scanning, then reclamping of the first vessel unclamping of the second vessel for 5 minutes before scanning, then reclamping of the second vessels and unclamping of the third vessel for 5 minutes before scanning, and finally reclamping of the third vessel and unclamping of the fourth vessel before scanning.

Clamping prior to free flap transfer should not be detrimental as this sort of 'ischaemic preconditioning' has been shown to be beneficial[31;175;176]. The surgeon was blinded to the results of the laser Doppler in this SIEA v DIEP study, as in the pilot study described in Chapter 4. The operation then proceeded normally with the flap being transferred from the abdomen and the surgeon's choice of right or left DIEP vessels anastomosed to the internal mammary vessels in the chest, and the DIEP flap inset to complete the breast reconstruction.

6.2.1 Data processing and statistical analysis

The scans were analysed using the Moor Laser Doppler Imager research software, Version 5.3. Areas within the scan can be identified by drawing polygons to trace the outline of the abdominal flap and the zones of the flap (Figure 6-3). Shapes can be duplicated within scans or across sequential scans. Divisions between zones were at the lateral border of the rectus sheath, as in Dinner's original description[244]. These divisions have also used by Hallock et al in a laser Doppler study[226]. Other authors (Scheflan[258],Holm[227]) have divided the abdominal flap into equal widths although this is dependent on the width of the

flap rather than any anatomical landmarks, and we have therefore used Dinner's original description. Descriptive statistics including the mean and median flux are then requested for the outlined area from the Moor software. All statistical analysis of laser Doppler images in chapters 4, 5 and 6 has been performed using the medians calculated by Moor Research software descriptive statistics. The choice of medians rather than means is discussed in Chapter 4, page 73.

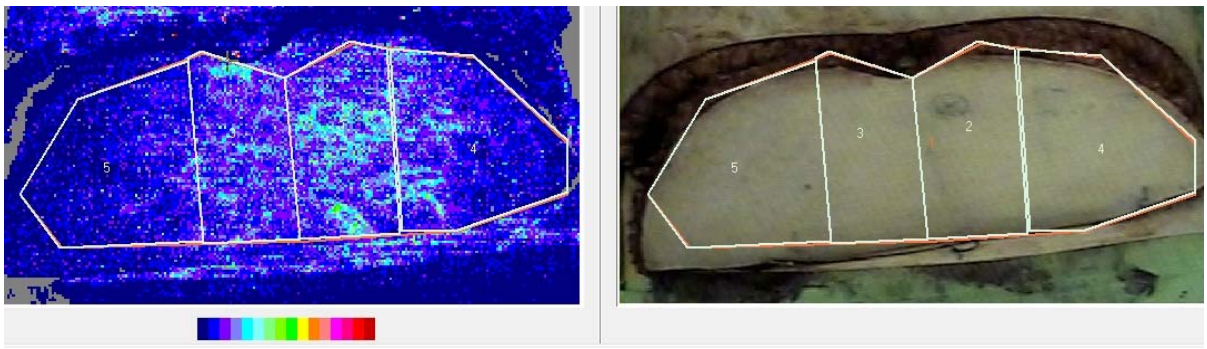

Figure 6-3 - Division of flux image into zones.
(NB numbers relate to Moor software & not zones.)

Ten patients were recruited for this study following review of the literature and comparison with similar cadaver[26;246;282-287], animal[288-290] and clinical studies[22;191;195;225-228;261;263;268;284;291-303]. A sample size calculation was performed using data from the pilot study, confirming 10 patients (with 4 scans per patient) to be a reasonable number. The results of the pilot study were analysed using parametric methods following Normal plots. The results of this study will be assessed with Normal plots and an Anderson-Darling test of normality before proceeding with parametric testing.

6.3 Results

Ten patients had DIEP flap breast reconstructions following mastectomies for breast cancer. Three were delayed procedures (mastectomy in a previous operation) and seven were immediate (mastectomy during the same surgical procedure as the reconstruction). Two reconstructions were bilateral. The patients had an average age of 54 (range 47 to 66) and an average BMI of 27.7 (range 24 to 34). All patients were non-smokers or ex-smokers at the time of the study. The mean operative time was 8 hours 36 minutes (6 hours 5 minutes to 15 hours), with one operative team. There was a bilateral flap failure in patient 8.

Right and left DIEP vessels and right and left SIEA vessels were found and dissected in nine of the ten patients. The DIEP perforators can be defined as 'medial row' or 'lateral row' in relation to their position emerging from the rectus abdominis muscle. 60% of the DIEP scans performed were medial row only (12/20), 25% were lateral row only (5/20) and 15% were a mixture of medial and lateral row (3/20) - see Table 6-2 for scans and patient details. In one patient (Patient No 7) no right SIEA was present and scans were performed on the other three vessels (left SIEA and bilateral DIEP vessels). All scans are in the Appendix.

6.3.1 Descriptive Statistics

The results for each scan are in Table 6-2 below. The flux value used for each individual vessel is the median value for flux over the whole flap. When the DIEP vessels were each supplying the lower abdominal flap (20 scans, 2 vessels per patient) the mean flux was 82.1 (s.d. 24.84, n=20 scans). This can be subgrouped into left and right DIEPS, the left DIEP vessels having a mean flux of 80.62 (s.d. 23.11, n=10 scans), and the right DIEP vessels having a mean flux of 83.58 (s.d. 26.67, n=10 scans). Two vessels per patient were also scanned for the SIEA vessels, other than patient 7 who had no SIEA vessel on the right side. The mean flux for the SIEA vessels supplying the lower abdominal flap is 69.0 (s.d. 26.37, n=19 scans), and for the left SIEAs 69.47 (s.d. 27.25, n=10 scans) and for the right SIEAs 68.47 (s.d. 68.47, n=9 scans).

The zones of the lower abdominal flap are referred to, for the descriptive purpose of this study for both SIEAs and DIEPs, in the traditional Hartrampf order, thought to be related to perfusion as illustrated below (Figure 6-4).

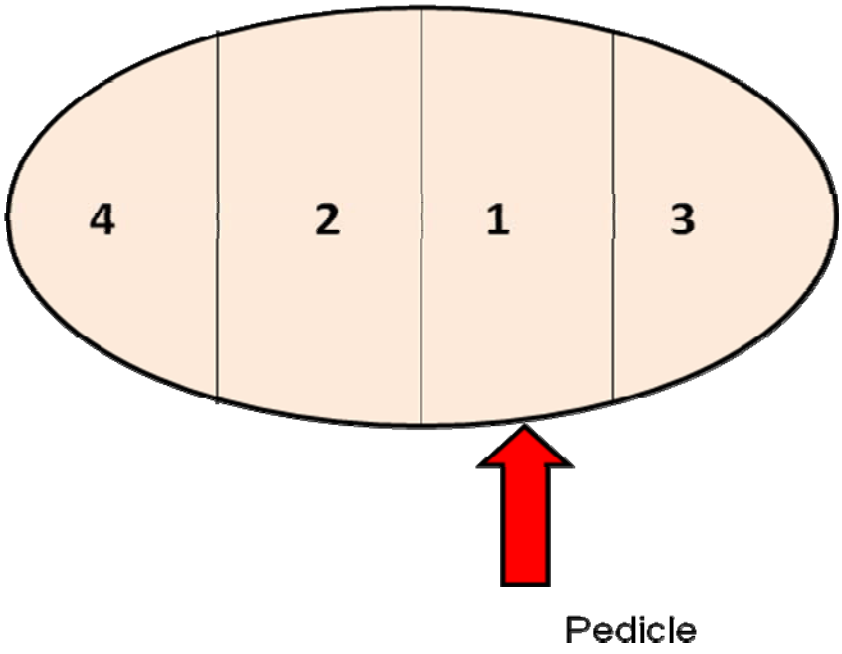

Figure 6-4 - Hartrampf's zones

The laser Doppler flux scans for patient 1 are shown below in Figure 6-5, Figure 6-6, Figure 6-7 & Figure 6-8. The flux images for all 10 patients grouped by vessel are in the Appendix.

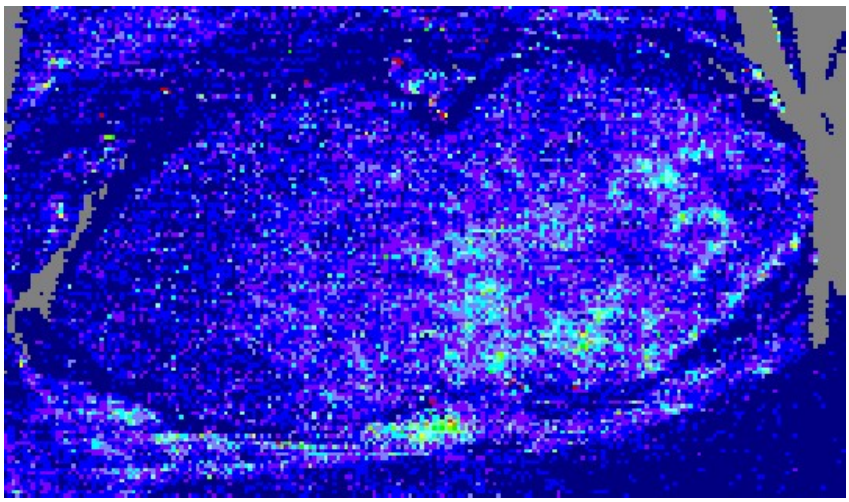

Figure 6-5 - Patient 1, scan 1. Left SIEA vessel supplying flap.

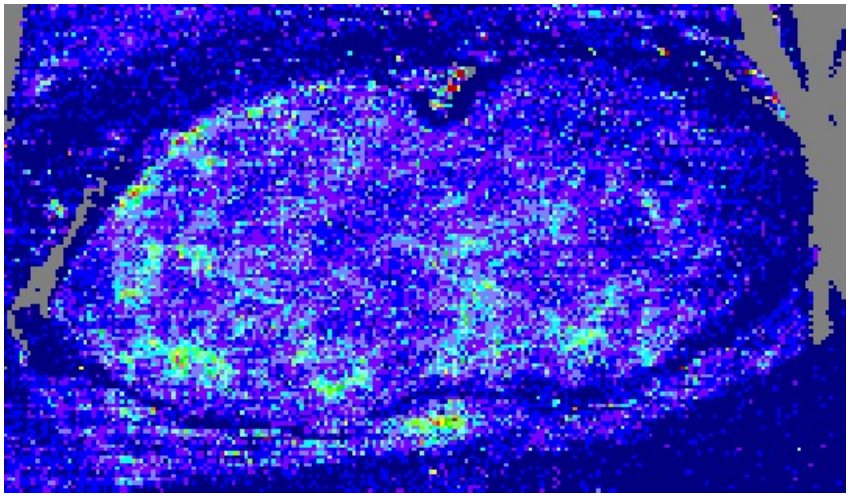

Figure 6-6 - Patient 1, scan 2. Right DIEP vessel supplying flap.

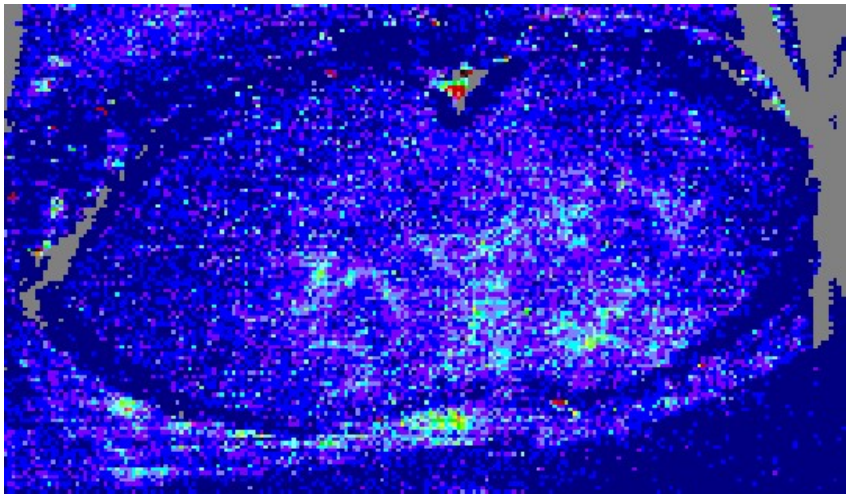

Figure 6-7 - Patient 1, scan 3. Right SIEA vessel supplying flap.

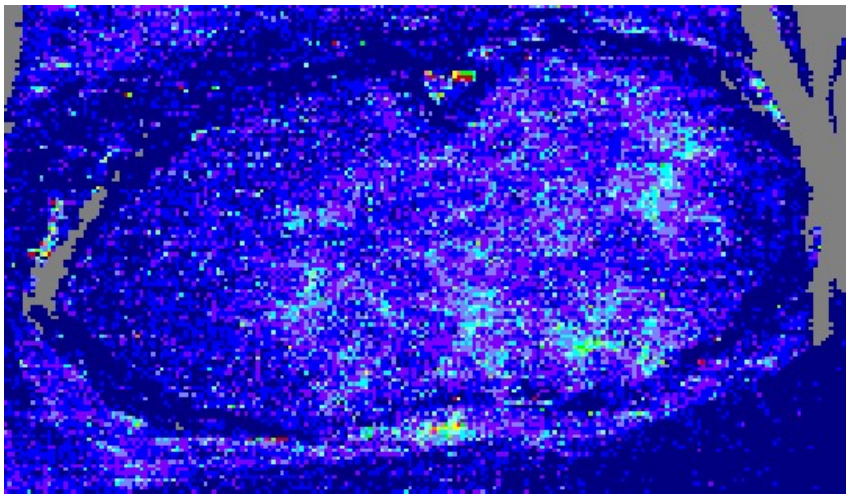

Figure 6-8 - Patient 1, scan 4. Left DIEP vessel supplying flap.

The zones were outlines using the Moor Laser Doppler software v5.3 and the flux for each scan was recorded, Table 6-2, the results are plotted in Figure 6-9.

Patient No	Vessel	Lateral perforators	Medial perforators	Zone 1	Zone 2	Zone 3	Zone 4	Whole flap
1	R DIEP†	2	0	106	112	120	76	104
	L DIEP†	2	0	109	88	97	59	89
	R SIEA	*	*	83	105	54	75	79
	L SIEA	*	*	109	83	99	55	87
2	R DIEP†	0	2	92	92	88	67	84
	L DIEP	0	2	101	98	82	67	86
	R SIEA	*	*	94	104	100	68	90
	L SIEA	*	*	112	124	97	68	97
3	R DIEP†	1	1	120	94	133	59	99
	L DIEP	0	2	100	53	70	38	63
	R SIEA	*	*	82	74	137	53	82
	L SIEA	*	*	55	43	47	35	45
4	R DIEP	0	1	81	100	88	94	91
	L DIEP†	0	2	99	88	110	71	91
	R SIEA	*	*	97	95	76	86	88
	L SIEA	*	*	99	88	110	71	91
5	R DIEP	1	0	66	46	112	31	59
	L DIEP†	0	1	128	108	77	51	86
	R SIEA	*	*	86	59	98	35	86
	L SIEA	*	*	74	52	111	34	74
6	R DIEP†	0	2	108	100	119	98	107
	L DIEP	1	0	103	87	93	61	85
	R SIEA	*	*	73	77	50	70	73
	L SIEA	*	*	98	92	91	63	98
7	R DIEP	0	3	97	99	100	66	85
	L DIEP†	0	2	108	99	72	96	89
	R SIEA	*	*	NA	NA	NA	NA	NA
	L SIEA	*	*	87	98	70	87	82
8	R DIEP†	0	1	65	42	67	35	51
	L DIEP†	1	0	82	70	77	59	72
	R SIEA	*	*	59	42	64	36	59
	L SIEA	*	*	43	45	39	49	43
9	R DIEP †	1	1	67	52	60	31	51
	L DIEP	1	1	58	42	92	27	49
	R SIEA	*	*	36	35	28	28	36
	L SIEA	*	*	41	41	33	30	41
10	R DIEP †	0	1	101	103	101	55	90
	L DIEP	0	3 small	98	60	97	49	75
	R SIEA	*	*	55	55	54	42	55
	L SIEA	*	*	55	55	42	54	55

Table 6-2 - Flux results per vessel. For whole flap per vessel, and also divided by zone. Number of perforators and position in medial or lateral row marked for DIEP vessels. † denotes vessel chosen clinically by surgeon for reconstruction.

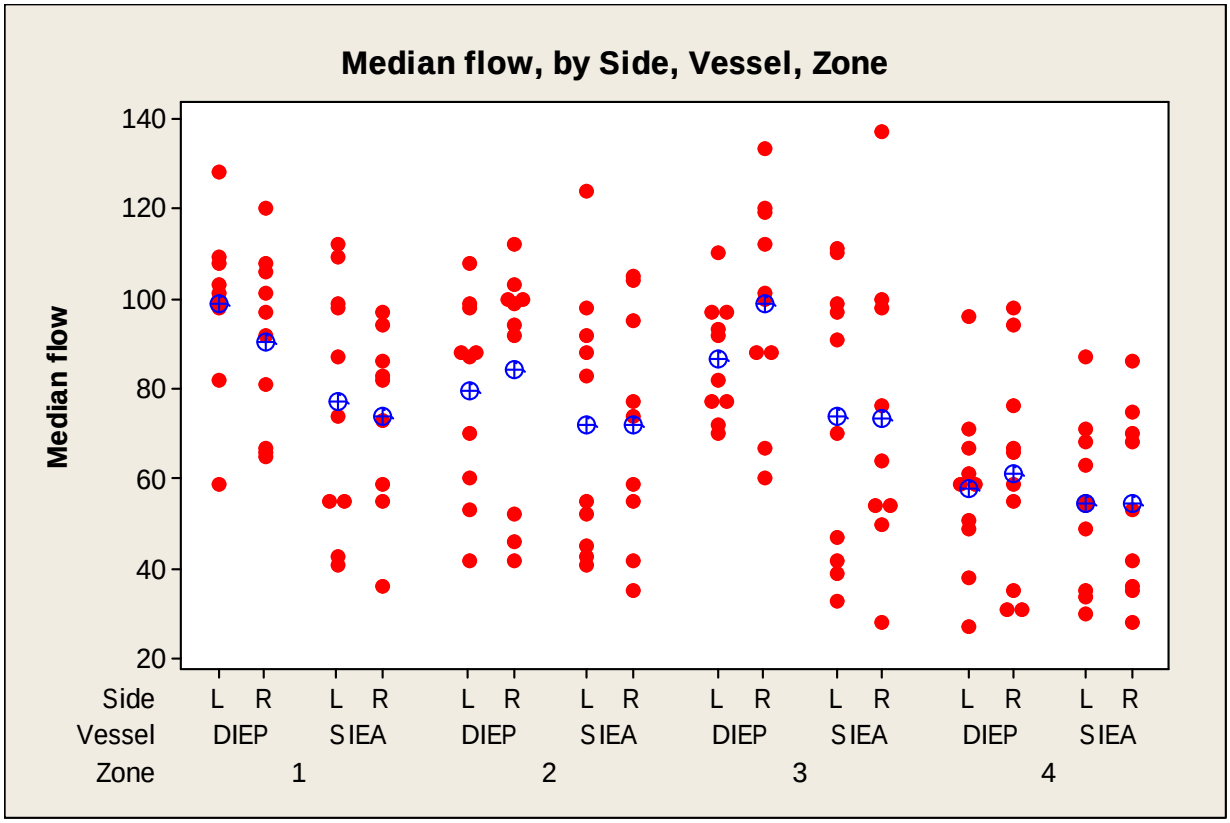

Figure 6-9 - Plot of individual values of median flow per laser Doppler scan. Means are marked in blue. The Values are grouped by side (left or right), vessel (SIEA or DIEP) and zone (1, 2, 3 or 4 as in figure 6.4 above).

Observing the pattern of flux values, there appears to be little difference between right and left side flow. DIEPs tend to have a higher flow than SIEA vessels, and zone 4 would appear to have reduced flow in both DIEPs and SIEAs with little difference between other zones. The flux values are displayed below, grouped by vessel, side and zone (Table 6-3).

Zone			1	2	3	4	All
Vessel	Side						
DIEP	L	Mean	98.70	79.30	86.70	57.80	80.62
		SD	18.05	21.89	13.03	18.84	23.11
		N	10	10	10	10	40
	R	Mean	90.30	84.00	98.80	61.20	83.58
		SD	19.62	26.41	23.47	24.17	26.67
		N	10	10	10	10	40
	L & R	Mean	94.50	81.65	92.75	59.50	82.10
		SD	18.85	23.73	19.49	21.17	24.84
		N	20	20	20	20	80
SIEA	L	Mean	77.30	72.10	73.90	54.60	69.47
		SD	27.29	28.63	31.24	18.30	27.25
		N	10	10	10	10	40
	R	Mean	73.89	71.78	73.44	54.78	68.47
		SD	20.15	25.97	33.19	20.67	25.72
		N	9	9	9	9	36
	L & R	Mean	75.68	71.95	73.68	54.68	69.00
		SD	23.58	26.64	31.27	18.90	26.37
		N	19	19	19	19	76
DIEP & SIEA	L	Mean	88.00	75.70	80.30	56.20	75.05
		SD	25.05	25.08	24.20	18.15	25.73
		N	20	20	20	20	80
	R	Mean	82.53	78.21	86.79	58.16	76.42
		SD	21.07	26.23	30.57	22.20	27.13
		N	19	19	19	19	76
	L & R	Mean	85.33	76.92	83.46	57.15	75.72
		SD	23.06	25.34	27.32	19.98	26.34
		N	39	39	39	39	156

Table 6-3 - Mean flow, standard deviation and number of observations, by vessel type, side and zone.

Considering the main effects of the data, the effects of each factor averaged over the levels of the other two, the mean flow for each side are very similar (75.05 left and 76.42 right), the mean flow associated with the DIEP flap is higher than the SIEA (82.10 DIEP and 69.00 SIEA), and there is variation in the zones 1,2 and 3 (85.33, 76.92 and 83.46 respectively) with a more substantial drop in flow in zone four (57.15). It is possible that the vessel and the zone are independently significant factors, although unlikely that the side is significant.

To look for interactions between the factors of vessel, side and zone they can be observed in pairs and in a group of three. Between vessel and side the differences in mean flow are small. For the DIEP vessels the mean flow on the left and right is 80.62 and 83.58 respectively, and for the SIEA vessels, mean flow on the left and right is 69.47 and 68.47. It would seem unlikely that there is a statistically significant interaction between vessel and side. Between zone and side, it also seems unlikely that there would be a statistically significant interaction. For zone 1 the mean flow between the left and right is 88.00 and

82.53 respectively. Corresponding left-right pairs for zones 2, 3 and 4 are 75.70 and 78.21, 80.30 and 86.79, 56.20 and 58.16. Finally, between vessel and zone, the DIEP means for zones 1 - 4 respectively are 94.50, 81.65, 92.75 and 59.50, and the SIEA means are 75.68, 71.95, 73.68 and 54.68. The differences (DIEP minus SIEA) are 18.82, 9.7, 19.07 and 4.82, and it would therefore appear that the differences in mean flow between vessel types depend on zone. There may be a two-factor interaction between vessel and zone of statistical significance.

To consider the effects of all three factors jointly, an interaction would be present if the difference between the type of vessel (DIEP minus SIEA) in the left-right difference (left minus right), does not depend on zone. The left-right differences for the two vessel types and zones, followed by the differences (DIEP minus SIEA) between these differences are (Table 6-4);

Zone	**1**	**2**	**3**	**4**
DIEP (L - R)	8.4	-4.7	-12.1	-3.4
SIEA (L - R)	3.41	0.32	0.46	-0.18
DIEP (L - R)- SIEA (L - R)	4.99	-5.02	-12.56	-3.22

Table 6-4 - Three factor interaction.

The differences (4.99, -5.02, -12.56, -3.22) are relatively small although the difference for zone 3 is larger and it is possible although unlikely that there is a three factor interaction between side, vessel and zone.

6.3.2 Analysis of variance

To check whether Normality is a reasonable assumption before interpreting the analysis of variance, the following four plots (Figure 6-10) provide a check on the assumptions of Normality of errors and homogeneity of variance of errors.

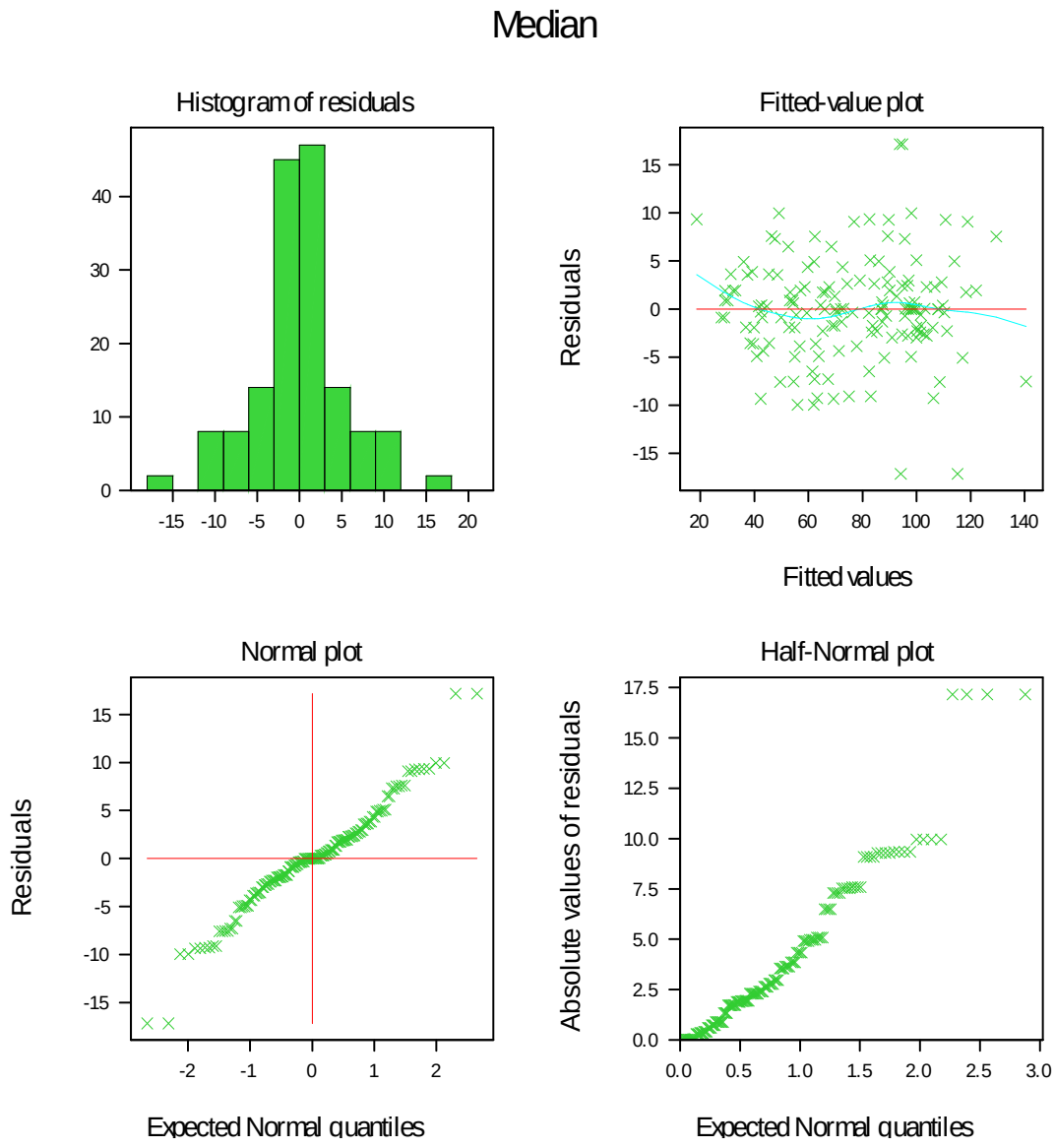

Figure 6-10 - Residual plots from ANOVA; Histogram of residuals, Fitted-value plot, Normal plot and Half-Normal plot.

The Normal plot and Half-Normal plot show four residuals appearing as outliers, and they correspond to Patient 5 zone 3. The outliers are also shown in the histogram and the fitted-value plot where they do not appear as especially prominent. The standardised residuals are all approximately equal to ±3.37. The Normal plots suggest that Normality would be a dubious assumption, even if the four large residuals are ignored. An Anderson-Darling test of Normality of residuals does indicate non-Normality ($p<0.005$). Repetition of the ANOVA, excluding these four observations, does not greatly affect the ANOVA table, the tables of means and the tables of standard errors. The conclusions would be unchanged. The largest standardised residuals are now ±2.92. However, the Anderson-Darling Normality test is still failed ($P=0.008$), although the P-value shows the departure from Normality is less.

The fitted-value plot shown no indication of non-homogeneity of variance.

In view of the non-Normality of errors, Armitage and Berry suggest that "it is often useful to be able to confirm the results of a normal theory significance test by also performing an appropriate distribution-free test"[304]. The seven hypotheses featuring in the ANOVA table (were therefore also tested using non-parametric methods (Table 6-6). The ANOVA and non-parametric test results agree apart from the Vessel and Zone interaction and therefore this interaction is regarded as suggestive only.

ANOVA of the full data set (Table 6-5) is however is reasonable to regard as having a valid result as;

i. homogeneity of variance is satisfactory,

ii. exclusions of the observations associated with the largest outliers only affects the ANOVA results in a minor way and does not alter the conclusions

iii. the non-parametric tests agree in terms of conclusions with those of the ANOVA (with one exception, the interaction between Vessel and Zone).

Source of variation	d.f.	(m.v.)	s.s.	m.s.	v.r.	F pr.
Patient_No stratum	9		38921.7	4324.6		
Patient_No.Vessel stratum						
Vessel	1		6325.8	6325.8	12.36	0.007
Residual	9		4605.9	511.8		
Patient_No.Side stratum						
Side	1		93.0	93.0	0.11	0.743
Residual	9		7326.0	814.0		
Patient_No.Zone stratum						
Zone	3		20097.0	6699.0	21.42	<.001
Residual	27		8444.6	312.8		
Patient_No.Vessel.Side stratum						
Vessel.Side	1		81.3	81.3	0.17	0.687
Residual	8	(1)	3726.0	465.8	2.65	
Patient_No.Vessel.Zone stratum						
Vessel.Zone	3		1451.8	483.9	3.23	0.038
Residual	27		4039.7	149.6	0.85	
Patient_No.Side.Zone stratum						
Side.Zone	3		775.5	258.5	0.86	0.474
Residual	27		8118.8	300.7	1.71	
Patient_No.Vessel.Side.Zone stratum						
Vessel.Side.Zone	3		362.1	120.7	0.69	0.569
Residual	24	(3)	4219.3	175.8		
Total	155	(4)	107569.6			

Table 6-5 - ANOVA. Analysis of variance of median flow.

The main effects of vessel (P<0.007) and zone (P<0.001) are statistically significant, and the main effect of side is not (P=0.743). The only significant two-factor interaction looking at the ANOVA results is between vessel and zone (P=0.038). As before, this cut-off value is close to 5% and the P-value for the non-parametric test (Friedman test) is 0.072 (see Table 6-6 below), and therefore the interaction between vessel and zone is regarded as suggestive only. The three-factor interaction is not statistically significant.

Model term	ANOVA P-value	Non-parametric test P-value	Type of non-parametric test
Vessel (V)	0.007	0.024	Wilcoxon signed rank test on Vessel differences in flow, averaged over zone and side
Side (S)	0.743	0.906	Wilcoxon signed rank test on side differences in flow, averaged over zone and vessel type
Zone (Z)	<0.001	<0.001	Friedman test on Zone differences in flow, averaged over side and vessel type
V.S	0.687	0.636	Wilcoxon signed rank test on interaction term: DIEP(L)-DIEP(R)-SIEA(L)+SIEA(R), where each of these 4 terms is an average over Zone
V.Z	0.038	0.072	Friedman test on vessel difference (averaged over side), by Zone
S.Z	0.474	0.352	Friedman test on side difference (averaged over vessel), by Zone
V.S.Z	0.569	0.694	Friedman test on interaction term: DIEP(L)-DIEP(R)-SIEA(L)+SIEA(R) by Zone

Table 6-6 - Comparison of ANOVA test results with non-parametric test results.

6.3.3 Analysis by Vessel, by Zone, and by Vessel and Zone

As above (Table 6-6), there is a significant difference between the Vessels, and between the Zones and the suggestion of an interaction between Vessel and Zone. To investigate this further, predicted means (from the fitted parameters of the ANOVA model) are used as there is an amount of missing data. The predicted means only differ slightly from the observed means in Table 6-4. For example, the observed marginal means for zone are 85.33, 76.92, 83.46 and 57.15, whereas the predicted means are 85.3, 77.4, 83.5 and 57.1.

The predicted means by vessel are 82.1 for the DIEP and 69.5 for the SIEA, with a standard error of difference of 3.58 on 9 degrees of freedom. The t-test statistic is 3.52, P=0.0065 and is therefore significant at the 1% level for a difference between the vessels, as before.

The predicted means by zone are (Table 6-7);

Zone	1	2	3	4
Predicted mean	85.2	77.4	83.5	57.1

Table 6-7 - Predicted means by zone (both SIEA and DIEP). Standard error of a difference between two of these means is 3.95 on 27 degrees of freedom.

Carrying out t-tests between zones 1 & 2 P=0.058 and is approaching significance, between zones 2 & 3 P=0.135 and is not significant, and between zones 3 & 4 P<0.001 and represents a very highly significant difference. If the zones were reordered by decreasing flux (1,3,2,4) the P-values of the differences between zones 1 & 3, and zones 2 & 4 would also be relevant. Between 1&3 the p-value is 0.671 which is not significant, although the p-value between zones 2&4 is very highly significant as P<0.001. These differences are more relevant clinically when the predicted means are calculated for each vessel.

Therefore, the predicted means by vessel and zone are (Table 6-8);

Zone	1	2	3	4
Predicted mean by vessel - DIEP	94.5	81.6	92.8	59.5
Predicted mean by vessel - SIEA	76.0	73.1	74.3	54.6

Table 6-8 - Predicted means by vessel and zone. Standard error of a difference between two means for the same vessel is 4.81 on 48.02 degrees of freedom. The standard error of a difference for two means in the same column is4.90, on 25.24 degrees of freedom.

These means by Vessel and by Zone are illustrated graphically in Figure 6-11.

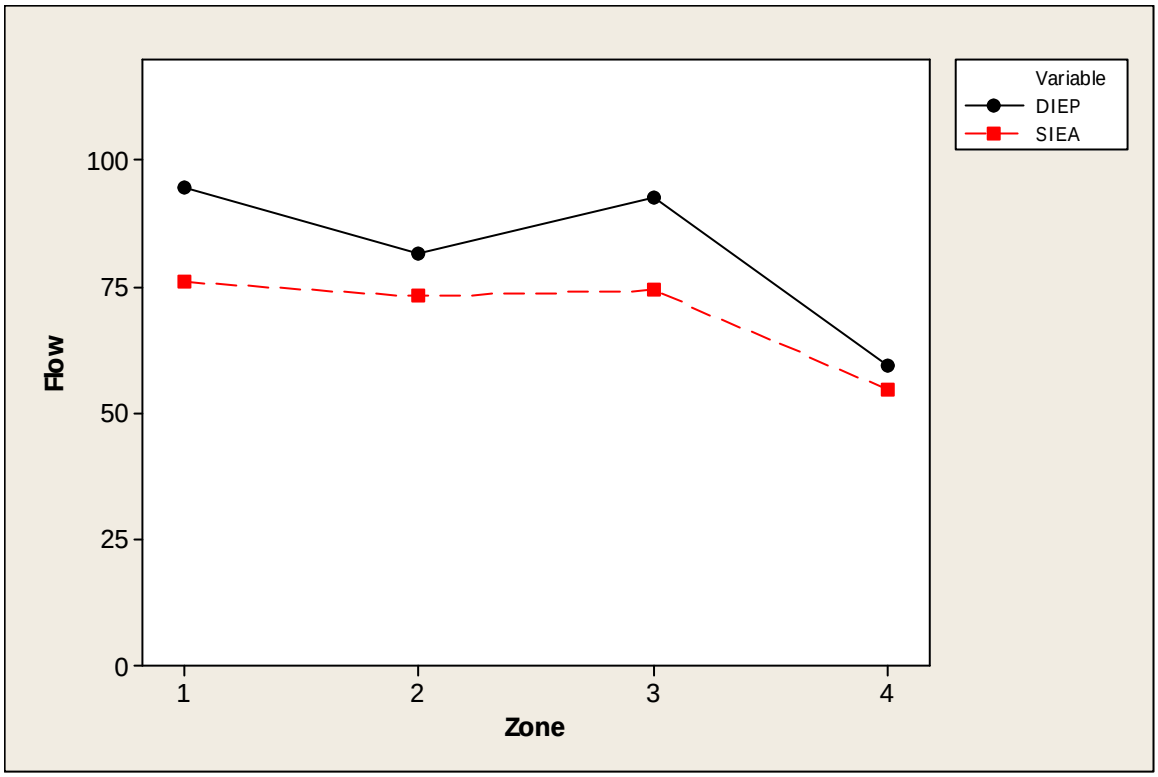

Figure 6-11 - Predicted means by Vessel and Zone.

There is a significant difference between DIEP zone 1 and SIEA zone 1, and between DIEP zone 3 and SIEA zone 3, P<0.001. There is no significant difference between the DIEP and SIEA zone 2 (P=0.095), and no significant difference between DIEP and SIEA zone 4 (P=0.327).

Considering the significance between DIEP zones (Table 6-8, Figure 6-11), between zone 1 and 2 the difference is 12.9 giving a t-test statistic of 2.68 and a P-value of 0.010, similarly between zone 2 and zone 3 P=0.025, and between zone 3 and zone 4 P<0.001. If the zones were reordered by descending flux i.e. 1,3, 2, 4, it would be relevant to also compare zones 1 & 3 P = 0.728, and zones 2 & 4 P<0.001. The clinical significance in this study for DIEPs is that zone 1 is the best perfused and is not statistically significantly different from zone 3 (the ispilateral zone, Figure 6-4). Zone 3 (and zone 1) are statistically significantly better perfused than zone 2 (contralateral midline, Figure 6-4), and zone 2 (and 3) are very highly significantly better perfused than zone 4 i.e. 1=3>2>4.

Similarly between SIEA zones (Table 6-8, Figure 6-11), the t-test statistic between zones 1 and 2 is 0.603 and the P value is 0.549, between zones 2 and 3 P=0.804, and between zones 3 and 4 P<0.001. Reordering the zones by descending flux (1, 3, 2, 4) would suggest comparison of zones 1 and 3, P=0.726, and between zones 2 and 4, P<0.001. Therefore zones 1, 2 and 3 are not statistically significant, but both zones 2 and 3 are very highly significantly better perfused than zone 4 i.e. 1=2=3>4.

In summary Table 6-9 displays the significance levels of the differences in flux between zones for both DIEP and SIEA vessels;

Difference between DIEP zones;	P-value	Difference between SIEA zones;	P-value
1 - 2	0.010	1 - 2	0.549
2 - 3	0.025	2 - 3	0.804
3 - 4	P < 0.001	3 - 4	P < 0.001
1 - 3	0.728	1 - 3	0.726
2 - 4	P < 0.001	2 - 4	P < 0.001

Table 6-9- Significance of difference between zones 1 - 4 for DIEP and SIEA vessels.

6.4 Conclusion

The overall perfusion of the lower abdominal skin by DIEP vessels is significantly higher than that of SIEA vessels ($P<0.05$). Side (left or right) has no significant effect on perfusion. The effect of zone however averaged over vessel side and type is very highly significant ($P<0.001$). When zones were examined, averaged over vessel and side, zone 4 was the only zone with significantly lower perfusion, and this reached a very high level of significance ($P<0.001$). The interaction between vessel and zone approached significance but can only be considered as suggestive.

Separating the data between vessel types, DIEP and SIEA vessels, provides more clinically relevant information regarding the perfusion of each of the zones. For DIEP vessels, the descending order of perfusion was zone 1, zone 3, zone2 and finally zone 4. The significance between these differences reveal that zone 1 is not significantly better than zone 3 (although better than zone 2, $P=0.01$), zone 3 is significantly better perfused than zone 2 ($P=0.025$), and zone 2 is significantly better perfused than zone 4 ($P<0.001$). 60% of the DIEPs were based only on medial perforators, 25% on lateral perforators, and 15% on both medial and lateral perforators.

For the SIEA vessels, the descending order of perfusion was zone 1, zone 3, zone 2 and finally zone 4, although there was no significant difference between perfusion of the first three zones. Zones 1 - 3 all have very highly significantly better perfusion than zone 4 ($P<0.001$). Subjectively, the SIEA flaps appear to have greater variability in perfusion than DIEP, and the standard deviations are very slightly though not significantly higher (Table 6-3).

Laser Doppler imaging is a safe, available method of non-invasive intraoperative imaging that can assist in physiologically assessing the vascular territory of vessels. This is of benefit in individual patients when there is a choice of vessel, and also when assessing the area of the flap to be discarded.

6.5 Discussion

The rapid progression of reconstructive surgery in the last 30 years has arisen following the pioneering free flap transfers in the 1970s and the corresponding re-evaluation of vascular anatomy to facilitate this development. The

'angiosome' concept has provided a theoretical framework for the design of flaps. Refinements such as perforator flaps have reduced donor site morbidity as can be seen with the use of the DIEP lower abdominal free flap for breast reconstruction[21], leaving behind the rectus abdominis muscle unlike its predecessor the TRAM flap. The quest to reduce donor site morbidity has also driven renewed interest in flaps such as the SIEA flap, often disregarded due to its small vessels and variable success rates[24;25;273;281;305]. The success of free flap transfer depends not only on minimising donor site morbidity, but on the flap failure rate, the risk of partial flap failure and fat necrosis. Large published series of each of these flaps with refinements to the operative procedure[295], algorithms suggested for their use, pre-operative scanning where necessary with CT and MRA, and increased knowledge of the variations in anatomy and perfusion, have all improved the results of free flap transfer in breast reconstruction.

6.5.1 Donor site

The differences in donor site between TRAM, DIEP and SIEA flaps is well documented. The DIEP flap has been presumed to reduce the possibility of hernias and muscle weakness, in comparison with the TRAM flap, given that there is less disruption to the abdominal wall musculature. A study by Lejour in 1991 of 57 patients undergoing TRAM flaps and with a minimum of 6 months follow-up were found to have no problems of clinical significance with return to normal function and sporting activities[300]. Physiotherapist assessment of these patients was more sceptical with 'no complete function of the rectus and obliques muscles' in any patient. Blondeel et al assessed 20 TRAM flap patients at an average of 32 months post-operatively and found that 44% of patients complained of decreased abdominal power, 28% of reduced ability to lift heavy objects, 42% of abdominal protrusion, 47% of pain in the lower abdominal wall with raised intra-abdominal pressure and 38% with difficulties getting up from a supine position[306]. Objectively patients had reduced abdominal flexion, extension and rotation. Similarly Blondeel later directly compared the donor site morbidity of 18 DIEPs, 20 TRAMs and 20 controls finding that TRAM flap patients had a statistically significant reduced ability to flex and rotate their trunk in comparison with the DIEP and control groups[294]. These findings of reduced abdominal wall function and bulge or hernia with TRAM versus DIEP flaps[22;261;263], are echoed by many other studies. Also, in the short term, a study

of DIEP flap patients showed that they had lower postoperative analgesia requirements than TRAM flap patients and are presumably in less pain[307]. Muscle sparing TRAM flaps, where a small section of muscle is removed with the perforating vessel, would appear to have a morbidity comparable to the DIEP flap[264;292].

Despite the seemingly logical operative progression from TRAM flaps to DIEP flaps in reducing donor site morbidity by maintaining anatomy, a systematic review by Sailon[265] in 2009 of eight studies[22;263;292;294;299;308-310] directly comparing DIEP and TRAM (including muscle-sparing TRAM) flaps did not find any statistical significance in reduced abdominal bulge with DIEP flaps although there was a trend towards this. The study did not include abdominal strength because of the differing methods of assessment, and did not include studies of DIEP or TRAM flaps alone to attempt to exclude bias. A meta-analysis published by Man et al the same year[311], included five of these eight studies[264;292;294;299;310] and one further comparative study[312], combined the abdominal donor site effects and found that DIEP patients had one-half the risk of abdominal bulge or hernia. They also pooled the data from 16 DIEP studies (1920 DIEP flaps) and 23 TRAM studies (3185 free TRAM flaps) and again found that DIEPs had less than one half the rate of abdominal hernia or bulge than TRAMs. It would seem apparent from the literature that there is a difference in donor site morbidity between DIEP and TRAM flaps. As the effects of this difference are debated[313], the significance of donor site morbidity as a factor in clinical decision of choice of flap will also depend upon the patients lifestyle, occupation and sporting activities.

The SIEA flap, in relation to donor site morbidity, is superior to the TRAM and DIEP flaps as outlined in the introduction, as it does not injure the rectus abdominis muscle or fascia. The superficial inferior epigastric vessels originate from the femoral artery and vein four to five centimetres below the inguinal ligament[314], coursing vertically upward towards the abdomen. The vessels are found in the subcutaneous fat roughly midway between the anterior superior iliac spine and the pubic symphysis, 75% within 1cm of the midpoint of the inguinal ligament[25] when incising the flap, and the donor site has the same lower abdominal or abdominoplasty scar as for the DIEP and free TRAM flaps. Several studies including SIEA flaps report no incidence of abdominal wall complications

such as hernia or bulge, for example; 14 SIEAs reported by Chevray in 2004[24], 94 SIEAs reported by Spiegel in 2007[281], and 69 SIEAs reported by Selber in 2008[303]. A prospective comparative study of 82 patients undergoing bilateral reconstructions with SIEAs, DIEPs and TRAMs showed a reduction in lower abdominal strength of bilateral TRAMs compared with SIEAs (p=0.04)[315]. Being the least invasive it has the lowest incidence of abdominal wall complications of the lower abdominal wall flaps, results in less post-operative pain[24;316]and requirement for analgesia, and a decreased post-operative hospital stay[24] than DIEP flaps. Despite the obvious benefits in reducing donor site morbidity, the variability of the presence of the SIEA vessels has been one of the perceived drawbacks when a SIEA flap is considered.

6.5.2 Blood supply to the lower abdomen

Taylor and Daniel in 1975 in their large anatomical study of 100 cadavers, 'The Anatomy of Several Free Flap Donor Sites', stated that the superficial inferior epigastric artery (SIEA) was absent in 35% of cadavers, replaced with a large superficial circumflex iliac artery[26]. The mean diameter of the SIEA was 1.1mm (0.8mm - 1.8mm range), and the vein described as 'constant', having a diameter of 2mm or greater. A further anatomical study of 16 cadavers by Hester et al in 1984 found the SIEA vessels inadequate for free flap transfer in 1 in 16 cases[317]. Stern & Nahai reported a clinical series in 1992 of 31 patients and only in 4 patients (13%) was the SIEA absent or unsuitable[268]. In 2004 an anatomical study of 22 cadaver dissections by Reardon et al found the SIEA present in 20 out of 22 (91%)[25]. They commented that the SIEA was therefore more consistently present than previously reported and consequently may be of greater clinical use. Of note a study by Gusenoff et al in 2008 found that maximum body mass index was related to the overall presence of a SIEA (p=0.009), a usable artery greater than 1.5mm (p=0.04), and to superficial inferior epigastric vein size (p<0.001)[298]. A small CT study of 17 patients by Fukaya in 2011[318] identified the SIEA vessel in only 64.7%, a number very similar to Taylor's 1975 cadaver study. The authors do comment however that it maybe a current technical limitation in visualising vessels of this calibre. It would appear from the literature that the SIEA is present more frequently than thought after Taylor's study in 1975, but it must be noted that Taylor's study has significantly more dissections than subsequent studies.

Further considerations when planning a SIEA flap include the pedicle length, being around 5.2cm from its origin to the inguinal ligament (range 3 - 7cm)[25], and therefore shorter than the DIEP (11.8cm mean, range 9.7 - 14.5cm)[21](10.3cm mean, range 9 - 13cm)[286] and muscle-sparing TRAM pedicles. The SIEA pedicle can be too short to allow anastomosis to the thoracodorsal vessels in the axilla. As described in the introduction Antia and Buch's original description of the free SIEA flap took a cuff of femoral artery and saphenous vein to increase the pedicle length[266] and Volpe in 1994 required saphenous vein interposition grafts in two of four patients to reach the thoracodorsal vessels[275]. The TRAM flap with its longer pedicle had allowed the use of the thoracodorsal vessels as the recipient vessels for breast reconstruction. The internal mammary vessels, which have been reported as recipient vessels, were largely disregarded as they were thought to be of 'unpredictable quality'[319], especially the vein. Dupin and Allen et al published 110 consecutive cases of use of the internal mammary artery and vein as a recipient vessels for breast reconstruction describing them as very reliable and recommending that 'the internal mammary system should be brought back into the armamentarium for free-flap breast reconstruction'[320]. They described the artery size at the 3rd and 4th rib as 3.2mm and 2.9mm respectively, and 3.4mm and 2.7mm for the vein. The series had 74 DIEP flaps and 32 superior gluteal artery flaps with only one flap failure which was unrelated to the recipient vessels. Although no SIEAs were included in this series, the use of internal mammary vessels as recipient vessels in breast reconstruction is crucial for the popularity and acceptance of the SIEA as it allows for a shorter pedicle length.

The artery diameter for the SIEA flap is smaller than that of the TRAM or DIEP flap[24;274;314], which combined with the shorter pedicle, and 'an absence or inadequacy of an arterial pedicle in most patients' as described by Chevray in 2004[24], has, as discussed, traditionally made the SIEA a less attractive option for many surgeons. Spiegel and Khan in 1997 reported performing 99 SIEAs out of 199 breast reconstructions, where SIEAs were the first choice dependent upon meeting suitability criteria[281]. The protocol of a pulsatile vessel of diameter 1.3mm at the point of entry to the flap was later modified to 1.5mm, as the difference between thrombotic and non thrombotic vessel sizes of 1.4mm versus 1.8mm was significant (p=0.002). Spiegel et al also felt that the diameter of the vessel at the point of entry to the flap mattered more than the SIEA diameter at

its origin. In an anatomical study in 2004, Reardon et al found a mean SIEA calibre of 1.9mm, ranging from 1.2mm to 2.5mm in 22 cadaver dissections[25]. Clinically, Chevray et al proposed selection criteria for performing a SIEA flap for breast reconstruction, including an arterial diameter of 1.2 - 1.5mm at the femoral origin (1mm at groin incision), visible and palpable pulsation of the SIEA, and the flap vessels based on the contralateral side to the breast reconstruction[24]. Allen in his discussion of Chevray's paper disagreed with Chevray's selection criteria for SIEA flaps as they only allowed 30% of patients to have SIEA flaps performed as a first choice in a series of 47 patients, with 17% of patients having DIEPs and 53% muscle-sparing free TRAMs. Allen similarly performed 40% SIEAs and 60% DIEPs with no TRAM flaps in 215 consecutive patients over the same time period, and states of the SIEA 'this may be the flap of the future'. Other authors have adopted protocols of exploring the SIEA vessels and considering their use if greater than or equal to 1.5mm at the vessel origin[303;321], converting to a DIEP flap (or muscle-sparing TRAM) if the SIEA vessels are not suitable.

The DIEP vessels have a longer pedicle length and therefore have more options for the flap orientation when inset in breast reconstruction, and also gives the option of using the thoracodorsal vessels. Heitmann et al in 1999 performed 40 cadaver dissections and found that the DIEP vessels were present in all dissections and that the average pedicle length was 10.3cm (9 - 13cm)[286]. The average vessel diameter was 3.6mm (range 2.8mm - 5mm) and the major perforators were located within a radius of 8cm below the umbilicus. The vessel size, constant presence and longer pedicle make the DIEP an easier choice than the SIEA for pre-operative planning, vessel anastomosis and flap inset.

6.5.3 Perforator topography

Blondeel in 1994, when describing the operative procedure of a patient undergoing bilateral DIEP flap breast reconstruction, stated that the main disadvantage of the DIEP in comparison with the TRAM flap is 'a more difficult pedicle dissection especially in the intramuscular portion of the pedicle'[295]. In 2001 Vandervoort et al documented this intramuscular perforator course in 100 consecutive patients, and similarly commented that 'it is the topography of the perforators within the flap and their relation to the rectus abdominis muscle and fascia that determines the degree of difficulty in dissecting these perforators

through the muscle down to their origin on the deep inferior epigastric artery'[322]. They identified five groups of perforators; short intramuscular course when the length in the muscle was less than 4 cm (65%), long intramuscular course when greater than 4cm in the muscle fibres (9%), subfascial perforators running under the fascia before entering the muscle (5%), paramedian perforators when located at the medial border of the rectus abdominis muscle (5%) and, and those perforators arising at the tendinous intersection (16%). The average time for dissection of the short intramuscular perforator was 110 minutes (138 minutes for two perforators), for the long intramuscular course 120 minutes (185 minutes for two perforators), 160 minutes for a subfascial perforator, 122 minutes for a paramedian perforator, and 103 minutes for a perforator at the tendinous intersection (150 minutes for two perforators). This study demonstrated that the course of the perforator chosen plays a large part in determining the patient's overall operative time. The location of the perforator is only one factor in the decision of which perforator to use, as the calibre of the perforators is a fundamentally important observation for flap perfusion. A medial perforator was thought to provide better perfusion to zone 4 than a lateral perforator, which is important if designing a large flap. It is also of note in this study, as in may other studies[21;294;296;299;323], that the authors felt that one large perforator (used in 74% of flaps) was sufficient for perfusion of the whole flap.

Munhoz et al in 2004 looked at medial and lateral row perforators in DIEP flaps, harvesting 30 cadaver DIEP flaps and 35 DIEP flaps in patients undergoing breast reconstruction[324]. An average of 6.1 perforators were dissected per flap with 66% being in the medial row (medial third of muscle) and 34% in the lateral row (lateral third of muscle), with the lateral row perforators following a rectilinear course and the medial row perforators a more oblique course. When harvesting the DIEP this means that a lateral row perforator is likely to be easier to dissect than a medial row perforator, as it has a perpendicular course through the muscle. Again, the authors do comment that although this is useful information it should not be used as a major selection criteria for the vessel used ahead of vessel calibre.

Carramenha e Costa et al in 1986 performed an anatomical study of 12 cadavers to investigate the venous drainage of the Transverse Rectus Abdominis flap and

found that drainage occurs from the cutaneous part of the flap to the deep inferior epigastric vessels through vertical perforators that are mainly periumbilical[287]. When designing a flap they emphasised the importance of including periumbilical perforators. Imanishi et al, 2003, performed arterial and venous injection studies on eight cadavers to investigate the relationship between the superficial inferior epigastric vein and the paraumbilical arterial and venous perforators[285]. They found that in the paraumbilical region there were relatively large paraumbilical arterial perforators, with a large skin territory, and accompanied by a vein. The superficial inferior epigastric vein (SIEV) did not accompany an artery, and formed a venous network. It was not clear which of these two pathways of venous drainage was dominant physiologically, but the authors suggested that the superficial inferior epigastric vein could lead to safe extension of the flap, analogous to using the cephalic vein in the free radial forearm flap.

The venous anatomy of the lower abdomen has been less extensively studied that the arterial anatomy, although venous congestion of flaps is not infrequently seen and can lead to partial or complete flap loss. In an anatomical study of 18 specimens by Blondeel et al in 1998 it was noted that branches always connected the superficial venous system to the deep system, and that in 18% there were large side branches crossing the midline, in 45% there were indirect connections through smaller veins, and in 36% there were no medial crosslinking branches. The potential clinical implications are discussed in 6.5.5 below. Rozen et al in 2009 studied 8 cadavers and 100 pre-operative lower abdominal CT scans in DIEP patients[284]. They found no SIEV branches crossing the midline in one out of 16 cadaver hemiabdomens and in 14% pre-operative CT scans. The SIEV had deep branches penetrating the anterior rectus sheath and draining into the venae comitantes of the deep inferior epigastric vein perforators, although this was only seen in 90% and for one to three perforators in these patients. The authors recommend the use of CT scanning preoperatively to identify the SIEV and its communication with the deep system, to look for midline crossover, and to help determine the dominance of the superficial or deep system for each individual patient.

6.5.4 Pre-operative imaging

Surgeons frequently use hand held Doppler devices preoperatively to identify the position of vessels and perforators, and then mark this position on the patient's skin. Unidirectional Doppler ultrasound is an quick and easy method of roughly identifying where vessels are, but it is not sensitive and does not give any indication of a perforators course through muscle[296;325]. Identification of the arterial and venous topography and location of the largest calibre vessels takes time and experience, and intraoperative decision making. Pre-operative imaging, by CT or MRI scanning, providing the location and evaluation of perforators and superficial inferior epigastric vessels, can aid in this decision making potentially reducing the operative time and improving the reconstructive outcome. Mihara et al in 2008 described multidetector computed tomography as 'illuminating reconstructive surgery in a manner analogous to Edison's development of the light bulb in 1879'[326].

Multidetector row CT angiography has in the last 5 years become the accepted standard for pre-operative imaging of lower abdominal flaps[327-330]. It has been shown to decrease the operative time[327-329;331;332], decrease the incidence of hernia[327] and abdominal wall bulge[332], increase the number of medial perforators used[327] and reduce the overall number of perforators used[327;332], and minimises surgical errors in the identification of the vascular anatomy[331]. The concordance of CT with intraoperative findings has been found to be very satisfactory by surgeons using this technique[329;332;333]. A cadaver study in 2008 of 10 cadavers and 154 perforators found CT angiography to have a sensitivity of 96% and a positive predictive value of 95% overall[334]. For mapping perforators greater than 1mm in diameter the sensitivity and positive predictive value both increased to an impressive 100%. Similarly Masia et al in 2008 in their first 36 clinical cases of using multidetector row CT found an 'absolute correlation' between the radiological information and the intraoperative findings[329].

The Navarra meeting in 2008 aimed to discuss the imaging modalities available and improve and standardise current techniques[330]. The 'ideal' vascular pedicle to maximise the speed and ease of the operation was described as; a large-calibre deep inferior epigastric perforating artery and veins, a central location within the flap, a short intramuscular course, perforating veins communicating with the superficial venous network, broad subcutaneous branching, and a

longer subfascial course and avoiding tendinous intersections. It was recommended that the surgeon and radiologist interpret the three-dimensional images together, and the two-dimensional images should be produced as the perforators emerge from the rectus sheath, and to show the DIEA and its main branching pattern, with the umbilicus as a point of reference. As well as being able to select out perforators preoperatively and hopefully maximise the vascularity of the flap, preoperative CT angiography can give the surgeon warning of any unfavourable and unusual variations in the anatomy[335;336].

CT scanning, although able to identify the vessels, has no clear way of differentiating between perforating arteries and veins, which can also be an issue with the SIEV and SIEA. An 'arterial-phase' scan where the contrast has reached only the arteries can improve accuracy for the arteries although this does not aid visualisation of the veins. Disadvantages of CT include the radiation dose, reported in one study as 5.6mSv, which is lower than a conventional abdominal CT scan[329]. Contraindications to the use of CT would include a sensitivity to IV contrast or renal impairment, and claustrophobia, although the number of CT detector rows influence how fast a scan can be preformed[325].

Other possible modalities of investigation include two-dimensional ultrasound and magnetic resonance angiography MRA. Two-dimensional ultrasound used pre-operatively in a comparative study by Rozen et al in 2008 was found to be inferior to CT scanning in 'all outcome measures', including identification of the major branches of the deep inferior epigastric artery, identifying the SIEA, and the intraoperative correlation with pre-operative findings[331]. MRA has the advantage over CT of avoiding ionizing radiation to the patient, although currently the images are not as detailed[325] (vessels are visible down to 1mm with MRA and down to 0.3mm with CTA[337;338]) and the scanning time is longer. It is the only other imaging modality to provide the three dimensional information required to have similar benefits to CT and may rival CT as technology progresses.

6.5.5 Flap perfusion

The number of perforators required for a DIEP flap and the position of these perforators either in the medial row or lateral row is one of the uncertainties among surgeons, and is often a compromise between donor site morbidity

related to the extent of the intramuscular dissection, operation time, and the size of the flap required. Venous anatomy and venous congestion are a confounding factor in flap perfusion, and reducing this perfusion can lead to fat necrosis or partial necrosis of the flap postoperatively. The pathophysiology of necrosis in flaps in relation to arterial and venous flow is not completely elucidated.

6.5.5.1 Number of perforators and row of perforators

Intraoperatively, the vessel chosen to perfuse a DIEP flap is the largest perforator, and similarly a SIEA flap is only undertaken if the vessel is above a certain size, for example many authors state greater than 1.5mm as discussed previously. With the DIEP flap, unlike the SIEA or TRAM flap, there is an option to include more than one perforator, dissecting the chosen vessels back to their common origin. A simple mathematical study, by Patel & Keller, comparing the resistance and flow circuits with one perforator or multiple perforators concludes that including the largest perforator and adding additional perforators will decrease the resistance and increase the flow, but the magnitude of the benefit may be small in comparison to donor site trauma[339]. For example choosing the largest perforator and adding a perforator with a diameter 0.9 times the largest diameter will decrease the resistance to 0.6 times the resistance of the largest perforator alone, whereas adding an additional perforator with 0.5 times the diameter of the single large perforator will only decrease the resistance to 0.9 times the largest perforator alone. Alternatively, not including the largest perforator but opting for two perforators with 0.84 times the radius of the largest perforator would give the same flow as the largest perforator alone. If three perforators are chosen, their radius would need to be 0.76 times the diameter of the largest perforator to give the same flow. The calculations also apply to the venous drainage of the flap, and as the venous system is of lower pressure than the arterial system, the authors comment that resistance in the venous system is even more significant. Practically, the logic of this study would support the use of the SIEV for additional drainage, although the use of one versus multiple perforators would depend very individually on perforators size and the impact on the muscle, fascia and operative time.

A study by Rubino et al in 2008 correlated the postoperative flow rate with the weight of the flap in 25 patients, 6 undergoing anterolateral thigh flaps and 19 undergoing DIEP flaps[302]. The flow in the flaps, measured one month postoperatively by Doppler ultrasound, was positively correlated with the weight of the flap ($p<0.001$). As the arterial inflow to a flap should equal the venous outflow, these data were then used to calculate the minimum diameter of veins to drain different sizes of flap, for example 1.3mm for a 300 gram flap, 1.5mm for a 500 gram flap, and 1.75mm for a 900 gram flap. If the venous diameter is not adequate, a higher pressure is required to drain the flap and the flap would then be at risk of venous congestion. The effect of the recipient vessels on flow rate has also been investigated, and in a study of 25 patients undergoing TRAM flaps by Lorenzetti et al in 2005, there was no difference found in TRAM flap flow whether anastomosed to the lower flow thoracodorsal vessels or the higher flow internal mammary vessels[340]. Lorenzetti concluded from this study and a prior study[301] that the 'intake of blood in a free flap is not dependent on the recipient artery but on the tissue components of the flap'.

More recently, a rat study by Miyamoto et al in 2008, aimed to investigate the effect of recipient arterial blood flow on free flap survival area[290]. Sixty-four rats were split into 3 groups and a 3 territory skin paddle (2 x 8 cm from scapula to hip) was designed on their abdomen. Group 1 had the flap raised on the axillary vessels, and the pedicle was then clamped to give an ischaemic time of 60 minutes after flap elevation. In group 2, the flap was raised in the same way as group 1, before being divided and anastomosed to the common carotid artery and external jugular vein. In group 3, the flap was raised and the axillary vessels were anastomosed to the femoral vessels. The flaps were examined at 5 days and whole-body angiography performed. Group 1, the pedicled flap control group, had an 81.2% survival rate. The authors thought that angiography showed that the first choke zone but not the second dilated to some extent, and thus the distal portion of the flap underwent necrosis. In group 2, the survival rate was 94.3%, and this was significantly better than group 1 ($p<0.01$). Multiple choke vessels of both zones dilated. In group 3 the survival rate was 82.3% and this was not significantly different from group 1 ($p=0.97$), but significantly different to group 2 ($p<0.01$). The structural changes on arteriography were similar to group 1. The mean arterial blood flow in the pedicle artery in group 2 (0.86 ml/min) was significantly greater than group 3 (0.64 ml/min), $p=0.04$. The

authors conclusion was that the choice of recipient artery affects the survival area of a free flap. They also comment that the literature suggests that free flap survival depends only upon its vascular anatomy, contrary to this study suggesting that blood inflow from a recipient artery is important in determining free flap survival area, especially in an extended flap. Of note, this study is a rat study examining an extreme, with an extended flap model, whereas patient studies by Rubino[302] and Lorenzetti[340], were of DIEP, TRAM and anterolateral thigh flaps. Rubino's study measured flap inflow one month postoperatively and found no difference in flow irrespective of recipient artery, whereas the rat study examines flow at five days, a period after choke vessel opening although perhaps prior to the vascular remodelling at one month. Lorenzetti conversely looks at flow immediately after TRAM transfer and anastomosis, and found that blood flow increased in the thoracodorsal artery and similarly decreased in the internal mammary artery to match the donor artery, within 30 minutes of anastomosis. It would seem likely from these apparently conflicting studies that the flap constituents and vascular anatomy is the main determinant of flow, provided that sufficient flow to the flap can be provided unlike the Miyamoto's extended flap model.

6.5.5.2 Venous congestion

Blondeel et al in 1998 performed a two centre retrospective study of 240 DIEP flaps and 271 TRAM flaps to look at the incidence of venous congestion of the entire flap and the incidence of venous congestion in zone 4, and strategies to deal with this[280]. Fifteen cadaver and 3 abdominoplasty specimens were also examined following injection to further investigate zone 4. The overall failure rate in DIEP flaps was 1.6%, and 1.5% in the TRAM group. Five DIEP flaps had severe diffuse venous congestion that required a microvascular anastomosis to the superficial inferior epigastric vein to save the flap. In these cases the superficial inferior epigastric vein was noted to be particularly large, and it is suggested by the authors that if a large SIEV is observed clinically the vein should be preserved for a secondary anastomosis if flap salvage is required. Alternatively the SIEV can be additionally primarily anastomosed. In the anatomical studies it was noted that branches always connected the superficial venous system to the deep system, and that in 18% there were large side branches crossing the midline, in 45% there were indirect connections through smaller veins, and in 36% there were no medial crosslinking branches. As

discussed above(6.5.3 Perforator topography), a later study by Rozen et al[284] in 2009 found in cadaveric and clinical studies that the SIEV failed to cross the midline in 13% of cases overall. Blondeel associated his findings with the poor venous drainage of zone 4 which is furthest from the midline, and with the variability and unpredictability of blood flow in zone 4. Blondeel and Kroll note that this problem in zone 4 appears to be more apparent in DIEP rather than free TRAM flaps, perhaps because there are only one or two perforating veins in the DIEP. Despite the variability in zone 4 the authors comment that the DIEP is their preferred option for breast reconstruction due to the donor site benefits.

The dominance of the superficial or deep venous systems in DIEP flaps suggested by Rozen et al on account of the current literature is a SIEV greater than 1.5mm for superficial system dominance, and a perforating DIEV greater than 1mm for deep system dominance[284]. Ayhan et al[291] investigated the correlation between the diameters of the superficial and deep inferior epigastric systems, following Kroll[299] and Blondeel's[280] impression that the size of the superficial inferior epigastric vein is inversely proportional to the perforators from the deep inferior epigastric system. Fifty patients undergoing breast reconstruction were preoperatively examined using colour Doppler ultrasound. They found a slight inverse correlation between the size of the superficial and deep systems, but this was not significant. There was a strong correlation between SIEVs on both sides, and a strong correlation between the deep inferior epigastric artery and vein on the same side and on the contralateral side.

Schaverien et al performed a retrospective study published in 2010 to further investigate the venous anatomy of the lower abdomen and its relationship to venous congestion[341]. Fifty-four DIEP flaps that had undergone contrast-enhanced magnetic resonance angiography (MRA) pre-operatively were reviewed. Seven of these flaps suffered from venous congestion and all of these were found to have had no direct connection between the venae comitantes of the deep system and the main arborisation of the SIEV. Only one of the remaining 46 flaps had a similar anatomy with no direct connection between the perforator venae comitantes and the SIEV. The occurrence of venous congestion and the lack of a direct connection between the superficial and deep systems was found to be extremely significant ($p<0.0001$). Additionally the number of perforators did not make a difference to the incidence of venous congestion

(p=0.33). Anatomically, only 68% of perforators had a direct connection with the main arborisation of the SIEV. The authors later suggested that in scenarios where one dominant perforator was not present, multiple perforators may increase the chance of including in the flap a perforator that directly drains the flap through a direct connection to the superficial system, and cited this as a possible partial explanation for the reduction in fat necrosis with multiple perforators seen in Baumann's paper[293;323].

The size of the perforating veins that had a direct connection was also investigated by Schaverian et al[341]. The veins had a mean diameter of 2.6mm which was significantly bigger than those without a direct connection of diameter 2.3mm (p=0.02). Also, those veins with a direct connection between superficial and deep systems were more likely to be in the medial row of perforators (p<0.01). These findings would suggest that in DIEP flaps where there is no direct connection between superficial and deep systems, there is a high risk of venous congestion leading to salvage procedures, for example performing a further anastomosis using the SIEV, and potentially flap failure. The findings are in support of other authors' technique of additionally performing and anastomosis using the SIEV during the original flap transfer or preserving it for a salvage procedure[280;285;299;322;342-347], although unlike Blondeel's study[280] no relationship was found between the size of the SIEV and the incidence of venous congestion.

6.5.5.3 Venous congestion versus arterial inflow

A rat study designed by Yamamoto et al in 1997 was designed to look at the relative importance of arterial inflow versus venous outflow in flap survival[289]. Thirty rats had abdominal perforator flaps and the femoral artery and vein, proximal to the superficial inferior epigastric system, were in various combinations clamped and unclamped to mimic increases in arterial and venous flow. The rats were then divided into three groups; a control group with both the SIEA and SIEV ligated, an enhanced arterial inflow group ('supercharged') with the SIEA retained and the SIEV ligated, and a supplemental venous outflow group ('superdrainage') with the SIEV retained and the SIEA ligated. The area of flap necrosis was recorded at 7 days. The surviving area was 77 ± 11.3% in the control group, 86.9 ± 8.8% in the supplemental venous outflow groups, and 93.3 ± 10.6% in the enhanced arterial inflow group. The enhanced arterial inflow

group was the only group to have a statistically significant improvement in survival area. The authors concluded that the major factor contributing to partial necrosis in the rat perforator flap model was arterial inflow rather than venous outflow. A similar study prior to this study by Hallock et al investigated only enhancing venous outflow again with the SIEV as a supplemental vein[348]. They found that enhancing venous outflow resulted in a significant ($p<0.027$) increase in flap survival at 48 hours. Of note in Yamamoto's study, of the enhanced arterial inflow group the flaps that entirely survived were those with the lower initial venous pressure. It would seem reasonable to presume that whilst arterial inflow may be the more important factor in flap survival, increased venous drainage is likely to be beneficial especially if indicated clinically.

6.5.6 Fat necrosis and partial necrosis

Partial necrosis is necrosis of any part of the visible skin paddle, and includes the underlying fat, and is often obvious within the first week. Fat necrosis is similar although does not involve the skin and is therefore detected as any palpable firmness which is not thought to be from any other cause, weeks to months post-operatively. On physical examination, necrotic, hard tissue apart from reducing the quality of the reconstruction, can mimic breast cancer causing the patient further anxiety and distress. Surgical excision if required, may reduce the aesthetic result of the breast reconstruction. If an area of partial necrosis is large, additional skin coverage maybe necessary depending upon the extent of the necrosis, and this may require a further flap and reconstructive procedure to bring healthy tissue into the area. Both can cause significant wound healing problems and can lead to infection deep in the reconstructed breast tissue. If the patient is having an immediate reconstruction at the time of mastectomy, problems healing can delay adjuvant radiotherapy and chemotherapy, and therefore also negatively affect cancer treatment. Surgeons attempt to minimise fat necrosis by intraoperatively excising areas of the flap, before transfer to the recipient site, that they from both experience and intraoperative observation suspect to have inadequate perfusion. This frequently involves zone 4[305], and then depending upon the positions of the perforators, and the size of the flap, parts of zones 2 and 3. Factors that have been associated with increased fat necrosis in autologous breast reconstructions

include smoking[293;297;310;349;350], chest wall irradiation[349-351], obesity[263;310;349;350;352], and flap size[299;350].

The rates quoted in the literature for partial necrosis of DIEP flaps range between 1.8% and 8.7%[299;350;353], and the rates of fat necrosis between 6% and 36%[262;264;299;310;311;350;353-356]. For TRAM flaps the rate of partial necrosis is around 2%[299], and the rate of fat necrosis between 4% and 12.9%[264;299;310-312;349]. A meta-analysis by Man et al including 1920 DIEPs and 3185 free TRAM flaps quotes the partial necrosis rate as 2.5% and 1.8% for DIEPs and TRAMs respectively, and similarly 10.1% and 4.9% for fat necrosis. There are fewer large series of SIEA flaps documented and a rate of partial loss quoted is 5.1%[281], and between 1%[281] and 14% for fat necrosis14%[24;293].

Fat necrosis can be difficult to document as it is difficult to quantify and does not appear in photographic records[293]. Peeters et al demonstrated this in 202 DIEPs with a 14% rate of clinically detected fat necrosis, and a 35% rate of ultrasound detected fat necrosis[355]. Seven percent of the total DIEPs performed required a further surgical procedure due to fat necrosis. Additionally Peeters et al found no association between fat necrosis and smoking or radiotherapy, two of the most implicated factors by other studies, and did not recommend delayed breast reconstruction in patients who possibly needed radiotherapy regarding fat necrosis. The published literature shows no definite association between fat necrosis and flap type, and although some authors have shown a trend of higher incidence of fat necrosis in DIEP flaps than TRAM flaps[280;299;311], this depends upon flap selection criteria and whether the TRAM flap group includes both muscle-sparing and non-muscle sparing TRAM flaps.

An early study by Kroll et al in 2000 compared the difference in fat necrosis between the free TRAM flap and the DIEP flap[299]. A retrospective review of 279 TRAM flaps revealed a partial flap loss or partial necrosis rate of 2.2% and a fat necrosis rate of 12.9%. The first eight DIEP flaps were selected in the same way as the TRAM flaps and the partial necrosis rate was found to be 37.5% and the fat necrosis rate 62.5%. These differences were statistically significant ($p=0.002$). Due to these high rates of necrosis more rigid selection criteria were introduced and DIEPs were performed only if no more than 70% of the TRAM flap skin paddle would be required to reconstruct the breast, and if the perforators

supplying the flap had a vein at least 1mm. In this selected group of 23 DIEP flap patients, the rate of partial necrosis was 8.7% and the rate of fat necrosis was 17.4%, which was not significantly different from the TRAM group (partial necrosis p=0.117, fat necrosis p=0.509). Multiple logistical regression was then used to analyse all flaps and control for confounding factors such as smoking and the use of bilateral reconstructions, and in this scenario the DIEP flap was predictive for partial necrosis (p=0.004) but not for fat necrosis (p=0.101). On account of these findings Kroll recommends judgement when using DIEP flaps including avoidance in smokers unless they have particularly large perforators and where more than 70% of the lower abdominal flap is likely to be required for the reconstruction. Preserving the SIEV is also suggested, as recommended by Blondeel[280] for additional flap drainage. The authors comment that the although blood supply of the DIEP flap is less robust than that of the TRAM, the DIEP flap is a very useful tool, with significantly reduced patient morbidity.

A meta-analysis published by Man et al[311] as discussed previously(6.5.1), included six studies that compared complications of both DIEPs and TRAMs[264;292;294;299;310;312], allowing relative risks to be calculated. There was found to be a two-fold increase in the risk for fat necrosis in patients receiving DIEP flaps compared to those with TRAM flaps. When the data were limited to the muscle-sparing TRAM flaps there was no difference in the rate of fat necrosis between DIEP and TRAM flaps. Man et al also pooled the data from 16 DIEP studies (1920 DIEP flaps) and 23 TRAM studies (3185 free TRAM flaps) and again found that DIEPs had twice the risk of fat necrosis (4.9% versus 10%) of all TRAM flaps. This study shows that the trade-off for improving the rate of fat necrosis for a DIEP would be instead to perform a full muscle free TRAM flap, which has understandably lost popularity due to donor site morbidity.

Baumann et al in 2010 investigated 228 consecutive abdominal free flap breast reconstructions, muscle-sparing TRAMs, DIEPs and SIEAs, to look for an association between perforator number and fat necrosis[293]. Fat necrosis was defined as any palpable firmness, nodule or mass greater than one centimetre in diameter that was present beyond 6 weeks after surgery. Flaps were categorised into four groups; group one was all 37 SIEAs, group two included all flaps with 1 - 2 musculocutaneous perforators (52 DIEPs, 12 TRAMs), group three included all flaps with 3 - 5 musculocutaneous perforators (19 DIEPs, 82 TRAMs),

and group four included all flaps with greater than 5 perforators (26 TRAMs). The incidence of fat necrosis for the SIEAs was 14%, 25% for one to two perforators, 5% for 3 - 5 perforators, and 19% for more than five perforators. The overall incidence of fat necrosis was 14%. Baumann found that the incidence of fat necrosis was significantly related to the number of perforators (p=0.007). Flaps with 1 - 2 perforators (25%) had a five-fold higher incidence of fats necrosis than those with the optimal number of 3 - 5 perforators (5%), and SIEAs had an intermediate rate of fat necrosis of 14%. Flaps with more than 5 perforators were inherently those flaps that lacked a dominant perforators and as many small perforators as practical were included. These flaps were often distressed and had a 19% incidence of fat necrosis. There was an increased risk of fat necrosis with smoking (p=0.018), and with inclusion of the midline zone contralateral to the pedicle of the flap (termed zone 3 in this study, Hartrampf zone 2) (p=0.049), and both were independent of the number of perforators. There were no data as to whether the perforating vessels were medial row or lateral row perforators.

Baumann et al found that flap type, laterality of reconstruction, recipient vessels, radiation therapy, timing of reconstruction, year of surgery, perforator score, ischaemia time, patient age, body mass index, bra size, and follow-up time did not have a significant independent effect on the incidence of fat necrosis. A study of 71 patients undergoing 80 DIEP flaps in normal (BMI < 25), overweight (BMI 25 - 29.9) and obese groups (BMI > 35), by Garvey et al similarly found no difference in the rate of fat necrosis with increasing weight, although there was a trend towards wound healing complications[357]. The perforator score used by Baumann et al was a score given for perforator size ('3' for <0.5mm, '5' for 0.5-1mm, '7' for >1mm) to account for blood flow to the flap rather than only perforator number[293]. This was not found to be significant and again it was thought to be the inadequate distribution of perforators rather than the blood flow though the perforators that was associated with fat necrosis. Interestingly there was no association between necrosis and flap type as in Kroll's study of DIEPs and TRAMs[299] and Man's analysis of studies comparing only muscle-sparing TRAM flaps and DIEPs[264;292;294;299;310-312]. Baumann notes that the flaps were evaluated intraoperatively for adequate perfusion, and in patients who were smokers or those who required inclusion of the flap across the midline, the threshold for performing a muscle-sparing TRAM was lower rather than insisting

on a DIEP flap. If areas of the flap were deemed inadequate intraoperatively they were excised. They concluded that DIEP flaps by design had fewer perforators than muscle-sparing TRAM flaps and that this was the reason for the higher rate of fat necrosis (20% versus 11%), rather than it being inherently associated with flap type.

Gill et al's 10 year retrospective review of 758 DIEP flaps found that the incidence of any complication and of fat necrosis was significantly lower with one perforator than with two or more perforators (p=0.0418), and this is in conflict with Baumann's study regarding the number of perforators. Baumann does not make reference to Gill's findings. In a response to Baunmann's study, Rozen et al question the use of external vessel diameter as a reflection of internal flow as the internal radius of the vessel determines this rather than the external radius which cannot account for different vessel wall thicknesses. The difficulty in both Gill and Baumann's studies is the unknown factor of blood flow into the flap, as this would help to clarify the confounding effects of the number of perforators. Other authors speculate that the calibre and flow through vessels are more important in the pathogenesis of fat necrosis then the number of perforators[355]. It would seem likely that the anatomy of individual perforator arteries and veins, know to be variable, and their interconnections, as suggested by Schaverien et al[323;341] fundamentally affect the perfusion of a flap. Increased knowledge related to perforator number, position in the medial or lateral row, order of zones of perfusion and pre-operative vessel imaging demonstrating size and branching patterns may all assist in optimising the perfusion of a flap. Physiological assessment of the flap intraoperatively is a further stage in assessing each individual combination of arteries and veins, and the resulting perfusion. Although the exact pathophysiology of necrosis within flaps has yet to be elucidated, optimisation of both patient factors, such as cessation of smoking, and surgical decision making, should be used to minimise the patients' morbidity due to fat necrosis.

6.5.7 Zones & experimental studies

The blood supply to the skin has been experimentally investigated and documented for over 100 years and reconstructive surgery has provided a very valuable application for this knowledge with the progression from random pattern flaps, to axial and pedicled flaps, and finally free tissue transfer with

the increasing refinement of perforator flaps. The angiosome concept has provided the theoretical background upon which investigation and observation of the blood supply to flaps has been based[2]. The choices available to the reconstructive surgeon are a balance of form and function, and donor site morbidity. The lower abdomen is a common donor site and provides tissue that is a very good match for breast tissue, hence its popularity for use in breast reconstruction. Free TRAM flaps have been almost entirely replaced by muscle-sparing TRAM flaps and DIEP flaps reducing the anatomical damage and donor site morbidity. Donor site morbidity has to be balanced with the recipient site reconstructive quality, and the risk of inadequate perfusion, venous congestion and ultimately fat necrosis, partial necrosis and flap failure[299]. Perforator flaps like the DIEP flap have added a subtle level of choice to the surgeon with each individual patient having a unique pattern of perforating vessels. The choice of perforating vessel, its diameter and flow, the position of the vessel in the medial or lateral row of perforators, its path through the muscle, and the requirement for additional perforators, the venous drainage and the size match of vessels to the recipient vessels must all be considered both pre-operatively and intra-operatively. The SIEA, whilst not a perforator flap, has a very favourable donor site although the variation in its presence, size and area of perfusion again make this choice of vessel individual to each patient.

Generic protocols have been devised by many surgeons based on the current knowledge, for example it is relatively common practice to excise zone 4 in a DIEP flap as it is poorly perfused and at risk of necrosis[305]. Despite this, there are case series of patients who have zone 4 maintained in their breast reconstruction with no significant increase in morbidity. The position of the vessel in the medial row rather than the lateral row has been postulated to increase the vascularity across the midline and increase the perfusion of zone 4. The medial row perforators may result in less donor site morbidity[358]. When more of the flap requires to be excised there is debate over Hartrampf original labelling of zones for DIEPs and TRAMs with zone 2 increasingly thought to be the ipsilateral lateral zone, rather than the contralateral midline zone. Again, perhaps the reallocation of zones is also dependent on whether the perforator is medial or lateral row, and may be more explicable by the concept of 'perforasomes', increasing the accuracy and detail of the angiosome concept. The overall perfusion of the flap and risk of fat necrosis and its relationship to

the number of perforators chosen is debated. The size and flow within each vessel is a confounding factor in the choice of perforators, although with the SIEA flap there is obviously one vessel therefore more specific recommendations regarding the size of vessel have been published.

6.5.7.1 Experimental DIEP studies

Flap perfusion has been subjectively described as more robust in the TRAM flap and muscle-sparing TRAM flap than the DIEP flap. A rat study by Hallock in 2005 compared the survival of TRAM flaps, multiple perforator DIEP flaps and single perforator DIEP flaps in three groups of five rats at 48 hours after flap elevation[348]. The TRAM flap had the greatest flap survival at 96.1%, followed by the muscle-sparing TRAM with 79.8% flap survival, and the DIEP flap with 77.1% survival. The differences were not statistically significant.

Perfusion zones of the DIEP flap are accepted terminology, and mostly referred to as originally described by Hartrampf with zone 2 being the contralateral midline zone, and zone 3 the ipsilateral lateral zone (Figure 6-1). A simplistic view is that both zones 2 and 3 should be re-numbered 2, and that zone 4 should become zone 3[359]. Henry et al[360] suggested calling the zones ipsilateral medial (I_M), ipsilateral lateral (I_L), contralateral medial (C_M) and contralateral lateral (C_L), although this may be cumbersome and doesn't reflect blood supply in any way. The placement of zones 2 and 3 has relevance when the size of the flap is being reduced with the higher the number of zone, the poorer the perfusion. By definition zone 3 would be preferentially excised over zone 2.

Holm et al in 2006 published a series entitled 'Perfusion Zones of the DIEP flap Revisited: A clinical study' aiming to quantitatively assess the perfusion of the lower abdomen and the validity of the Hartrampf perfusion zones[227]. Fifteen DIEP patients were intraoperatively assessed using the method of laser-induced fluorescence of indocyanine green with laser illumination of 780 nanometres. Indocyanine green is a dye injected that absorbs light in the near-infrared range, maximal at 805 nanometres. The indocyanine green dye emits fluorescence at 835 nanometers. The absorption and emission light is said to penetrate to a depth of '3mm and more' in the skin, allowing fluorescence from the deep dermal plexus and subcutaneous fat to be recorded by a near-infrared sensitive videocamera[193]. Perfusion of zones 1, 2, 3 and 4 was seen 25, 41, 32 and 67

seconds respectively after injection. The perfusion index was 76, 25, 47 and 33 percent of normal tissue in zones 1, 2, 3 and 4. Zone four perfusion was completely absent in 5 patients (33%). Zone 3 was perfused more quickly than zone 2 and the perfusion index was of greater intensity. The authors therefore suggest re-numbering zones 2 & 3, with zone 2 being ipsilateral to the pedicle. They suggest that choke vessel anastomoses between vascular territories on the ipsilateral side of the flap are stronger than those across the midline, that the ipsilateral half of the flap has an axial blood supply and the contralateral side a variable random-pattern perfusion, and that the poor perfusion of zone 4 is due to distance from the perforator and the need to pass two choke vessel watersheds.

The finding of better perfusion in zone 3 than zone 2 in Holm et al's study[227] is in agreement with the findings of our study, and would suggest that the order of zones should be changed with zone 2 becoming the ipsilateral lateral zone, as in Dinner's original description[244]. Similarly zone 4 had the worst perfusion. The anatomical basis for these findings stated by Holm et al of a random pattern of blood flow in the midline contralateral zone yet an axial blood supply in the ipsilateral lateral zone, is no more than supposition with the data available. This re-ordering of the zones has been questioned by other authors as being related to the position of perforators in the lateral or medial row[243;245;246], with the lateral row being seen as more likely to have an order of zones as per Holm's or Dinner's original description. Holm's study lists the position of the perforators for each of the 15 flaps and it can be calculated that 53.3% are supplied only by lateral row perforators, 33.3% by both medial and lateral row perforators, and only 13.3% by medial row perforators. Our study has a higher number of flaps supplied by medial row perforators, 60%, with 35% being supplied by both medial and lateral perforators, and 15% being supplied by lateral row perforators. Despite the higher number of medial perforators our data still supports zone 3 (ipsilateral lateral zone) having significantly higher perfusion than zone 2 (contralateral medial zone)($p = 0.025$). Twelve of our flaps were supplied only by medial perforators. In 4 of these 12 flaps (33%) perfusion appears to be better in Hartrampf zone 3 (ipsilateral lateral zone) than zone 2 (contralateral medial zone), as shown in examples Figure 6-12, Figure 6-13 & Figure 6-14 below.

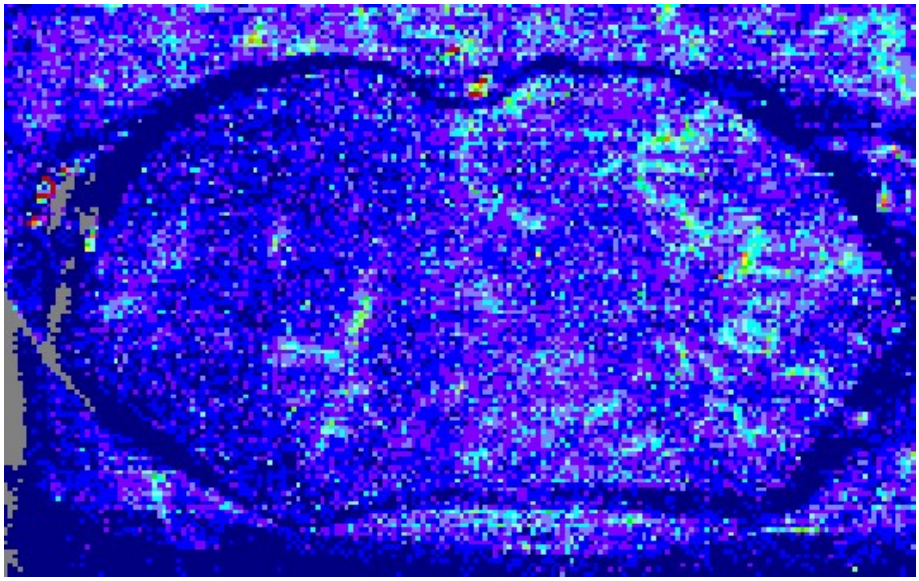

Figure 6-12 - Patient 4 left DIEP laser Doppler scan. Supplied by two medial perforators. Hartrampf zone 3 appears to be better perfused than zone 2.

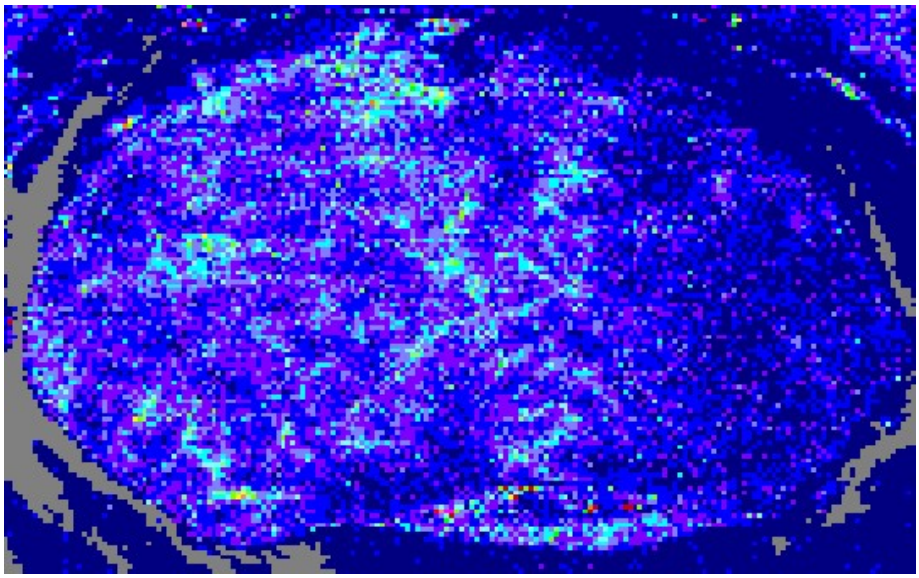

Figure 6-13 - Patient 10, right DIEP laser Doppler scan. Supplied by one medial perforator. Hartrampf zone 3 appears to be better perfused than zone 2.

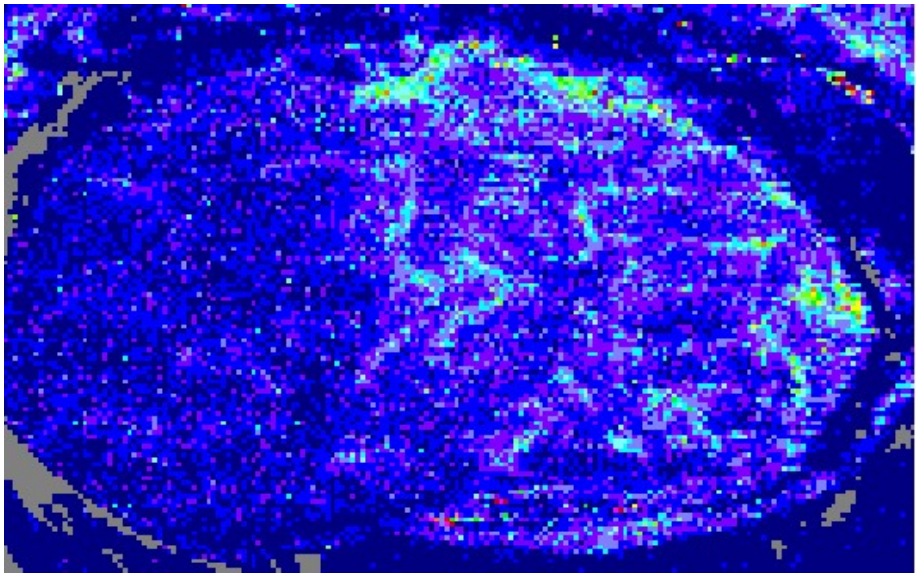

Figure 6-14 - Patient 10, left DIEP laser Doppler scan. Supplied by 3 small medial perforators. Hartrampf zone 3 appears to be better perfused than zone 2.

Schaverien et al, from the Dallas group, investigated the arterial and venous anatomy of the lower abdomen in 12 specimens (10 cadavers and 2 abdominoplasties) using three- and four-dimensional computed tomographic angiography and venography[282]. The injection CT studies compared the medial and lateral perforator rows of the DIEP flap. The medial row perfused a central ellipse with declining perfusion at the edges. Large-diameter vessels connected the medial row perforators across the midline at the level of the subdermal plexus, and the lateral row perforators were perfused bilaterally and this extended to zone four. Injection of a lateral row perforator perfused the ipsilateral lateral flap and lateral row, and perfused the ipsilateral medial row by means of recurrent flow through the subdermal plexus. Perfusion reached the contralateral medial row perforators in some cases, but did not reach the contralateral lateral row perforators. Dye studies of the fresh abdominoplasty specimens confirmed these findings. Schaverien et al postulated that the limit of perfusion is when flow has to pass through the subdermal plexus more than twice. The superficial and deep venous systems were also investigated, with injection of either venous system resulting in filling of all the adjacent venae commitantes. Filling of the adjacent superficial inferior epigastric vein across the midline occurred through vessels crossing the midline at the level of the subdermal plexus. There were no venous branches crossing the midline in one specimen, and this according to the authors may explain why some flaps clinically have diffuse venous congestion. The authors additionally compared the results of cadaveric injections with fresh abdominoplasty specimen dye

injections concluding that cadaveric studies are an underestimate of in vivo perfusion. Schaverien et al's study further clarifies the influence of the medial and lateral perforator rows when defining the DIEP zones of the lower abdomen, and the position of perforators is an important observation in studies of the zones of perfusion.

Two further studies from the Dallas group used CT angiography to investigate the differences in vascular territory based on flap type, and also the differences in vascular territory of the single most dominant DIEP perforator[243;246]. Wong et al used 11 lower abdominal flaps (9 cadaver and 2 abdominoplasty specimens), and simulated the perfusion of 43 flaps; 7 pedicled TRAMs, 8 full TRAMs, 8 muscle-sparing TRAMs, 14 DIEPs and 6 SIEAs[246]. Intravenous omnipaque contrast was used and washed out with saline between simulated perfusions, which according to the authors does not affect the vessel diameter or vascular territory. The pedicled TRAM had the lowest estimated percentage of skin paddle perfused with 32.6% perfused, followed by a lateral perforator DIEP with 32.9%, the SIEA flap with 33.3%, a lateral row muscle-sparing TRAM with 43.2%, a medial perforator DIEP with 44.6%, a medial row muscle-sparing TRAM with 45.7%, and finally the full-width TRAM flap with 48.4% perfused. The results that reached statistical significance included the lateral DIEP versus the full TRAM ($p<0.007$) and the lateral DIEP versus medial DIEP (32.9% v 44.6%)($p<0.02$). The territory of the lateral DIEP appeared similar to the SIEA. The authors therefore recommend the use of a medial row perforator, rather than lateral row perforator, when a large abdominal flap is required. Also noted by four-dimensional computed tomographic angiography in the TRAM models was that if the medial perforator was dominant, Hartrampf zone 2 was perfused earlier and more intensely than zone 3. Conversely, if the lateral row perforator were dominant, then zone 3 was perfused earlier and more intensely than zone 2. This therefore notes Hartrampf's zones of perfusion with zone 2 being the contralateral midline zone, to be correct for medial row perforators, and Holm's proposed change to Dinner's original description with zone 2 being the ipsilateral lateral zone to be correct for lateral row perforators. Holm's study, as mentioned previously had only 2 of 15 flaps that were supplied only by medial perforators, and therefore Wong's assertion of the ordering of the zones being dependent on whether the perforator is medial or lateral could still hold true. Although our study found better perfusion in Hartrampf zone 3 (lateral

ipsilateral zone) for the overall group of DIEPs (60% medial perforators, 35% medial and lateral, 15% lateral), we have examples of medial and lateral row perforators that would support Wong's version of the dominance of Hartrampf zone 2 in the medial perforators (and Hartrampf zone 3 in the lateral perforators), Figure 6-15 & Figure 6-16;

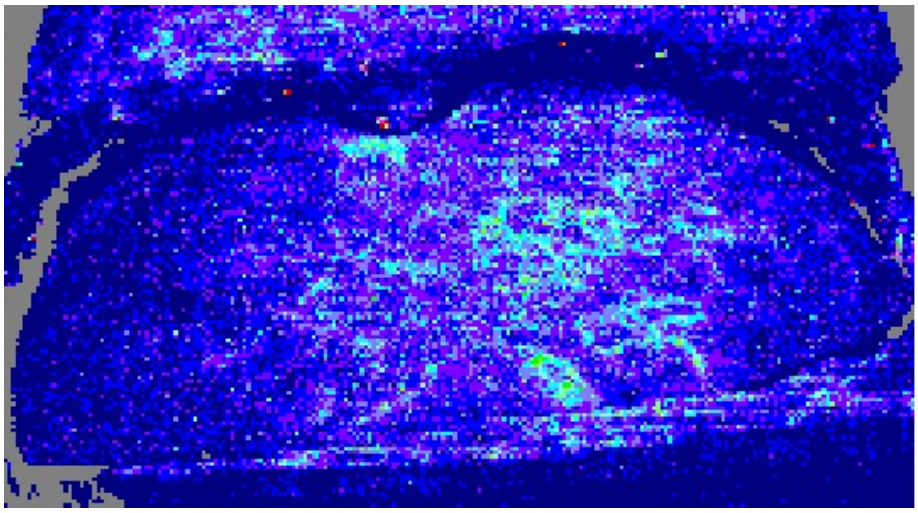

Figure 6-15 - Patient 5, laser Doppler scan of left DIEP with one medial perforator. Hartrampf zone 2 appears to be better perfused than zone 3, and the perfusion area of the flap is centralised.

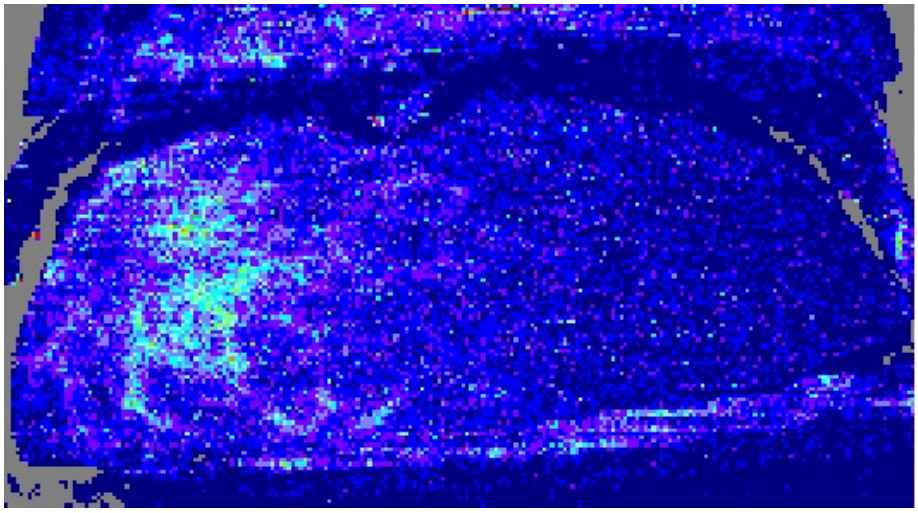

Figure 6-16 - Patient 5, laser Doppler scan of right DIEP with one lateral perforator. Hartrampt zone 3 is better perfused than zone 2, and the perfusion of the flap appears to be hemiabdominal.

Wong's study illustrates this order of perfusion between medial and lateral row with two videos from two individual flaps. It is not clear whether there would be interflap variability in this finding. Additionally as before, it is not a physiological study and involves repeated injections of cadaver specimens which although the authors ascertain the diameter of vessels remains the same, it does

not account for the in vivo vascular reactivity and action of pre-capillary sphincters.

A second study from the Dallas group by Bailey et al investigated the single dominant medial row perforator in the DIEP in 11 abdominal cadaver flaps and 16 patients undergoing DIEP flaps[243]. In the cadaver study they found that injection of the single dominant medial row perforator resulted in vascularisation across the midline in all flaps, predominantly by indirect linking vessels by means of the subdermal plexus. Perfusion was consistently found in all flap dissections in the entire portions of zones 1 and 2, and in the midportions of zones 3 and 4. In the 16 clinical patients, fat necrosis of less than 5 % occurred in 3 patients (16.7% of flaps), and in all cases occurred in the lateral portion of zone 3, concurring with the anatomical results. The authors concluded that the DIEP medial row perforators are the largest perforators in the lower abdomen, and when used, the lateral half of zone 3 and all of zone 4 should be discarded to avoid fat necrosis.

Tregaskiss et al in 2008 used CT scanning in a 10 cadaver injection study of the lower abdomen, with the aim of investigating the arterial anatomy[361]. Their main finding was that the perforators of the deep inferior epigastric artery varied markedly in their orientation and course. There were an average of 7 large (≥0.5mm) DIEA perforators per hemiabdomen (range 5 - 12), with significant differences in the size of their anatomical territories, and no single morphology predominating. Tregaskiss et al found no consistent pattern of deep inferior epigastric perforators, and suggested that a considerable proportion of abdominal flaps rely on a truly random network for their survival. They compare their findings with an in vivo angiographic study by Ohijimi et al of 11 TRAM free flaps[362]. Three of these flaps suffered partial necrosis and 2 of the 3 had no axial artery, the third having an axial artery running alongside the skin paddle. Of the 8 flaps with no necrosis, all had axial arteries. Ohijimi et al also comment that the arterial density is lower in Hartrampf zones 2 and 4, and that there were poor connections across the midline.

Wong et al in a further study in 2010 specifically compared the medial and lateral row DIEP perforators in 22 cadaver flaps, again using CT angiography[363]. They found that zone 2 perfusion was greater in a medial perforator (65.8% of

zone 2 perfused) compared with a lateral perforator (4.8% of zone 2 perfused), and that zone 3 perfusion was greater in a lateral perforator (85.2% of zone 3 perfused) compared with a medial perforator (43.9% of zone 3 perfused) ($p<0.01$). The mean vascular territory for a medial perforator was 296.4cm^2 compared to 195.6cm^2 in the lateral row perforators ($p<0.008$). Their study demonstrates that the lateral row and medial row have different perfusion characteristics which is relevant in flap design when choosing a single perforator. This individual territory for a perforator has been termed a 'perforasome' by Saint-Cyr et al in 2009[283].

Saint-Cyr et al performed an injection and CT angiography study of 217 perforator flaps in 40 cadavers[283]. They set out five principles describing the vascular anatomy of perforasomes, the arterial territory of a perforator. Firstly, perforasomes are linked directly and indirectly, and these two patters of flow are protective mechanisms in the event of a vascular injury. Secondly, flap design and skin paddle orientation should be based on the direction of the linking vessels, which is axial in the extremities and perpendicular in the midline trunk. Thirdly, preferential filling of perforasomes occurs within perforators of the same source artery first, followed by perforators of other adjacent source arteries. Fourthly, mass vascularity near a joint is directed away from that articulation, and where the perforator is at a midpoint between two articulations the flow is multidirectional. Rozen et al similarly described the 'perforator angiosome' in 2010 in a clinical and cadaveric study of 155 abdominal walls[364]. They concluded that there were fundamental differences between the medial and lateral rows, and that the perforator angiosome depends upon location. This would mean that zone 1 represents two different perforasomes, and the next zone is immediately adjacent in all directions. For example a medial row perforator would capture Hartrampf zone 2 and the lateral row of zone 1 as the immediately adjacent perforators. These differences in understanding of the perforator angiosome or perforasome, and additionally Keller's observation of decreased oxygen perfusion in the inferior sections of zone 1[245], led Hallock to note that 'any devised system of schematics or theories must represent no more than a rough guideline' for the designing and planning of a DIEP flap[365]. Hallock recommended an individualised approach and intraoperative mapping, and in view of the many factors including the venous drainage, we would support this view.

6.5.7.2 Experimental SIEA studies

The zones of the SIEA, often referred to in the literature as the same four lower abdominal zones of the DIEP or TRAM flap, are less clearly understood and thought by many to represent hemiabdominal perfusion, with zones 1 and two being ipsilateral to the SIEA vessel[24;274;366]. Holmes et al in 2006 looked at the vascular territory in vivo using indocyanine green injections, in 10 patients undergoing SIEAs and in 5 patients who had SIEA flaps raised before having abdominoplasties performed. The mean body mass index was 30kg/$m^{2.}$ The perfusion of Hartrampf zone 3 occurred first, 25 seconds after dye injection with a perfusion index of 89% of normal tissue, and zone 1 was perfused 30 seconds after injection with a perfusion index of 80%. Zone 2, the contralateral midline zone only had a perfusion index of 8% and was completely missing in four patients. There was no perfusion in zone 4 in any of the patients. This does not correlate with our findings that there is no statistical evidence of a difference between Hartrampf zones 1, 2 and 3 in the SIEA flap. It maybe that the physiological nature of laser Doppler imaging of reveals a larger area of perfusion than indocyanine green injections. In clinical series of 14 patients, Chevray et al describe using a hemiabdominal SIEA flap based on uncertainty of perfusion across the midline as the SIEA vessels enter lateral to the lateral row of DIEP perforators[24].

In contrast to the findings of Holm et al, a study in 2006 by Ulusal et al aimed to estimate the adequacy of perfusion from the superficial system across the midline[191]. Forty four breast reconstructions were recruited and of these, six cases were chosen for SIEA flaps, with pulsatile arteries greater than 1mm diameter. A laser Doppler probe was used to quantify the perfusion from each zone from each of the superficial and deep systems with clamping of each system in turn. With the deep system supplying the flap, zone 1 was significantly better perfused than zone 4 ($p=0.04$). When the superficial system was supplying the flap there was no significant difference between any of the zones, and there was also no statistically significant difference between the superficial and deep systems. Our study compared 19 potential SIEAs and 20 potential DIEPs and therefore has more power than this study in reaching significance, especially in the order of DIEP zones. Regarding the SIEA flap, Ulusal et al state that their study is the 'first documenting the reliability of cutaneous perfusion in all zones (1 - 4) of the abdominal flap by using laser

Doppler flowmetry'. Also the postoperative follow-up in Ulusal's study, shows a 92.3% area survival of the six SIEA flaps, especially impressive as zone 4 was not routinely discarded. This, contrary to the general hemiabdominal perception of SIEA flaps, is in support of our studies findings of no significant difference found in intraoperative perfusion between zones 1, 2 and 3 of the SIEA flap. Examples of our laser Doppler scan are shown in the figures below; Figure 6-17, Figure 6-18, Figure 6-19, Figure 6-20 & Figure 6-21. Although not in vivo studies, two previous cadaveric studies that add support to our findings were; a fluorescein study by Hester et al in 1984[317] who found that in all 20 specimens the only area with questionable or no fluorescence in the equivalent of zone 4, and an ink injection study by Volpe et al in 1994[275] who found that a large area of the medial aspect of the contralateral hemiabdomen was supplied by the SIEA.

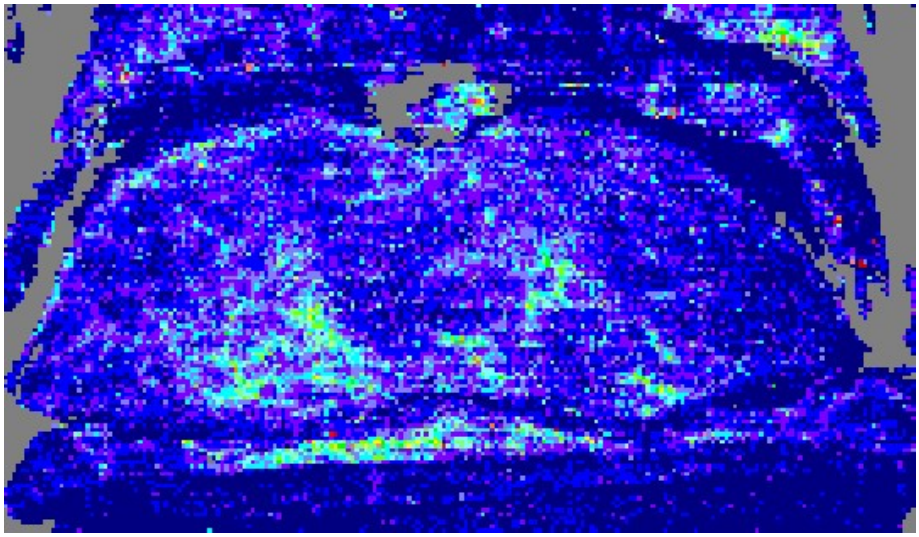

Figure 6-17 - Patient 2, laser Doppler scan of right SIEA.

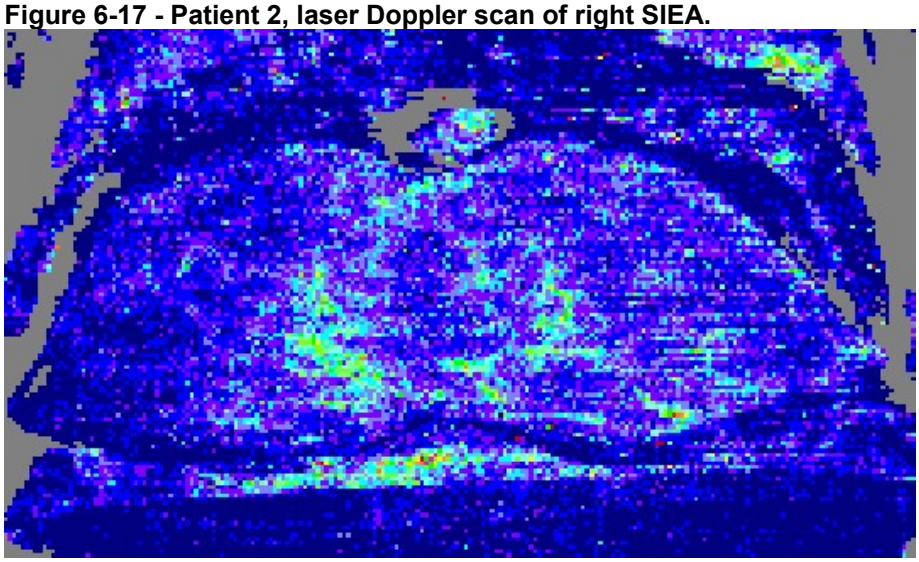

Figure 6-18 - Patient 2. Laser Doppler scan of left SIEA.

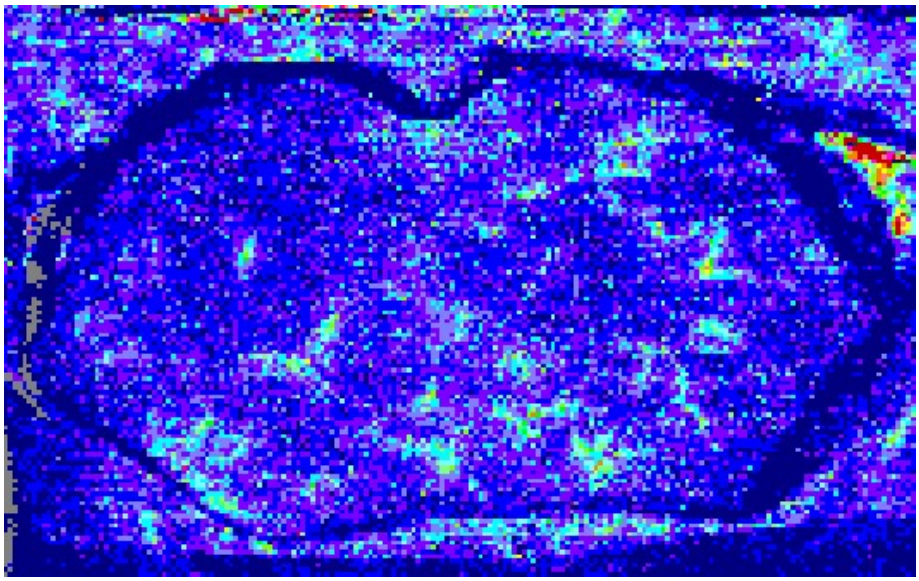

Figure 6-19 - Patient 4. Laser Doppler scan of right SIEA.

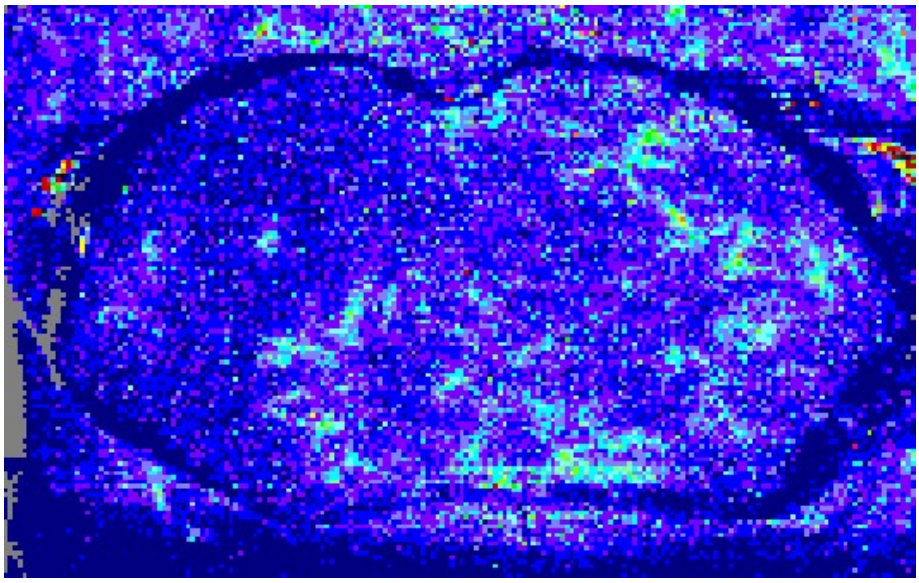

Figure 6-20 - Patient 4. Laser Doppler scan of left SIEA.

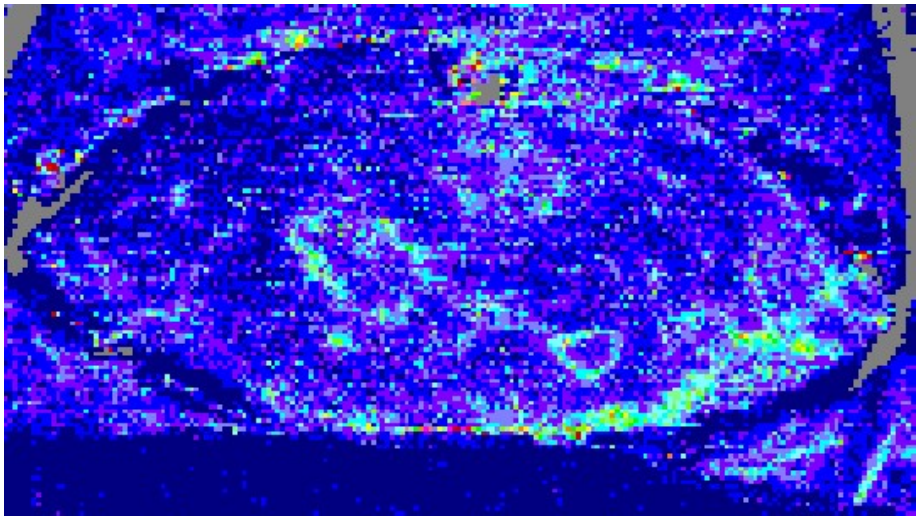

Figure 6-21 - Patient 6. Laser Doppler scan of left SIEA.

Schaverien et al's three- and four-dimensional computed tomographic cadaveric study of the lower abdomen, as discussed previously, also looked at perfusion of the superficial system by cannulating and injecting the SIEA[282]. Branches coursed to the subdermal plexus followed by filling of the ipsilateral lateral and medial row perforators by recurrent flow through the subdermal plexus. Perfusion was not seen contralateral to the midline in any of the specimens. This is in contrast to our findings(examples Figure 6-17 - Figure 6-21), where although a minority of SIEAs appeared hemiabdominal (Figure 6-22 & Figure 6-23), there was no statistical significance between zones 1, 2 &3. The perfusion of the SIEA only appears to have been studied in the cadaveric specimens despite the acknowledgement in the paper that cadaveric studies are an underestimate of in vivo perfusion as shown by the injection of dye into fresh abdominoplasty specimens. Dye does not appear to have been injected into the abdominoplasty SIEA vessel to confirm the territory as hemiabdominal.

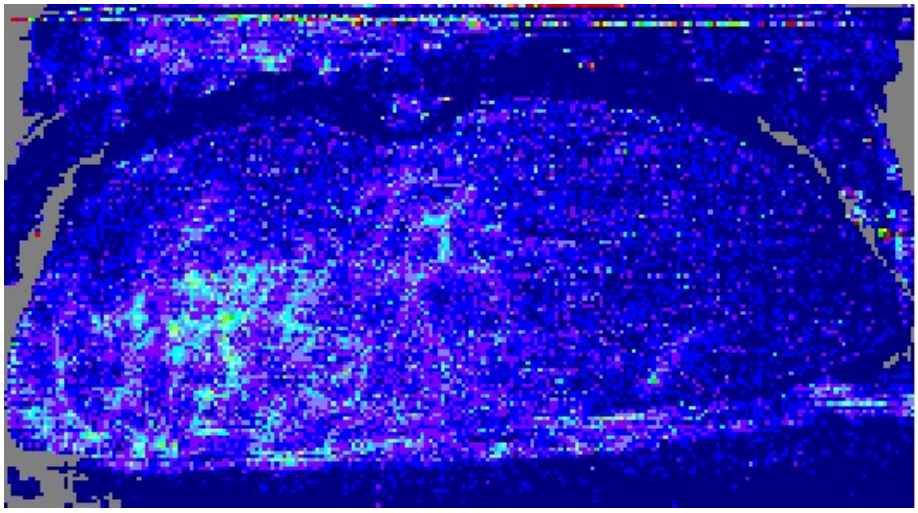

Figure 6-22 - Patient 5. Laser Doppler scan of right SIEA.

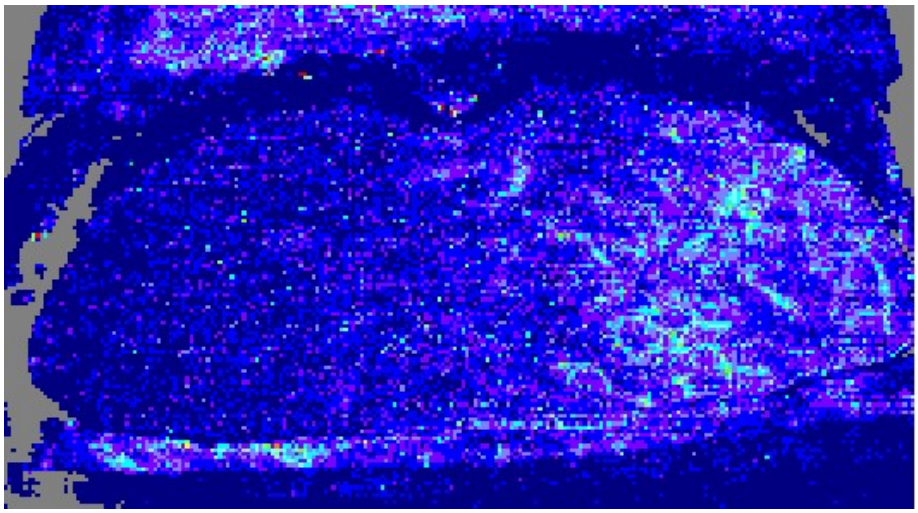

Figure 6-23 - Patient 5. Laser Dopper scan of left SIEA.

Whilst our study found no statistical difference between hartrampf zones 1, 2 & 3 of the SIEA flap, it would appear that there is variability in the territory of the SIEA, with some having more lateral territories and others centralised over zone 1 and crossing the midline (see Appendix for further laser Doppler scans). Holm et al looked at the interindividual variability of the SIEA in 25 SIEA flaps by using laser-induced fluorescence of indocyanine green[196]. The study compared the contributions of the superficial and then deep systems to the lower abdominal flap by sequentially clamping the pedicles. There is no reference in the method to a stabilisation period for completion of reactive hyperaemia before measuring the deep system. Of the 25 patients selected for SIEA flaps, 19 patients had SIEA flaps, the remaining 6 patients underwent DIEP flaps on the basis of intraoperative perfusion measurements. The SIEA territory did not cross the midline in 64% of patients (16 patients), with a dramatic range from zero

percent territory (2 patients) to the entire abdominal ellipse. Four patients (16%) SIEAs stained zones 1 - 4, and four patients (16%) SIEAs stained zone 1 - 3. The remaining 14 SIEAs (56%) stained zone 1 or zones 1 & 2. They felt that the ability to harvest only half the SIEA flap was the main concern with choosing to use a SIEA flap, and recommend bilateral dissection of the superficial system when the whole flap is required. Holm's et al explain the findings by a variably developed anastomotic network at the dermal vessels. Due to this variability, Holm's et al also stress the importance of intraoperative imaging as they found the algorithms of other authors too undifferentiated, and note that intraoperative imaging changed their plan in 44% of patients. Whilst a positive perfusion test is reassuring, it is not clear however whether a negative indocyanine green perfusion test results in inadequate postoperative blood flow. Like Tregaskiss, Holm et al also noted that when the superficial system is well developed, the deep system is smaller in size and vice versa[361].

In conclusion, based on the variability of the superficial system, and the choice of perforators in the deep system, we would suggest laser Doppler scanning as a non-invasive physiological method of intraoperative assessment that can aid in determining the vascular territories. This is especially relevant when there is a choice of vessels, as although poor perfusion may be difficult to correlate with post-operative outcome, preoperative imaging has yet to be correlated with intraoperative perfusion. Intraoperative imaging can therefore provide valuable additional information, aiding surgical judgement and modification of plans based on intraoperative findings. Sequentially clamping the possible vessels, leaving an adequate time for reactive hyperaemia (Chapter 4) between scans, allows the system with optimal flow to be chosen. It also aids in the clinical decision of the areas of the flap to discard. The laser Doppler can additionally be used to check the patency of the anastomosis after flap transfer. The laser Doppler is readily available in many plastic surgery units as it is commonly used for burns assessment. It is non-invasive intraoperative method, unlike laser-induced fluorescence of indocyanine green which requires the indocyanine green dye to be injected. Laser Doppler imaging has a similar wavelength to the laser used in indocyanine green fluorescence, and therefore penetrates the flap to a similar depth in the range of a few millimeters.

Our findings do not support a hemiabdominal SIEA flap, as there was no significance difference between Hartrampf zones 1, 2, and 3. The DIEP flap ordering of zones appears to be Hartrampf zone 1, zone 3, zone 2 and then zone 4 in our study, although this included medial and lateral row perforators, and a mixture of medial and lateral row perforators. A further study would required with a significant number of only medial row perforators to assess whether Hartrampf's zone 2, the midline contralateral zone, is the second zone perfused for a medial perforator. As Rozen et al have suggested, the traditional four lower abdominal zones may not apply to the perforator angiosome or perforasome, further subdividing the zones around the perforator. There are many vascular combinations of arterial perforators, veins and flap dimensions, and whilst the prescribed ordering of zones along with operative protocols is attractive, it is unlikely that this can ever be completely reliable. Individual variability and the combinations of perforators available require intraoperative physiological imaging.

7 Microdialysis analysis of DIEP flaps

7.1 Introduction

The objective of this study is to investigate factors mediating circulatory change within free flaps after free flap transfer.

As discussed in the Introduction (Chapter 1) and Chapter 5, Laser Doppler post-operative perfusion pilot study, angiosomes are three dimensional blocks of tissue supplied by a source artery and vein. These territories are linked to adjacent territories by reduced calibre anastomotic vessels theoretically known as 'choke vessels'[2;367;368]. Choke vessels are thought to dilate in the first 72 hours when blood flow to an area is disrupted, either following surgical delay where the flap is raised in stages, or following immediate flap transfer[30;31]. This dilation continues for 7 days at which point the choke vessels are thought to become irreversibly larger diameter vessels[31].

Delay procedures improve flap survival and have been carried out for hundreds of years. Tagliacozzi in the 16th century was aware that the division of vessels along a flap's length would improve the viable dimensions of the flap. The technique of tubed pedicled flaps was recorded by Filatov, a Russian ophthalmologist using it on the lower eyelid in 1916[369]. Other surgeons followed and the technique of tubed pedicles was popularised by Sir Harold Gilles following his first procedure in 1917 on a burns patient in the First World War[369]. Delay procedures can be carried out surgically, pharmacologically[370] and using laser[371-373]. The physiological mechanism of choke vessel opening has yet to be elucidated and this study was designed to trial the microdialysis technique in investigation of mediators that may be influential in the increase in perfusion in the first 72 hours after flap transfer.

Microdialysis catheters have been used in patient monitoring and research for over 10 years[63;64;69;72-75;374-382]. A small dialysis catheter, which is no bigger than a small surgical drain, is inserted into the area to be monitored. Microdialysis catheters function by using a semipermeable membrane (usually allowing molecules of up to 20 kDaltons to pass) and a dialysis fluid, collecting the dialysate to be analysed in a microvial. They monitor the chemistry of the tissue and do not consume any blood. Lactate, pyruvate, glucose and glycerol are the

routinely used markers of tissue ischaemia when microdialysis is used for flap monitoring. Although originally designed for patients in neurointensive care, many medical specialties have made use of the benefits of early warning of tissue ischaemia. In plastic surgery several of the Scandinavian units use microdialysis routinely for free flap monitoring, and others including Canniesburn Plastic Surgery unit have more recently used microdialysis for 'buried' flaps that cannot be monitored by direct vision, without any significant adverse effects to the patient. Microdialysis catheters to be used in this study have a modification of the semipermeable membrane allowing molecules of up to 100kDaltons to be measured.

Sites of insertion of the microdialysis catheters will be in Hartrampf zones 1, 2 and 4, shown below (Figure 7-1). As discussed in previous chapters the lower abdomen is though to have four zones representing different angiosomes and quality of blood supply when raised as a flap. The DIEP is thought to have four zones, corresponding to angiosomes, two on either side of the midline (Figure 7-1). Zone 1 is the zone in which the anastomosed perforator vessels enter, zone 2 is usually considered to be adjacent to this across the midline (i.e. corresponding contralateral zone), and zone 4 is the next zone adjacent to zone 2. Zone 4 has the poorest blood supply as it is two angiosomes away from the perforating vessels supplying the DIEP flap. Zones 1, 2 and 4 were chosen for insertion of microdialysis catheters to represent contrasting quality of perfusion across the flap.

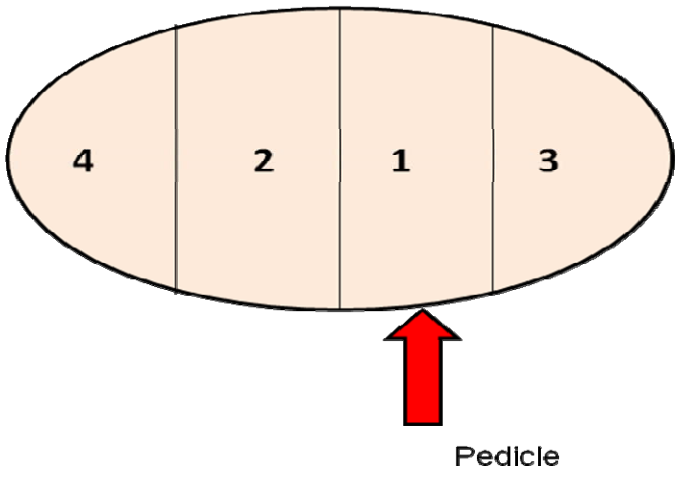

Figure 7-1 - Zones of lower abdomen.
Pedicle marks the vessels that supply the flap.

The samples will be analysed for factors that may be implicated in changes in circulation. This will include markers from an inflammatory response Tumour Necrosis Factor alpha (TNFα, 26 kDaltons)[383] and Interleukin 6 (IL-6, 22-27 kDaltons)[384;385], and Fibroblast Growth Factor basic (FGFβ, 18 kDaltons)[386] involved in angiogenesis. It has been recommended that initial samples are tested for the factors highlighted above to ensure adequate yield before running all samples (54 per patient & 11 patients, 594 samples in total). This has been common practice in similar work they have performed on dialysate samples from muscle, and allows the investigative phase to gain as much information as possible from the small sample volumes.

7.2 Method

Eleven patients undergoing DIEP flap breast reconstruction following mastectomy for breast cancer, were recruited for this study between October 2008 and August 2009. A sample size calculation was performed based on a 20% change in measurement being of physiological significance with probability of type 1 error 0.05, and probability of type 2 error 0.90. There are no previous studies using high-cut off catheters in free flap plastic surgery and therefore this study was a pilot study.

Microdialysis catheters (CMA Stockholm) were used to measure changes in tissue fluid in the DIEP flaps. The catheters chosen were CMA71 'High Cut-Off' Brain Microdialysis catheters (Figure 7-2). This dialysing membrane allows molecules as large as 100 kiloDaltons to pass. The membrane length was 10mm.

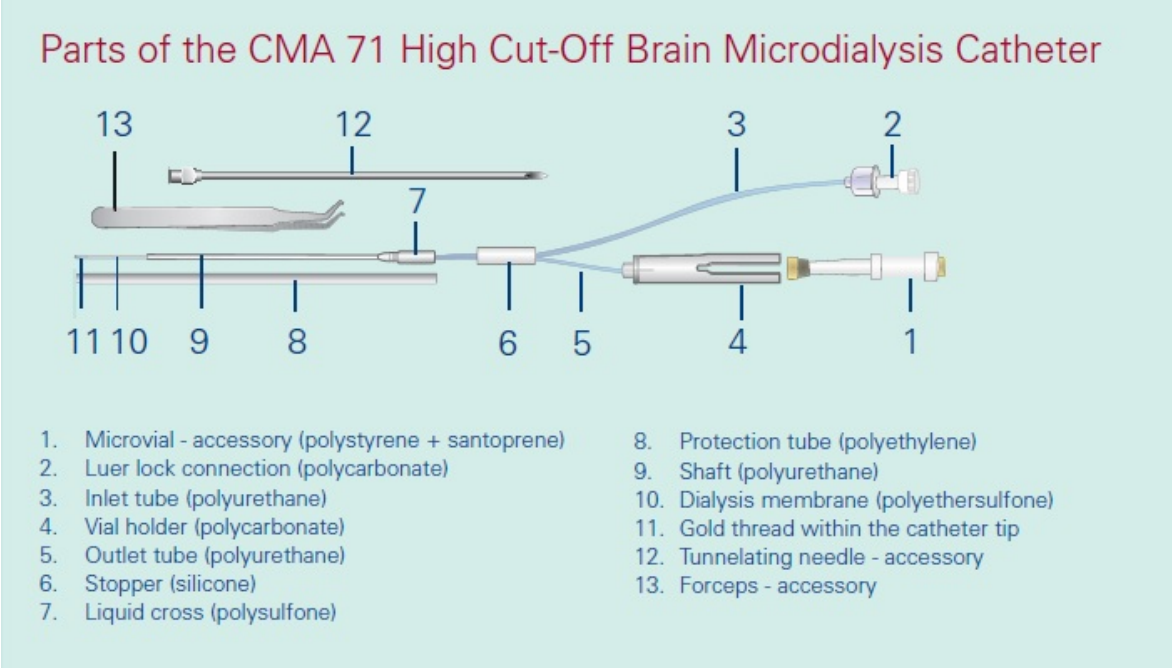

Figure 7-2 - CMA 71 High Cut-Off catheter and accessories.
(Pictures courtesy of CMA Stockholm / Dipylon Medical AB)

Intraoperatively, each patient had three high cut-off microdialysis catheters inserted into DIEP flap zones 1, 2 and 4. The catheters in zones 1, 2 and 4 were labelled a, b and c respectively. Three microdialysis pumps, CMA106 and CMA 107, set at a flow rate of 0.3µl/min perfused 'Perfusion Fluid T1' through the catheters and the microvials collecting dialysate were changed every 4 hours (Figure 7-3). Perfusion Fluid T1 is an isotonic perfusion fluid containing Na^+ 147mmol, K^+ 4mmol, Ca^{2+} 2.3mmol and Cl^- 156mmol. The catheters, inserted much like intravenous lines although with a splitable introducer, were secured with an occlusive dressing.

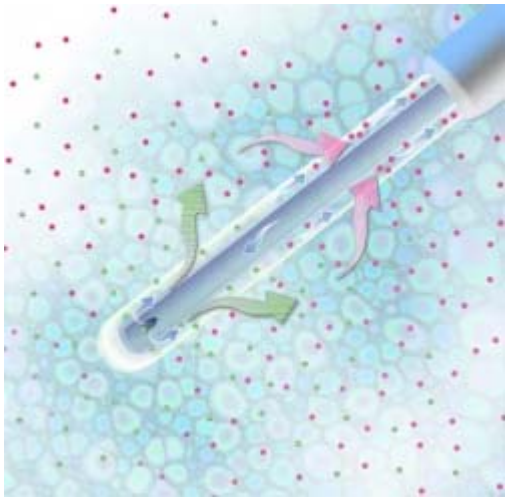

Figure 7-3 - Microdialysis catheter tip showing molecule collection through dialysing membrane.
(Pictures courtesy of CMA Stockholm / Dipylon Medical AB)

Microdialysis continued for 76 hours, and with vials collected every 4 hours from all three catheters, a maximum of 627 vials would be collected (19 time points x 3 catheters x 11 patients). The microvials containing the microdialysis samples when removed from the catheter were immediately stored in a minus 80 degrees Celsius freezer on the patients' ward. The vials were later transferred for storage at Glasgow University.

Analysis was performed initially, as planned, on six of the eleven patients as part of an investigative phase to gain information and ensure adequate yield before progressing with further analysis, as recommended by Dr Niall MacFarlane. ELISA kits (Quantikine High Sensitivity, R&D Systems) were used to detect human Interleukin-6 (IL-6), Fibroblast Growth Factor basic (FGFβ) and Tumour Necrosis Factor alpha (TNFα) and this was carried out by / under direction of Dr Niall MacFarlane, College of Medical, Veterinary and Life Sciences, University of Glasgow.

7.3 Results

Six patients samples were analysed for each of three molecules; interleukin-6 (IL-6), Fibroblast Growth Factor basic (FGFβ) and Tumour Necrosis Factor alpha (TNFα). Patient 4 did not have zone 4 transferred with the flap and therefore only had two catheters, a and b in zones 1 and 2. Patient 5 had no collection beyond 56 hours due to the catheters dislodging inadvertently with dressing removal by the patient. Patient 4 was not analysed for FGFβ due to a technical

error. 324 samples were analysed by high sensitivity ELISA for each IL-6 and TNFα, and 267 for FGFβ, totalling 915 analyses from 324 vials.

7.3.1 Interleukin-6 (IL-6)

7.3.1.1Data description of IL-6

Six patient's concentrations of interleukin-6, collected by three microdialysis catheters (a, b and c) over 4 hourly periods, are displayed in the graphs below (Figure 7-4, Figure 7-5, Figure 7-6, Figure 7-7, Figure 7-8 & Figure 7-9). The unit of concentration is µg/ml

Between catheters a, b and c there does not appear to be any difference.

There appears to be an increasing trend in patients 1, 4 and 5 in the first 20 hours. There is a more gradual increase in patients 2 and 6.

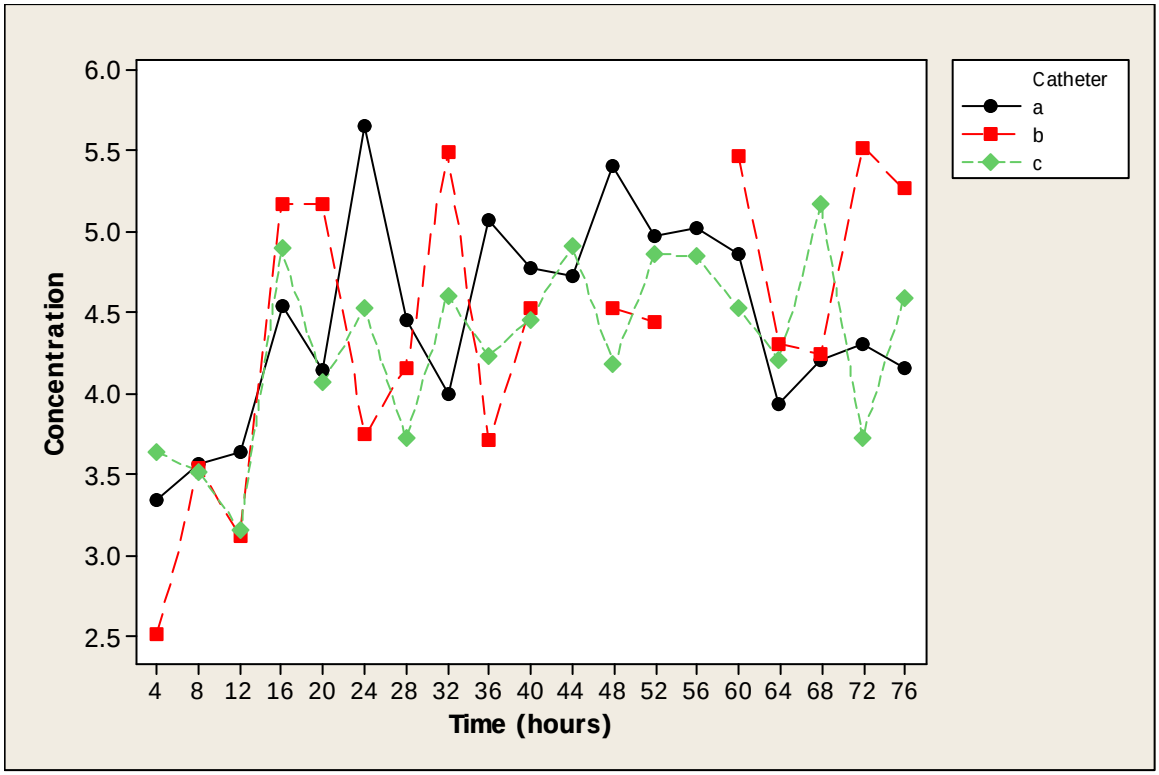

Figure 7-4 - Patient 1. Concentration versus time by catheter.

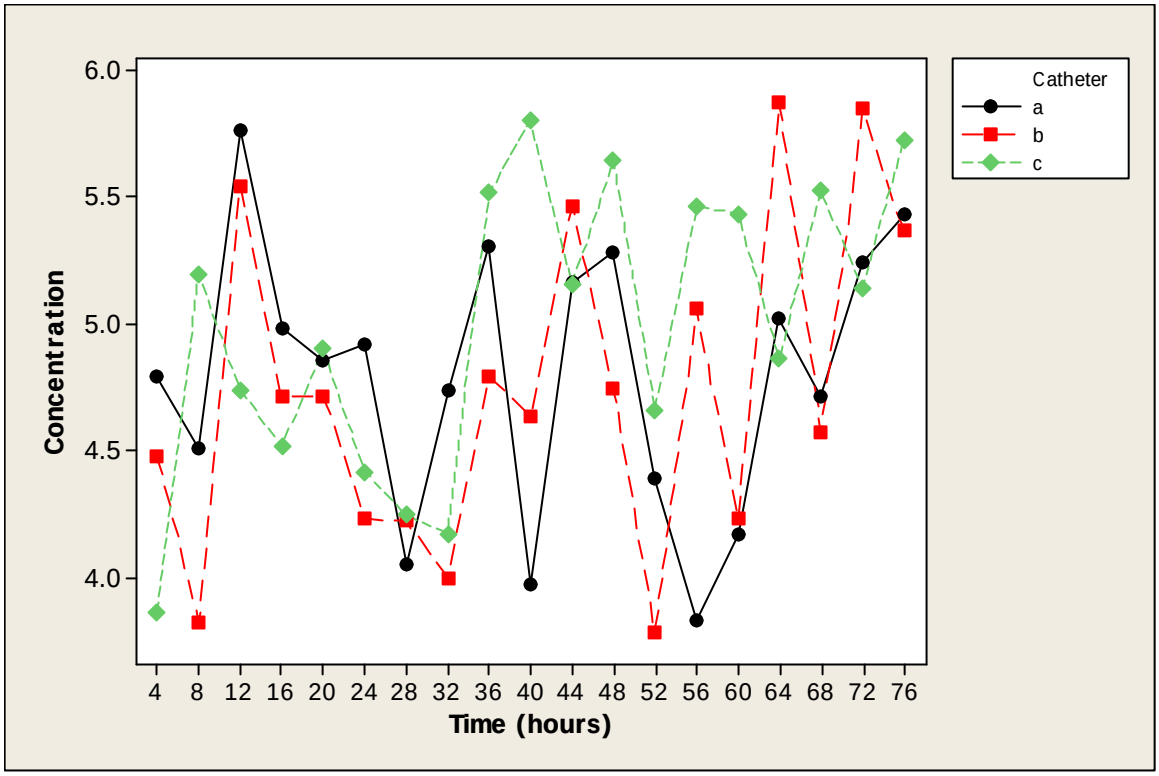

Figure 7-5 - Patient 2. Concentration versus time by catheter.

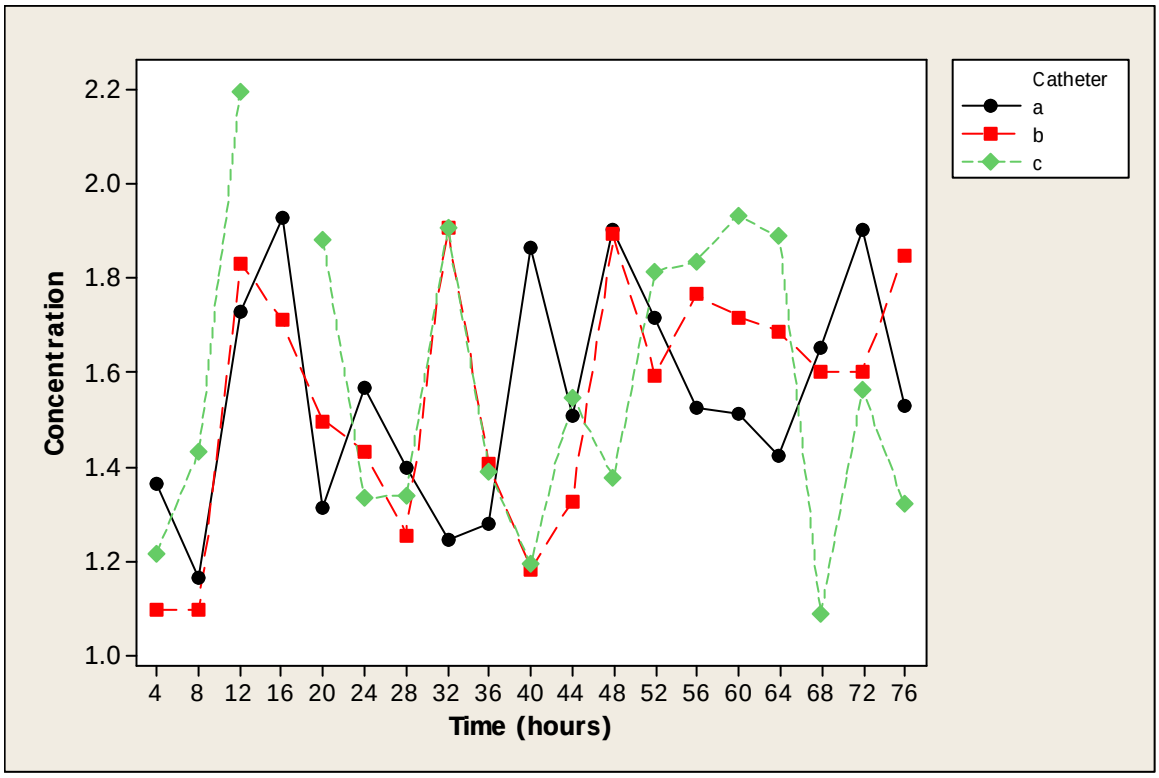

Figure 7-6 - Patient 3. Concentration versus time by catheter.

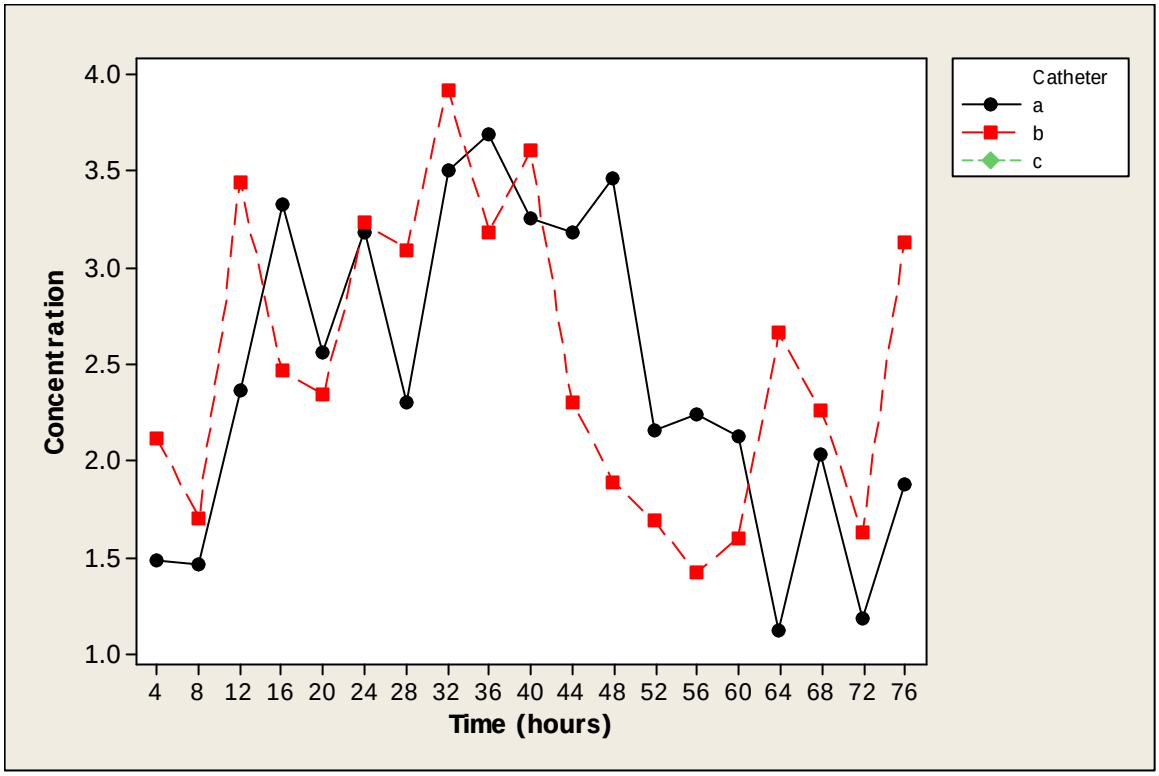

Figure 7-7 - Patient 4. Concentration versus time by catheter.

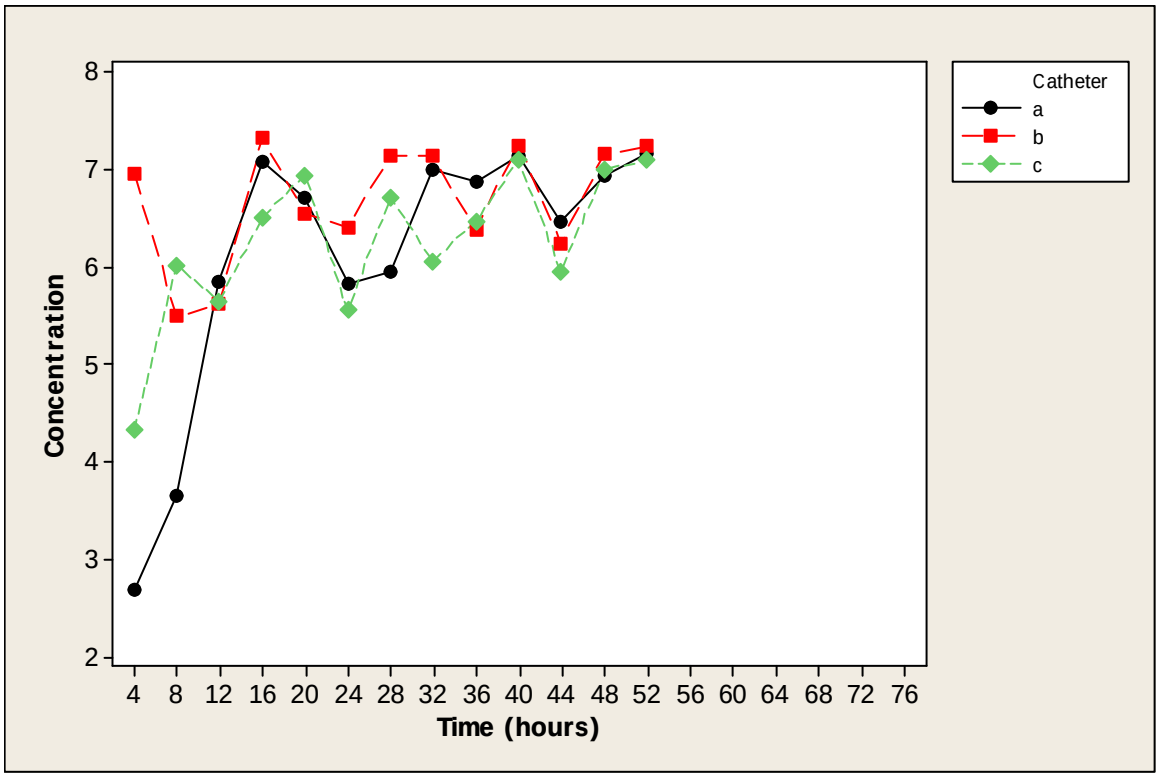

Figure 7-8 - Patient 5. Concentration versus time by catheter.

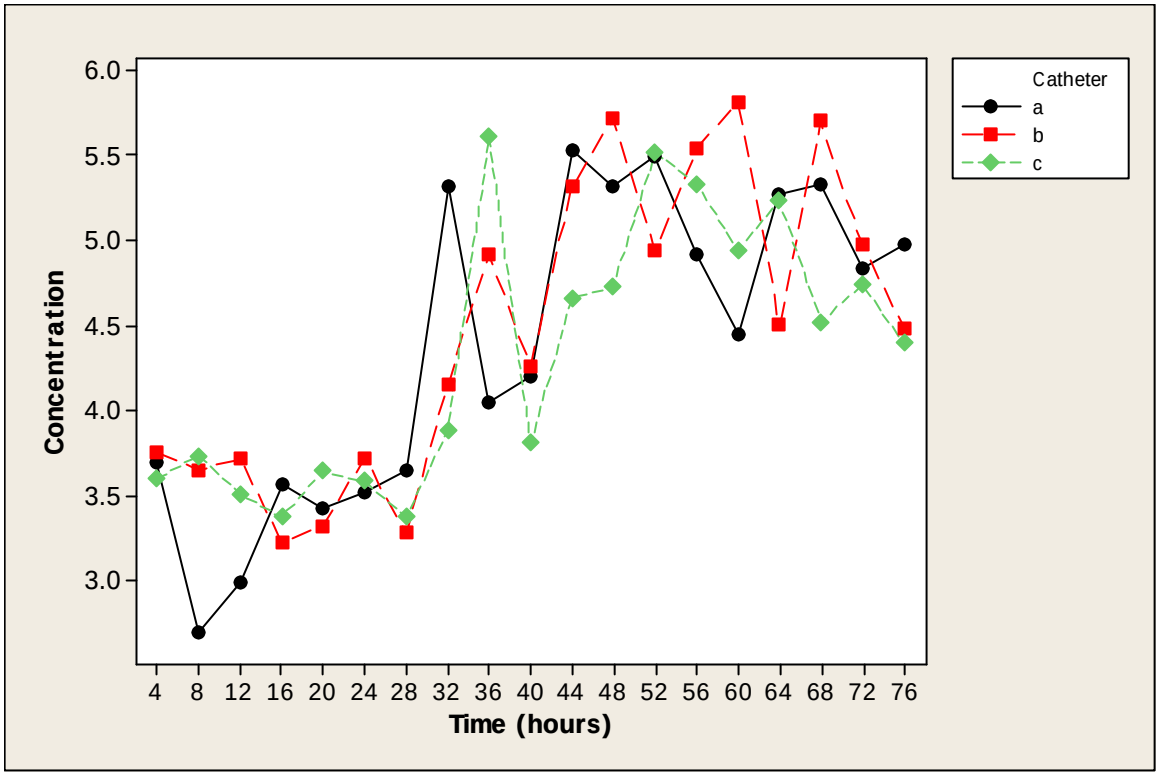

Figure 7-9 - Patient 6. Concentration versus time by catheter.

Figure 7-10 shows the mean concentration averaged over all 6 patients (patient 4 has no data for catheter c and the readings for patient 5 stop after 52 hours). There is an initial increase to 16 hours, followed by fairly constant concentrations until about 52 hours, then a decline. Concentrations in catheter c (zone 4) tend to be the greatest although there is no clear separation and this is not the same at all time points.

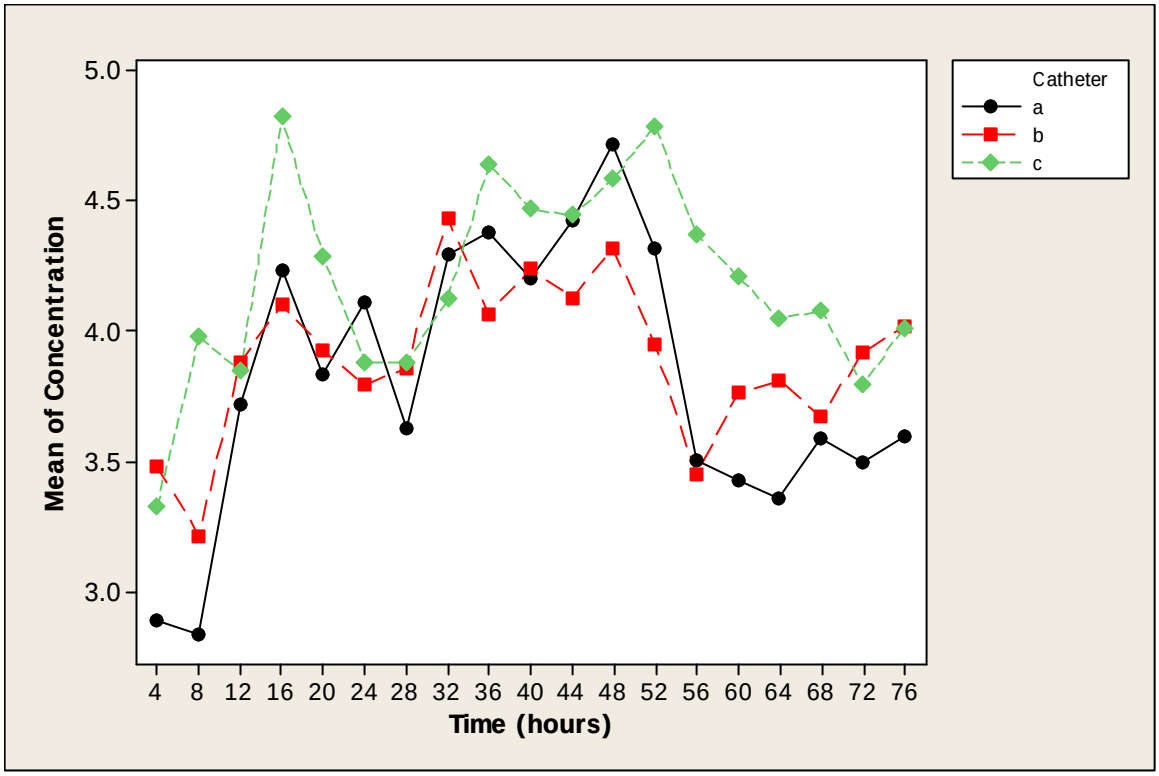

Figure 7-10 - Mean concentration averaged over 6 patients versus time, by catheter.

7.3.1.2 Statistical modelling, IL-6

A linear model was initially fitted to the data. The method of residual maximum likelihood (REML) was used to fit the model[229]. The fixed effects were; the main effects of time (T) and catheter (C), the two-factor interaction T.C. A random factor 'patient' was included in the model to allow for correlation between measurements made on the same patient. Statistical significance was assessed using approximate F-tests, Table 7-1.

Variable	Approximate F-Test statistic	Numerator d.f.	Denominator d.f.	P-value
Time (T)	2.73	18	81.6	0.001
T|Catheter(C)	2.73	18	81.6	0.001
C	0.56	2	7.9	0.592
C|T	0.58	2	7.9	0.580
C.T|T+C	1.08	36	149.8	0.360

Table 7-1- Approximate F-tests of main effects and interactions, IL-6.

Differences between time points in mean concentration, averaged over catheter, are statistically significant, whether allowance is made for the effect of catheter or not (p=0.001).

The effect of catheter upon concentration is not statistically significant whether allowance is made for the effect of time point or not (p=0.580 and p=0.592).

The interaction between time point and catheter is not statistically significant (p=0.360), and therefore the differences in mean concentration between time points do not depend upon catheter.

7.3.1.2.1 Predicted means of IL-6 concentrations

The predicted means by time point are shown below. It would appear that there is an increase in concentration until about 36 hours, after which it remains roughly constant. The effect of time point has been shown to be significant (p=0.001). T-tests can be carried out between specific time points using the matrix of standard errors given in the appendix, on 81.6 d.f..

Time4	8	12	16	20	24	28	32
3.138	3.246	3.737	4.074	3.917	3.857	3.705	4.217
Time36	40	44	48	52	56	60	64
4.289	4.231	4.261	4.427	4.221	4.218	4.154	4.095
Time68	72	76					
4.147	4.062	4.250					

Table 7-2 - Predicted mean concentrations by time point.

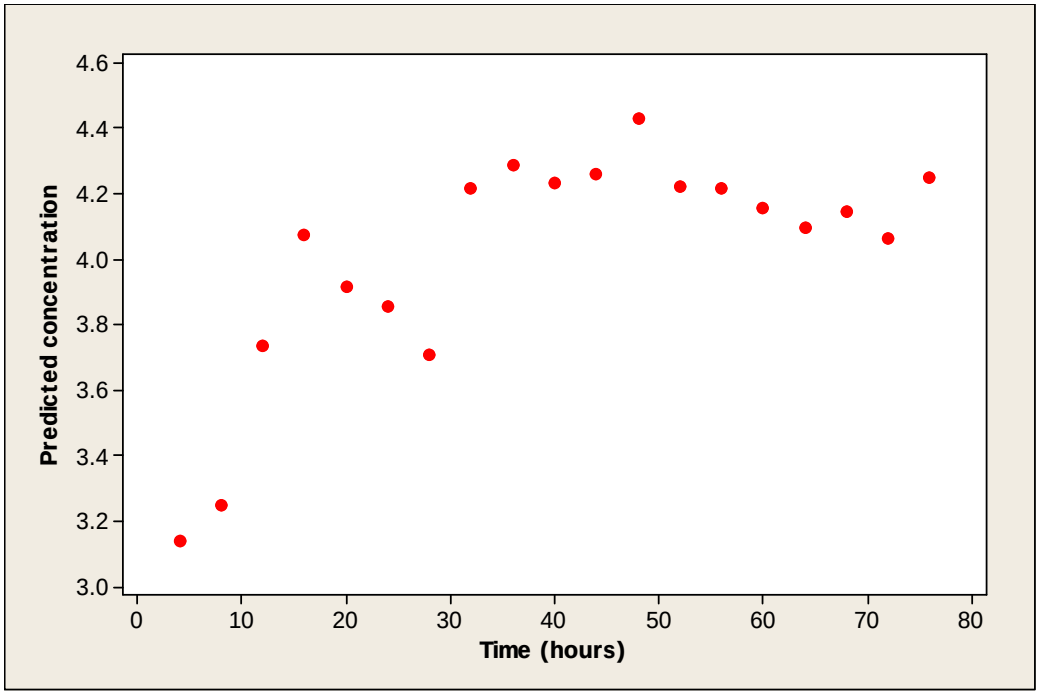

Figure 7-11 - Predicted concentrations by time, IL-6.

The increase after 4 hours is significant by 12 hours (p=0.046). There appears to be a further rise between 28 hours and 32 hours (p=0.08) (28 hours to 48 hours, p=0.02). The difference in concentration between first collection at 4 hours and the final collection at 76 hours is also significant, p=0.001.

7.3.1.3Test of linear trend with hours post-operatively, IL-6

The F-tests of time point were significant, p=0.01, meaning that the concentration for IL-6 was not the same at all time points. To further test any trend in concentration, rather than differences between individual time points or groups of time points, the original test of the factor 'time' was split into two subsets. One subset was a linear trend of time, and the other of the effect of time not captured by a linear trend (Table 7-3).

Similarly, the test of interaction between time and catheter is split into two subtests; one of the extent to which the linear trend varies with catheter, and the other of the extent to which those effects of time not captured by a linear trend vary with catheter (Table 7-4).

Variable	Approximate F-Test statistic	Numerator d.f.	Denominator d.f.	P-value
Time (T)	2.73	18	81.6	0.001
Linear	23.19	1	81.6	<0.001
Non-linear	1.53	17	81.6	0.106
Catheter (C)|T	0.58	2	7.9	0.580
C. T|T+C	1.08	36	149.8	0.360
Linear	0.05	2	154.9	0.95
Non-linear	1.14	34	149.5	0.287

Table 7-3- Approximate F-tests of main effects and interactions (time fitted first).

Variable	Approximate F-Test statistic	Numerator d.f.	Denominator d.f.	P-value
C	0.56	2	7.9	0.592
T|C	2.73	18	81.6	0.001
Linear	23.22	1	81.6	<0.001
Non-linear	1.53	17	81.6	0.106
C. T|T+C	1.08	36	149.8	0.360
Linear	0.05	2	154.9	0.95
Non-linear	1.14	34	149.5	0.287

Table 7-4 - Approximate F-tests of main effects and interactions (catheter fitted first).

Considering the effect of time, the linear trend is significant (p<0.001), whether or not an allowance is made for catheter. The remaining non-linear effects of

time are not statistically significant (p=0.106) whether or not allowance is made for the effect of catheter. IL-6 therefore tends to increase in a linear fashion with time although appears to begin to level off at 32 hours post-operatively.

7.3.2 Fibroblast Growth Factor basic (FGFβ)

The five patients' samples in microdialysis vials were analysed for FGFβ (patients 1, 2, 3, 5 & 6). Due to a technical error there were no results for patient 4. The vials as before were collected every 4 hours from catheters a, b and c. The concentrations for each patient are displayed in the graphs below (Figure 7-12, Figure 7-13, Figure 7-14, Figure 7-15, & Figure 7-16).

There does not appear to be any differences between catheters in any of the patients, nor does there appear to be any difference in concentration with time.

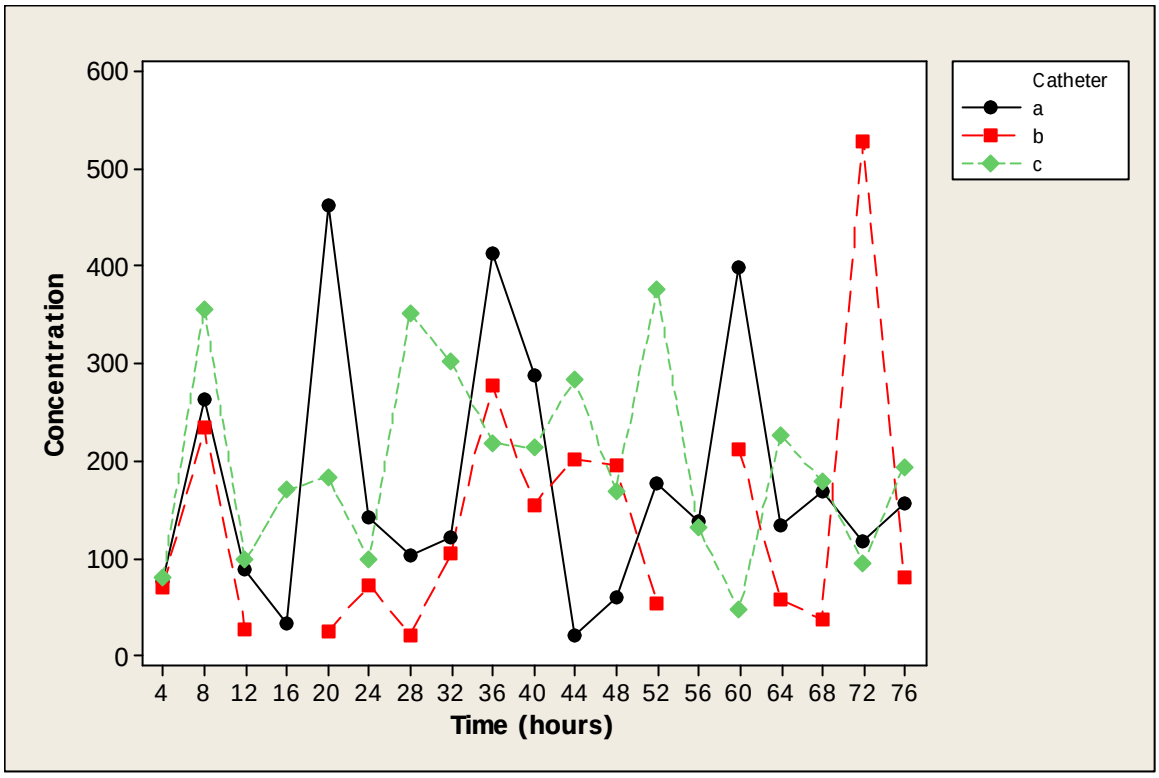

Figure 7-12 - Patient 1. Concentration versus time by catheter. FGFβ.

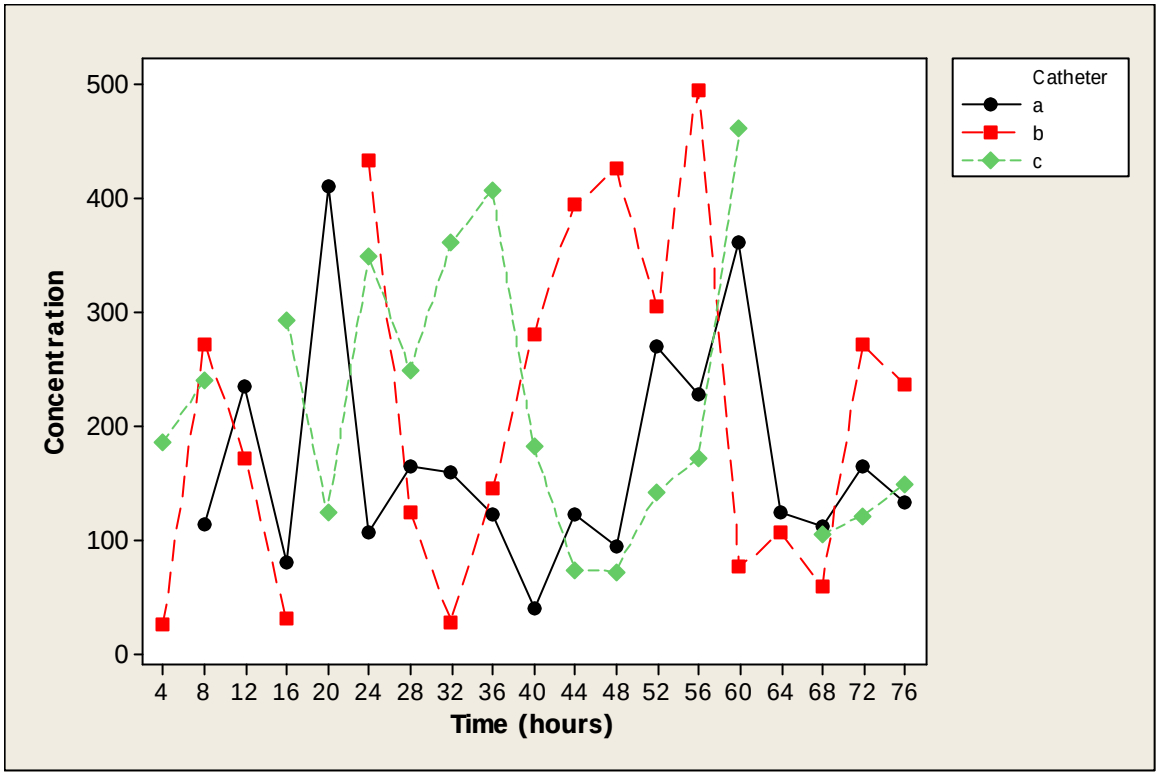

Figure 7-13 - Patient 2. Concentration versus time by catheter. FGFβ.

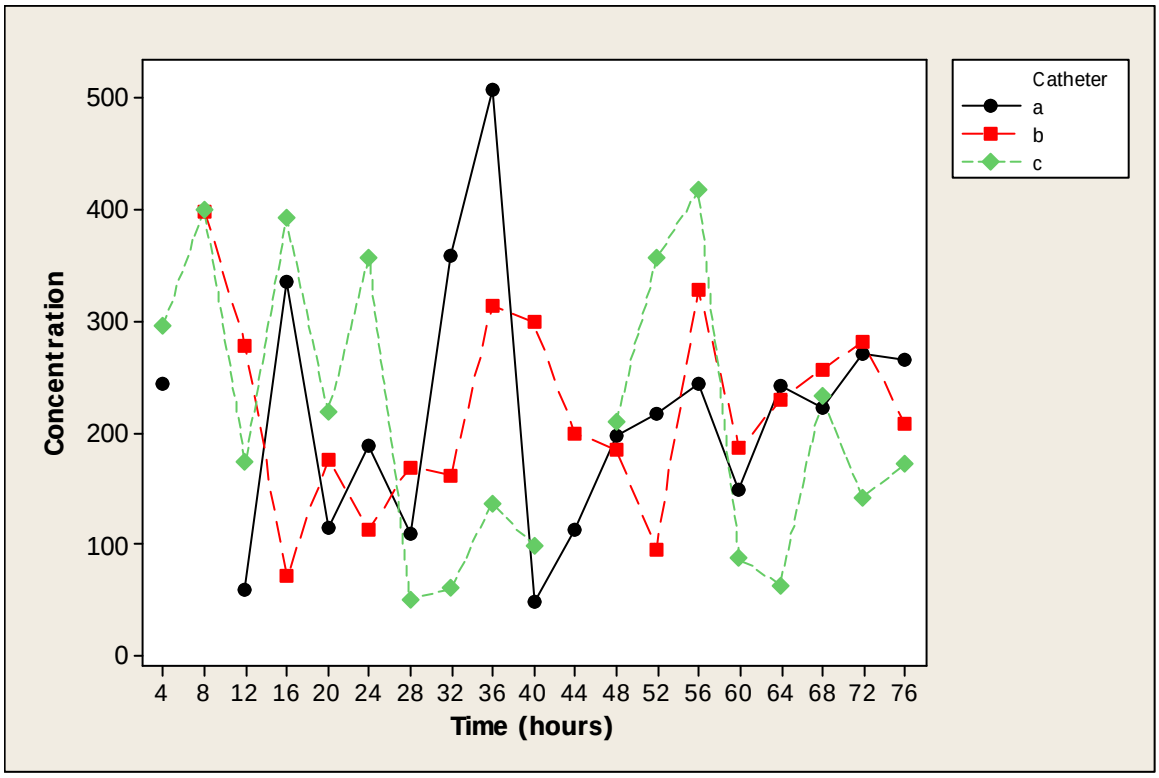

Figure 7-14 - Patient 3. Concentration versus time by catheter. FGFβ.

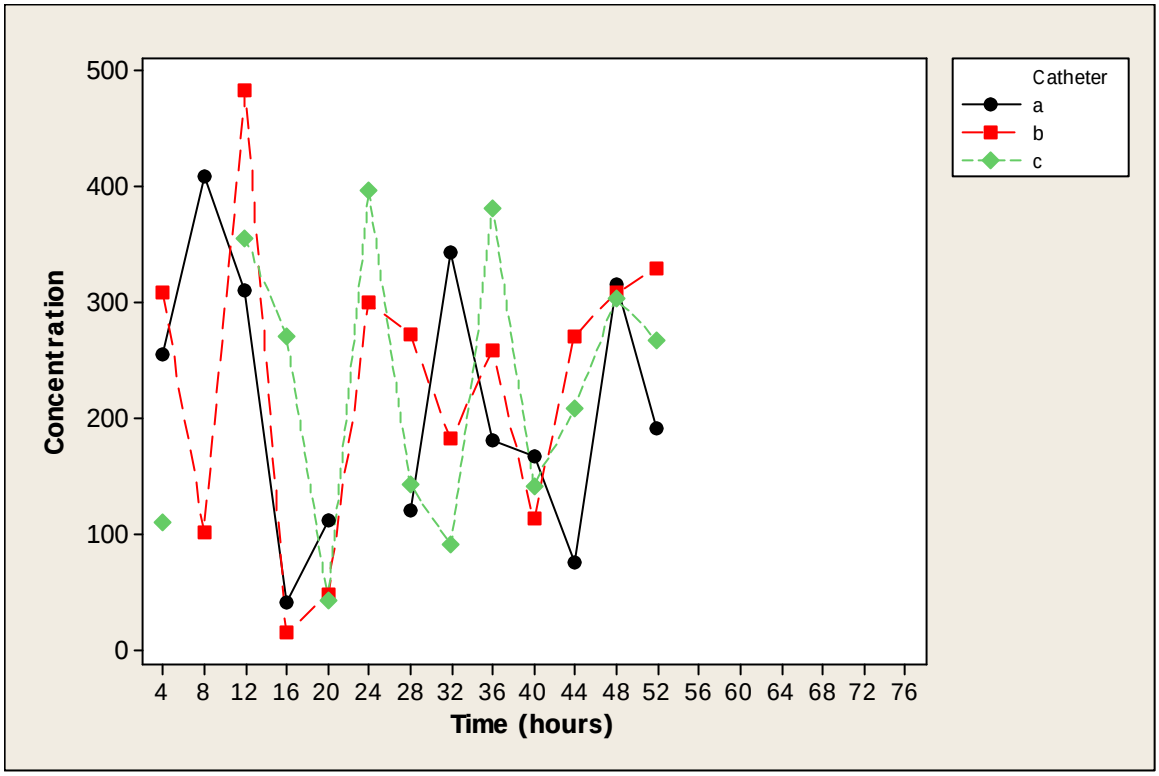

Figure 7-15 - Patient 5. Concentration versus time by catheter. FGFβ.

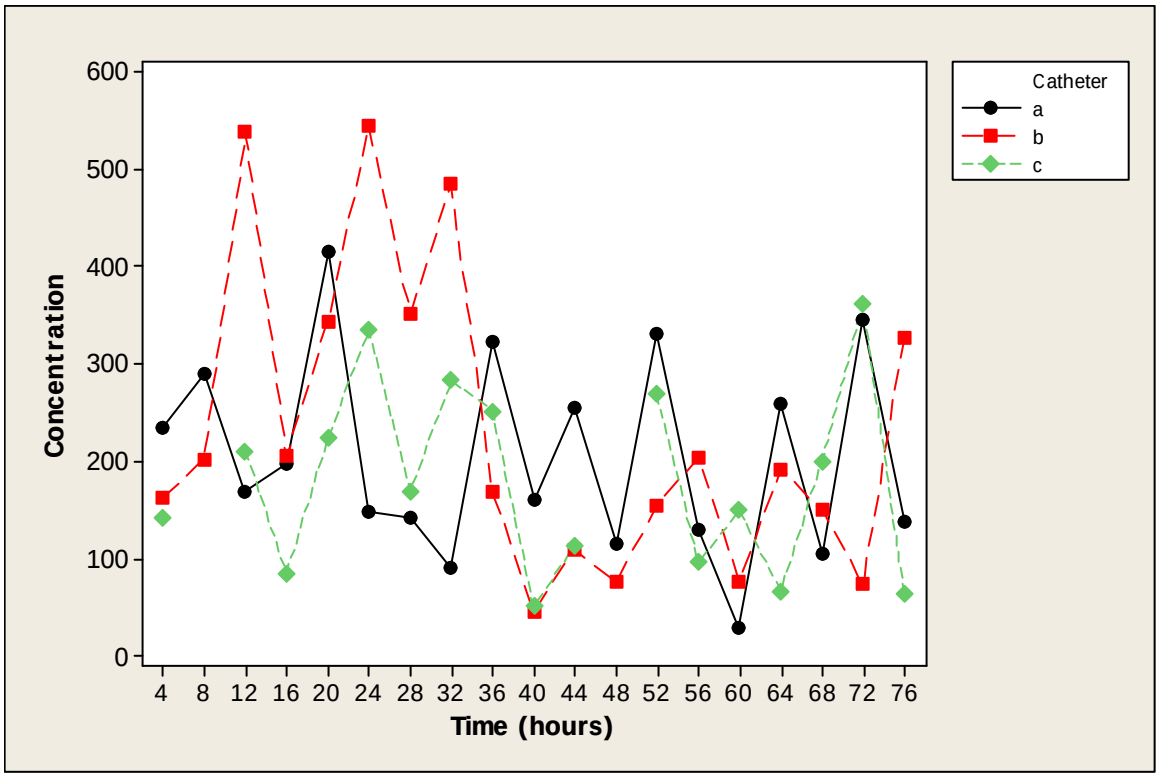

Figure 7-16 - Patient 6. Concentration versus time by catheter. FGFβ.

Figure 7-17 below shows mean concentration averaged over all patients. There does not appear to be any uniform differences between catheters and no obvious time trend. There does appear to be a pattern of cyclical variation.

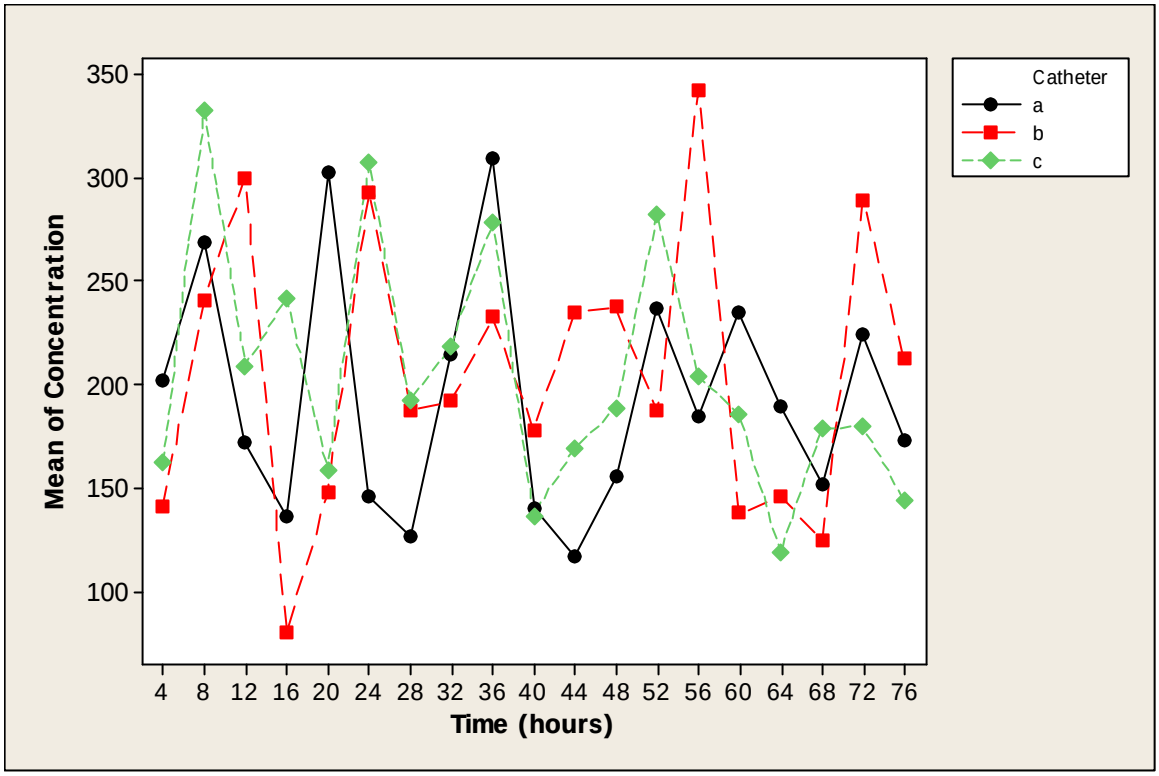

Figure 7-17 - Mean concentration averaged over 5 patients versus time, by catheter.

7.3.2.1 Statistical modelling & tests of linear trend, FGFβ

As before the time factor was split into two subsets to test for the linear trend of time and the effect of time not captured by a linear trend.

REML modelling of the log concentration produced a residual plot in which the residuals tended to decrease in absolute magnitude with increasing mean concentration. The square root transformation was found to be the most appropriate in terms of homogeneity of variance and was used in this analysis.

The results of the fixed effects where time was fitted before catheter are shown in Table 7-5. Table 7-6 shows the results of fixed effects where catheter was fitted first.

Variable	Approximate F-Test statistic	Numerator d.f.	Denominator d.f.	P-value
Time (T)	1.70	18	65.1	0.061
Linear	0.40	1	69.0	0.530
Non-linear	1.78	17	65.0	0.050
Catheter (C)|T	0.38	2	7.5	0.698
C. T|T+C	0.90	36	126	0.640
Linear	1.32	2	133.7	0.270
Non-linear	0.87	34	125.7	0.673

Table 7-5 - Approximate F-tests of main effects and interactions, FGFβ. Time fitted first.

Variable	Approximate F-Test statistic	Numerator d.f.	Denominator d.f.	P-value
C	0.35	2	7.5	0.718
T|C	1.71	18	65.1	0.060
Linear	0.39	1	69.0	0.535
Non-linear	1.79	17	65.0	0.049
C. T|T+C	0.90	36	126	0.640
Linear	1.32	2	133.7	0.270
Non-linear	0.87	34	125.7	0.673

Table 7-6 - Approximate F-tests of main effects and interactions, FGFβ. Catheter fitted first.

The test of interaction (C.T) shows that there is no evidence that the linear trend in concentration differs between catheters (p=0.270), or that the remaining non-linear effects of time point on concentration differs between catheters (p=0.673).

The differences between catheters are not statistically significant, whether allowance is made for the effect of time is allowed for (0.698) or not (p=0.719).

Considering the effect of time, the linear trend is not statistically significant, whether allowance is made for the effect of catheter (p=0.535), or not (p=0.530). The non-linear effects of time are on the borderline of statistical significance (p=0.050 not allowing for catheter, p=0.049 allowing for catheter).

7.3.2.1.1 Predicted means of FGFB concentrations

The predicted mean concentrations (square root scale) by time point are shown in Table 7-7 below. Figure 7-18 shows the predictions of Table 7-7 back-transformed) i.e. squared. There is no apparent time trend, however there is possibly a pattern of cyclical variation which may explain the border line F-statistic (non-linear effects of time p=0.050 and p=0.049 allowing for catheter). Differences between some of the peaks and troughs of the cycle are significant individually (e.g. 8 hours to 16 hour p<0.001, 24 hours to 28 hours p=0.088).

Table of predicted means for Time

Time4	8	12	16	20	24	28	32
12.45	16.54	14.23	11.27	13.24	15.12	12.45	13.65
Time36	**40**	**44**	**48**	**52**	**56**	**60**	**64**
16.19	11.77	12.64	13.46	14.97	15.17	12.74	11.95

Time68	72	76
12.03	14.66	13.06

Standard errors of differences

Average:	1.614
Maximum:	1.780
Minimum:	1.506

Average variance of differences: 2.609

Table 7-7 - Predicted means by time point (square root scale). FGFβ

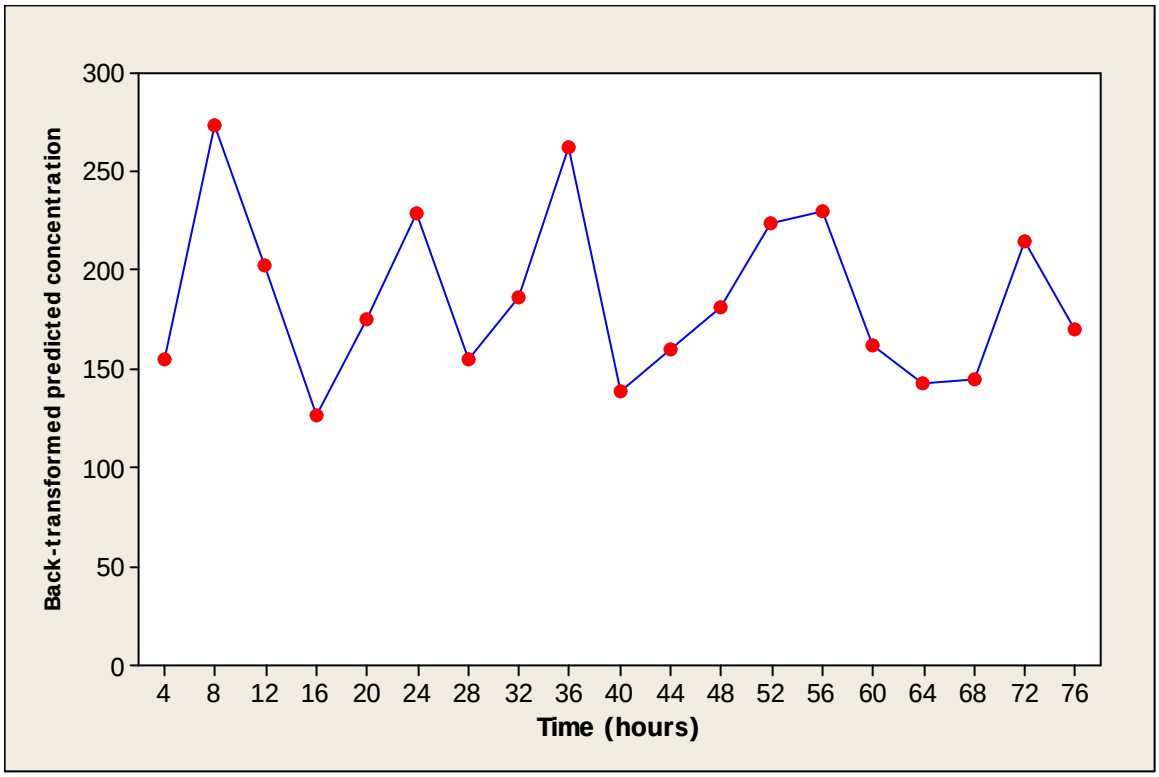

Figure 7-18 - Predicted back-transformed concentrations by time. FGFβ.

7.3.3 Tumour Necrosis Factor alpha (TNFα)

The same six patients' samples were analysed (as for IL-6 and FGFß). The concentrations for each patient are displayed in the graphs below (Figure 7-19, Figure 7-20, Figure 7-21, Figure 7-22, Figure 7-23 & Figure 7-24). Patient 4 did not have a catheter c as there was no zone 4 in the flap.

There is no clear evidence of uniform differences between catheters in any of the six graphs. Concentrations for patients 1, 4, and 5 show a slight decrease with time.

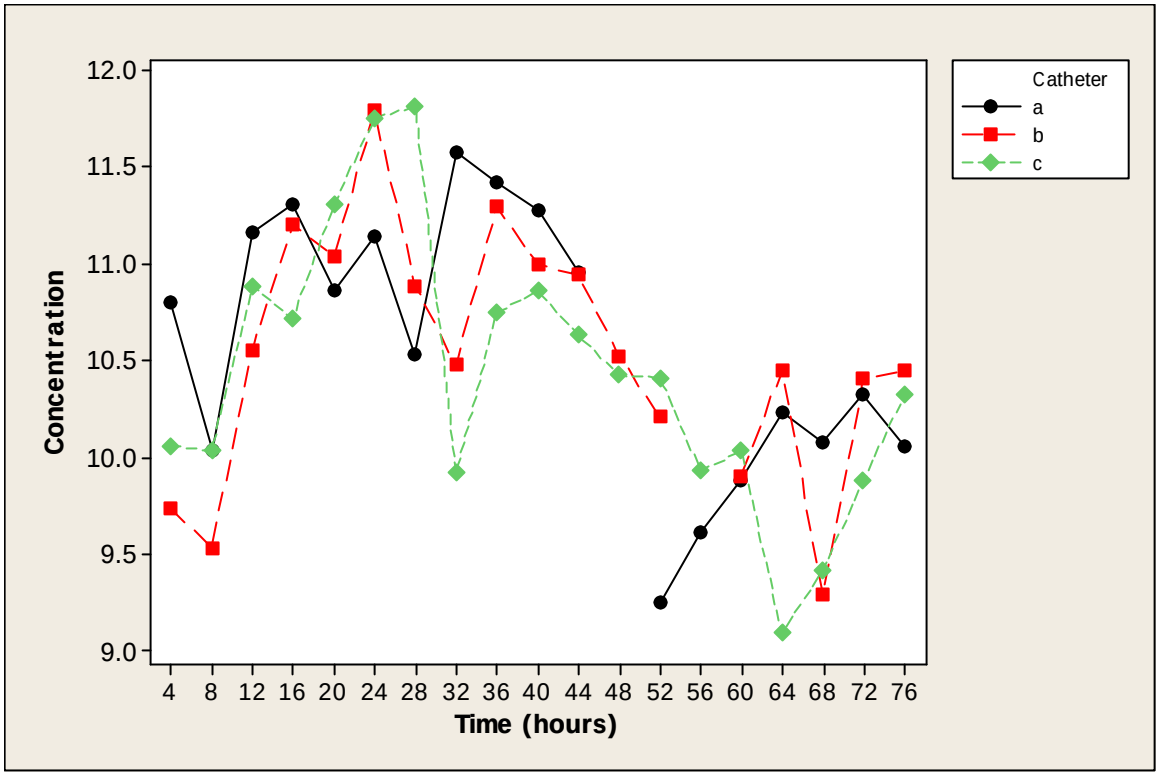

Figure 7-19 - Patient 1. Concentration versus time by catheter. TNFα.

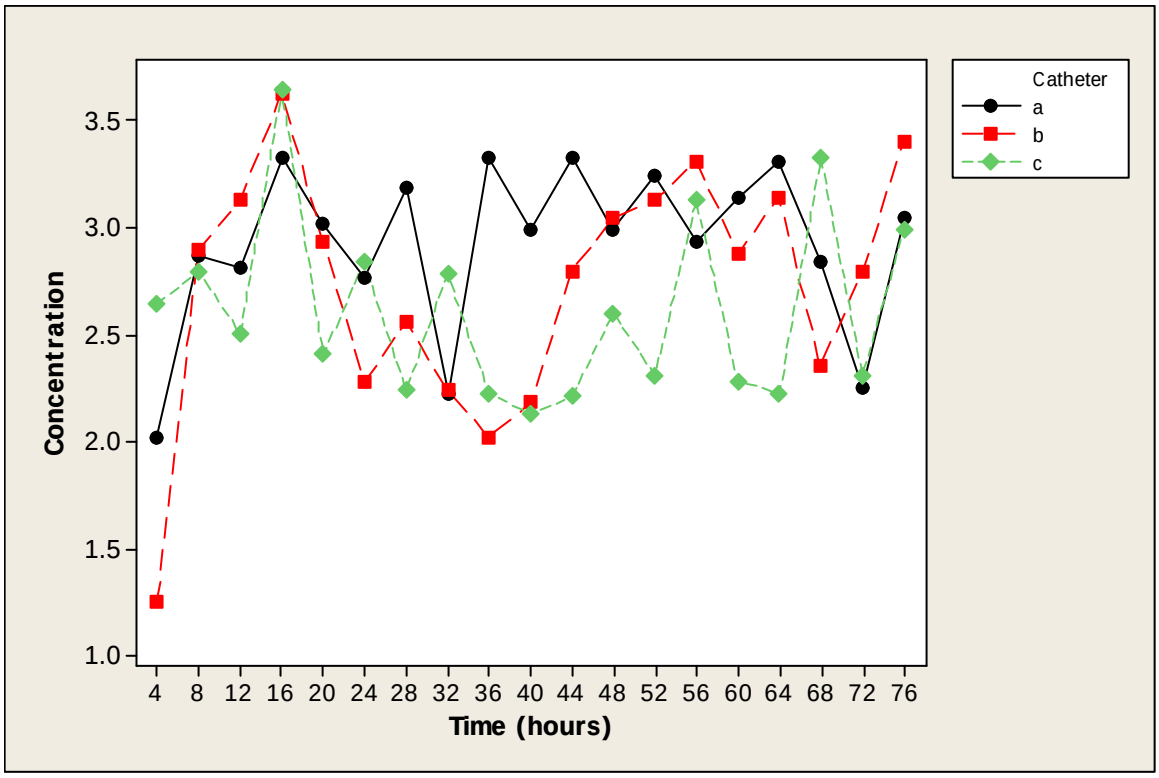

Figure 7-20 - Patient 2. Concentration versus time by catheter. TNFα.

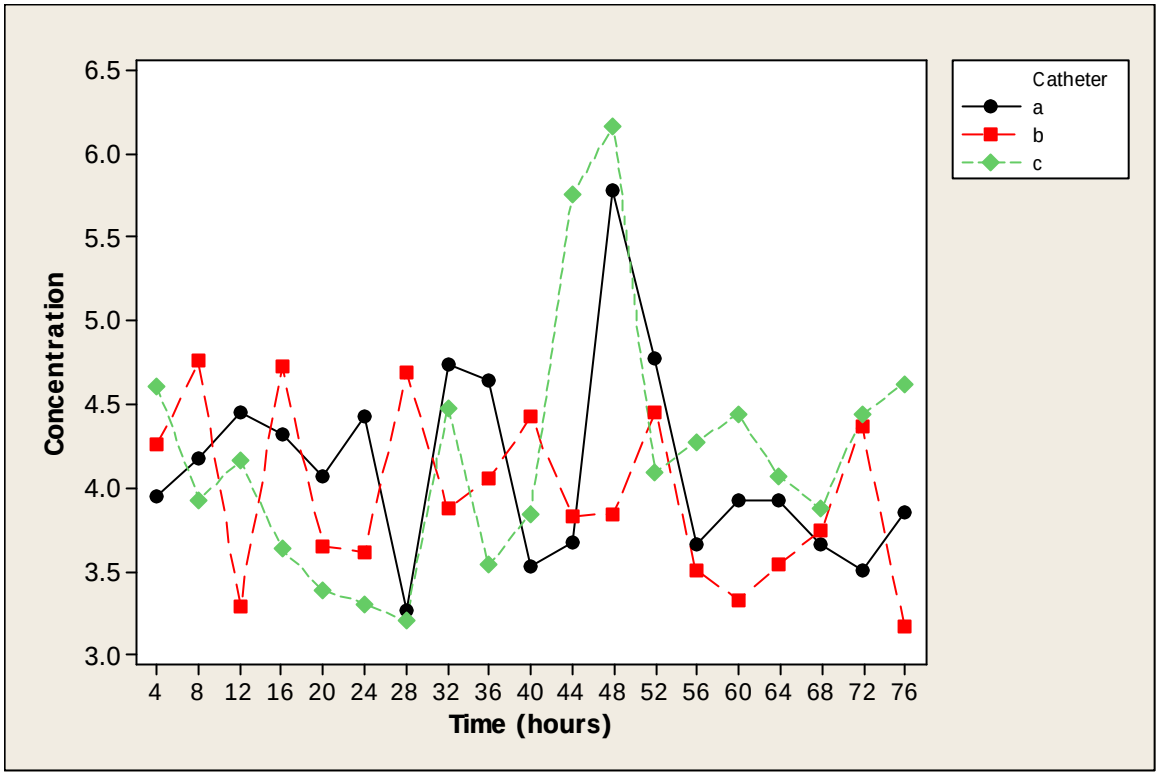

Figure 7-21 - Patient 3. Concentration versus time by catheter. TNFα.

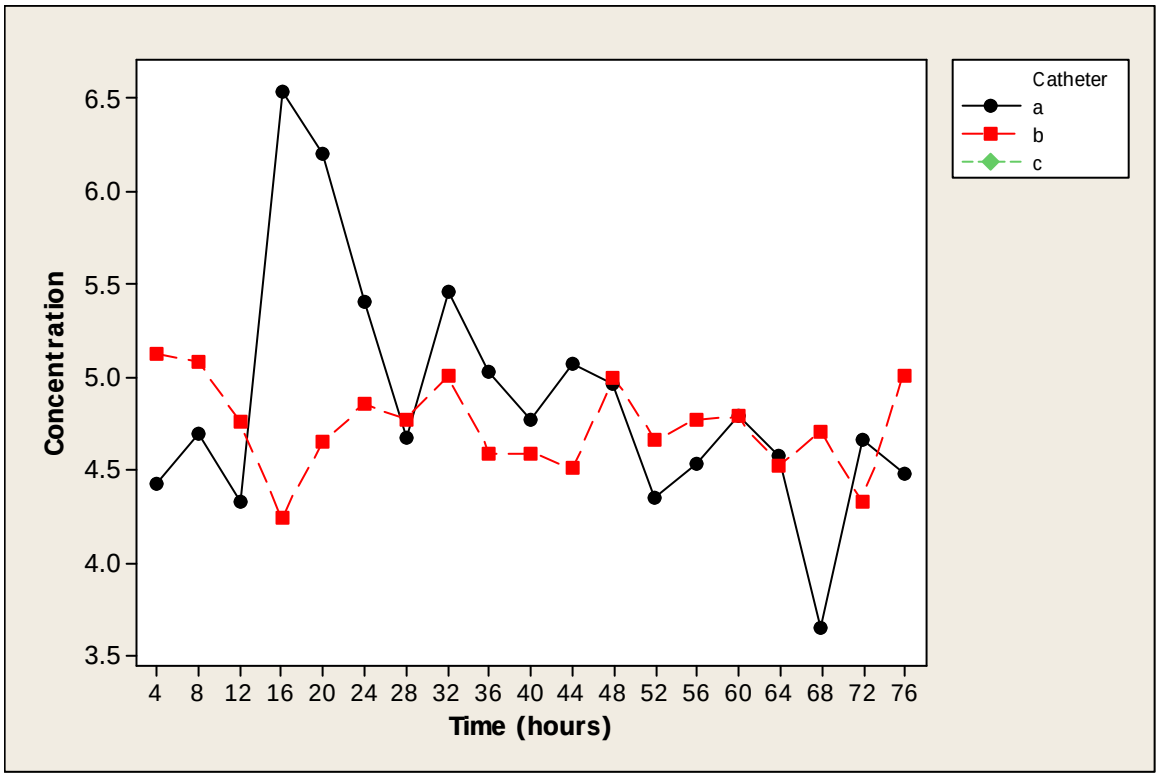

Figure 7-22 - Patient 4. Concentration versus time by catheter. TNFα.

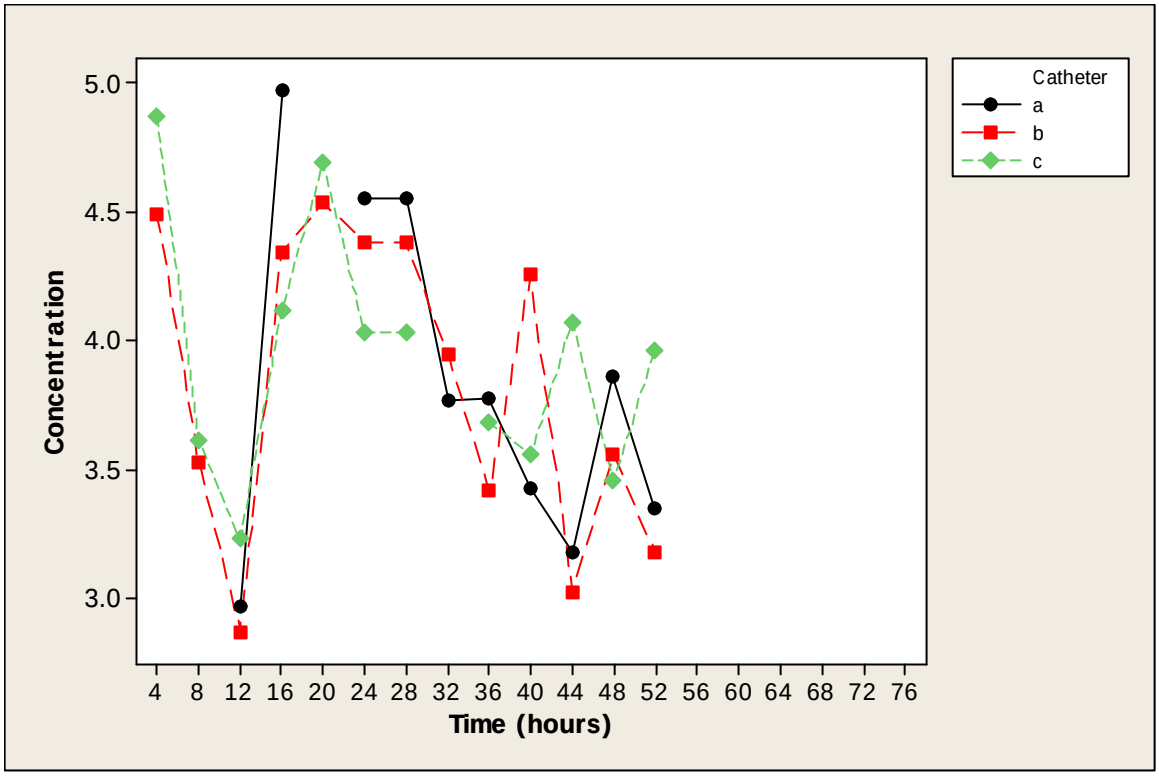

Figure 7-23 - Patient 5. Concentration versus time by catheter. TNFα.

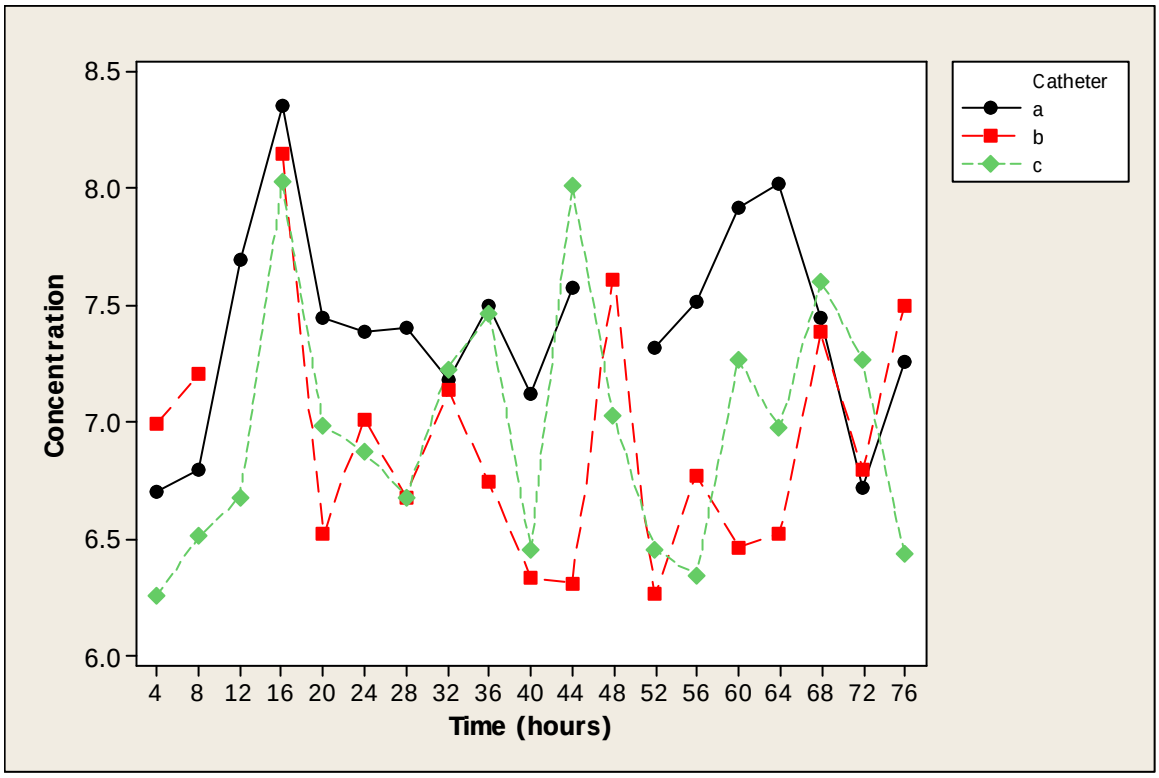

Figure 7-24 - Patient 6. Concentration versus time by catheter. TNFα.

Figure 7-25 below shows the mean concentration of TNFα averaged over all patients. There do not appear to be any uniform differences between catheters and there is no obvious time trend.

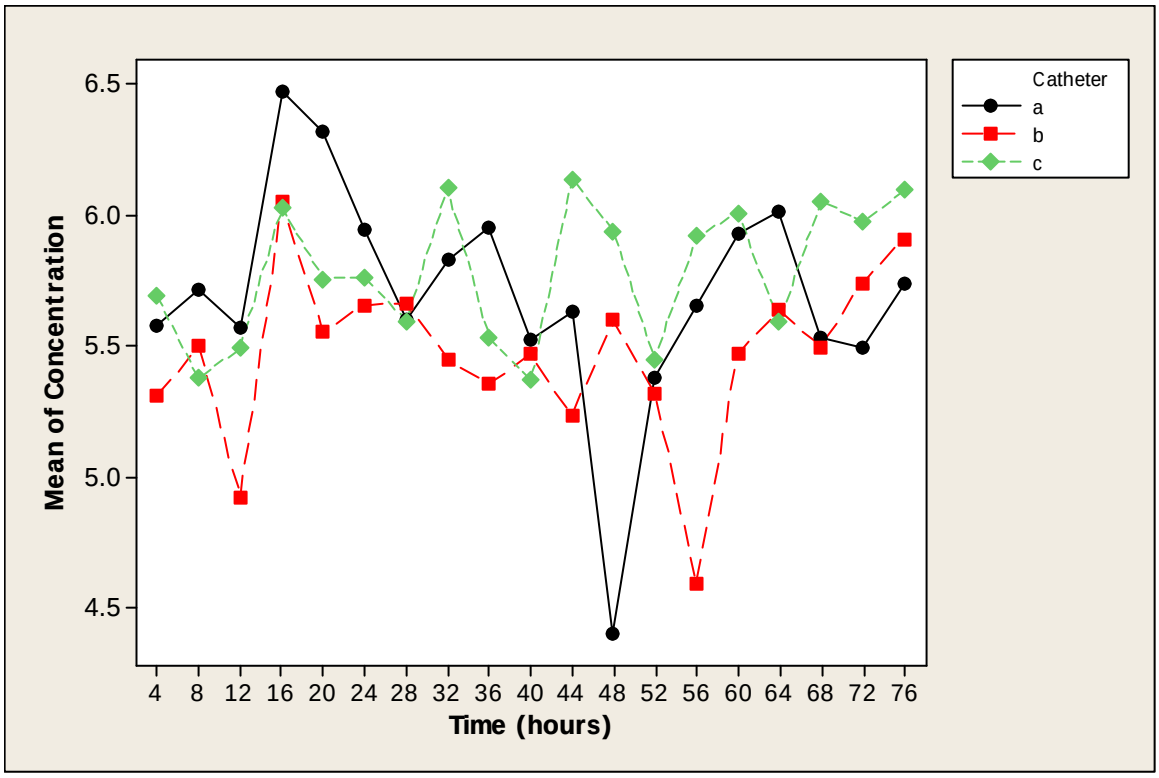

Figure 7-25 - Mean concentration averaged over 6 patients versus time, by catheter. TNFα.

7.3.3.1 Statistical modelling & tests of linear trend, TNFα

As before the time factor was split into two subsets to test for the linear trend of time and the effect of time not captured by a linear trend.

The results of tests of fixed effects where time was fitted before catheter are shown in Table 7-8. Table 7-9 shows the results of fixed effects where catheter was fitted first.

Variable	Approximate F-Test statistic	Numerator d.f.	Denominator d.f.	P-value
Time (T)	1.78	18	83.3	0.041
Linear	4.95	1	82.8	0.029
Non-linear	1.60	17	83.3	0.083
Catheter (C)|T	3.38	2	8.4	0.084
C. T|T+C	0.83	36	152.8	0.735
Linear	0.69	2	155.8	0.502
Non-linear	0.84	34	152.7	0.717

Table 7-8 - Approximate F-tests of main effects and interactions, TNFα. Time fitted first.

Variable	Approximate F-Test statistic	Numerator d.f.	Denominator d.f.	P-value
C	3.29	2	8.4	0.088
T|C	1.79	18	83.3	0.040
Linear	5.02	1	82.5	0.028
Non-linear	1.60	17	83.4	0.082
C. T|T+C	0.83	36	152.8	0.735
Linear	0.69	2	155.8	0.502
Non-linear	0.84	34	152.7	0.717

Table 7-9 - Approximate F-tests of main effects and interactions. TNFα. Catheter fitted first.

The test of interaction (C.T) shows that there is no evidence that the linear trend in concentration differs between catheters (p=0.503), or that the remaining non-linear effects of time point on concentration differ between catheters (p=0.717).

The differences between catheters are suggestive, whether the effect of time is allowed for (p=0.084) or not (p=0.088).

Considering the effect of time, the linear trend is statistically significant whether allowance is made for catheter (p=0.028) or not (p=0.029). Remaining non-linear effects of time are approaching significance (p=0.083 not allowing for catheter, p=0.082 allowing for catheter).

7.3.3.1.1 Predicted means of TNFa concentrations

The predicted mean concentrations by time point are shown in Table 7-10 & Figure 7-26 below. Further details including matrices of standard errors are in the appendix.

There is a significant initial increase between 12 hours and 16 hours p=0.002. (Between 12 hours and 20 hours p=0.126.)

Overall all slight decreasing time trend is apparent, which is statistically significant (Table 7-8 & Table 7-9, p=0.029 and p=0.028 allowing for the effect of catheter). The value of the estimated trend was equal to -0.004 µg/ml per hour.

Table of predicted means for Time

Time4	8	12	16	20	24	28	32

5.391	5.366	5.382	6.129	5.740	5.741	5.565	5.600

Time36	40	44	48	52	56	60	64
5.559	5.400	5.620	5.809	5.329	5.333	5.379	5.310

Time68	72	76
5.257	5.305	5.485

Standard errors of differences

Average:	0.2386
Maximum:	0.2546
Minimum:	0.2288

Average variance of differences: 0.05699

Table 7-10 - Predicted mean concentrations by time point. TNFα.

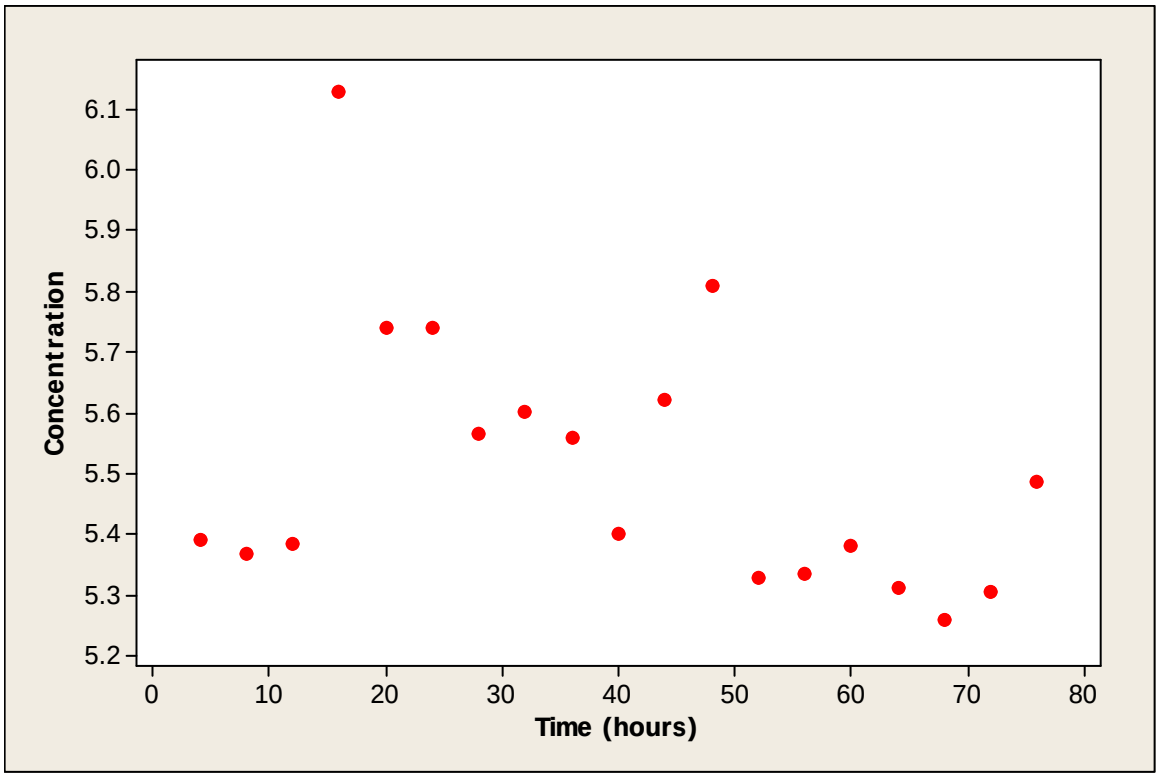

Figure 7-26 - Predicted concentrations by time point. TNFα.

7.4 Conclusion

Interleukin-6 shows an increasing trend until about 36 hours before remaining relatively constant. The effect of catheter is not significant. The effects of time, in a linear trend are significant ($p<0.001$). Effects of time in a non-linear trend are not significant ($p=0.106$). The concentration of IL-6 therefore tends to

increase ($p<0.001$) over the period form 4 hours to 72 hours and this can best be explained by a linear trend.

Fibroblast Growth Factor basic does not display a time trend between 4 and 76 hours on the square root scale ($p=0.061$ when time is fitted first, and $p=0.060$ when time is fitted after catheter). There is no sign of a linear trend ($p=0.530$ and $p=0.535$). The test of remaining differences in concentration is just significant ($p=0.050$ and $p=0.049$) which would mean if real, that the oscillations about the trend line (essentially horizontal, Figure 7-18) are of biological significance.

Tumour Necrosis Factor alpha has a significant linear trend between 4 and 76 hours ($p=0.029$, and $p=0.028$ with catheter fitted first). This trend is a slightly decreasing trend over the time period, -0.004 units of concentration µg/ml per hour. The remaining non-linear effects of time are not significant, although p-values approach significance ($p=0.083$, and $p=0.082$ when time is fitted after catheter). Observing Figure 7-26, there does appear to be a peak around 20 - 24 hours before a gradual decrease.

7.5 Discussion

7.5.1 Mechanism of delay

Delay has been known for centuries to improve flap survival although the mechanism has yet to be elucidated. Delay, involving a staged division of vessels along the length of a flap, has been known clinically to have effect within one week although flap transfer does often not happen until at least two weeks[387-390]. It is generally agreed that the delay phenomenon occurs primarily due to ischaemia and that this the induces changes in the vascularity of the flap[30;391]. Similarly, the transfer of a pedicled or free flap induces changes in the flap vascularity in the first few days post-operatively and increased flow in the pedicle. Delay and the improved vascularity within flaps after transfer have both been described as theoretically being related to the opening of anastomotic choke vessels between angiosomes[32;34;392].

Callegari et al in 1992 designed an experimental study in dogs looking at the anatomical changes in flaps with and without surgical delay[32]. Laser Doppler

probes were used followed by lead oxide injection anatomical studies 5 days after flaps were raised, with or without prior surgical delay 5 to 10 days earlier. They noted that; the necrosis line in flaps usually appeared in the zone of choke vessels connecting adjacent territories and that neovascularization did not appear to occur, surgical delay resulted in dilatation of existing vessels with maximal effect in the zone of choke arteries, that tissue expansion was a form of surgical delay, and that similar changes occurred when muscle was delayed. An earlier pig study using radioactive microspheres, by Pang et al in 1986, compared time periods of delay finding that between 2 and 14 days of delay, capillary blood flow reached a plateau after 3 days[393]. Pang noted in accordance with Callegari's findings, that angiogenesis did not account for the increase in blood flow as the time period of 4 days was too short and there was no increase in the density of vessels. The improvement in blood flow theoretically occurs in too short a time period, days, to be attributable to angiogenesis and this has been supported by these and many other studies[30;32;372;393;394]. Dilatation of vessels has become the focus of research in delay phenomenon.

Morris and Taylor designed a study to elucidate the chronological sequence of the events that occur in choke vessel opening, by using surgical delay in a rabbit model[30]. Thirty rabbits were used and total body arteriograms were performed in pairs of rabbits at 1, 2, 3, 4, 6, 8, 12, 24, 48 and 72 hours after delay. A final two rabbits were examined at 7 days. Flap viability at 24, 48 and 72 hours closely matched the viability assessment at 7 days. Angiographic studies at 48 and 72 hours showed a marked increase in the diameter of vessels in the flap, particularly in the zone of the choke vessels. Again this is in agreement with Pang et al's findings on the timing of delay, showing a maximal increase in nutrient blood flow in the first 3 days following a delay procedure before reaching a plateau at 4 days. Morris et al summarised their impression of surgical delay as involving an initial vasoconstriction between 1 and 4 hours due to the systemic release of vasoconstrictive substances, followed by a diminished effect of these substances between 4 and 12 hours with vessel dilation, then between 24 and 72 hours an active process of dilation and dramatic enlargement of choke vessels.

In 1999 a detailed study was carried out by Dhar and Taylor involving 200 rabbits and 17 dog models to investigate anatomical changes occurring in the delayed

choke arterioles in both the early and late post delay period, the microscopic changes in the cellular elements of the vessel wall, and to provide further information on the mechanism of delay[31]. Using fluorescein, angiographic, light microscopic, immunohistochemical and electron microscopic techniques in 7 experiments, Dhar summarised the events of the delay procedure in 4 phases. Phase 1, between 0 and 24 hours there was an initial vasoconstriction up to 3 hours and then gradual vasodilation to 24 hours. There was minimal change in the cellular elements during this period. Phase 2 occurred between 24 and 72 hours, especially between 48 and 72 hours, with an accelerated increase in vessel diameter especially at the choke vessel level. A dramatic increase in cell division in the vessel wall was noted. Phase 3 occurred between 72 hours and 7 days with continued more gradual dilation of the vessel lumen and a thickening of the media of the vessel wall. Phase 4 occurred from 7 days to one year, the end of the study period, and showed permanent dilation of the choke vessels. The post-operative study of 72 hours of flap perfusion measured by laser Doppler in Chapter 5 displays a zone 3 fall in perfusion between 0 and 16 hours, which then appears to peak at 48 hours before decreasing to 72 hours. The other zones have a less dramatic course although have peak perfusions at 48 hours. This is in agreement with Dhar's outline of the stages in a delay phenomenon, which shares an ischaemic stimulus and alteration in vascular flow in common with free flap transfer.

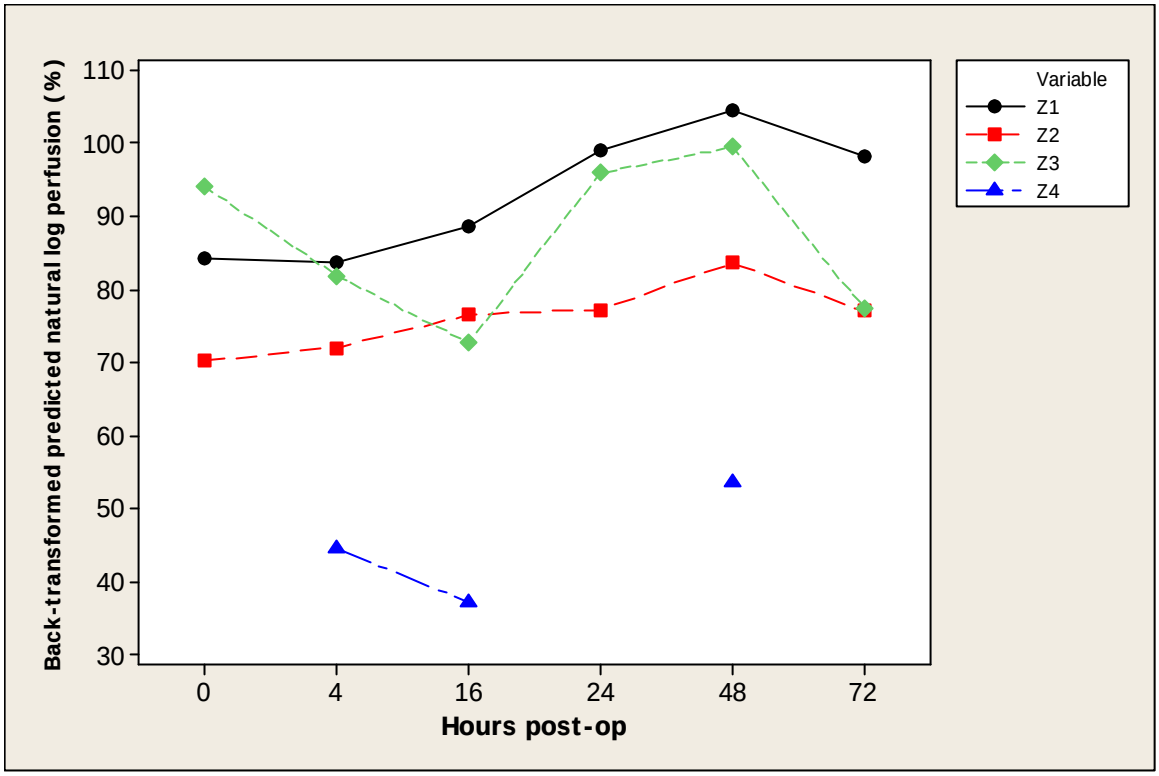

Figure 7-27 - Anti-logged predicted natural log perfusion by zone and time point, Chapter 5. 72 hour post-operative laser Doppler study of flow in DIEP flaps.

Dhar also proposed two possible mechanisms of active dilation of the choke vessels[31]. The first is the physical effect of the blood flow with a new pulsatile flow following anastomosis and a fall in pressure across the choke vessels with other blood supplies (e.g. deep circumflex iliac vessels) disconnected when raising the flap. The second mechanism is hypoxia and this is regarded as an undisputed stimulus for neovascularization although it is unknown how this effects the choke vessels. Mechanisms investigated by other authors include free radicals, nitric oxide and other vascular endothelium derived relaxing factors.

7.5.2 Molecular mechanisms

Delay has been used as a mechanism of improving flap survival and experimentally to improve understanding of the chemical signalling that may be involved in the dilation of choke vessels and intraflap vessels. Inadequate blood perfusion and perhaps ischaemia-reperfusion injury during flap transfer lead to partial flap necrosis. Knowledge of the changes that occur, the pathophysiology and the molecular signalling, may allow flap viability to be improved through pharmacological manipulation.

Pharmacological agents that have experimentally increased flap survival in animals include guanethidine[395], topical nitroglycerine[395;396], prostaglandin E1 and E2[395;397;398](angiogenesis improved[399]), basic fibroblast growth factor (FGFß)[400], platelet derived growth factor (PDGF)[158] and thromboxane A2 synthase inhibition[401]. Decreases in survival have been shown with thromboxane, prostaglandin F1α[401] and epinephrine[402].

A study by Hendel et al in 1982 attempted to determine the pharmacological control of delayed flaps by directly comparing acute and delayed flaps in a series of experiments in rats[403]. They concluded that there were two components to the delay phenomenon, one being passive vasodilation in acute flaps due to loss of sympathetic nerve terminals, and the second was an active vasodilation that did not involve loss of a vasoconstrictor mechanism or sensitization of beta receptors. Hendel et al concluded that this second mechanism was related to an effect on smooth muscle rather than nerves and a vasodilator such as a prostaglandin could perhaps explain this. Murphy et al in 1985 measured the levels of prostaglandin E2 and vasoconstrictive prostaglandin F2α and thromboxane in acute and delayed flaps[398]. The delayed flaps showed a reduced thromboxane production with increased prostaglandin E2, whereas the acute flaps had elevated prostaglandin E2 and thromboxane, and decreased flap survival.

Endothelial dysfunction is a known consequence of ischaemia-reperfusion injury, when tissue has been ischaemic for a period before being reperfused[404]. In a study of 16 rat cremaster muscles, Wang et al 1997, sodium nitroprusside infusion, a direct donor of nitric oxide and thus an endothelium-independent vasodilator, prevented ischaemia-reperfusion vasoconstriction[405]. Acetylcholine however, which stimulates endothelium release of endogenous nitric oxide, does not prevent the vasoconstriction. This indicates that vasospasm and vasoconstriction after ischaemia-reperfusion may be related to temporary endothelial dysfunction, and reduced nitric oxide bioavailability. Free flaps have had a period of ischaemia during transfer and microvascular anastomosis at the recipient site (mean 93 minutes range 56 - 135 minutes in this study, and in Chapter 5 post-operative laser Doppler study 113 minutes mean, range 95 - 155 minutes) and there may be effects caused by temporary endothelial dysfunction. In our laser Doppler post-operative study of perfusion, a decrease in perfusion

was only clearly apparent in zone 3 between 0 - 4 hours postoperatively, although zones 1 and 2 did not show any significant change (Figure 7-27).

7.5.2.1 IL-6, FGFβ and TNFα

Cytokines are cell-signalling protein molecules secreted by a variety of cell types that can modulate immune response. They are transiently produced and act on specific cell-surface receptors. IL-6 and TNF alpha are cytokines produced by T-cells, macrophages and endothelial cells. IL-6 and TNF alpha are both involved in signalling the acute phase response and fever, and are inflammatory cytokines[151]. Fibroblast Growth Factor basic (FGFβ or FGF2) is part of a family of growth factors involved in angiogenesis, wound healing and embryonic development. It is one of the most powerful angiogenic factors identified[406-408]. Vascular endothelial Growth Factor (VEGF) is a heparin-binding glycoprotein that increases vascular permeability. It is also a stimulator of angiogenesis.

In 1995 Most et al carried out a study of dermal cytokine expression in dorsal flaps in rats[409]. Flap biopsies were taken at 0, 8, 16, 24 and 48 hours after the flaps were raised (n=3 for each time point). They were taken 0.5cm, 2.5cm, 5cm and 10cm distances from the distal edge of the flap. Cytokine mRNA profiles were then examined, using in-situ hybridisation, for interleukin-1 alpha (IL-1α), interleukin-2 (IL-2), interleukin-6 (IL-6), basic fibroblast growth factor (FGFβ), interferon gamma IFNγ), transforming growth factor beta (TGFβ) and platelet derived growth factor (PDGF). The highest cytokine expression was detected 8 hours post-operatively for PDGF, TGFβ and FGFβ, with each of these cytokines having a 20-fold increase in signal in comparison with controls($p<0.002$). FGFβ expression was highest 10cm from the flap tip. IL-6 expression was highest at 8 hours with a 14-fold increase, and it was highest 2.5cm and 5cm from the flap tip. 90% of this signal was localised to fibroblasts, keratinocytes and dermal dendritic cells, with the remainder in intravascular and infiltrating lymphocytes and macrophages. IFNγ, IL-1α and IL-2 expression levels were highest at 16 hours with 19-fold elevations with peak expression at the base of the flaps. Clinical oedema, erythema and cyanosis of the flaps appeared at a mean time of 15.7 hours, and by 48 hours the distal tip region appeared partially necrotic. The authors concluded that detecting these cytokines using immunoassays could be useful in a hospital setting for early detection of ischaemia and also as a way of monitoring the effects of pharmacological agents in the prevention or

reversal of flap ischaemia. We would question the feasibility and cost of this, as for detection of impending flap problems 8 hour sampling windows would seem insufficient despite the early warning provided. In addition clinical correlation in patients developing necrosis in comparison with those patients who do not develop necrosis is vital, as cytokines may rise in response to the operative trauma and changes in perfusion within the flap without necessarily signifying impending necrosis. The authors also noted that there was dramatic cytokine elevation at the flap bases in comparison with the ischaemic tips, and that this would be the optimal site for sampling. Our study similarly did not find increased cytokines in zone 4 furthest from the pedicle although there was no significant difference in cytokine concentration in any of the zones.

In a delayed TRAM flap model in rats published by Wong et al in 2002[410], FGFß was measured by biopsy and enzyme-linked immunosorbent assays. A surgical delay was performed 7 days (n=12), 14 days (n=10) or 21 days (n=7) before the flap was raised. FGFß was found to be significantly higher in all delayed flaps than the control flaps with no delay (n=6) at day 3 post-operatively. There was no difference in FGFß across zones 1 - 4. The delayed flaps had higher superficial survival although there was no difference in the deep survival between delay and control groups. The authors concluded that the increase in FGFß at day 3 in delayed flaps may be a factor in improved flap viability, and that further investigation was required. Lineaweaver et al demonstrated a significant increase in cytokine expression of FGFß and VEGF in delayed rat TRAM flaps postoperatively, with no significant differences between zones[411]. In Most's study above, the increase in FGFß increased maximally at 8 hours post operatively, and along with the rise in other cytokines most notable at the flap bases, was thought to represent early ischaemia and that the rise could be used as an early indicator of impending necrosis[409]. The flaps were not delayed. Wong's study however notes an increase in FGFß at in the delayed flaps 3 days post-operatively (the only time point for measurement of FGFß), but no similar rise in non-delayed flaps[410]. They presumed FGFß to therefore be protective. It is likely from these two studies that FGFß increases in response to ischaemia, and perhaps this is why the level is greater in the delayed flaps at 3 days. It may be protective but does not obviously correlate with impending ischaemia as suggested by Most et al.

Cytokine expression is also increased following ischaemia-reperfusion. A rat study by Zhang et al in 2005 subjected rat gracilis muscle to two episodes of ischaemia, a primary episode for one hour and then a 24 hours later a secondary ischemia of 4 hours[412]. Gene expression of TNFα, interleukin 1 beta (IL1ß) and platelet derived growth factor (PDGF) mRNA was determined by PCR at 4 and 18 hours after the primary ischaemia and at 0, 4 and 18 hours after the secondary ischaemia. IL-1 was upregulated 4hours after the primary ischaemia and PDGF was upregulated immediately after the secondary ischaemia. TNFα was significantly upregulated 18 hours after secondary ischaemia. Our highest concentration was at 16 hours which was significantly higher than the concentration at 12 hours post-operatively ($p=0.002$). Following this there was a slowly decreasing significant trend. Our average ischaemia time for the DIEP flap during microvascular anastomosis was 93 minutes. This is shorter than the secondary ischaemia time in the rat model, and the rat model is a muscle flap rather than a perforator flap like the DIEP. It is therefore difficult to make comparisons regarding the timing of the rise in TNFα, although there does appear to be a post operative rise in this cytokine.

The levels of cytokines expressed may vary in relation to the type of operative reconstruction as a reflection of differing levels of trauma. In a clinical study, Schmidt et al compared the level of proinflammatory cytokines in blood samples of thirty patients undergoing delayed breast reconstruction with either lateral thoracodorsal flaps, latissimus dorsi flaps or pedicled transverse rectus abdominis flaps (pedicled TRAM flaps)[413]. Blood samples were taken pre-operatively, at 24 hours and 2 weeks post-operatively, and tested using immunoassay kits for TNF, IL-6 and IL-8. IL-6 levels were significantly elevated in all groups 24 hours after surgery, and the levels were significantly higher in the TRAM group. IL-8 was significantly increased in all groups after surgery although the TRAM patients had the lowest rise. TNF remained at normal levels. The authors concluded that IL-6 levels were highest in the patients undergoing TRAM flaps as this was the most extensive operation. We found that IL-6 had an increasing trend from zero to around 30 hours post-operatively before levelling off.

In the design of future studies, a study by Erdmann et al highlighted differences between the levels of the cytokine vascular endothelial growth factor between

the skin of a flap and the muscle of a flap[414]. In an ischaemia-reperfusion study of latissimus dorsi muscles flaps in pigs, looking at both skin and muscle within the flap, Erdmann showed an increase in expression of vascular endothelial growth factor (VEGF) in both the ischaemic flaps and the control latissimus dorsi flaps. The VEGF was detected using immunoassays in biopsies, at a fixed time point of 2 hours reperfusion following 4 hours of ischaemia. VEGF expression in the muscle of the flaps was significantly higher than VEGF expression in flap skin (~30-85pg/mg versus ~5-15pg/mg). Ischaemia-reperfusion latissimus dorsi muscle in comparison with the control flap showed higher levels of VEGF than the control flap in zones 1 and 2, and the levels of VEGF decreased from zone 1 to 3. The same pattern was repeated in the skin zones, albeit at lower levels. Due to cost implications we were unable to have a control catheter in adjacent skin which displays significantly lower levels of VEGF than the flaps in this study. Erdmann's study unlike our study showed a trend towards decreasing levels of cytokine further from the pedicle. This could be related to the method of sampling using biopsies rather than microdialysis catheters before similarly using immunoassays. A suggested explanation was that the ischaemia, especially in muscle, resulted in the most ischaemic area (zone 3) being unable to produce as much VEGF. We have no example of this level of ischaemia, although patient 5 developed a haematoma requiring evacuation in theatre around 52 hours post-operatively (Figure 7-8). There was an increase in IL-6 towards this time point in all zones, but no obvious change for FGFß or TNFα. This patient may have suffered from mild ischaemia within the flap due to pressure effects and congestion, but if so this has resulted in an increase rather than decrease of cytokines.

Clinically, varying scenarios would need to be encountered to appreciate patterns of cytokine release in relation to outcome. There may be differences across zones and with time, and also between different flap compositions. The use of microdialysis catheters is a more acceptable method of analysis of cytokine levels than biopsies as used in animal studies. Our patients had no complications related to use of the catheters. Microdialysis fluid can be collected continuously and high cut-off catheters would appear to collect cytokines IL-6, FGFß and TNFα all less than 100 kilo Daltons. It would be useful to directly compare the levels of cytokines in biopsy specimen immunoassays and though MRNA expression with microdialysis catheters, to compare time lines

between techniques and also assess the percentage pick-up of the catheters. The use of high cut-off catheters as a research tool in plastic surgery is not reported in the literature, and without further study it is difficult to ascertain whether there could be confounding factors in the measurement of molecules observed in the biological setting. For example when there are other unknown molecules in circulation perhaps close to the membrane pore size, it is not unfeasible that these could cause temporary occlusions or alter the amount of researched molecule reaching the microvial in other ways. The levels of FGFß appeared to oscillate around a constant concentration over the time period in a way that did not appear to be physiological. Whether this was artefact perhaps at the point of analysis from the stored microvials, or whether this occurred during collection is not clear. We chose to have a low flow rate through the microdialysis pumps to try and maximise the concentration of molecule collected. This conversely reduces the rate of fluid collection in the microvials necessitating a 4 hour rather than 15 minutes or less use in flap monitoring with 20k Dalton catheters. We do not feel that 4 hour collection periods would be detrimental when using microdialysis catheters as a research tool as many studies use 12 hours, or greater, biopsy intervals.

7.5.2.2 Manipulation of flap survival & factors improving flap survival

Some cytokines have been shown in animal studies to improve the survival of flaps. Transforming growth factor beta, fibroblast growth factor, endothelial growth factor and vascular endothelial growth factor shown some of the more impressive results[400;415-419].

Carroll et al designed a study to investigate the benefit of exogenous FGFß in a muscle flap[400]. Exogenous FGFß is thought to act in an autocrine fashion and enhance the release of endogenous FGFß. Intra-arterial administration of 100µg of basic fibroblast growth factor immediately following a delay procedure on a latissimus dorsi in nine canines resulted in increased expression of native FGFß on completion of the flap 10 days later. There was a 20% increase in perfusion compared with the control, and 300% improvement in fatigue resistance of the muscle. This would be of benefit in functional muscle transfers and cardiomyoplasty. Carroll et al note that other authors have not found survival advantage of FGFß[420], but suggest that the key to benefit is injection into

ischaemic rather than well-perfused tissue as described in the case of cardiac infarction by Yanagisawa-Miwa et al in 1992[421]. Ishiguro et al investigated the effect of exogenous FGFβ at the time of operation on the viability of random skin flaps in rats and also found a survival advantage at day 7[417]. FGFβ has also been shown to upregulate the expression of VEGF, another angiogenic factor, in smooth muscle cells synergistic with hypoxia[422]. A further study by Carroll et al in mice demonstrated the flap survival advantage of Platelet Derived Growth Factor (PDGF), another angiogenic factor, directly into the injected directly into the latissimus dorsi muscle 10 days before flap elevation[423]. These studies present further possibilities of increasing flap survival, although as the growth factor manipulation is 10 days prior to flap elevation, these would presumably be an unsuccessful adjunct in acute flap failure. The timings are comparable with angiogenesis and this is the authors' suggested mechanism. More work is required to assess the potential of more immediate benefits from these growth factors such as the dilation of choke vessels, and whether improvement in flap survival is as significant in all flap types as in muscle flaps.

Tumour necrosis factor alpha (TNFα) and interleukin-1 (IL-1) were found to be decreased by the exogenous Vascular Endothelial Growth Factor (VEGF) in a rat study by Pang et al in 2002[424]. Rats (n=24) were placed into two groups and 3cm by 10cm dorsal flaps raised. Half of the control groups had injection of 1ml of saline and the other half of the control group had no injection. The treatment group had 1ml (1μg/ml) of exogenous VEGF injected into several points in the flap. Biopsies were taken from both groups at 12 hours and 24 hours post-operatively and cytokine mRNA expression was determined by PCR. There was no detection of insulin-like growth factor-1, transforming growth factor beta, FGFβ, and platelet derived growth factor mRNA. Interleukin-1 expression was decreased in both the saline and VEGF injection groups at both time points. TNFα was also significantly reduced at 12 hours and 24 hours in the distal parts of the flap, and in the middle of the flap at 12 hours, in comparison with controls. Inducible nitric oxide synthase expression was decreased in the middle of the VEGF treated flaps at 12 hours, and decreased in the middle and distal sections at 24 hours. TNFα and IL-1 are pro-inflammatory cytokines contributing to local inflammation, and may therefore lead to tissue damage. Their role in flap survival is not clear. Inducible nitric oxide synthase mediates the cytotoxic action of macrophages and leads to the formation of tissue damaging free

radical. The authors conclude that VEGF's advantage in ischaemic flap survival may be related to its inhibition of TNFα and attenuation of inducible nitric oxide synthase. Endogenous VEGF has been shown to rise 3 days after delay in animal models, with an increase in perfusion observed after 7 days[425].

The pathophysiology of ischaemia-reperfusion injury, the delay phenomenon and the changes occurring following flap surgery requires further investigation, as a better understanding may allow a treatment to improve flap survival, for example a monoclonal antibody to proinflammatory cytokines[412] or the exogenous administration of cytokines preoperatively.

8 Summary

The aim of this thesis was to investigate factors controlling cutaneous microcirculation, and patterns of perfusion within the microcirculation in relation to lower abdominal flaps.

The application of the topical anaesthetic creams EMLA and ametop prior to laser treatment of capillary malformations provided an accessible example of a pharmacological agent affecting the microcirculation. In capillary malformations we found that topical EMLA reduced vessel diameter during a 90 minute application time. Ametop subjectively increased vessels' diameter although this was not significant. Vasoconstriction could potentially be deterimental to the outcome of laser treatment. The technique of videomicroscopy was compared to a confocal laser scanning microscope. Similar results were found with no significant differences between the diameters measured.

To compare the physiological territories of SIEA and DIEP vessels supplying the lower abdomen, a pilot study was devised to ensure that reactive hyperaemia did not account for differences in area perfused. Within operative time constraints, the assessment of a vessel by any technique involves clamping those vessels not being assessed, and then allowing a period for blood flow to stabilise when clamps are switched, before assessment of sequential vessels. We validated a methodology that would allow multiple vessels to be assessed in free flap transfers by illustrating with laser Doppler that there was no significant differences between the clamp times, or between scanning times over 5 minutes. This protocol allows maximal information to be gained in the intra-operative period in further research studies. We also confirmed that the subjective choice of good and poor areas of perfusion within the flap are statistically significant and this may be of benefit clinically should uncertainty arise in the choice of vessel or design of flap.

The methodology of this pilot study described in Chapter 4 was used to compare SIEA and DIEP lower abdominal flaps intraoperatively (Chapter 6). The overall perfusion of the DIEP vessels was significantly higher than that of the SIEA. The DIEP vessels perfused the traditional Hartrampf perfusion zones in the order 1,

3, 2 and then 4. There was no significant difference in the perfusion of zones 1 and 3, but both were significantly better perfused than zone 2, and this in turn was better perfused than zone 4. 60% of the DIEPs were based only on medial perforators, 25% on medial and lateral perforators, and 15% on both medial and lateral perforators. The SIEA vessels' descending order of perfusion was zone 1, 3, 2 and then 4. Unlike the DIEP vessels there was no significant difference in perfusion between zones 1, 2 and 3, and all were significantly better perfused than zone 4. This is not in support of SIEAs being described as hemiabdominal.

A 72 hour post-operative laser Doppler study of DIEP flap perfusion was performed to observe any changes in perfusion around the theoretical time of opening of choke vessels between angiosomes. Although no statistical differences were found, the differences between zones with time approached significance ($p=0.051$). The most dramatic changes in perfusion occurred between 16 and 48 hours. This study did not elucidate a definite pattern of perfusion between angiosomes during the immediate post-operative period, and did not change the design for a further study using microdialysis catheters to investigate possible changes in tissue cytokines over the same period.

Our final study involved the use of high cut-off microdialysis catheters in DIEP flaps, a use that has not previously been reported in the literature. Microdialysis has been used increasingly in flap monitoring and in other surgical fields to provide early detection of ischaemia, however the use of high-cut off catheters for the collection of larger molecules in tissue other than brain is not well documented. The investigation of three cytokines resulted in linear trends of IL-6 and TNFα, with IL-6 increasing to around 28 hours before stabilizing, and TNFα showing an initial peak around 16 to 20 hours before decreasing gradually. FGFβ had the most unusual pattern with oscillations around a constant trend. Further work would be required to establish if this had physiological significance.

In conclusion, the study of the microcirculation in flaps is in an attempt to reduce the risk of partial necrosis and morbidity for the patient. Intraoperative studies have potential to be of benefit in the planning and design of flaps, although there are no absolute correlations with flap outcome. Similarly as there is a large variability in perfusion patterns within the same nominal vessels, newer concepts such as the perforasome allow for consideration of this

individuality. Ultimately, knowledge of the process of choke and anastomotic vessel dilation in the immediate post-operative period and the ability to control this period would be a fundamental step for plastic surgery.

Appendix

Chapter 3

Estimates of variance components

The estimates of components of variance associated with each random term are shown in below.

Random term	Estimated variance component
Patient	0.00961
Patient.Treatment	-0.00058
Patient.Microscope	0.00251
Patient.Treatment.Microscope	0.00282
Residual	0.0262

Estimates of variance components

The variance between patients is 0.01444 which is the sum of the first four components. This represents the variability between patients of the true mean diameter of a patient's vessels. It is approximately half the within-patient variance (0.0262) which measures the variability between the measurements of individual vessels for a given patient.

Most of the random variation in the data are between measurements of different vessels for a given patient.

Checking model assumptions: homogeneity of variance

The residual variation is greater for the videomicroscope than the confocal microscope.

The figure below shows boxplots of residuals ('observed' minus 'predicted' where 'predicted' includes random effects) by treatment and microscope. Looking at the inter-quartile range, within-patient variability for the videomicroscope appears greater than for the confocal microscope.

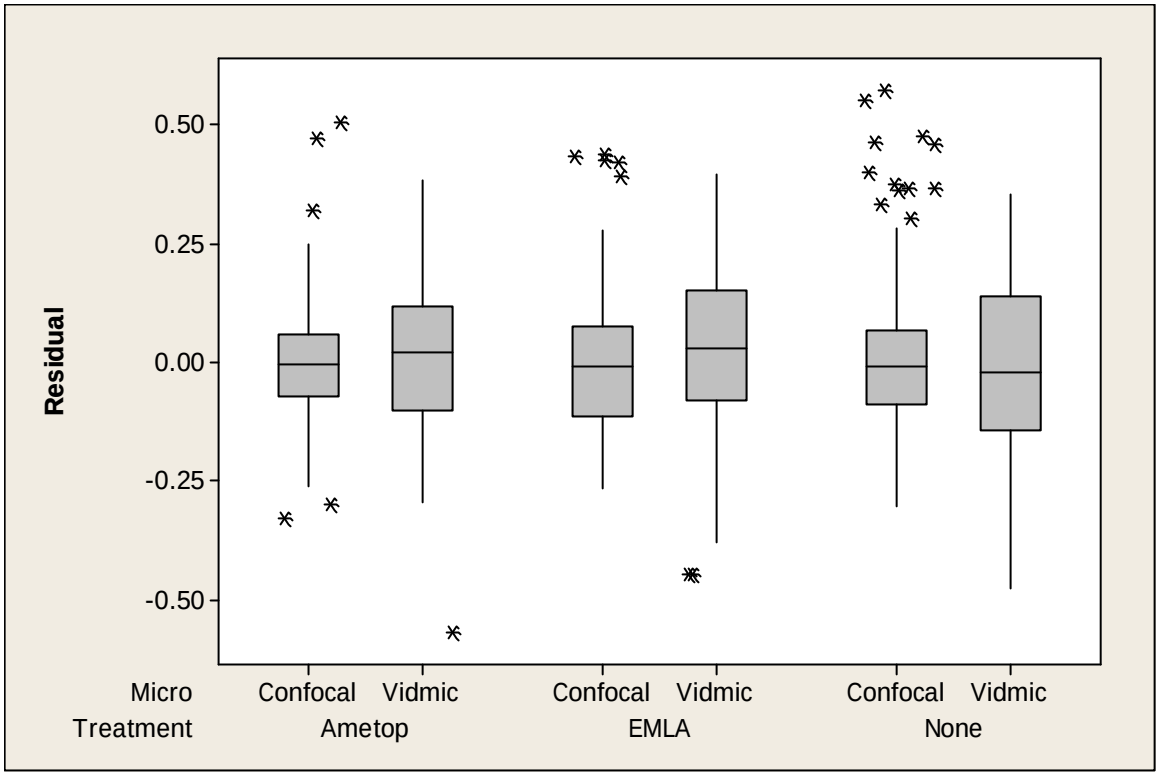

Residuals (log scale base 10) by treatment and by microscope (fitted values include random effects)

The table below compares the summary statistics of the residuals (observed minus predicted, where predicted includes random effects) among the six groups defined by treatment and microscope type. Within each treatment category, the tendency for the variability of measurements made with the videomicroscope to be greater can be seen by comparing the s.d. and interquartile ranges.

Results for Treatment = Ametop

Variable	Micro	N	N*	Mean	SE Mean	StDev	Minimum	Q1	Median
Resi	Confocal	92	0	-0.0000	0.0137	0.1317	-0.3303	-0.0728	-0.0039
	Vidmic	36	0	0.0000	0.0320	0.1919	-0.5698	-0.1036	0.0214

Variable	Micro	Q3	Maximum
Resi	Confocal	0.0592	0.5065
	Vidmic	0.1183	0.3844

Results for Treatment = EMLA

Variable	Micro	N	N*	Mean	SE Mean	StDev	Minimum	Q1	Median
Resi	Confocal	88	0	0.0000	0.0168	0.1575	-0.2676	-0.1169	-0.0078
	Vidmic	36	0	0.0000	0.0377	0.2264	-0.4467	-0.0794	0.0305

Variable	Micro	Q3	Maximum
Resi	Confocal	0.0766	0.4371
	Vidmic	0.1490	0.3978

Results for Treatment = None

Variable	Micro	N	N*	Mean	SE Mean	StDev	Minimum	Q1
Resi	Confocal	241	0	0.00000	0.00947	0.14695	-0.30340	-0.08905
	Vidmic	72	0	0.0000	0.0201	0.1705	-0.4797	-0.1427

Variable	Micro	Median	Q3	Maximum
Resi	Confocal	-0.00990	0.06695	0.57230
	Vidmic	-0.0222	0.1396	0.3525

Summary statistics of residuals ('Resi'). Residuals are calculated as 'observed' minus 'predicted' includes random effects.

The homogeneity of variance by predicted diameter is shown in the figure below. The residuals (observed minus predicted where predicted includes random effects) are plotted against predicted (fitted values). There does not appear to be any evidence that variability increases or decreases markedly with fitted value.

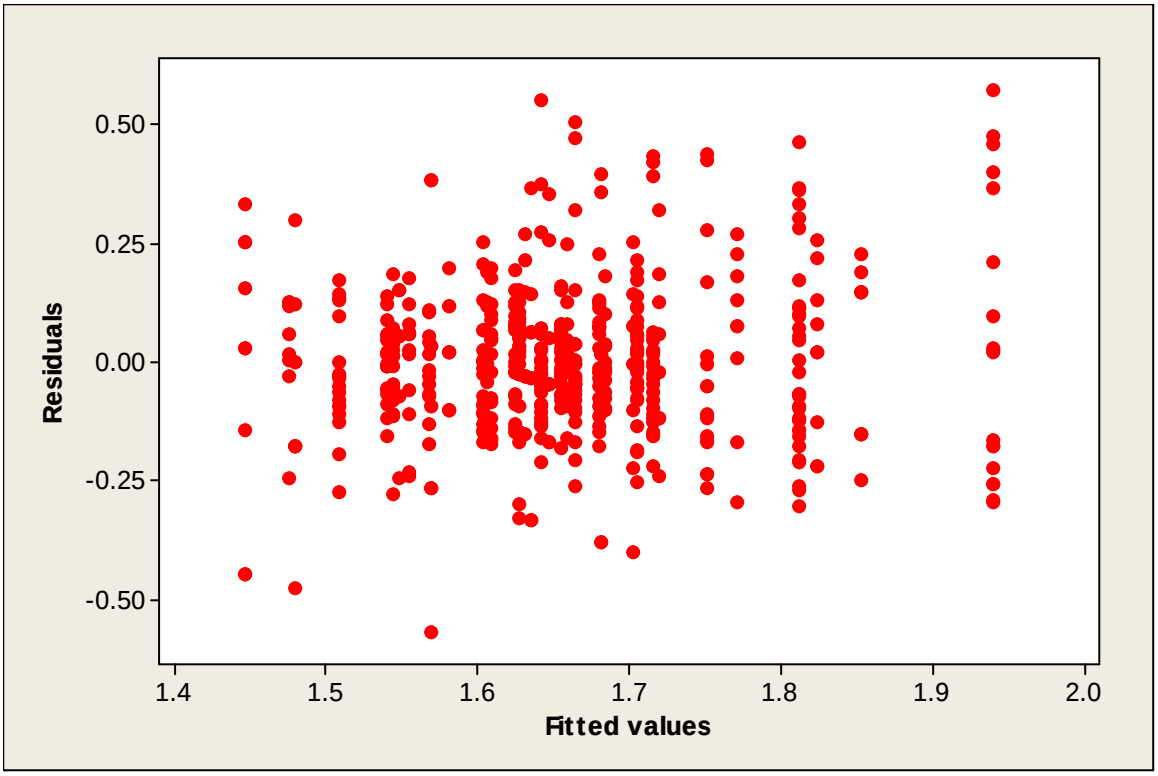

Residuals (observed minus predicted where predicted includes random effects) plotted against predicted (fitted values).

Normality of residuals

The figures below show normality of the residuals. The residuals are 'observed' minus 'predicted' where 'predicted' includes random effects.

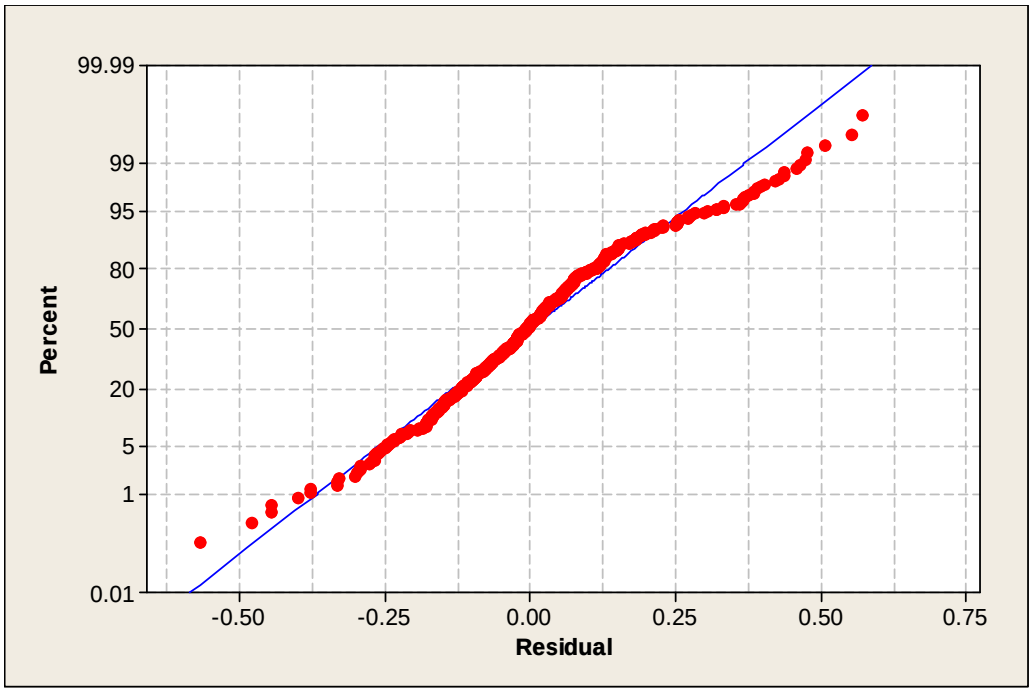

Normal plot of residuals

The Anderson-Darling test statistic is significant ($p<0.005$).

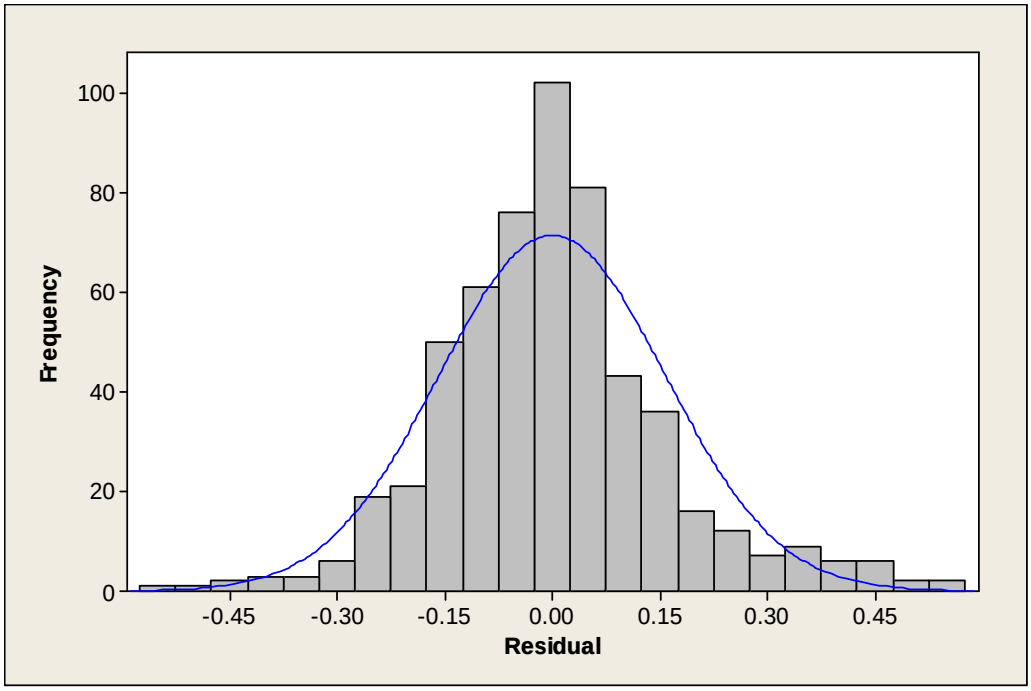

Histogram of residuals with added normal curve.

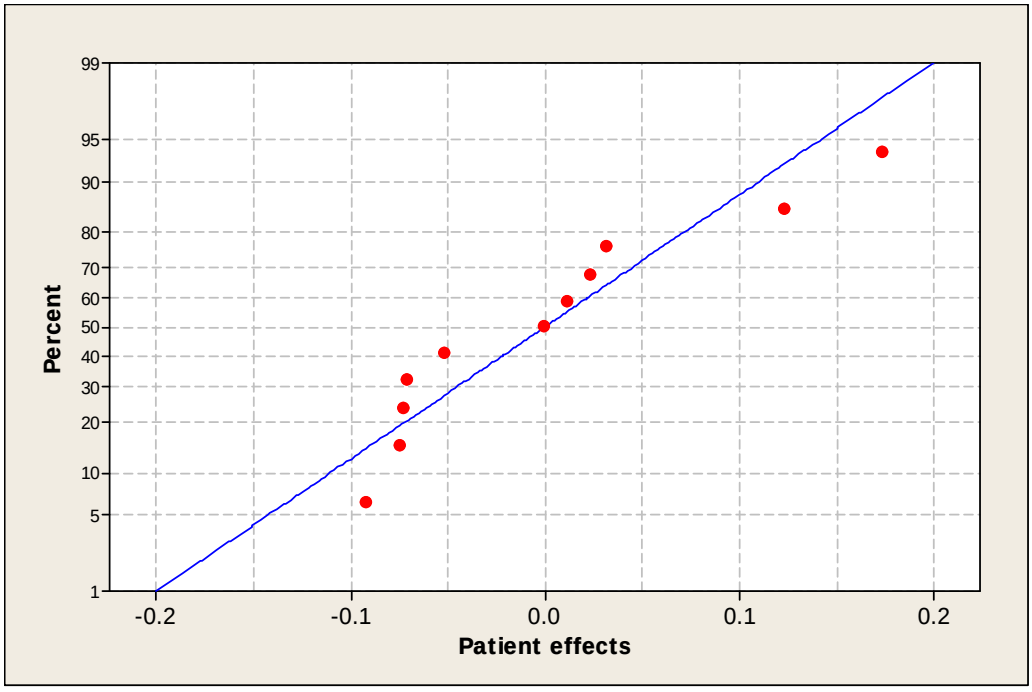

Normal plot for patient effects.

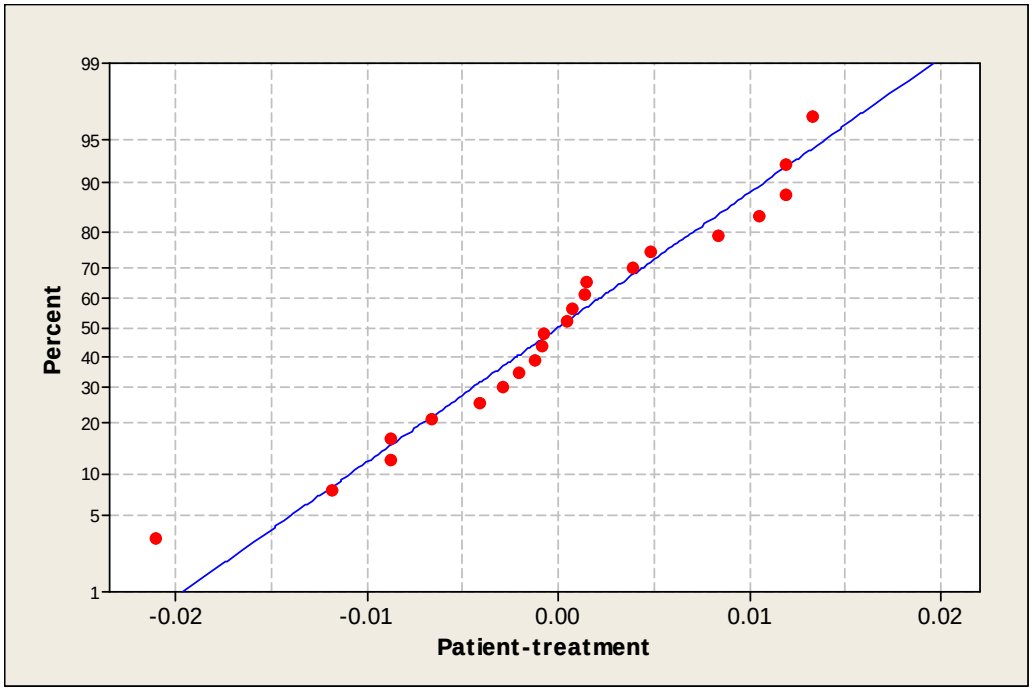

Normal plot for patient-treatment interaction effects.

The estimated variance component is negative (-0.00058). If this value is interpreted as zero, all 'patient.treatment' effects should be zero.

The Anderson-Darling test statistic is not significant (p=0.551).

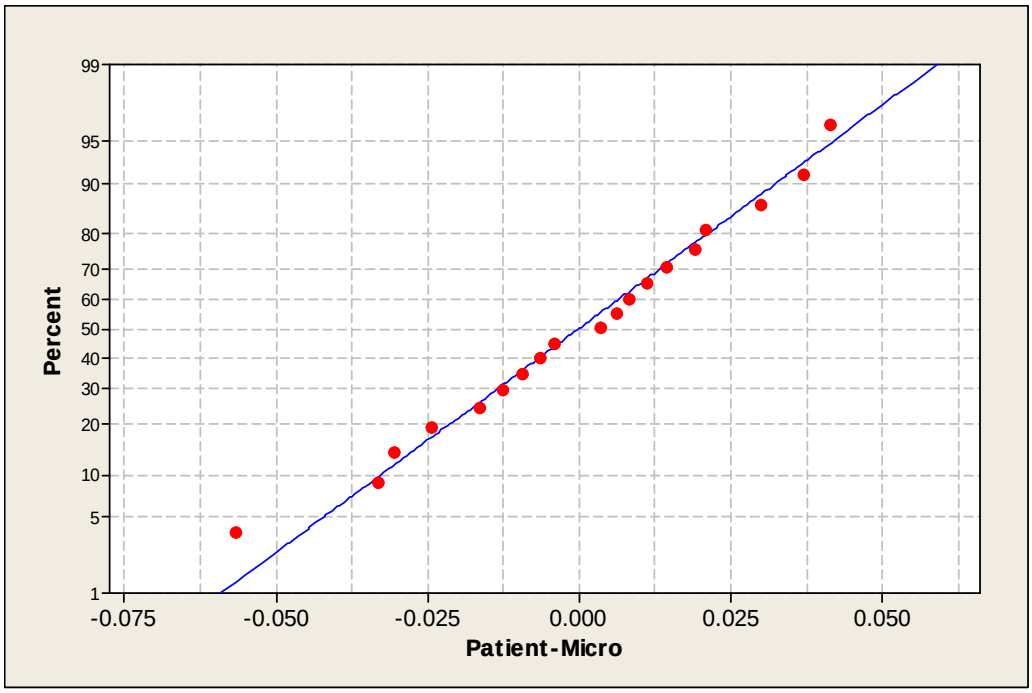

Normal plot for patient-microscope interaction effects.

The Anderson-Darling test statistic is not significant (p=0.989).

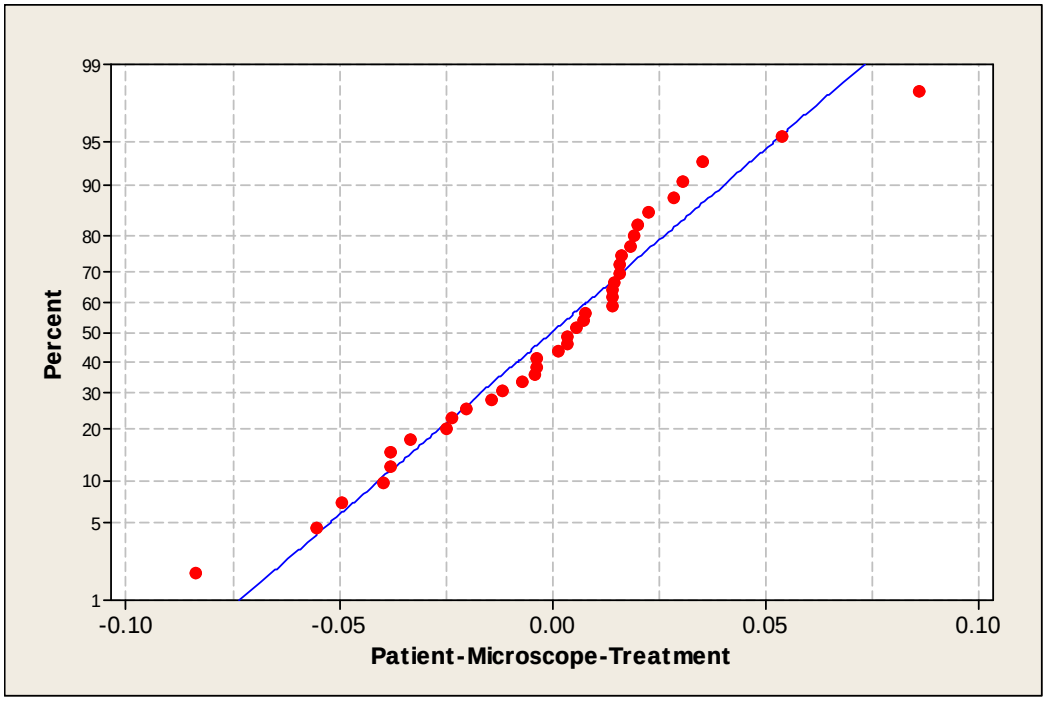

Normal plot for patient-microscope interaction effects.

The Anderson-Darling test statistic is not significant (p=0.096).

Non-parametric tests

Due to evidence of non-normality of the residual errors, the effects of anaesthetic and the difference between types of microscope were tested using non-parametric tests. The log (base 10) diameters for each patient were averaged (patients 4 - 11 used as these had measurements from both microscopes).

Row	Anaesthetic1	Patient1	Con Pre	Con Post	Video Pre	Video Post
1	Ametop	4	1.642	1.610	1.640	1.602
2	Ametop	8	1.585	1.665	1.682	1.827
3	Ametop	9	1.662	1.689	1.393	1.602
4	Ametop	10	1.521	1.678	1.668	1.519
5	EMLA	5	1.638	1.552	1.728	1.562
6	EMLA	6	1.817	1.719	1.841	1.631
7	EMLA	7	1.481	1.498	1.663	1.448
8	EMLA	11	1.984	1.730	1.869	1.669

Mean log diameters for patients 4 to 11.

Interaction between treatment and microscope type was tested in two stages. First the difference between microscope types, of pre-post differences. These differences of differences were compared between the two groups, ametop and EMLA, using a Mann Whitney test. The null hypothesis was that the interaction could be described by a single parameter. This hypothesis was not rejected (p=0.471). Secondly, the complete set of differences of differences was tested against zero using a Wilcoxon signed rank test. The null hypothesis is that the interaction parameter is zero, and this was not rejected (p=0.363).

Row	Anaesthetic1	Patient1	Interaction
1	Ametop	4	-0.006
2	Ametop	8	0.065
3	Ametop	9	0.182
4	Ametop	10	-0.306
5	EMLA	5	-0.080
6	EMLA	6	-0.112
7	EMLA	7	-0.232
8	EMLA	11	0.054

Linear combination of log mean diameters for testing equality of interaction parameters.

Mann-Whitney Test and CI: Interaction_Ametop, Interaction_EMLA

	N	Median
Interaction_Ametop	4	0.0295
Interaction_EMLA	4	-0.0960

Point estimate for ETA1-ETA2 is 0.1170
97.0 Percent CI for ETA1-ETA2 is (-0.3600,0.4139)
W = 21.0
Test of ETA1 = ETA2 vs ETA1 not = ETA2 is significant at 0.4705

Test of equality of interaction parameters.

Wilcoxon Signed Rank Test: Interaction

Test of median = 0.000000 versus median not = 0.000000

	N	N for Test	Wilcoxon Statistic	P	Estimated Median
Interaction	8	8	11.0	0.363	-0.05100

Test of zero interaction.

Assuming no interaction, the mean effect of microscope was tested. The differences in log diameter between microscope types were computed (i) for pre-treatment and (ii) for post-treatment, and these differences added. These sums of differences were tested against zero using a Wilcoxon signed ranks test (see tables below). The test statistic was not statistically significant, p=0.834.

Row	Anaesthetic1	Patient1	Micro
1	Ametop	4	0.010
2	Ametop	8	-0.259

3	Ametop	9	0.356
4	Ametop	10	0.012
5	EMLA	5	-0.100
6	EMLA	6	0.064
7	EMLA	7	-0.132
8	EMLA	11	0.176

Linear combination of log diameters for testing difference between microscope types, in the absence of interaction.

Wilcoxon Signed Rank Test: Micro

```
Test of median = 0.000000 versus median not = 0.000000

          N for   Wilcoxon          Estimated
       N   Test  Statistic      P     Median
Micro  8      8       20.0  0.834    0.01150
```

Test of no difference between microscope types.

The null hypothesis that the effects of the two anaesthetics are identical was tested. For each patient, the pre-post differences obtained with the two microscopes were added. The two groups, Ametop and EMLA, were compared with respect to these sums of differenced using a Mann Whitney test, which was statistically significant, p=0.0304.

Row	Anaesthetic1	Patient1	Treatment
1	Ametop	4	0.070
2	Ametop	8	-0.225
3	Ametop	9	-0.236
4	Ametop	10	-0.008
5	EMLA	5	0.252
6	EMLA	6	0.308
7	EMLA	7	0.198
8	EMLA	11	0.454

Linear combination of log diameters for testing equality of effects of anaesthetic.

Mann-Whitney Test and CI: Treatment_Ametop, Treatment_EMLA

```
                  N   Median
Treatment_Ametop  4  -0.1165
Treatment_EMLA    4   0.2800


Point estimate for ETA1-ETA2 is -0.4285
97.0 Percent CI for ETA1-ETA2 is (-0.6900,-0.1281)
W = 10.0
Test of ETA1 = ETA2 vs ETA1 not = ETA2 is significant at 0.0304
```

Test of equality of effects for anaesthetic.

The non-parametric tests and REML analysis give the same findings as regards the statistical significance of experimental factors.

Chapter 4

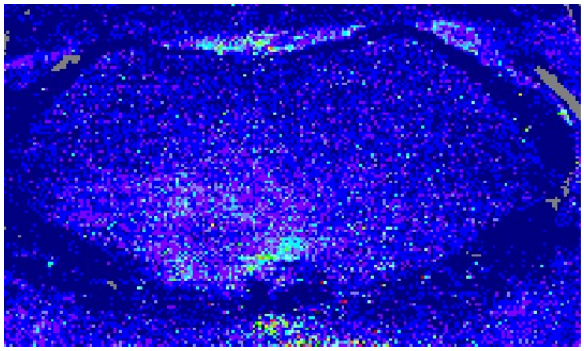

Patient 1 - 20 minute clamp time 5 minute scan time

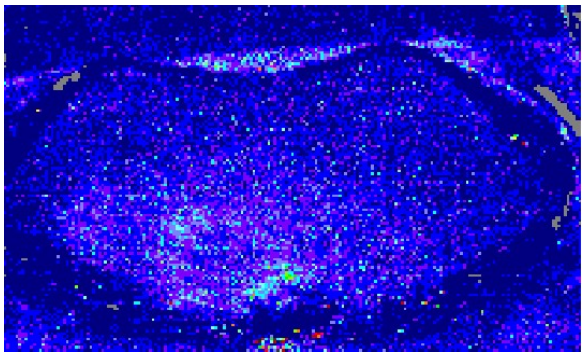

Patient 1 - 20 minute clamp time, 10 minute scan time.

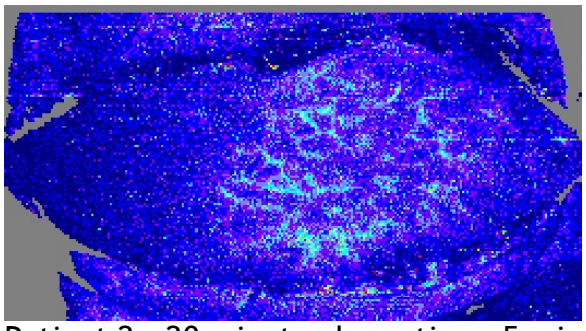

Patient 2 - 20 minute clamp time, 5 minute scan time.

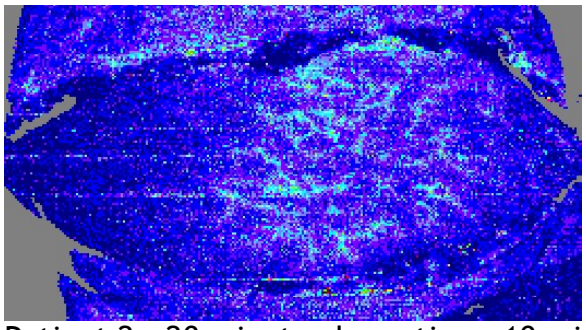

Patient 2 - 20 minute clamp time, 10 minute scan time.

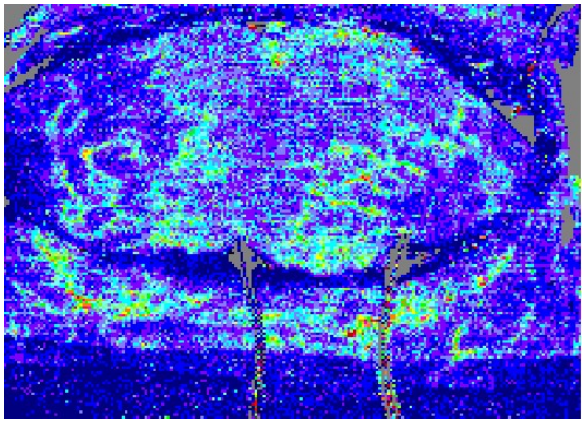

Patient 3 - 20 minute clamp time, 5 minute scan time.

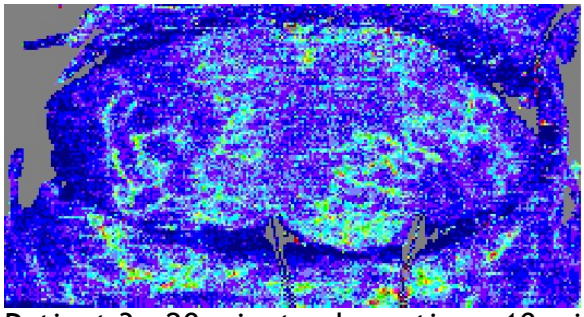

Patient 3 - 20 minute clamp time, 10 minute scan time.

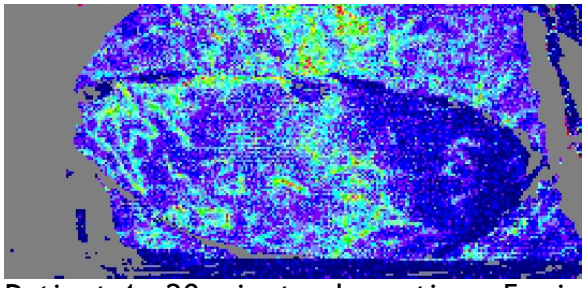

Patient 4 - 20 minute clamp time, 5 minute scan time.

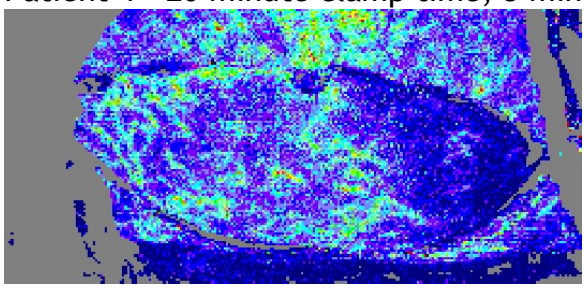

Patient 4 - 20 minute clamp time, 10 minute scan time.

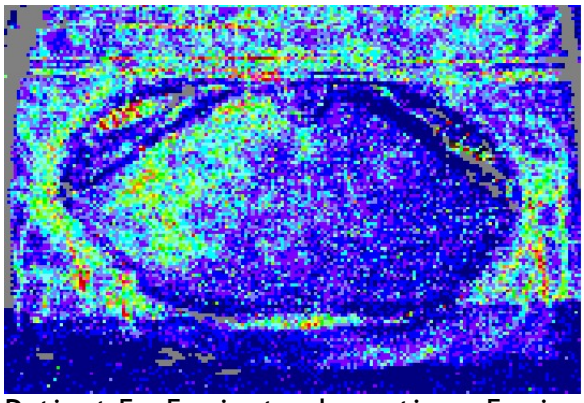

Patient 5 - 5 minute clamp time, 5 minute scan time.

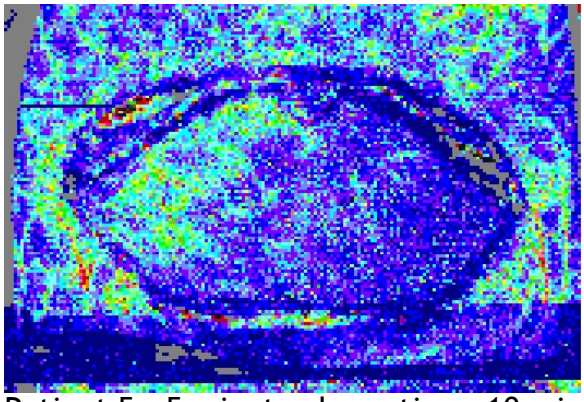

Patient 5 - 5 minute clamp time, 10 minute scan time.

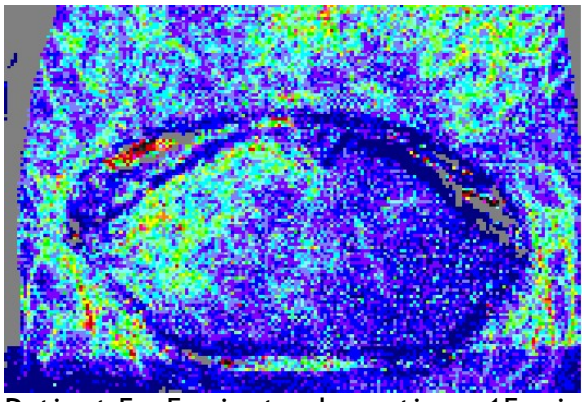

Patient 5 - 5 minute clamp time, 15 minute scan time.

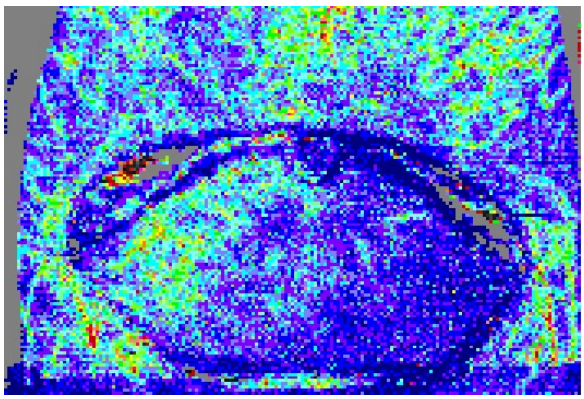

Patient 5 - 5 minute clamp time, 20 minute scan time.

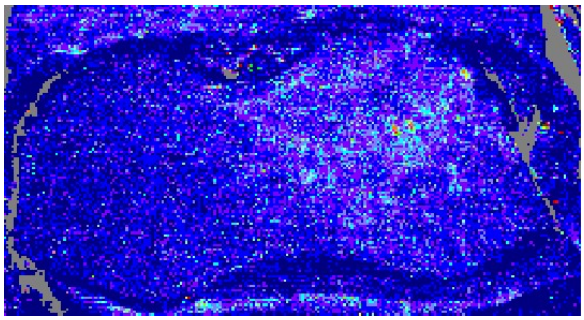

Patient 6 - 5 minute clamp time, 5 minute scan time.

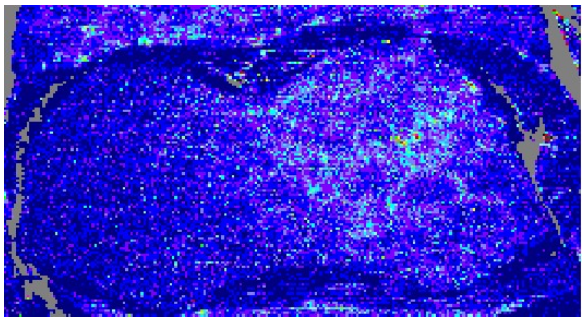

Patient 6 - 5 minute clamp time, 10 minute scan time.

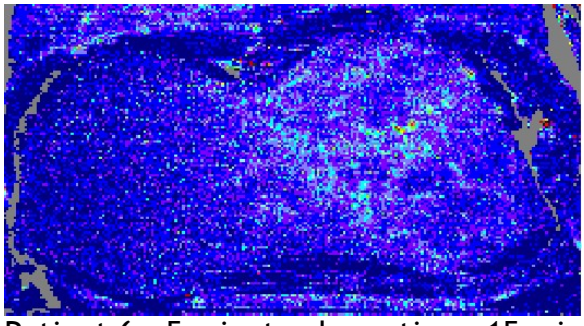

Patient 6 - 5 minute clamp time, 15 minute scan time.

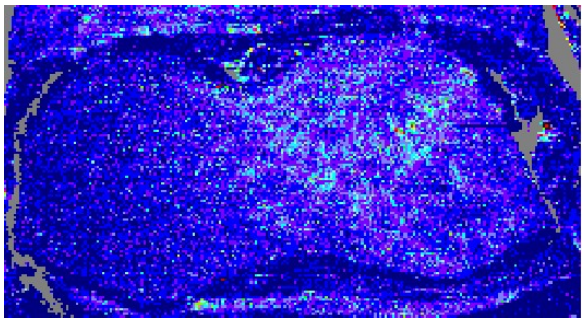

Patient 6 - 5 minute clamp time, 20 minute scan time.

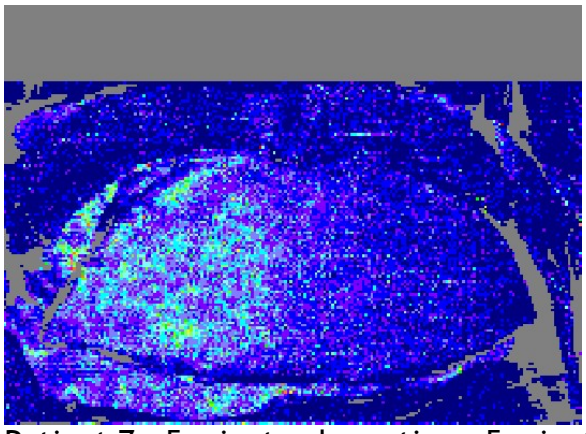

Patient 7 - 5 minute clamp time, 5 minute scan time.

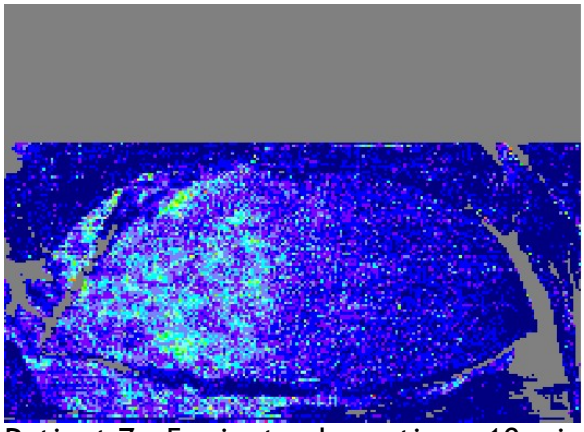

Patient 7 - 5 minute clamp time, 10 minute scan time.

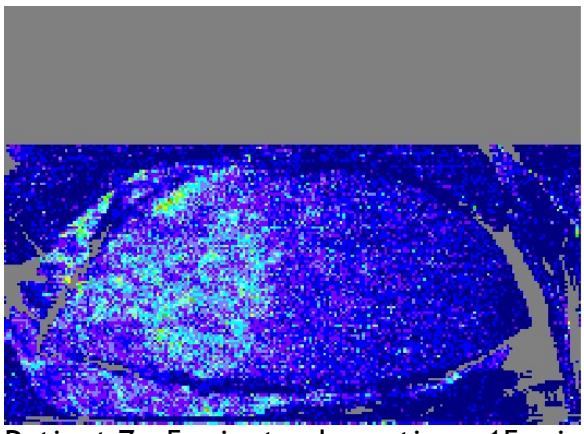

Patient 7 - 5 minute clamp time, 15 minute scan time.

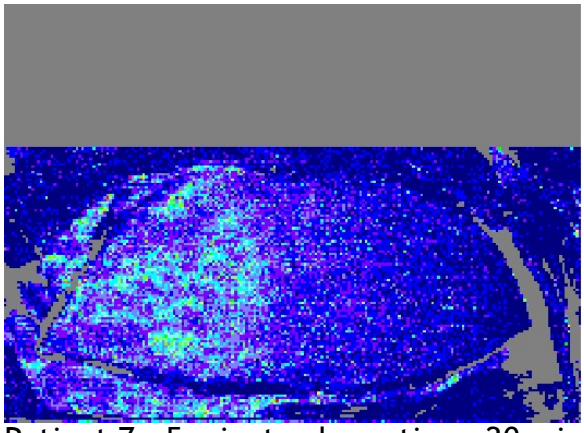

Patient 7 - 5 minute clamp time, 20 minute scan time.

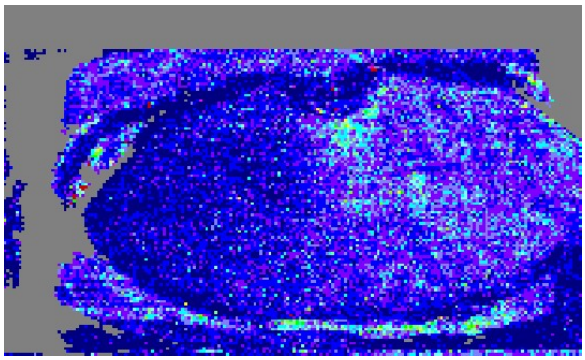
Patient 8 - 5 minute clamp time, 5 minute scan time.

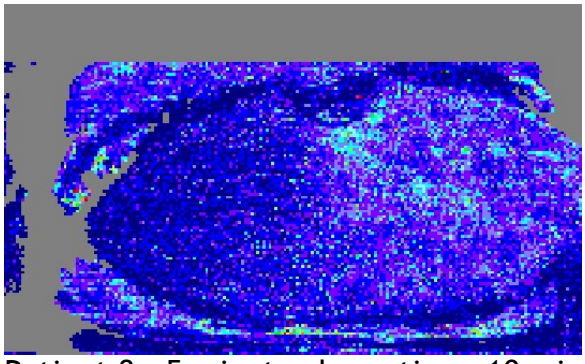
Patient 8 - 5 minute clamp time, 10 minute scan time.

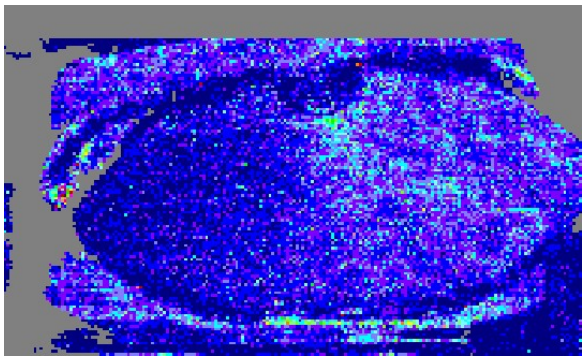
Patient 8 - 5 minutes clamp time, 15 minutes scan time.

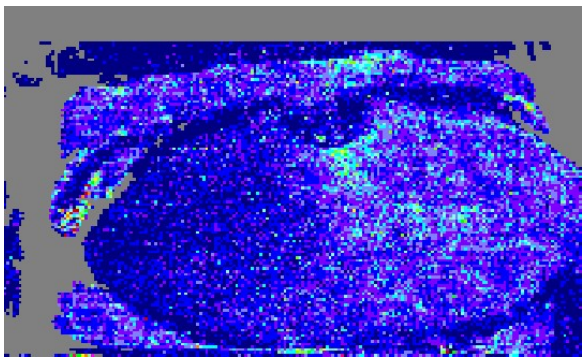
Patient 8 - 5 minutes clamp time, 20 minutes scan time.

Confidence intervals

95% confidence intervals for mean differences in flow, between scan times (at clamp time 5 minutes).

Contrast between scan times (minutes)	Difference between mean flow (higher scan time *minus* lower)	Difference	95% c.i. for difference
10 minus 5	97.75-97.00	0.75	(-1.96, 3.46)
15 minus 5	97.50-97.00	0.50	(-2.21, 3.21)
20 minus 5	98.50-97.00	1.50	(-1.21, 4.21)
15 minus 10	97.50-97.75	-0.25	(-2.96, 2.46)
20 minus 10	98.50-97.75	0.75	(-1.96, 3.46)
20 minus 15	98.50-97.50	1.00	(-1.71, 3.71)

Diagnostic plots for ANOVA

The following graph shows residuals plotted against fitted values. Although random variability tends to decrease with increasing fitted value over the full range of fitted values, the trend is not consistent. There does not appear to be a compelling reason to re-analyse on a transformed scale.

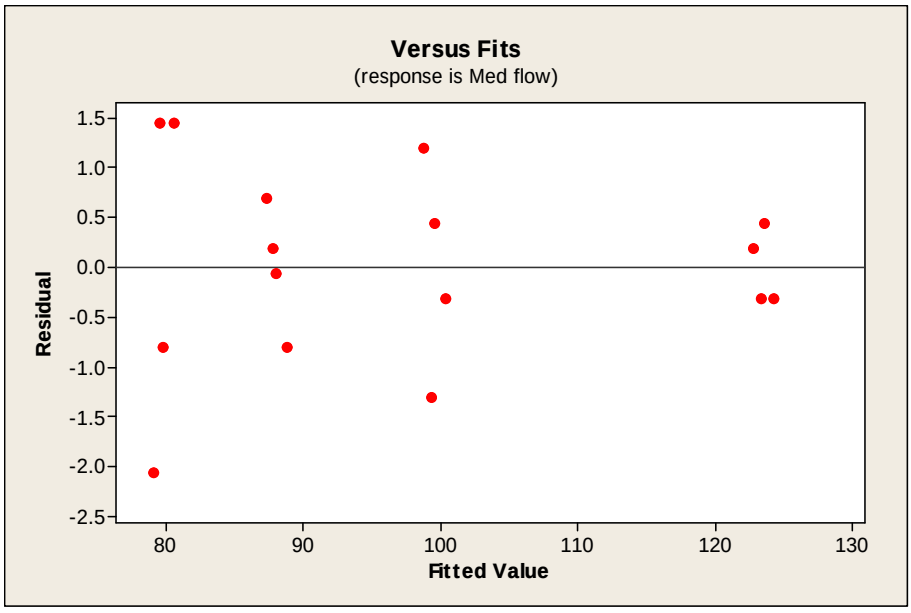

The next graph shows a Normal plot of residuals. Points follow a straight line reasonably well, suggesting that Normality is a reasonable assumption.

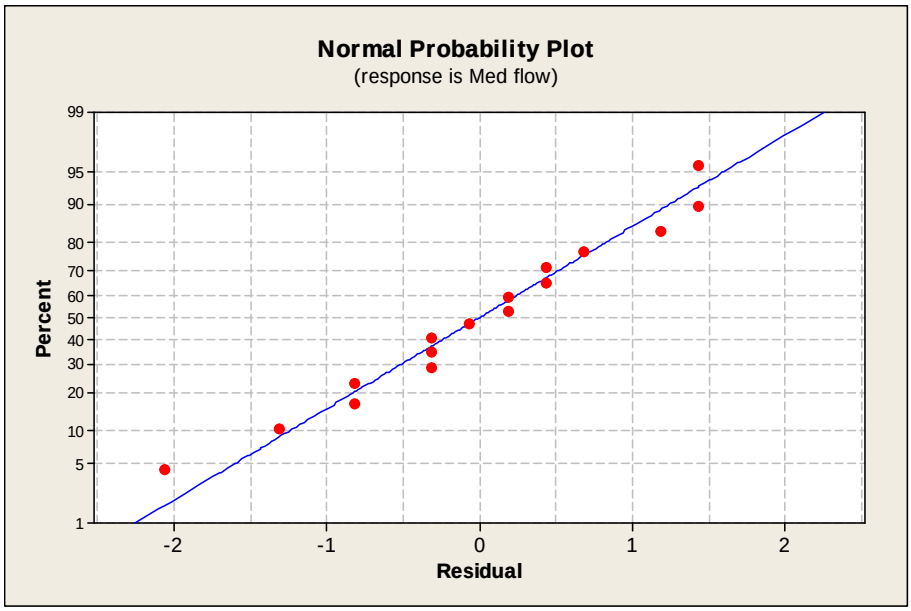

Raw data: median perfusion, by Patient, Clamp time (minutes), and quality of perfusion.

Patient	Clamp Time	Perfusion Good	Perfusion Poor
1	20	98	47
2	20	125	41
3	20	148	99
4	20	154	76
5	5	188	82
6	5	115	43
7	5	158	53
8	5	125	44

Raw data: median perfusion, by Patient, Clamp time (minutes), and Scan Time (minutes).

Patient	Clamp time	Scan Time	Median
1	20	5	59
1	20	10	63
2	20	5	91
2	20	10	91
3	20	5	138
3	20	10	131
4	20	5	125
4	20	10	125
5	5	5	123
5	5	10	124
5	5	15	123
5	5	20	124
6	5	5	77
6	5	10	79
6	5	15	81
6	5	20	82
7	5	5	100
7	5	10	100
7	5	15	98
7	5	20	100
8	5	5	88
8	5	10	88
8	5	15	88
8	5	20	88

Analysis of variance

A repeated measures analysis of variance was carried out, with patients as "subjects factor" and scan times (5, 10, 15 and 20) as the "time point factor" (see following box).

Two-way ANOVA: Median flow versus Patient, Scan Time

Source	DF	SS	MS	F	P
Patient	3	4340.69	1446.90	926.01	
ScanTime	3	4.69	1.56	1.00	0.436
Error	9	14.06	1.56		

Total	**15**	**4359.44**

The F-statistic to test differences in mean flow between the four scan times is not statistically significant (F = 1.00 on 3 and 9 d.f., P=0.436).

Chapter 5

The plots show the residuals and fitted values for the model in Results.

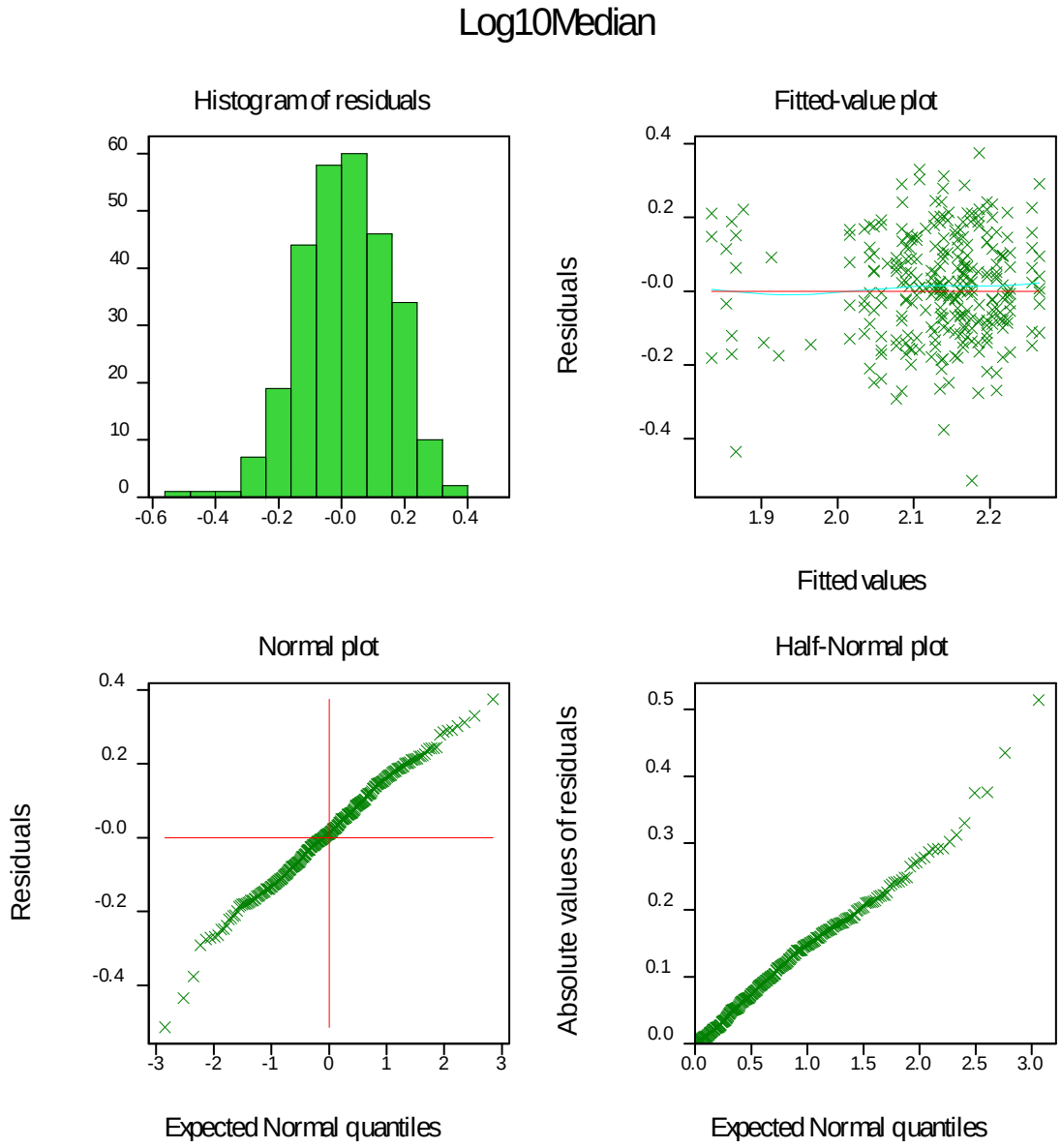

The histogram of residuals is roughly bell-shaped, with three outlying negative residuals.

The fitted plot shows no evidence of non-homogeneity of variance, or of trend. The three outlying negative residuals can be identified, and do not appear to be particularly extreme.

Setting aside the three lowest negative residuals, the Normal plots appear satisfactory.

Chapter 6

Right DIEP laser Doppler images

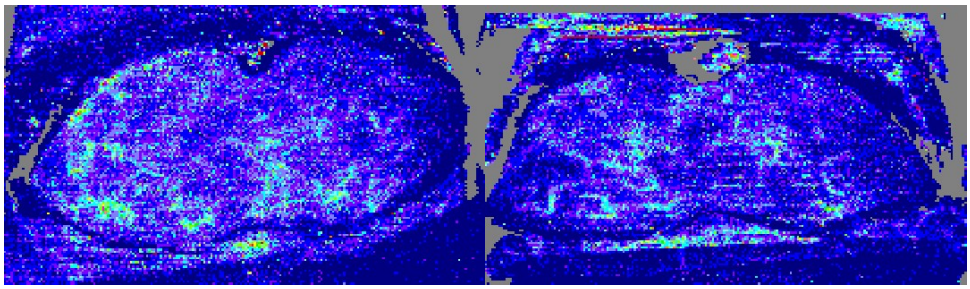
Patient 1 - Right DIEP

Patient 2 - Right DIEP

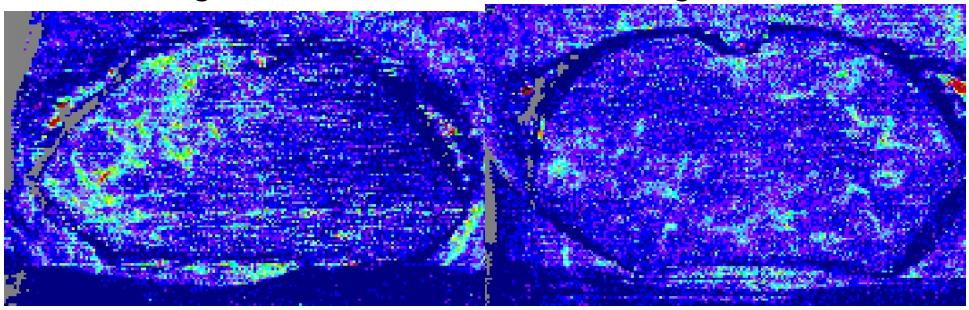
Patient 3 - Right DIEP

Patient 4 - Right DIEP

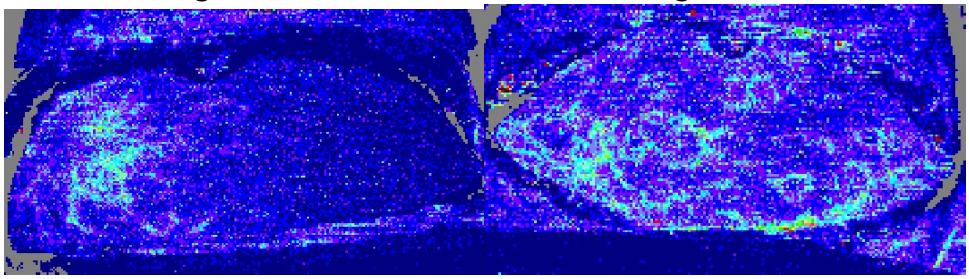
Patient 5 - Right DIEP

Patient 6 - Right DIEP

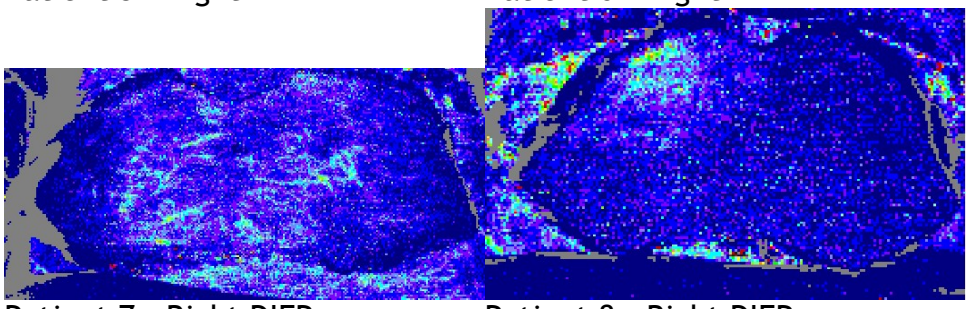
Patient 7 - Right DIEP

Patient 8 - Right DIEP

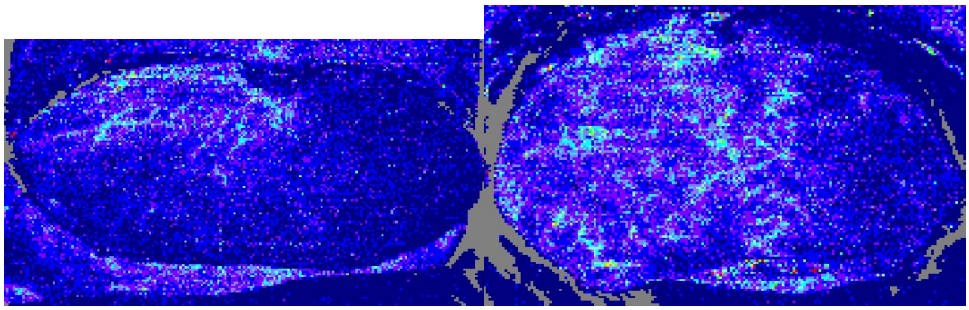
Patient 9 - Right DIEP

Patient 10 - Right DIEP

Left DIEP laser Doppler images

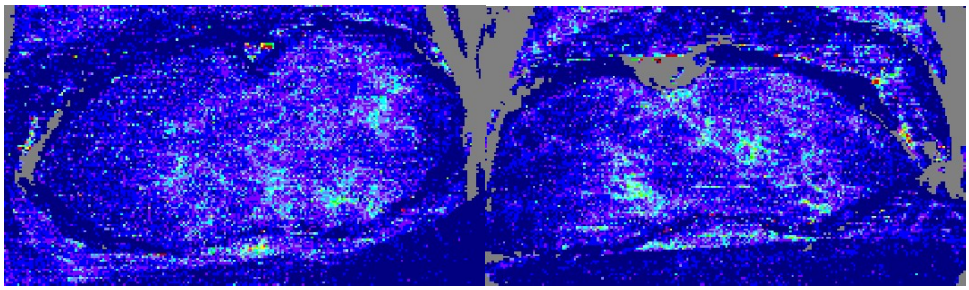
Patient 1 - Left DIEP

Patient 2 - Left DIEP

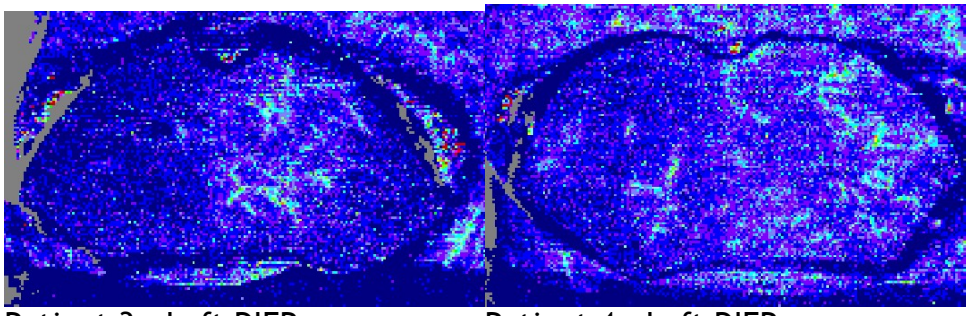
Patient 3 - Left DIEP

Patient 4 - Left DIEP

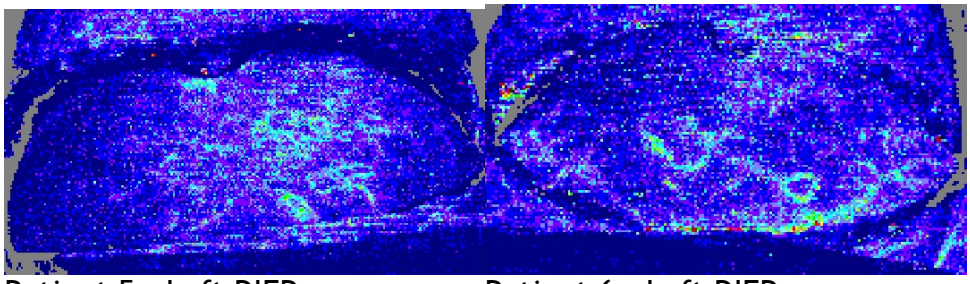
Patient 5 - Left DIEP

Patient 6 - Left DIEP

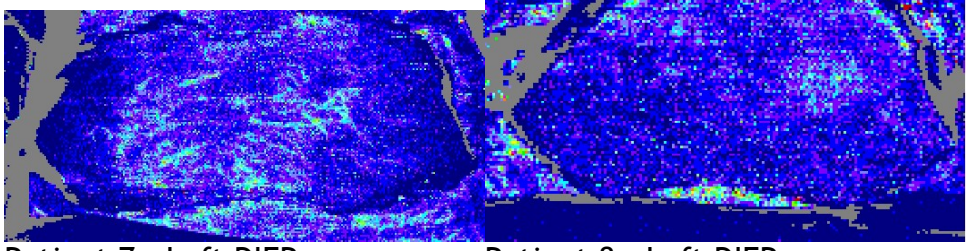
Patient 7 - Left DIEP

Patient 8 - Left DIEP

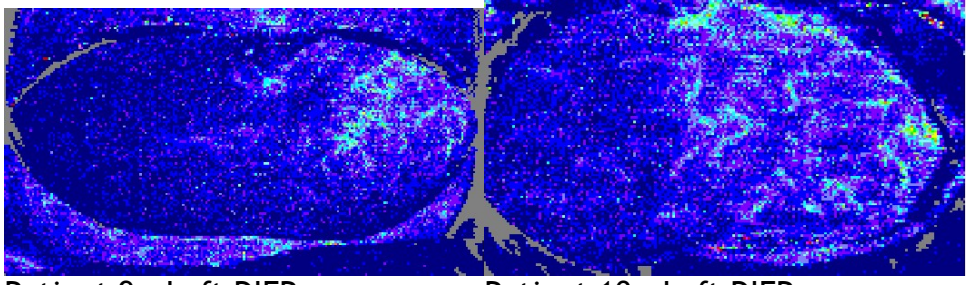
Patient 9 - Left DIEP

Patient 10 - Left DIEP

Right SIEA laser Doppler images

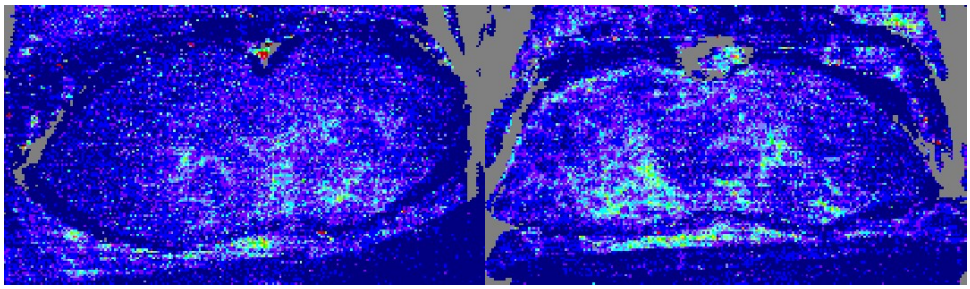

Patient 1 - Right SIEA

Patient 2 - Right SIEA

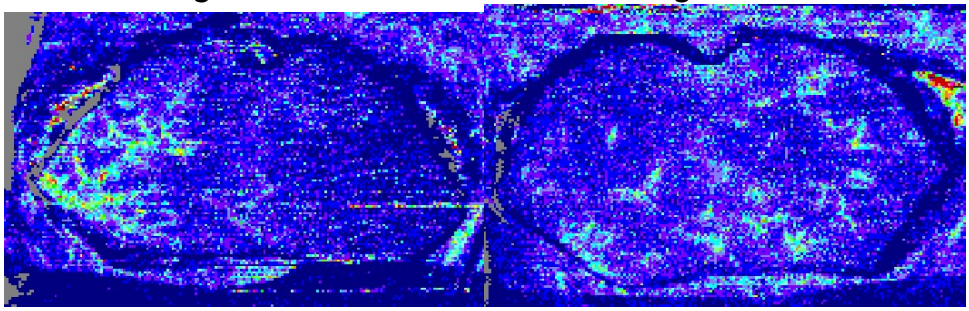

Patient 3 - Right SIEA

Patient 4 - Right SIEA

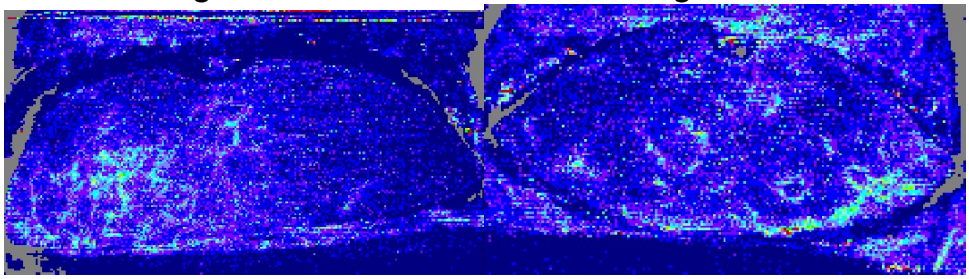

Patient 5 - Right SIEA

Patient 6 - Right SIEA

Patient 7 did not have right SIEA

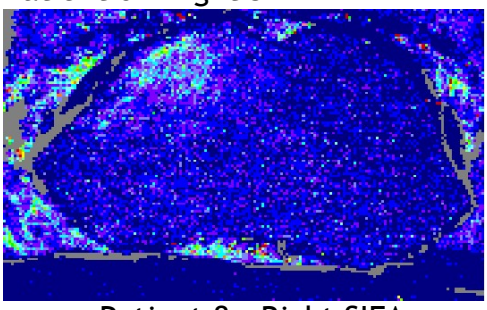

Patient 8 - Right SIEA

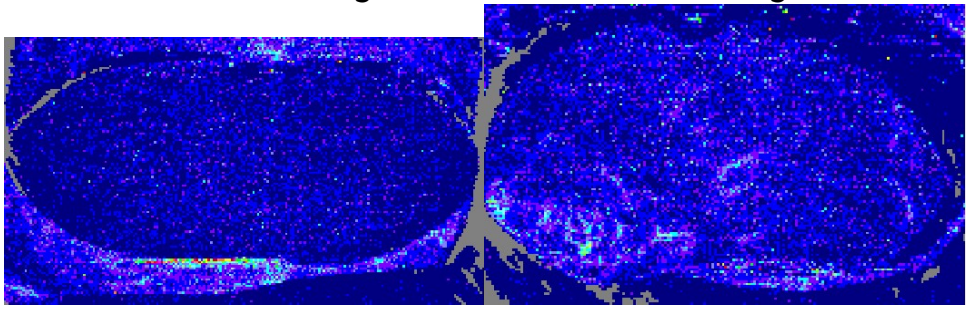

Patient 9 - Right SIEA

Patient 10 - Right SIEA

Left SIEA laser Doppler images

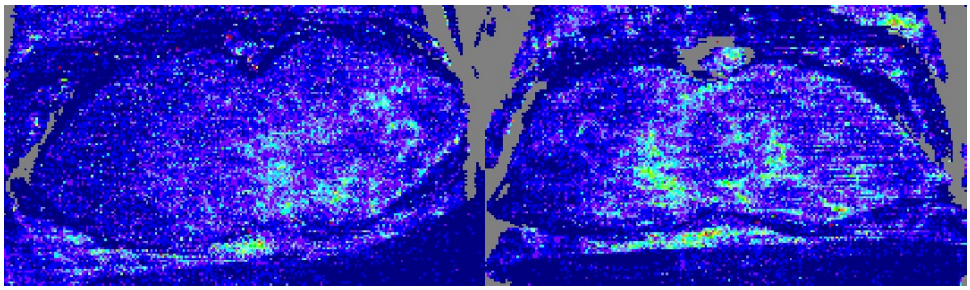
Patient 1 - Left SIEA

Patient 2 - Left SIEA

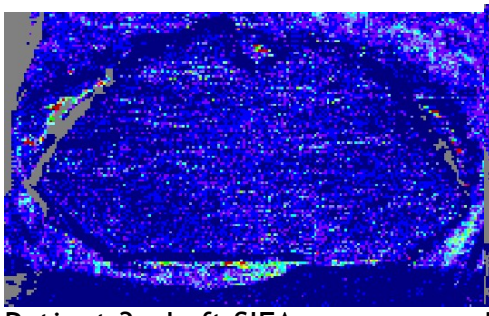
Patient 3 - Left SIEA

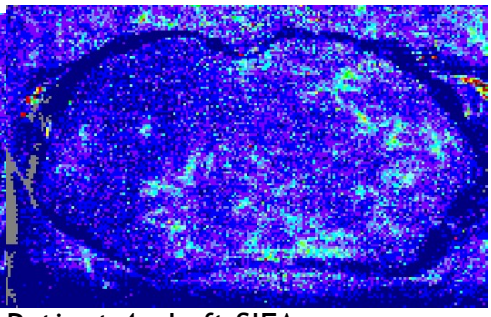
Patient 4 - Left SIEA

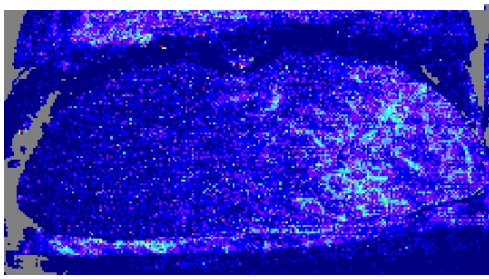
Patient 5 - Left SIEA

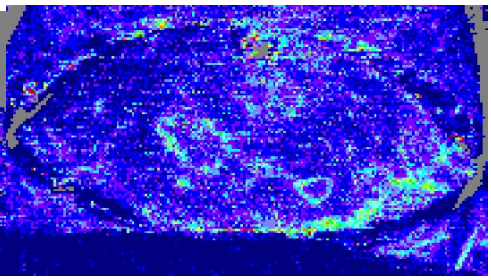
Patient 6 - Left SIEA

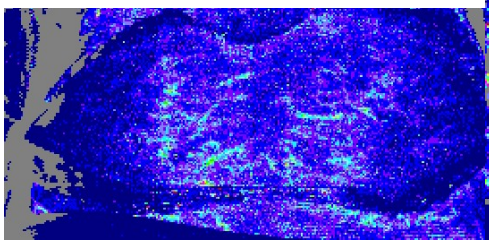
Patient 7 - Left SIEA

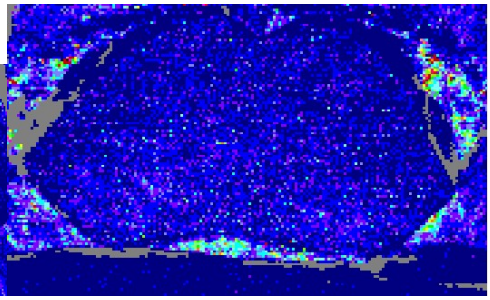
Patient 8 - Left SIEA

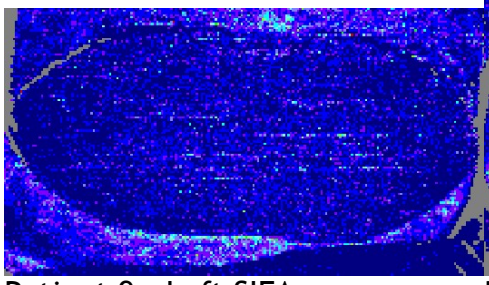
Patient 9 - Left SIEA

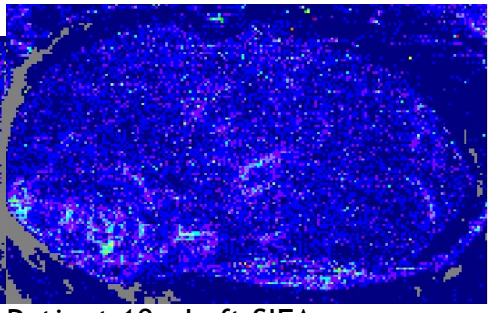
Patient 10 - Left SIEA

Chapter 7

Interleukin IL-6

Estimates of variance components, REML analysis

Estimated variance components

Random term	component	s.e.
Patient	3.0034	1.9120
Patient.Time	0.1721	0.0427
Patient.Catheter	0.0099	0.0123

Residual variance model

Term	Factor	Model(order)	Parameter	Estimate
Patient.Time.Catheter		Identity	Sigma2	0.253

Checks on model with main effects of time point, catheter and their interaction, IL-6.

Concentration

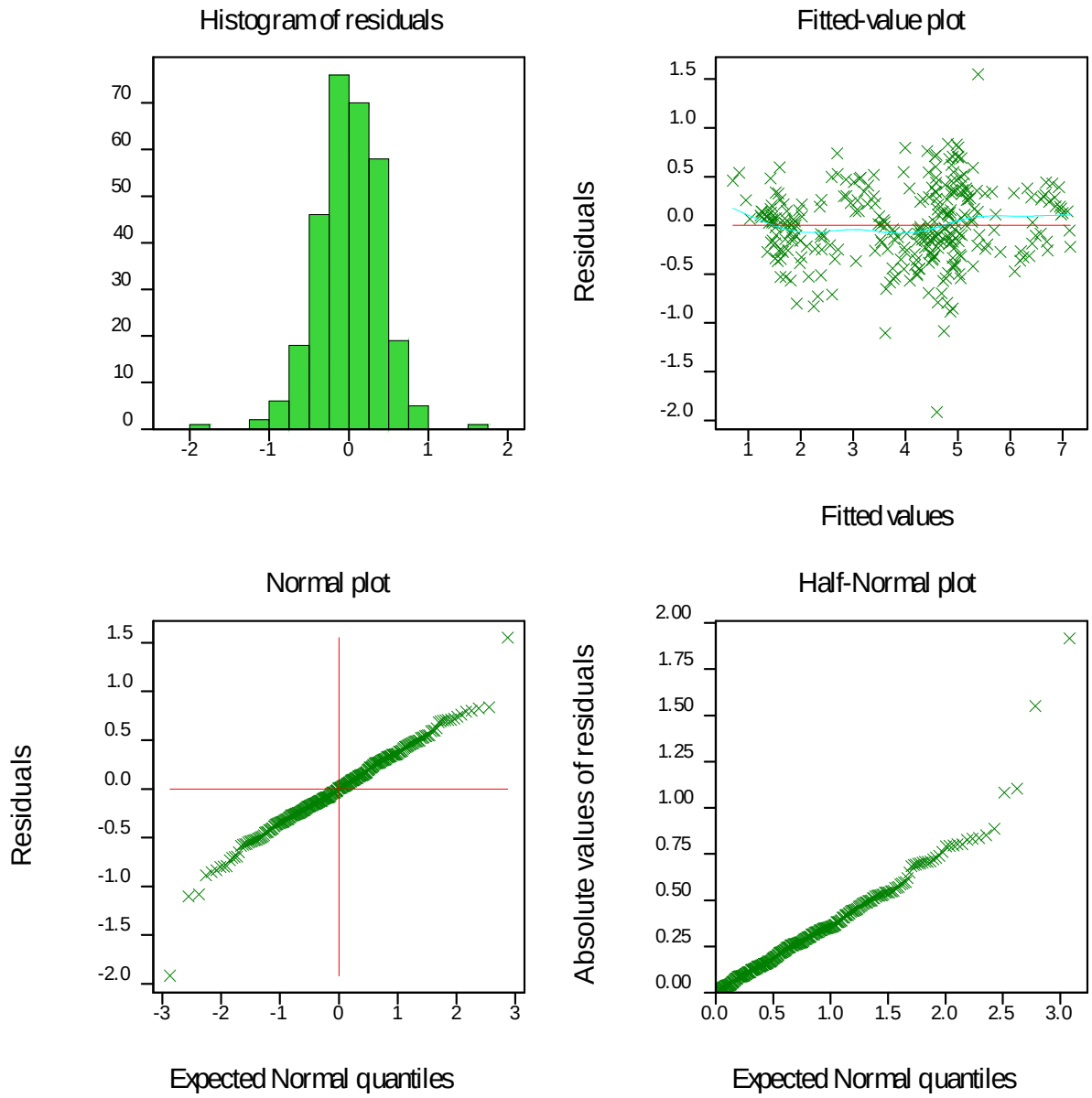

There are two large residuals, but the other residuals do not depart from Normality, as shown by the Normal plot. The fitted value plot shows no indication of non-homogeneity of variance.

Standard errors of differences between predicted concentrations of IL-6, by time point

Standard errors of differences between pairs

Time 4	1	*						
Time 8	2	0.296	*					
Time 12	3	0.296	0.296	*				
Time 16	4	0.300	0.300	0.300	*			
Time 20	5	0.296	0.296	0.296	0.300	*		
Time 24	6	0.296	0.296	0.296	0.300	0.296	*	
Time 28	7	0.296	0.296	0.296	0.300	0.296	0.296	*
Time 32	8	0.296	0.296	0.296	0.300	0.296	0.296	0.296
Time 36	9	0.296	0.296	0.296	0.300	0.296	0.296	0.296
Time 40	10	0.296	0.296	0.296	0.300	0.296	0.296	0.296
Time 44	11	0.298	0.298	0.298	0.301	0.298	0.298	0.298
Time 48	12	0.296	0.296	0.296	0.300	0.296	0.296	0.296
Time 52	13	0.296	0.296	0.296	0.300	0.296	0.296	0.296
Time 56	14	0.315	0.315	0.315	0.318	0.315	0.315	0.315
Time 60	15	0.313	0.313	0.313	0.316	0.313	0.313	0.313
Time 64	16	0.313	0.313	0.313	0.316	0.313	0.313	0.313
Time 68	17	0.313	0.313	0.313	0.316	0.313	0.313	0.313
Time 72	18	0.313	0.313	0.313	0.316	0.313	0.313	0.313
Time 76	19	0.313	0.313	0.313	0.316	0.313	0.313	0.313
		1	2	3	4	5	6	7

Time 32	8	*						
Time 36	9	0.296	*					
Time 40	10	0.296	0.296	*				
Time 44	11	0.298	0.298	0.298	*			
Time 48	12	0.296	0.296	0.296	0.298	*		
Time 52	13	0.296	0.296	0.296	0.298	0.296	*	
Time 56	14	0.315	0.315	0.315	0.317	0.315	0.315	*
Time 60	15	0.313	0.313	0.313	0.314	0.313	0.313	0.328
Time 64	16	0.313	0.313	0.313	0.314	0.313	0.313	0.328
Time 68	17	0.313	0.313	0.313	0.314	0.313	0.313	0.328
Time 72	18	0.313	0.313	0.313	0.314	0.313	0.313	0.328
Time 76	19	0.313	0.313	0.313	0.314	0.313	0.313	0.328
		8	9	10	11	12	13	14

Time 60	15	*						
Time 64	16	0.326	*					
Time 68	17	0.326	0.326	*				
Time 72	18	0.326	0.326	0.326	*			
Time 76	19	0.326	0.326	0.326	0.326	*		
		15	16	17	18	19		

Standard errors of differences

Average:	0.3071
Maximum:	0.3282
Minimum:	0.2964

Average variance of differences: 0.09442

Fibroblast Growth Factor beta

Estimates of variance components, FGFß

Estimated variance components

Random term	component	s.e.
Patient	0.37	0.47
Patient.Time	-0.51	1.32
Patient.Catheter	-0.24	0.45

Residual variance model

TermFactor	Model(order)	Parameter	Estimate	s.e.
Patient.Time.Catheter	Identity	Sigma2	18.55	2.39

The variance component values are small, especially in comparison with the standard error. This suggests that the effect of these interaction terms in the population is small.

Checks on REML model which includes main effects of Time, Catheter and their interaction- FGFß

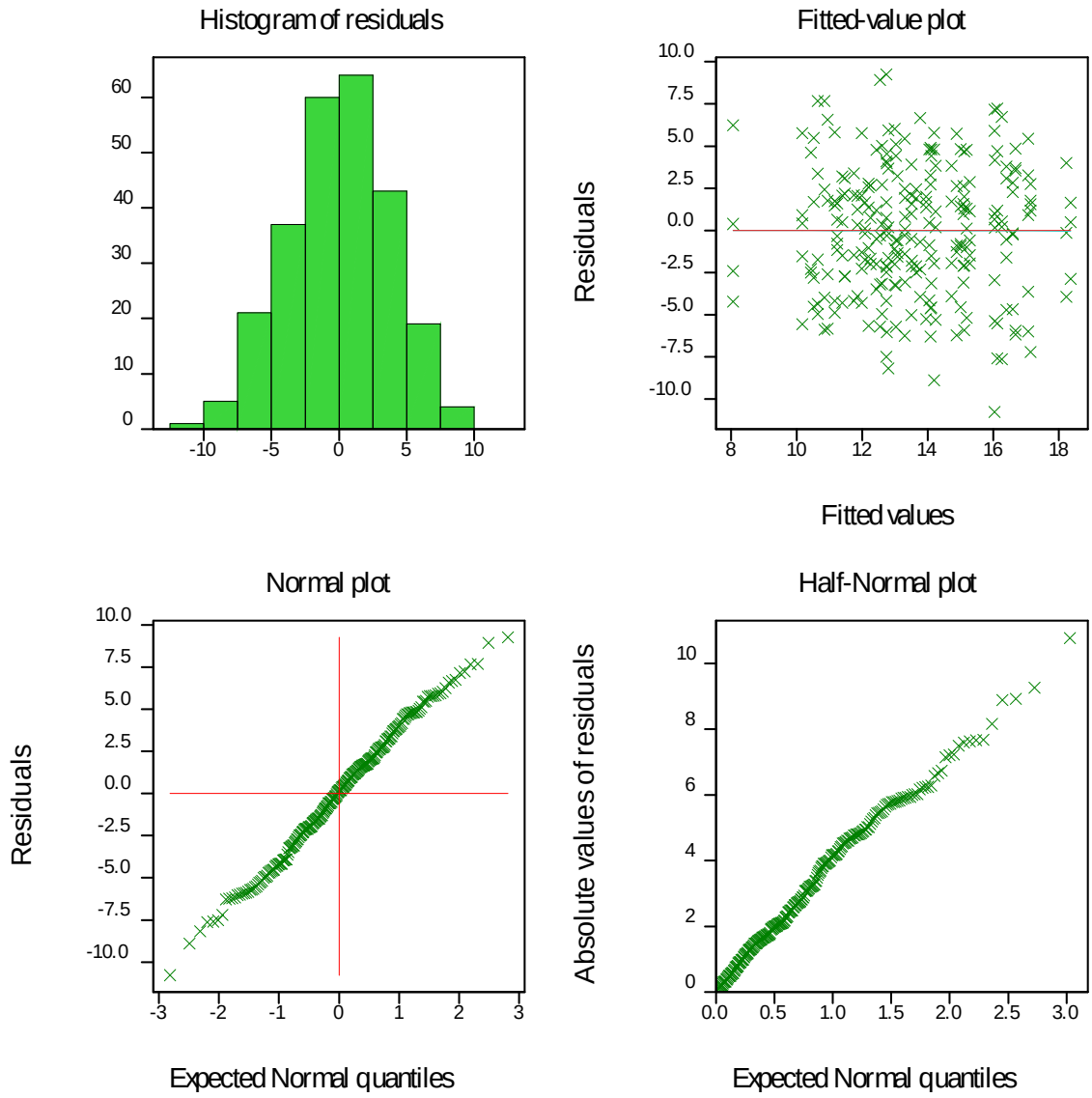

The histogram and Normal plot confirm that normality is a reasonable assumption. There is no evidence of lack of homogeneity of variance on the square-root scale.

Tumour Necrosis Factor alpha

Estimated variance components

Random term	component	s.e.
Patient	8.1188	5.1418
Patient.Time	0.0749	0.0262
Patient.Catheter	0.0059	0.0094

Residual variance model

Term	Factor	Model(order)	Parameter	Estimate	s.e.
Patient.Time.Catheter		Identity	Sigma2	0.228	0.0267

Compared to the estimated error variance (0.228), the variance component for patients (8.1188) is large. The variance components corresponding to random terms Patient.Time and Patient.Catheter are considerably smaller than the error variance.

The values of the estimated variance components show that the estimated correlation between repeat measurements of concentration made on the same patient is high.

Checks on REML model which includes main effects of Time, Catheter and their interaction - TNFα

The histogram and Normal plot confirm that normality is a reasonable assumption. There is no evidence of lack of homogeneity of variance.

Concentration

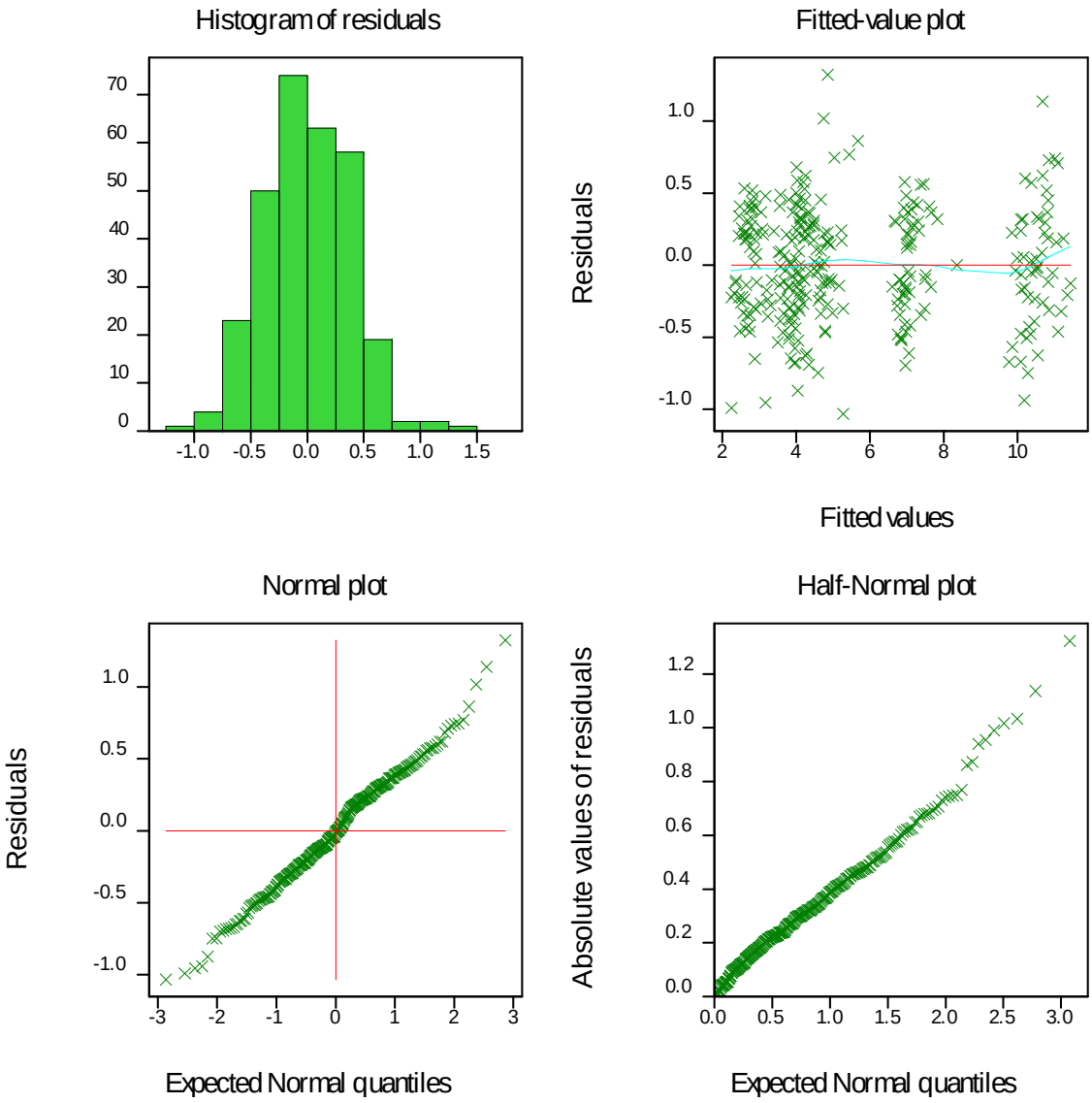

Ethics approval for Chapters 4 & 5

07/S0704/4

North Glasgow University Hospitals Division

Glasgow Royal Infirmary LREC
4th floor, Walton Building
Glasgow Royal Infirmary
84 Castle Street
GLASGOW
G4 0SF

Telephone: 0141 211 4020
Email: sharon.macgregor@northglasgow.scot.nhs.uk

NHS Greater Glasgow

15 March 2007

Mr Iain R MacKay
Consultant Plastic Surgeon
Canniesburn Plastic Surgery Unit
Jubilee Building
Glasgow Royal Infirmary

Dear Mr MacKay

Full title of study: **Assessing changes in skin blood flow to the lower abdomen using laser Doppler imaging.**

REC reference number: **07/S0704/4**

Thank you for your letter of 22 February 2007, responding to the Committee's request for further information on the above research and submitting revised documentation.

The further information has been considered on behalf of the Committee by the Chair.

Confirmation of ethical opinion

On behalf of the Committee, I am pleased to confirm a favourable ethical opinion for the above research on the basis described in the application form, protocol and supporting documentation as revised.

Conditions of approval

The favourable opinion is given provided that you comply with the conditions set out in the attached document. You are advised to study the conditions carefully.

Approved documents

The final list of documents reviewed and approved by the Committee is as follows:

Document	*Version*	*Date*
Application	(2)	10 January 2007
Investigator CV		
Protocol	2	22 February 2007
Covering Letter		10 January 2007
GP/Consultant Information Sheets	1	10 January 2007
Participant Information Sheet	2	22 February 2007
Participant Consent Form	2	22 February 2007
Response to Request for Further Information		22 February 2007

R&D approval

The study should not commence at any NHS site until the local Principal Investigator has obtained final approval from the R&D office for the relevant NHS care organisation.

Statement of compliance

The Committee is constituted in accordance with the Governance Arrangements for Research Ethics Committees (July 2001) and complies fully with the Standard Operating Procedures for Research Ethics Committees in the UK.

07/S0704/4	**Please quote this number on all correspondence**

With the Committee's best wishes for the success of this project

Yours sincerely

for

Dr Brian Neilly
Chair

Enclosures: Standard approval conditions

Copy to: GRI R&D office

North Glasgow University Hospitals
Division

Research & Development Office
Glasgow Royal Infirmary
4th Floor, Walton Building
84 Castle Street
Glasgow G4 0SF
Telephone 0141 211 1114
Fax 0141 232 0752
Fiona.Graham.gri@northglasgow.scot.nhs.uk

NHS Greater Glasgow

Mr Iain R Mackay
Department of Plastic Surgery
Jubilee Building
Glasgow Royal Infirmary

Enquiries to Dr Fiona Graham
Direct Line 0141 211 0475

16th March 2007

Dear Mr Mackay

Research Project Registration
RN07BU001:- Assessing skin blood flow in the lower abdomen.

I write to acknowledge receipt of your research project submission.

The project proposal has been registered on the Trust Research Database and will be sent to the Department of Finance for approval.

I enclose a copy of the corresponding entry for the National Research Register. If you wish to have this entry modified, please contact me at the address below.

With kind regards

Yours sincerely

L. Hickey

p.p. Dr Fiona Graham
Academic Research Co-ordinator

Encl.

Ethics approval for Chapter 6

RN07BU001 func

North Glasgow University Hospitals
Division

NHS
Greater Glasgow

Glasgow Royal Infirmary REC
4th floor, Walton Building
Glasgow Royal Infirmary
84 Castle Street
GLASGOW
G4 0SF

Telephone: 0141 211 4020
Facsimile: 0141 232 0752

15 January 2008

Mr Iain R MacKay
Consultant Plastic Surgeon
Canniesburn Plastic Surgery Unit
Jubilee Building, Glasgow Royal Infirmary
84 Castle Street,
Glasgow
G4 0SF

Dear Mr MacKay

Full title of study: **Assessing changes in skin blood flow to the lower abdomen using laser Doppler imaging.**

REC reference number: **07/S0704/95**

Thank you for your letter of 21 December 2007, responding to the Committee's request for further information on the above research and submitting revised documentation.

The further information has been considered on behalf of the Committee by the Chair.

Confirmation of ethical opinion

On behalf of the Committee, I am pleased to confirm a favourable ethical opinion for the above research on the basis described in the application form, protocol and supporting documentation as revised.

Conditions of approval

The favourable opinion is given provided that you comply with the conditions set out in the attached document. You are advised to study the conditions carefully.

Approved documents

The final list of documents reviewed and approved by the Committee is as follows:

Document	*Version*	*Date*
Application	(2)	21 December 2007
Investigator CV		15 November 2007
Protocol	2	21 December 2007
Covering Letter		15 November 2007
GP/Consultant Information Sheets	1	15 November 2007
Participant Information Sheet	2	21 December 2007
Participant Consent Form	2	21 December 2007

Response to Request for Further Information		21 December 2007

R&D approval

All researchers and research collaborators who will be participating in the research at NHS sites should apply for R&D approval from the relevant care organisation, if they have not yet done so. R&D approval is required, whether or not the study is exempt from SSA. You should advise researchers and local collaborators accordingly.

Guidance on applying for R&D approval is available from http://www.rdforum.nhs.uk/rdform.htm.

Statement of compliance

The Committee is constituted in accordance with the Governance Arrangements for Research Ethics Committees (July 2001) and complies fully with the Standard Operating Procedures for Research Ethics Committees in the UK.

After ethical review

Now that you have completed the application process please visit the National Research Ethics Website > After Review

Here you will find links to the following

a) Providing feedback. You are invited to give your view of the service that you have received from the National Research Ethics Service on the application procedure. If you wish to make your views known please use the feedback form available on the website.
b) Progress Reports. Please refer to the attached Standard conditions of approval by Research Ethics Committees.
c) Safety Reports. Please refer to the attached Standard conditions of approval by Research Ethics Committees.
d) Amendments. Please refer to the attached Standard conditions of approval by Research Ethics Committees.
e) End of Study/Project. Please refer to the attached Standard conditions of approval by Research Ethics Committees.

We would also like to inform you that we consult regularly with stakeholders to improve our service. If you would like to join our Reference Group please email referencegroup@nationalres.org.uk .

07/S0704/95	**Please quote this number on all correspondence**

With the Committee's best wishes for the success of this project

Yours sincerely

Dr Brian Neilly
Chair

Email: rose.gallacher@northglasgow.scot.nhs.uk

Enclosures: *Standard approval conditions*

Copy to: Dr Fiona Graham,
NHS Greater Glasgow and Clyde

North Glasgow University Hospitals Division

NHS
Greater Glasgow and Clyde

Research & Development Office
4th Floor Walton Building
Glasgow Royal Infirmary
84 Castle St
Glasgow
G4OSF
Telephone: 0141 211 0475
Fax: 0141 232 0752
Email: Fiona.Graham.gri@northglasgow scot.nhs.uk

Friday, 01 February 2008

Mr Iain R. McKay
Consultant Plastic Surgeon
Canniesburn Plastic Surgery Unit
84 Castle St
Glasgow
G4 0SF

Dear McKay,

Project Title: Assessing skin blood flow in the lower abdomen.
Investigator: Mr Iain B. McKay
R&D Reference: RN07BU001
COREC: 07/S0704/95

We are pleased to inform you that, based on the information provided, the above project has been granted overall Management Approval and you may now proceed. This approval includes Finance and favourable Research Ethics Committee opinions.

Further management approval will be required for amendments that increase patient numbers, increase or change the test procedures or bring about a change in pharmacy requirements. Please contact the R&D office if you wish to discuss any future amendments.

Thank you for your current and future collaboration

Yours Sincerely,

Dr Fiona Graham
Academic Research Co-ordinator
Glasgow Royal Infirmary

Ethics approval for Chapter 7

ETHICS

North Glasgow University Hospitals
Division

NHS
Greater Glasgow

Glasgow Royal Infirmary REC
4th floor, Walton Building
Glasgow Royal Infirmary
84 Castle Street
GLASGOW
G4 0SF

Telephone: 0141 211 4020
Facsimile: 0141 232 0752

09 June 2008

Mr Iain R MacKay
Consultant Plastic Surgeon
Canniesburn Plastic Surgery Unit
Jubilee Building, Glasgow Royal Infirmary
84 Castle Street,
Glasgow
G4 0SF

Dear Mr MacKay

Full title of study: **Microdialysis analysis of DIEP flaps**
REC reference number: **08/S0704/20**

Thank you for your letter of 04 June 2008, responding to the Committee's request for further information on the above research and submitting revised documentation, subject to the conditions specified below.

The further information has been considered on behalf of the Committee by the Vice-Chair.

Confirmation of ethical opinion

On behalf of the Committee, I am pleased to confirm a favourable ethical opinion for the above research on the basis described in the application form, protocol and supporting documentation as revised.

Conditions of the favourable opinion

The favourable opinion is subject to the following conditions being met prior to the start of the study.

Management permission or approval must be obtained from each host organisation prior to the start of the study at the site concerned.

Management permission at NHS sites ("R&D approval") should be obtained from the relevant care organisation(s) in accordance with NHS research governance arrangements.

Guidance on applying for NHS permission is available in the Integrated Research Application System or at http://www.rdforum.nhs.uk.

Approved documents

The final list of documents reviewed and approved by the Committee is as follows:

Document	*Version*	*Date*
Application	(2)	05 June 2008
Investigator CV		
Protocol	1	12 March 2008

01811

Covering Letter		14 March 2008
GP/Consultant Information Sheets	1	12 March 2008
Participant Information Sheet	2	04 June 2008
Participant Consent Form	2	04 June 2008
Response to Request for Further Information		04 June 2008

Statement of compliance

The Committee is constituted in accordance with the Governance Arrangements for Research Ethics Committees (July 2001) and complies fully with the Standard Operating Procedures for Research Ethics Committees in the UK.

After ethical review

Now that you have completed the application process please visit the National Research Ethics Website > After Review

You are invited to give your view of the service that you have received from the National Research Ethics Service and the application procedure. If you wish to make your views known please use the feedback form available on the website.

The attached document "After ethical review – guidance for researchers" gives detailed guidance on reporting requirements for studies with a favourable opinion, including:

- Notifying substantial amendments
- Progress and safety reports
- Notifying the end of the study

The NRES website also provides guidance on these topics, which is updated in the light of changes in reporting requirements or procedures.

We would also like to inform you that we consult regularly with stakeholders to improve our service. If you would like to join our Reference Group please email referencegroup@nres.npsa.nhs.uk.

08/S0704/20	**Please quote this number on all correspondence**

With the Committee's best wishes for the success of this project

Yours sincerely

R Gallacher

pp **Dr K James**
Vice-chair

Email: rose.gallacher@ggc.scot.nhs.uk

Enclosures: "After ethical review – guidance for researchers"

Copy to: *Dr Fiona Graham, NHS Greater Glasgow & Clyde* ✓

List of References

Reference List

(1) **Milton SH. Pedicled skin-flaps--the fallacy of the length: width ratio. *Br J Surg* 1969; 56(5):381.**

(2) **Taylor GI, Palmer JH. The vascular territories (angiosomes) of the body: experimental study and clinical applications. *Br J Plast Surg* 1987; 40(2):113-141.**

(3) **Milton SH. The tubed pedicle flap. *Br J Plast Surg* 1969; 22(1):53-59.**

(4) **Bakamjian VY. A TWO-STAGE METHOD FOR PHARYNGOESOPHAGEAL RECONSTRUCTION WITH A PRIMARY PECTORAL SKIN FLAP. *Plast Reconstr Surg* 1965; 36:173-184.**

(5) **McGregor IA, Jackson IT. The groin flap. *Br J Plast Surg* 1972; 25(1):3-16.**

(6) **Mathes SJ, Alpert BS. Advances in muscle and musculocutaneous flaps. *Clin Plast Surg* 1980; 7(1):15-26.**

(7) **Ponten B. The fasciocutaneous flap: its use in soft tissue defects of the lower leg. *Br J Plast Surg* 1981; 34(2):215-220.**

(8) **Cormack GC, Lamberty BG. Cadaver studies of correlation between vessel size and anatomical territory of cutaneous supply. *Br J Plast Surg* 1986; 39(3):300-306.**

(9) **Geddes CR, Morris SF, Neligan PC. Perforator flaps: evolution, classification, and applications. *Ann Plast Surg* 2003; 50(1):90-99.**

(10) **Harii K, Omori K, Omori S. Free deltopectoral skin flaps. *Br J Plast Surg* 1974; 27(3):231-239.**

(11) **Harii K, Omori K, Omori S. Successful clinical transfer of ten free flaps by microvascular anastomoses. *Plast Reconstr Surg* 1974; 53(3):259-270.**

(12) **Hart AM, Tollan CJ, Dabernig J, Acland R, Taggart I. Tertiary resurfacing after one of the first free flaps in Europe, a reflection on 30 years of microsurgical progress. *J Plast Reconstr Aesthet Surg* 2007; 60(11):1263-1267.**

(13) **Hough M, Fenn C, Kay SP. The use of free groin flaps in children. *Plast Reconstr Surg* 2004; 113(4):1161-1166.**

(14) Koshima I, Soeda S. Inferior epigastric artery skin flaps without rectus abdominis muscle. *British Journal of Plastic Surgery 42(6):645-8*, **1989.**

(15) Blondeel PN, Van Landuyt KH, Monstrey SJ, Hamdi M, Matton GE, Allen RJ et al. The "Gent" consensus on perforator flap terminology: preliminary definitions. *Plast Reconstr Surg* **2003; 112(5):1378-1383.**

(16) Hallock GG. Direct and indirect perforator flaps: the history and the controversy. *Plast Reconstr Surg* **2003; 111(2):855-865.**

(17) Kim JT. New nomenclature concept of perforator flap. *Br J Plast Surg* **2005; 58(4):431-440.**

(18) Wei FC, Jain V, Suominen S, Chen HC. Confusion among perforator flaps: what is a true perforator flap? *Plast Reconstr Surg* **2001; 107(3):874-876.**

(19) Maxwell GP, Stueber K, Hoopes JE. A free latissimus dorsi myocutaneous flap: case report. *Plast Reconstr Surg* **1978; 62(3):462-466.**

(20) Moore C, Lee S, Hart A, Watson S. Use of Integra to resurface a latissimus dorsi free flap. *Br J Plast Surg* **2003; 56(1):66-69.**

(21) Allen RJ, Treece P. Deep inferior epigastric perforator flap for breast reconstruction. *Annals of Plastic Surgery 32(1):32-8*, **1994.**

(22) Futter CM, Webster MH, Hagen S, Mitchell SL. A retrospective comparison of abdominal muscle strength following breast reconstruction with a free TRAM or DIEP flap. *Br J Plast Surg* **2000; 53(7):578-583.**

(23) Kimura N, Satoh K. Consideration of a thin flap as an entity and clinical applications of the thin anterolateral thigh flap. *Plast Reconstr Surg* **1996; 97(5):985-992.**

(24) Chevray PM. Breast reconstruction with superficial inferior epigastric artery flaps: a prospective comparison with TRAM and DIEP flaps. *Plast Reconstr Surg* **2004; 114(5):1077-1083.**

(25) Reardon CM, O'Ceallaigh S, O'Sullivan ST. An anatomical study of the superficial inferior epigastric vessels in humans. *Br J Plast Surg* **2004; 57(6):515-519.**

(26) Taylor GI, Daniel RK. The anatomy of several free flap donor sites. *Plast Reconstr Surg* **1975; 56(3):243-253.**

(27) Taylor GI, Daniel RK. The free flap: composite tissue transfer by vascular anastomosis. *Aust N Z J Surg* **1973; 43(1):1-3.**

(28) Cobbett JR. Microvascular surgery. *Surg Clin North Am* **1967; 47(2):521-542.**

(29) Taylor GI, Minabe T. The angiosomes of the mammals and other vertebrates. *Plast Reconstr Surg* **1992; 89(2):181-215.**

(30) Morris SF, Taylor GI. The time sequence of the delay phenomenon: when is a surgical delay effective? An experimental study. *Plast Reconstr Surg* **1995; 95(3):526-533.**

(31) Dhar SC, Taylor GI. The delay phenomenon: the story unfolds. *Plast Reconstr Surg* **1999; 104(7):2079-2091.**

(32) Callegari PR, Taylor GI, Caddy CM, Minabe T. An anatomic review of the delay phenomenon: I. Experimental studies. *Plast Reconstr Surg* **1992; 89(3):397-407.**

(33) Morris SF, Taylor GI. Predicting the survival of experimental skin flaps with a knowledge of the vascular architecture. *Plast Reconstr Surg* **1993; 92(7):1352-1361.**

(34) Taylor GI, Corlett RJ, Caddy CM, Zelt RG. An anatomic review of the delay phenomenon: II. Clinical applications. *Plast Reconstr Surg* **1992; 89(3):408-416.**

(35) Fagrell B, Fronek A, Intaglietta M. Capillary flow components and reactive hyperemia in human skin capillaries studied by clinical television microscopy. *Bibl Anat* **1977;(16 Pt 2):112-115.**

(36) Fagrell B. Advances in microcirculation network evaluation: an update. *Int J Microcirc Clin Exp* **1995; 15 Suppl 1:34-40.**

(37) Motley RJ, Lanigan SW, Katugampola GA. Videomicroscopy predicts outcome in treatment of port-wine stains. *Arch Dermatol* **1997; 133(7):921-922.**

(38) Eubanks LE, McBurney EI. Videomicroscopy of port-wine stains: correlation of location and depth of lesion. *J Am Acad Dermatol* **2001; 44(6):948-951.**

(39) Sivarajan V, Mackay IR. The depth measuring videomicroscope (DMV): a non-invasive tool for the assessment of capillary vascular malformations. *Lasers in Surgery & Medicine 34(2):193-7*, **2004.**

(40) Sivarajan V, Mackay IR. Noninvasive in vivo assessment of vessel characteristics in capillary vascular malformations exposed to five pulsed dye laser treatments. *Plastic & Reconstructive Surgery 115(5):1245-52*, **2005.**

(41) Sivarajan V, Smith G, Mackay IR. The validation of the Depth Measurement Videomicroscope (DMV) as a noninvasive tool for the assessment of capillary vascular malformations. *Journal of Plastic, Reconstructive & Aesthetic Surgery: JPRAS 60(1):79-86*, **2007.**

(42) Kang HY, Bahadoran P, Suzuki I, Zugaj D, Khemis A, Passeron T et al. In vivo reflectance confocal microscopy detects pigmentary changes in melasma at a cellular level resolution. *Exp Dermatol* **2010; 19(8):e228-e233.**

(43) Kang HY, Bahadoran P, Ortonne JP. Reflectance confocal microscopy for pigmentary disorders. *Exp Dermatol* **2010; 19(3):233-239.**

(44) Richtig E, Ahlgrimm-Siess V, Koller S, Gerger A, Horn M, Smolle J et al. Follow-up of actinic keratoses after shave biopsy by in-vivo reflectance confocal microscopy--a pilot study. *J Eur Acad Dermatol Venereol* **2010; 24(3):293-298.**

(45) Gerger A, Koller S, Weger W, Richtig E, Kerl H, Samonigg H et al. Sensitivity and specificity of confocal laser-scanning microscopy for in vivo diagnosis of malignant skin tumors. *Cancer* **2006; 107(1):193-200.**

(46) Agero AL, Busam KJ, Benvenuto-Andrade C, Scope A, Gill M, Marghoob AA et al. Reflectance confocal microscopy of pigmented basal cell carcinoma. *J Am Acad Dermatol* **2006; 54(4):638-643.**

(47) Gerger A, Hofmann-Wellenhof R, Samonigg H, Smolle J. In vivo confocal laser scanning microscopy in the diagnosis of melanocytic skin tumours. *Br J Dermatol* **2009; 160(3):475-481.**

(48) Stern MD. In vivo evaluation of microcirculation by coherent light scattering. *Nature* **1975; 254(5495):56-58.**

(49) Wright CI, Kroner CI, Draijer R. Non-invasive methods and stimuli for evaluating the skin's microcirculation. *J Pharmacol Toxicol Methods* **2006; 54(1):1-25.**

(50) Stern MD, Lappe DL, Bowen PD, Chimosky JE, Holloway GA, Jr., Keiser HR et al. Continuous measurement of tissue blood flow by laser-Doppler spectroscopy. *Am J Physiol* **1977; 232(4):H441-H448.**

(51) Nilsson GE, Tenland T, Obert PA. A new instrument for continuous measurement of tissue blood flow by light beating spectroscopy. *IEEE Trans Biomed Eng* **1980; 27(1):12-19.**

(52) Schabauer AM, Rooke TW. Cutaneous laser Doppler flowmetry: applications and findings. *Mayo Clin Proc* **1994; 69(6):564-574.**

(53) Vongsavan N, Matthews B. Some aspects of the use of laser Doppler flow meters for recording tissue blood flow. *Exp Physiol* **1993; 78(1):1-14.**

(54) Hovell CJ, Beasley CR, Mani R, Holgate ST. Laser Doppler flowmetry for determining changes in cutaneous blood flow following intradermal injection of histamine. *Clin Allergy* **1987; 17(5):469-479.**

(55) Leslie SJ, Affolter J, Denvir MA, Webb DJ. Validation of laser Doppler flowmetry coupled with intra-dermal injection for investigating effects of vasoactive agents on the skin microcirculation in man. *Eur J Clin Pharmacol* **2003; 59(2):99-102.**

(56) Clinton MS, Sepka RS, Bristol D, Pederson WC, Barwick WJ, Serafin D et al. Establishment of normal ranges of laser Doppler blood flow in autologous tissue transplants. *Plast Reconstr Surg* **1991; 87(2):299-309.**

(57) Soderstrom T, Svensson H, Koop T, Moller KO. Processing of laser-Doppler signals from free flaps. *Technol Health Care* 1999; 7(2-3):219-223.

(58) Yuen JC, Feng Z. Distinguishing laser Doppler flowmetric responses between arterial and venous obstructions in flaps. *J Reconstr Microsurg* 2000; 16(8):629-635.

(59) Yuen JC, Feng Z. Monitoring free flaps using the laser Doppler flowmeter: five-year experience. *Plast Reconstr Surg* 2000; 105(1):55-61.

(60) Jeng JC, Bridgeman A, Shivnan L, Thornton PM, Alam H, Clarke TJ et al. Laser Doppler imaging determines need for excision and grafting in advance of clinical judgment: a prospective blinded trial. *Burns* 2003; 29(7):665-670.

(61) Niazi ZB, Essex TJ, Papini R, Scott D, McLean NR, Black MJ. New laser Doppler scanner, a valuable adjunct in burn depth assessment. *Burns* 1993; 19(6):485-489.

(62) Pape SA, Skouras CA, Byrne PO. An audit of the use of laser Doppler imaging (LDI) in the assessment of burns of intermediate depth. *Burns* 2001; 27(3):233-239.

(63) Benveniste H, Huttemeier PC. Microdialysis--theory and application. *Prog Neurobiol* 1990; 35(3):195-215.

(64) Ungerstedt U. Microdialysis--principles and applications for studies in animals and man. *J Intern Med* 1991; 230(4):365-373.

(65) Lindefors N, Amberg G, Ungerstedt U. Intracerebral microdialysis: I. Experimental studies of diffusion kinetics. *Journal of Pharmacological Methods* 1989; 22(3):141-156.

(66) Tossman U, Ungerstedt U. Microdialysis in the study of extracellular levels of amino acids in the rat brain. *Acta Physiologica Scandinavica* 1986; 128(1):9-14.

(67) Ungerstedt U, Hallstrom A. In vivo microdialysis--a new approach to the analysis of neurotransmitters in the brain. *Life Sciences* 1987; 41(7):861-864.

(68) Rojdmark J, Blomqvist L, Malm M, Adams-Ray B, Ungerstedt U. Metabolism in myocutaneous flaps studied by in situ microdialysis. *Scand J Plast Reconstr Surg Hand Surg* 1998; 32(1):27-34.

(69) Setala L, Papp A, Romppanen EL, Mustonen P, Berg L, Harma M. Microdialysis detects postoperative perfusion failure in microvascular flaps. *J Reconstr Microsurg* 2006; 22(2):87-96.

(70) Setala L, Joukainen S, Uusaro A, Alhava E, Harma M. Metabolic response in microvascular flaps during partial pedicle obstruction and hypovolemic shock. *J Reconstr Microsurg* 2007; 23(8):489-496.

(71) Setala L, Koskenvuori H, Gudaviciene D, Berg L, Mustonen P. Cost analysis of 109 microsurgical reconstructions and flap monitoring with microdialysis. *J Reconstr Microsurg* 2009; 25(9):521-526.

(72) Setala LP, Korvenoja EM, Harma MA, Alhava EM, Uusaro AV, Tenhunen JJ. Glucose, lactate, and pyruvate response in an experimental model of microvascular flap ischemia and reperfusion: a microdialysis study. *Microsurgery* 2004; 24(3):223-231.

(73) Birke-Sorensen H, Toft G, Bengaard J. Pure muscle transfers can be monitored by use of microdialysis. *J Reconstr Microsurg* 2010; 26(9):623-630.

(74) Udesen A, Lontoft E, Kristensen SR. Monitoring of free TRAM flaps with microdialysis. *J Reconstr Microsurg* 2000; 16(2):101-106.

(75) Whitaker IS, Rozen WM, Chubb D, Acosta R, Kiil BJ, Birke-Sorensen H et al. Postoperative monitoring of free flaps in autologous breast reconstruction: a multicenter comparison of 398 flaps using clinical monitoring, microdialysis, and the implantable Doppler probe. *J Reconstr Microsurg* 2010; 26(6):409-416.

(76) Abdel-Galil K, Mitchell D. Postoperative monitoring of microsurgical free-tissue transfers for head and neck reconstruction: a systematic review of current techniques--part II. Invasive techniques. *Br J Oral Maxillofac Surg* 2009; 47(6):438-442.

(77) Jyranki J, Suominen S, Vuola J, Back L. Microdialysis in clinical practice: monitoring intraoral free flaps. *Ann Plast Surg* 2006; 56(4):387-393.

(78) Nielsen HT, Gutberg N, Birke-Sorensen H. Monitoring of intraoral free flaps with microdialysis. *Br J Oral Maxillofac Surg* 2010.

(79) Brueggemann A, Noltze A, Lange T, Kaun M, Gliemroth J, Goerg S et al. Significant [C3a] increase in free flaps after prolonged ischemia. *J Surg Res* 2008; 150(1):125-130.

(80) Contaldo C, Harder Y, Plock J, Banic A, Jakob SM, Erni D. The influence of local and systemic preconditioning on oxygenation, metabolism and survival in critically ischaemic skin flaps in pigs. *J Plast Reconstr Aesthet Surg* 2007; 60(11):1182-1192.

(81) Hiltunen P, Palve J, Setala L, Mustonen PK, Berg L, Ruokonen E et al. The effects of hypotension and norepinephrine on microvascular flap perfusion. *J Reconstr Microsurg* 2011; 27(7):419-426.

(82) Ionac M, Schaefer D, Geishauser M. Thromboxane A2 release in ischemia and reperfusion of free flaps in rats, studied by microdialysis. *J Reconstr Microsurg* 2001; 17(2):139-143.

(83) Rydh M, Malm M, Jernbeck J, Dalsgaard CJ. Ectatic blood vessels in port-wine stains lack innervation: possible role in pathogenesis. *Plastic & Reconstructive Surgery 87(3):419-22*, 1991.

(84) Jernbeck J, Malm M. Calcitonin gene-related peptide increases the blood flow of port-wine stains and improves continuous-wave dye laser treatment. *Plast Reconstr Surg* **1993; 91(2):245-251.**

(85) Huang YC, Ringold TL, Nelson JS, Choi B. Noninvasive blood flow imaging for real-time feedback during laser therapy of port wine stain birthmarks. *Lasers Surg Med* **2008; 40(3):167-173.**

(86) Mulliken JB, Glowacki J. Hemangiomas and vascular malformations in infants and children: a classification based on endothelial characteristics. *Plast Reconstr Surg* **1982; 69(3):412-422.**

(87) Jacobs AH, Walton RG. The incidence of birthmarks in the neonate. *Pediatrics 58(2):218-22*, **1976.**

(88) Portilla P, Husson B, Lasjaunias P, Landrieu P. Sturge-Weber disease with repercussion on the prenatal development of the cerebral hemisphere. *Ajnr: American Journal of Neuroradiology 23(3):490-2*, **2002.**

(89) Lanigan SW. Lasers in Dermatology. New York: Springer Verlag; 2000.

(90) Maiman T. Stimulated optic radiation in ruby. *Nature* **1960; 187:493-494.**

(91) GOLDMAN L, BLANEY DJ, KINDEL DJ, Jr., RICHFIELD D, FRANKE EK. Pathology of the effect of the laser beam on the skin. *Nature* **1961;912-914.**

(92) Dixon JA, Rotering RH, Huether SE. Patient's evaluation of argon laser therapy of port wine stain, decorative tattoo, and essential telangiectasia. *Lasers Surg Med* **1984; 4(2):181-190.**

(93) Anderson RR, Parrish JA. Selective photothermolysis: precise microsurgery by selective absorption of pulsed radiation. *Science* **1983; 220(4596):524-527.**

(94) Dierickx CC, Casparian JM, Venugopalan V, Farinelli WA, Anderson RR. Thermal relaxation of port-wine stain vessels probed in vivo: the need for 1-10-millisecond laser pulse treatment. *J Invest Dermatol* **1995; 105(5):709-714.**

(95) Pickering JW, Butler PH, Ring BJ, Walker EP. Thermal profiles of blood vessels heated by a laser. *Australas Phys Eng Sci Med* **1989; 12(1):11-15.**

(96) Goldman MP, Fitzpatrick RE, Ruiz-Esparza J. Treatment of port-wine stains (capillary malformation) with the flashlamp-pumped pulsed dye laser. *Journal of Pediatrics 122(1):71-7*, **1993.**

(97) Katugampola GA, Lanigan SW. Five years' experience of treating port wine stains with the flashlamp-pumped pulsed dye laser. *British Journal of Dermatology 137(5):750-4*, **1997.**

(98) Lanigan SW. Port-wine stains unresponsive to pulsed dye laser: explanations and solutions. [Review] [39 refs]. *British Journal of Dermatology 139(2):173-7*, **1998.**

(99) Tan OT, Carney JM, Margolis R, Seki Y, Boll J, Anderson RR et al. Histologic responses of port-wine stains treated by argon, carbon dioxide, and tunable dye lasers. A preliminary report. *Archives of Dermatology 122(9):1016-22*, **1986.**

(100) Kauvar AN, Geronemus RG. Repetitive pulsed dye laser treatments improve persistent port-wine stains. *Dermatologic Surgery 21(6):515-21*, **1995.**

(101) van der Horst CM, Koster PH, de Borgie CA, Bossuyt PM, van Gemert MJ. Effect of the timing of treatment of port-wine stains with the flash-lamp-pumped pulsed-dye laser. *New England Journal of Medicine 338(15):1028-33*, **1998.**

(102) Fiskerstrand EJ, Svaasand LO, Kopstad G, Ryggen K, Aase S. Photothermally induced vessel-wall necrosis after pulsed dye laser treatment: lack of response in port-wine stains with small sized or deeply located vessels. *Journal of Investigative Dermatology 107(5):671-5*, **1996.**

(103) van Gemert MJ, Nelson JS, Milner TE, Smithies DJ, Verkruysse W, de Boer JF et al. Non-invasive determination of port wine stain anatomy and physiology for optimal laser treatment strategies. *Phys Med Biol* **1997; 42(5):937-950.**

(104) Garden JM, Tan OT, Kerschmann R, Boll J, Furumoto H, Anderson RR et al. Effect of dye laser pulse duration on selective cutaneous vascular injury. *J Invest Dermatol* **1986; 87(5):653-657.**

(105) Waner M. Recent developments in lasers and the treatment of birthmarks. *Archives of Disease in Childhood 88(5):372-4*, **2003.**

(106) Tan OT, Motemedi M, Welch AJ, Kurban AK. Spotsize effects on guinea pig skin following pulsed irradiation. *Journal of Investigative Dermatology 90(6):877-81*, **1988.**

(107) Keijzer M, Pickering JW, van Gemert MJ. Laser beam diameter for port wine stain treatment. *Lasers in Surgery & Medicine 11(6):601-5*, **1991.**

(108) Aguilar G, Svaasand LO, Nelson JS. Effects of hypobaric pressure on human skin: feasibility study for port wine stain laser therapy (part I). *Lasers in Surgery & Medicine 36(2):124-9*, **2005.**

(109) van Gemert MJ, Welch AJ, Amin AP. Is there an optimal laser treatment for port wine stains? *Lasers in Surgery & Medicine 6(1):76-83*, **1986.**

(110) Nelson JS, Milner TE, Anvari B, Tanenbaum BS, Kimel S, Svaasand LO et al. Dynamic epidermal cooling during pulsed laser treatment of

port-wine stain. A new methodology with preliminary clinical evaluation. *Archives of Dermatology 131(6):695-700*, **1995.**

(111) Svaasand LO, Aguilar G, Viator JA, Randeberg LL, Kimel S, Nelson JS. Increase of dermal blood volume fraction reduces the threshold for laser-induced purpura: implications for port wine stain laser treatment. *Lasers in Surgery & Medicine 34(2):182-8*, **2004.**

(112) Franco W, Childers M, Nelson JS, Aguilar G. Laser surgery of port wine stains using local vacuum [corrected] pressure: changes in calculated energy deposition (Part II). *Lasers Surg Med* **2007; 39(2):118-127.**

(113) McGill DJ, Mackay IR. The effect of ambient temperature on capillary vascular malformations. *British Journal of Dermatology 154(5):896-903*, **2006.**

(114) McGill DJ, Mackay IR. Capillary vascular malformation response to increased ambient temperature is dependent upon anatomical location. *Ann Plast Surg* **2007; 58(2):193-199.**

(115) Friedman PM, Mafong EA, Friedman ES, Geronemus RG. Topical anesthetics update: EMLA and beyond. *Dermatologic Surgery 27(12):1019-26*, **2001.**

(116) Fiala S, Jones SA, Brown MB. A fundamental investigation into the effects of eutectic formation on transmembrane transport. *Int J Pharm* **2010; 393(1-2):68-73.**

(117) Hallen B, Olsson GL, Uppfeldt A. Pain-free venepuncture. Effect of timing of application of local anaesthetic cream. *Anaesthesia* **1984; 39(10):969-972.**

(118) Kurien L, Kollberg H, Uppfeldt A. Venepuncture pain can be reduced. *J Trop Med Hyg* **1985; 88(6):397-399.**

(119) Maunuksela EL, Korpela R. Double-blind evaluation of a lignocaine-prilocaine cream (EMLA) in children. Effect on the pain associated with venous cannulation. *Br J Anaesth* **1986; 58(11):1242-1245.**

(120) Cooper CM, Gerrish SP, Hardwick M, Kay R. EMLA cream reduces the pain of venepuncture in children. *Eur J Anaesthesiol* **1987; 4(6):441-448.**

(121) Hopkins CS, Buckley CJ, Bush GH. Pain-free injection in infants. Use of a lignocaine-prilocaine cream to prevent pain at intravenous induction of general anaesthesia in 1-5-year-old children. *Anaesthesia* **1988; 43(3):198-201.**

(122) Watson AR, Szymkiw P, Morgan AG. Topical anaesthesia for fistula cannulation in haemodialysis patients. *Nephrol Dial Transplant* **1988; 3(6):800-802.**

(123) Bucalo BD, Mirikitani EJ, Moy RL. Comparison of skin anesthetic effect of liposomal lidocaine, nonliposomal lidocaine, and EMLA using 30-minute application time. *Dermatol Surg* **1998; 24(5):537-541.**

(124) Ohlsen L, Englesson S, Evers H. An anaesthetic lidocaine/prilocaine cream (EMLA) for epicutaneous application tested for cutting split skin grafts. *Scand J Plast Reconstr Surg* **1985; 19(2):201-209.**

(125) Lahteenmaki T, Lillieborg S, Ohlsen L, Olenius M, Strombeck JO. Topical analgesia for the cutting of split-skin grafts: a multicenter comparison of two doses of a lidocaine/prilocaine cream. *Plast Reconstr Surg* **1988; 82(3):458-462.**

(126) Goodacre TE, Sanders R, Watts DA, Stoker M. Split skin grafting using topical local anaesthesia (EMLA): a comparison with infiltrated anaesthesia. *Br J Plast Surg* **1988; 41(5):533-538.**

(127) Arendt-Nielsen L, Bjerring P. Laser-induced pain for evaluation of local analgesia: a comparison of topical application (EMLA) and local injection (lidocaine). *Anesth Analg* **1988; 67(2):115-123.**

(128) Hernandez E, Gonzalez S, Gonzalez E. Evaluation of topical anesthetics by laser-induced sensation: comparison of EMLA 5% cream and 40% lidocaine in an acid mantle ointment. *Lasers Surg Med* **1998; 23(3):167-171.**

(129) Molodecka J, Stenhouse C, Jones JM, Tomlinson A. Comparison of percutaneous anaesthesia for venous cannulation after topical application of either amethocaine or EMLA cream. *British Journal of Anaesthesia 72(2):174-6*, **1994.**

(130) Lawson RA, Smart NG, Gudgeon AC, Morton NS. Evaluation of an amethocaine gel preparation for percutaneous analgesia before venous cannulation in children. *British Journal of Anaesthesia 75(3):282-5*, **1995.**

(131) O'Connor B, Tomlinson AA. Evaluation of the efficacy and safety of amethocaine gel applied topically before venous cannulation in adults. *British Journal of Anaesthesia 74(6):706-8*, **1995.**

(132) Taddio A, Gurguis MG, Koren G. Lidocaine-prilocaine cream versus tetracaine gel for procedural pain in children. [Review] [22 refs]. *Annals of Pharmacotherapy 36(4):687-92*, **2002.**

(133) Sivarajan V, Mackay IR. The relationship between location, color, and vessel structure within capillary vascular malformations. *Annals of Plastic Surgery 53(4):378-81*, **2004.**

(134) Sivarajan V, Maclaren WM, Mackay IR. The effect of varying pulse duration, wavelength, spot size, and fluence on the response of previously treated capillary vascular malformations to pulsed-dye laser treatment. *Annals of Plastic Surgery 57(1):25-32*, **2006.**

(135) Harville DA. Maximum Likelihood Approaches to Variance Component Estimation and to Related Problems. *Journal of the American Statistical Association* **1977; 72(358):320-338.**

(136) Militino AF. Applied Mixed Models in Medicine, 2nd edn by H. Brown and R. Prescott. *Journal of the Royal Statistical Society: Series A (Statistics in Society)* **2007; 170(1):252-253.**

(137) Biro P, Meier T, Cummins AS. Comparison of topical anaesthesia methods for venous cannulation in adults. *Eur J Pain* **1997; 1(1):37-42.**

(138) Friedman PM, Fogelman JP, Nouri K, Levine VJ, Ashinoff R. Comparative study of the efficacy of four topical anesthetics. *Dermatologic Surgery 25(12):950-4*, **1999.**

(139) Doshi SN, Friedman PM, Marquez DK, Goldberg LH. Thirty-minute application of the S-Caine peel prior to nonablative laser treatment. *Dermatologic Surgery 29(10):1008-11*, **2003.**

(140) Chen JZ, Alexiades-Armenakas MR, Bernstein LJ, Jacobson LG, Friedman PM, Geronemus RG. Two randomized, double-blind, placebo-controlled studies evaluating the S-Caine Peel for induction of local anesthesia before long-pulsed Nd:YAG laser therapy for leg veins. *Dermatologic Surgery 29(10):1012-8*, **2003.**

(141) Bryan HA, Alster TS. The S-Caine peel: a novel topical anesthetic for cutaneous laser surgery. *Dermatologic Surgery 28(11):999-1003; discussion 1003*, **2002.**

(142) Alster TS, Lupton JR. Evaluation of a novel topical anesthetic agent for cutaneous laser resurfacing: a randomized comparison study. *Dermatologic Surgery 28(11):1004-6; discussion 1006*, **2002.**

(143) Ramos-Zabala A, Perez-Mencia MT, Fernandez-Garcia R, Cascales-Nunez MR. Anesthesia technique for outpatient facial laser resurfacing. *Lasers in Surgery & Medicine 34(3):269-72*, **2004.**

(144) Herd DW, Newbury C, Brown PM. Cost benefit analysis of amethocaine (Ametop) compared with EMLA for intravenous cannulation in a children's emergency department. *Emerg Med J* **2010; 27(6):456-460.**

(145) Kilmer SL, Chotzen V, Zelickson BD, McClaren M, Silva S, Calkin J et al. Full-face laser resurfacing using a supplemented topical anesthesia protocol. *Archives of Dermatology 139(10):1279-83*, **2003.**

(146) Kaweski S. Topical anesthetic creams. *Plast Reconstr Surg* **2008; 121(6):2161-2165.**

(147) Eaglstein NF. Chemical injury to the eye from EMLA cream during erbium laser resurfacing. *Dermatologic Surgery 25(7):590-1*, **1999.**

(148) Arildsson M, Asker CL, Salerud EG, Stromberg T. Skin capillary appearance and skin microvascular perfusion due to topical application of analgesia cream. *Microvasc Res* **2000; 59(1):14-23.**

(149) Bjerring P, Andersen PH, Arendt-Nielsen L. Vascular response of human skin after analgesia with EMLA cream. *Br J Anaesth* 1989; 63(6):655-660.

(150) Wiles MD, Dickson E, Moppett IK. Transient hyperaemic response to assess vascular reactivity of skin: effect of topical anaesthesia. *Br J Anaesth* 2008; 101(3):320-323.

(151) Ganong W. Review of Medical Physiology. 18th ed. Stamford, Connecticut: Appleton & Lange; 1997.

(152) Aps C, Reynolds F. The effect of concentration on vasoactivity of bupivacaine and lignocaine. *Br J Anaesth* 1976; 48(12):1171-1174.

(153) Reynolds F, Bryson TH, Nicholas AD. Intradermal study of a new local anaesthetic agent aptocaine. *Br J Anaesth* 1976; 48(4):347-354.

(154) Arildsson M, Nilsson GE, Stromberg T. Effects on skin blood flow by provocation during local analgesia. *Microvasc Res* 2000; 59(1):122-130.

(155) Haggblad E, Larsson M, Arildsson M, Stromberg T, Salerud EG. Reflection spectroscopy of analgesized skin. *Microvasc Res* 2001; 62(3):392-400.

(156) Hafner HM, Thomma SR, Eichner M, Steins A, Junger M. The influence of Emla cream on cutaneous microcirculation. *Clin Hemorheol Microcirc* 2003; 28(3):121-128.

(157) Berghoff M, Kathpal M, Kilo S, Hilz MJ, Freeman R. Vascular and neural mechanisms of ACh-mediated vasodilation in the forearm cutaneous microcirculation. *J Appl Physiol* 2002; 92(2):780-788.

(158) Caselli A, Rich J, Hanane T, Uccioli L, Veves A. Role of C-nociceptive fibers in the nerve axon reflex-related vasodilation in diabetes. *Neurology* 2003; 60(2):297-300.

(159) Caselli A, Uccioli L, Khaodhiar L, Veves A. Local anesthesia reduces the maximal skin vasodilation during iontophoresis of sodium nitroprusside and heating. *Microvasc Res* 2003; 66(2):134-139.

(160) Hsieh CH, Huang KF, Liliang PC, Huang PC, Shih HM, Rau CS. EMLA and water immersion cause similar vasodilatation in replanted fingers. *J Surg Res* 2007; 143(2):265-269.

(161) Larkin SW, Williams TJ. Evidence for sensory nerve involvement in cutaneous reactive hyperemia in humans. *Circ Res* 1993; 73(1):147-154.

(162) Wiles MD, Dobson SA, Moppett IK. The effect of a new topical local anaesthetic delivery system on forearm skin blood flow reactivity. *Anaesthesia* 2010; 65(2):178-183.

(163) Tahir A, Webb JB, Allen G, Nancarrow JD. The effect of local anaesthetic cream (EMLA) applied with an occlusive dressing on skin

thickness. Does it matter? *J Plast Reconstr Aesthet Surg* **2006; 59(4):404-408.**

(164) Villringer A, Haberl RL, Dirnagl U, Anneser F, Verst M, Einhaupl KM. Confocal laser microscopy to study microcirculation on the rat brain surface in vivo. *Brain Res* **1989; 504(1):159-160.**

(165) Selim MM, Kelly KM, Nelson JS, Wendelschafer-Crabb G, Kennedy WR, Zelickson BD. Confocal microscopy study of nerves and blood vessels in untreated and treated port wine stains: preliminary observations. *Dermatol Surg* **2004; 30(6):892-897.**

(166) Astner S, Gonzalez S, Cuevas J, Rowert-Huber J, Sterry W, Stockfleth E et al. Preliminary evaluation of benign vascular lesions using in vivo reflectance confocal microscopy. *Dermatol Surg* **2010; 36(7):1099-1110.**

(167) Pellacani G, Cesinaro AM, Seidenari S. Reflectance-mode confocal microscopy of pigmented skin lesions--improvement in melanoma diagnostic specificity. *J Am Acad Dermatol* **2005; 53(6):979-985.**

(168) Langley RG, Walsh N, Sutherland AE, Propperova I, Delaney L, Morris SF et al. The diagnostic accuracy of in vivo confocal scanning laser microscopy compared to dermoscopy of benign and malignant melanocytic lesions: a prospective study. *Dermatology* **2007; 215(4):365-372.**

(169) Lakmaker O, Pickering JW, van Gemert MJ. Modeling the color perception of port wine stains and its relation to the depth of laser coagulated blood vessels. *Lasers Surg Med* **1993; 13(2):219-226.**

(170) Hohenleutner U, Hilbert M, Wlotzke U, Landthaler M. Epidermal damage and limited coagulation depth with the flashlamp-pumped pulsed dye laser: a histochemical study. *J Invest Dermatol* **1995; 104(5):798-802.**

(171) Kelly KM, Choi B, McFarlane S, Motosue A, Jung B, Khan MH et al. Description and analysis of treatments for port-wine stain birthmarks. *Arch Facial Plast Surg* **2005; 7(5):287-294.**

(172) Fitzpatrick RE, Lowe NJ, Goldman MP, Borden H, Behr KL, Ruiz-Esparza J. Flashlamp-pumped pulsed dye laser treatment of port-wine stains. *J Dermatol Surg Oncol* **1994; 20(11):743-748.**

(173) Taieb A, Touati L, Cony M, Leaute-Labreze C, Mortureux P, Renaud P et al. Treatment of port-wine stains with the 585-nm flashlamp-pulsed tunable dye laser: a study of 74 patients. *Dermatology* **1994; 188(4):276-281.**

(174) Altintas MA, Altintas AA, Guggenheim M, Steiert AE, Aust MC, Niederbichler AD et al. Insight in human skin microcirculation using in vivo reflectance-mode confocal laser scanning microscopy. *J Digit Imaging* **2010; 23(4):475-481.**

(175) Zahir KS, Syed SA, Zink JR, Restifo RJ, Thomson JG. Ischemic preconditioning improves the survival of skin and myocutaneous flaps in a rat model. *Plast Reconstr Surg* 1998; 102(1):140-150.

(176) Greenbaum AR. The nutrition of active muscle flaps. *Ann R Coll Surg Engl* 2005; 87(2):77-84.

(177) Baker RD, Weinand C, Jeng JC, Hoeksema H, Monstrey S, Pape SA et al. Using ordinal logistic regression to evaluate the performance of laser-Doppler predictions of burn-healing time. *BMC Med Res Methodol* 2009; 9:11.

(178) Newton DJ, Khan F, Belch JJ. Assessment of microvascular endothelial function in human skin. *Clin Sci (Lond)* 2001; 101(6):567-572.

(179) Ferrell WR, Balint PV, Egan CG, Lockhart JC, Sturrock RD. Metacarpophalangeal joints in rheumatoid arthritis: laser Doppler imaging--initial experience. *Radiology* 2001; 220(1):257-262.

(180) Levene H. Robust test for equality of variance. In: Oilkin I, Ghurye SG, Hoeffding W, Madow WG, Mann HB, editors. Contributions to Probability and Statistics. California: Stanford University Press; 1960.

(181) Jones BM, Mayou BJ. The Laser Doppler flowmeter for microvascular monitoring: a preliminary report. *Br J Plast Surg* 1982; 35(2):147-149.

(182) Smit JM, Zeebregts CJ, Acosta R, Werker PM. Advancements in free flap monitoring in the last decade: a critical review. *Plast Reconstr Surg* 2010; 125(1):177-185.

(183) Heller L, Levin LS, Klitzman B. Laser Doppler flowmeter monitoring of free-tissue transfers: blood flow in normal and complicated cases. *Plast Reconstr Surg* 2001; 107(7):1739-1745.

(184) Stone CA, Dubbins PA, Morris RJ. Use of colour duplex Doppler imaging in the postoperative assessment of buried free flaps. *Microsurgery* 2001; 21(5):223-227.

(185) Hirigoyen MB, Urken ML, Weinberg H. Free flap monitoring: a review of current practice. *Microsurgery* 1995; 16(11):723-726.

(186) Soderstrom T, Svensson H, Koop T, Moller KO. Processing of laser-Doppler signals from free flaps. *Technol Health Care* 1999; 7(2-3):219-223.

(187) Yuen JC, Feng Z. Monitoring free flaps using the laser Doppler flowmeter: five-year experience. *Plast Reconstr Surg* 2000; 105(1):55-61.

(188) Yoshino K, Nara S, Endo M, Kamata N. Intraoral free flap monitoring with a laser Doppler flowmeter. *Microsurgery* 1996; 17(6):337-340.

(189) Figus A, Mosahebi A, Ramakrishnan V. Microcirculation in DIEP flaps: a study of the haemodynamics using laser Doppler flowmetry and

lightguide reflectance spectrophotometry. *J Plast Reconstr Aesthet Surg* **2006; 59(6):604-612.**

(190) Walkinshaw M, Holloway A, Bulkley A, Engrav LH. Clinical evaluation of laser Doppler blood flow measurements in free flaps. *Ann Plast Surg* **1987; 18(3):212-217.**

(191) Ulusal BG, Cheng MH, Wei FC, Ho-Asjoe M, Song D. Breast reconstruction using the entire transverse abdominal adipocutaneous flap based on unilateral superficial or deep inferior epigastric vessels. *Plast Reconstr Surg* **2006; 117(5):1395-1403.**

(192) Holzle F, Loeffelbein DJ, Nolte D, Wolff KD. Free flap monitoring using simultaneous non-invasive laser Doppler flowmetry and tissue spectrophotometry. *J Craniomaxillofac Surg* **2006; 34(1):25-33.**

(193) Holm C, Tegeler J, Mayr M, Becker A, Pfeiffer UJ, Muhlbauer W. Monitoring free flaps using laser-induced fluorescence of indocyanine green: a preliminary experience. *Microsurgery* **2002; 22(7):278-287.**

(194) Rubben A, Eren S, Krein R, Younossi H, Bohler U, Wienert V. Infrared videoangiofluorography of the skin with indocyanine green--rat random cutaneous flap model and results in man. *Microvasc Res* **1994; 47(2):240-251.**

(195) Scheufler O, Exner K, Andresen R. Investigation of TRAM flap oxygenation and perfusion by near-infrared reflection spectroscopy and color-coded duplex sonography. *Plast Reconstr Surg* **2004; 113(1):141-152.**

(196) Holm C, Mayr M, Hofter E, Raab N, Ninkovic M. Interindividual variability of the SIEA Angiosome: effects on operative strategies in breast reconstruction. *Plast Reconstr Surg* **2008; 122(6):1612-1620.**

(197) Holm C, Dornseifer U, Sturtz G, Basso G, Schuster T, Ninkovic M. The intrinsic transit time of free microvascular flaps: clinical and prognostic implications. *Microsurgery* **2010; 30(2):91-96.**

(198) Guyton A, Hall J. Textbook of Medical Physiology. 9th Edition ed. Philadelphia: W.B. Saunders Company; 1996.

(199) Levick J. An Introduction to Cardiovascular Physiology. 3rd ed. 2000.

(200) Tee GB, Rasool AH, Halim AS, Rahman AR. Dependence of human forearm skin postocclusive reactive hyperemia on occlusion time. *J Pharmacol Toxicol Methods* **2004; 50(1):73-78.**

(201) Hallock GG. Critical threshold for tissue viability as determined by laser Doppler flowmetry. *Ann Plast Surg* **1992; 28(6):554-558.**

(202) Khan MS, Kairinos N, Cadier M. The use of laser Doppler in determining timing for division of cross leg free flaps. *Br J Plast Surg* **2005; 58(1):120-121.**

(203) Kinnunen I, Laurikainen E, Schrey A, Aitasalo K. Changes in blood flow in the epigastric free flap after microsurgical artery anastomoses in rats. *Acta Otolaryngol Suppl* **2000; 543:254-256.**

(204) Kinnunen I, Laurikainen E, Schrey A, Laippala P, Aitasalo K. Effect of hypothermia on blood-flow responses in pedicled groin flaps in rats. *Br J Plast Surg* **2002; 55(8):657-663.**

(205) Kinnunen I, Laurikainen E, Schrey A, Laippala P, Aitasalo K. Effect of acute ischemic preconditioning on blood-flow response in the epigastric pedicled rat flap. *J Reconstr Microsurg* **2002; 18(1):61-68.**

(206) Kinnunen I, Laurikainen E, Schrey A, Laippala P, Aitasalo K. Effect of blood loss on vascular responsiveness in pedicled groin flaps in a rat model. *J Reconstr Microsurg* **2002; 18(7):599-608.**

(207) Sigdell JE. Venous occlusion plethysmography. Part 1: basic principles and applications. *Biomed Eng* **1975; 10(8):300-302.**

(208) Sigdell JE. Venous occlusion plethysmography. Part 2: methods. *Biomed Eng* **1975; 10(9):342-5, 349.**

(209) Cracowski JL, Minson CT, Salvat-Melis M, Halliwill JR. Methodological issues in the assessment of skin microvascular endothelial function in humans. *Trends Pharmacol Sci* **2006; 27(9):503-508.**

(210) Morales F, Graaff R, Smit AJ, Bertuglia S, Petoukhova AL, Steenbergen W et al. How to assess post-occlusive reactive hyperaemia by means of laser Doppler perfusion monitoring: application of a standardised protocol to patients with peripheral arterial obstructive disease. *Microvasc Res* **2005; 69(1-2):17-23.**

(211) Thijssen DH, Bleeker MW, Smits P, Hopman MT. Reproducibility of blood flow and post-occlusive reactive hyperaemia as measured by venous occlusion plethysmography. *Clin Sci (Lond)* **2005; 108(2):151-157.**

(212) Tew GA, Klonizakis M, Saxton JM. Effects of ageing and fitness on skin-microvessel vasodilator function in humans. *Eur J Appl Physiol* **2010; 109(2):173-181.**

(213) Lenasi H, Strucl M. Effect of regular physical training on cutaneous microvascular reactivity. *Med Sci Sports Exerc* **2004; 36(4):606-612.**

(214) Roche DM, Rowland TW, Garrard M, Marwood S, Unnithan VB. Skin microvascular reactivity in trained adolescents. *Eur J Appl Physiol* **2010; 108(6):1201-1208.**

(215) Tur E, Yosipovitch G, Oren-Vulfs S. Chronic and acute effects of cigarette smoking on skin blood flow. *Angiology* **1992; 43(4):328-335.**

(216) Ijzerman RG, Serne EH, van Weissenbruch MM, de Jongh RT, Stehouwer CD. Cigarette smoking is associated with an acute impairment of microvascular function in humans. *Clin Sci (Lond)* **2003; 104(3):247-252.**

(217) Sieg-Dobrescu D, Burnier M, Hayoz D, Brunner HR, Waeber B. The return of increased blood pressure after discontinuation of antihypertensive treatment is associated with an impaired post-ischemic skin blood flow response. *J Hypertens* **2001; 19(8):1387-1392.**

(218) Monsuez JJ, Dufaux J, Vittecoq D, Vicaut E. Reduced reactive hyperemia in HIV-infected patients. *J Acquir Immune Defic Syndr* **2000; 25(5):434-442.**

(219) Maggi P, Bellacosa C, Grattagliano V, Pastore G, Lapadula G. Functional impairments of microcirculation in HIV-positive patients: a laser Doppler fluxometry-based investigation. *HIV Clin Trials* **2008; 9(6):428-433.**

(220) Hansell J, Henareh L, Agewall S, Norman M. Non-invasive assessment of endothelial function - relation between vasodilatory responses in skin microcirculation and brachial artery. *Clin Physiol Funct Imaging* **2004; 24(6):317-322.**

(221) Wollersheim H, Reyenga J, Thien T. Postocclusive reactive hyperemia of fingertips, monitored by laser Doppler velocimetry in the diagnosis of Raynaud's phenomenon. *Microvasc Res* **1989; 38(3):286-295.**

(222) Bungum L, Kvernebo K, Oian P, Maltau JM. Laser doppler-recorded reactive hyperaemia in the forearm skin during the menstrual cycle. *Br J Obstet Gynaecol* **1996; 103(1):70-75.**

(223) Agarwal SC, Allen J, Murray A, Purcell IF. Comparative reproducibility of dermal microvascular blood flow changes in response to acetylcholine iontophoresis, hyperthermia and reactive hyperaemia. *Physiol Meas* **2010; 31(1):1-11.**

(224) Bender D. Introduction to Nutrition and Metabolism. 2nd ed. London: Taylor & Francis; 1997.

(225) Hallock GG. Zones of the lower transverse rectus abdominis musculocutaneous flap based on laser Doppler flowmetry. *Ann Plast Surg* **1992; 29(2):117-121.**

(226) Hallock GG. Physiological studies using laser Doppler flowmetry to compare blood flow to the zones of the free TRAM flap. *Ann Plast Surg* **2001; 47(3):229-233.**

(227) Holm C, Mayr M, Hofter E, Ninkovic M. Perfusion zones of the DIEP flap revisited: a clinical study. *Plast Reconstr Surg* **2006; 117(1):37-43.**

(228) Holm C, Mayr M, Hofter E, Ninkovic M. The versatility of the SIEA flap: a clinical assessment of the vascular territory of the superficial epigastric inferior artery. *J Plast Reconstr Aesthet Surg* **2007; 60(8):946-951.**

(229) Brown H, Prescott R. Applied mixed models in medicine (second edition) Brown H, Prescott R (2006) . Wiley, Chichester, England.; 2006.

(230) Stern MD, Bowen PD, Parma R, Osgood RW, Bowman RL, Stein JH. Measurement of renal cortical and medullary blood flow by laser-Doppler spectroscopy in the rat. *Am J Physiol* **1979; 236(1):F80-F87.**

(231) Clinton MS, Sepka RS, Bristol D, Pederson WC, Barwick WJ, Serafin D et al. Establishment of normal ranges of laser Doppler blood flow in autologous tissue transplants. *Plast Reconstr Surg* **1991; 87(2):299-309.**

(232) Hallock GG. A "True" false-negative misadventure in free flap monitoring using laser Doppler flowmetry. *Plast Reconstr Surg* **2002; 110(6):1609-1611.**

(233) Jallali N, Ridha H, Butler PE. Postoperative monitoring of free flaps in UK plastic surgery units. *Microsurgery* **2005; 25(6):469-472.**

(234) Ferguson RE, Jr., Yu P. Techniques of monitoring buried fasciocutaneous free flaps. *Plastic & Reconstructive Surgery* **2009; 123(2):525-532.**

(235) Yuen JC. Techniques of external monitoring of buried free flaps. *Annals of Plastic Surgery* **2005; 55(5):460-465.**

(236) Furnas H, Rosen JM. Monitoring in microvascular surgery. [Review] [75 refs]. *Annals of Plastic Surgery* **1991; 26(3):265-272.**

(237) Yuen JC, Feng Z. Reduced cost of extremity free flap monitoring. *Ann Plast Surg* **1998; 41(1):36-40.**

(238) Brenman SA, Barber WB, Pederson WC, Barwick WJ. Pedicled free flaps: indications in complex reconstruction. *Ann Plast Surg* **1990; 24(5):420-426.**

(239) Abdel-Galil K, Mitchell D. Postoperative monitoring of microsurgical free tissue transfers for head and neck reconstruction: a systematic review of current techniques--part I. Non-invasive techniques. [Review] [25 refs]. *British Journal of Oral & Maxillofacial Surgery* **2009; 47(5):351-355.**

(240) Kaiser M, Yafi A, Cinat M, Choi B, Durkin AJ. Noninvasive assessment of burn wound severity using optical technology: a review of current and future modalities. [Review]. *Burns* **2011; 37(3):377-386.**

(241) Monstrey SM, Hoeksema H, Baker RD, Jeng J, Spence RS, Wilson D et al. Burn wound healing time assessed by laser Doppler imaging. Part 2: validation of a dedicated colour code for image interpretation. *Burns* **2011; 37(2):249-256.**

(242) Nguyen K, Ward D, Lam L, Holland AJ. Laser Doppler Imaging prediction of burn wound outcome in children: is it possible before 48 h? *Burns* **2010; 36(6):793-798.**

(243) Bailey SH, Saint-Cyr M, Wong C, Mojallal A, Zhang K, Ouyang D et al. The single dominant medial row perforator DIEP flap in breast reconstruction: three-dimensional perforasome and clinical results. *Plast Reconstr Surg* **2010; 126(3):739-751.**

(244) Dinner MI, Dowden RV, Scheflan M. Refinements in the use of the transverse abdominal island flap for postmastectomy reconstruction. *Annals of Plastic Surgery 11(5):362-72*, **1983.**

(245) Keller A. Perfusion zones of the DIEP flap revisited: a clinical study. *Plast Reconstr Surg* **2006; 118(4):1076-1077.**

(246) Wong C, Saint-Cyr M, Arbique G, Becker S, Brown S, Myers S et al. Three- and four-dimensional computed tomography angiographic studies of commonly used abdominal flaps in breast reconstruction. *Plast Reconstr Surg* **2009; 124(1):18-27.**

(247) de WL, Miland AO, Mercer JB. Perfusion dynamics of free DIEP and SIEA flaps during the first postoperative week monitored with dynamic infrared thermography. *Ann Plast Surg* **2009; 62(1):42-47.**

(248) Figus A, Ramakrishnan V, Rubino C. Hemodynamic changes in the microcirculation of DIEP flaps. *Ann Plast Surg* **2008; 60(6):644-648.**

(249) Heitland AS, Markowicz MP, Koellensperger E, Schoth F, Pallua N. Early and long-term evaluation of perfusion changes in free DIEP-flaps for breast reconstruction via IC-view and duplex ultrasound: autonomous or peripheral perfusion? *J Reconstr Microsurg* **2009; 25(2):139-145.**

(250) Tai Y, Hasegawa H. A transverse abdominal flap for reconstruction after radical operations for recurrent breast cancer. *Plastic & Reconstructive Surgery 53(1):52-4*, **1974.**

(251) Pennington DG, Pelly AD. The rectus abdominis myocutaneous free flap. *British Journal of Plastic Surgery 33(2):277-82*, **1980.**

(252) Mathes SJ, Bostwick J, III. A rectus abdominis myocutaneous flap to reconstruct abdominal wall defects. *British Journal of Plastic Surgery 30(4):282-3*, **1977.**

(253) Holmstrom H. The free abdominoplasty flap and its use in breast reconstruction. An experimental study and clinical case report. *Scandinavian Journal of Plastic & Reconstructive Surgery 13(3):423-27*, **1979.**

(254) Drever JM. The epigastric island flap. *Plast Reconstr Surg* **1977; 59(3):343-346.**

(255) Brown RG, Vasconez LO, Jurkiewicz MJ. Transverse abdominal flaps and the deep epigastric arcade. *Plastic & Reconstructive Surgery 55(4):416-21*, **1975.**

(256) SHAW DT, PAYNE RL, Jr. One stage tubed abdominal flaps; single pedicle tubes. *Surgery, Gynecology & Obstetrics 83:205-9*, **1946.**

(257) Hartrampf CR, Scheflan M, Black PW. Breast reconstruction with a transverse abdominal island flap. *Plastic & Reconstructive Surgery 69(2):216-25*, **1982.**

(258) Scheflan M, Hartrampf CR, Black PW. Breast reconstruction with a transverse abdominal island flap. *Plastic & Reconstructive Surgery 69(5):908-9*, **1982.**

(259) Boyd JB, Taylor GI, Corlett R. The vascular territories of the superior epigastric and the deep inferior epigastric systems. *Plastic & Reconstructive Surgery 73(1):1-16*, **1984.**

(260) Taylor GI, Corlett R, Boyd JB. The extended deep inferior epigastric flap: a clinical technique. *Plastic & Reconstructive Surgery 72(6):751-65*, **1983.**

(261) Blondeel PN. One hundred free DIEP flap breast reconstructions: a personal experience. *Br J Plast Surg* **1999; 52(2):104-111.**

(262) Hamdi M, Weiler-Mithoff EM, Webster MH. Deep inferior epigastric perforator flap in breast reconstruction: experience with the first 50 flaps. *Plast Reconstr Surg* **1999; 103(1):86-95.**

(263) Nahabedian MY, Momen B, Galdino G, Manson PN. Breast Reconstruction with the free TRAM or DIEP flap: patient selection, choice of flap, and outcome. *Plastic & Reconstructive Surgery 110(2):466-75; discussion 476-7*, **2002.**

(264) Nahabedian MY, Tsangaris T, Momen B. Breast reconstruction with the DIEP flap or the muscle-sparing (MS-2) free TRAM flap: is there a difference? *Plastic & Reconstructive Surgery 115(2):436-44; discussion 445-6*, **2005.**

(265) Sailon AM, Schachar JS, Levine JP. Free transverse rectus abdominis myocutaneous and deep inferior epigastric perforator flaps for breast reconstruction: a systematic review of flap complication rates and donor-site morbidity. *Ann Plast Surg* **2009; 62(5):560-563.**

(266) Antia NH, Buch VI. Transfer of an abdominal dermo-fat graft by direct anastomosis of blood vessels. *British Journal of Plastic Surgery 24(1):15-9*, **1971.**

(267) Boeckx WD, de Coninck A, Vanderlinden E. Ten free flap transfers: use of intra-arterial dye injection to outline a flap exactly. *Plastic & Reconstructive Surgery 57(6):716-21*, **1976.**

(268) Stern HS, Nahai F. The versatile superficial inferior epigastric artery free flap. *British Journal of Plastic Surgery 45(4):270-4*, **1992;-Jun.**

(269) Iwahira Y, Maruyama Y, Shiba T. One-stage abdominal wall reconstruction with oblique abdominal fasciocutaneous flaps. *Annals of Plastic Surgery* **1919;(5):475-477.**

(270) Chen ZJ, Chen MY, Chen C, Wu N. Vaginal reconstruction with an axial subcutaneous pedicle flap from the inferior abdominal wall: a new method. *Plastic & Reconstructive Surgery 83(6):1005-12*, **1989.**

(271) Sun GC, Huang JJ. One-stage reconstruction of the penis with composite iliac crest and lateral groin skin flap. *Annals of Plastic Surgery 15(6):519-28*, **1985.**

(272) Stevenson TR, Hester TR, Duus EC, Dingman RO. The superficial inferior epigastric artery flap for coverage of hand and forearm defects. *Ann Plast Surg* **1984; 12(4):333-339.**

(273) Grotting JC. The free abdominoplasty flap for immediate breast reconstruction. *Ann Plast Surg* **1991; 27(4):351-354.**

(274) Arnez ZM, Khan U, Pogorelec D, Planinsek F. Breast reconstruction using the free superficial inferior epigastric artery (SIEA) flap. *Br J Plast Surg* **1999; 52(4):276-279.**

(275) Volpe AG, Rothkopf DM, Walton RL. The versatile superficial inferior epigastric flap for breast reconstruction. *Ann Plast Surg* **1994; 32(2):113-117.**

(276) Scheflan M, Dinner MI. The transverse abdominal island flap: part I. Indications, contraindications, results, and complications. *Annals of Plastic Surgery 10(1):24-35*, **1983.**

(277) Scheflan M, Dinner MI. The transverse abdominal island flap: Part II. Surgical technique. *Annals of Plastic Surgery 10(2):120-9*, **1983.**

(278) Dinner MI, Dowden RV. The value of the anterior rectus sheath in the transverse abdominal island flap. *Plastic & Reconstructive Surgery 72(5):724-6*, **1983.**

(279) Rickard R. TRAM and DIEP flap zones. *Br J Plast Surg* **2001; 54(3):272-273.**

(280) Blondeel PN, Arnstein M, Verstraete K, Depuydt K, Van Landuyt KH, Monstrey SJ et al. Venous congestion and blood flow in free transverse rectus abdominis myocutaneous and deep inferior epigastric perforator flaps. *Plast Reconstr Surg* **2000; 106(6):1295-1299.**

(281) Spiegel AJ, Khan FN. An Intraoperative algorithm for use of the SIEA flap for breast reconstruction. *Plast Reconstr Surg* **2007; 120(6):1450-1459.**

(282) Schaverien M, Saint-Cyr M, Arbique G, Brown SA. Arterial and venous anatomies of the deep inferior epigastric perforator and superficial inferior epigastric artery flaps. *Plast Reconstr Surg* **2008; 121(6):1909-1919.**

(283) Saint-Cyr M, Wong C, Schaverien M, Mojallal A, Rohrich RJ. The perforasome theory: vascular anatomy and clinical implications. *Plast Reconstr Surg* **2009; 124(5):1529-1544.**

(284) Rozen WM, Pan WR, Le Roux CM, Taylor GI, Ashton MW. The venous anatomy of the anterior abdominal wall: an anatomical and clinical study. *Plast Reconstr Surg* **2009; 124(3):848-853.**

(285) Imanishi N, Nakajima H, Minabe T, Chang H, Aiso S. Anatomical relationship between arteries and veins in the paraumbilical region. *Br J Plast Surg* 2003; 56(6):552-556.

(286) Heitmann C, Felmerer G, Durmus C, Matejic B, Ingianni G. Anatomical features of perforator blood vessels in the deep inferior epigastric perforator flap. *Br J Plast Surg* 2000; 53(3):205-208.

(287) Carramenha e Costa MA, Carriquiry C, Vasconez LO, Grotting JC, Herrera RH, Windle BH. An anatomic study of the venous drainage of the transverse rectus abdominis musculocutaneous flap. *Plast Reconstr Surg* 1987; 79(2):208-217.

(288) Hallock GG, Rice DC. Comparison of TRAM and DIEP flap physiology in a rat model. *Plast Reconstr Surg* 2004; 114(5):1179-1184.

(289) Yamamoto Y, Sakurai H, Nakazawa H, Nozaki M. Effect of vascular augmentation on the haemodynamics and survival area in a rat abdominal perforator flap model. *J Plast Reconstr Aesthet Surg* 2009; 62(2):244-249.

(290) Miyamoto S, Minabe T, Harii K. Effect of recipient arterial blood inflow on free flap survival area. *Plast Reconstr Surg* 2008; 121(2):505-513.

(291) Ayhan S, Oktar SO, Tuncer S, Yucel C, Kandal S, Demirtas Y. Correlation between vessel diameters of superficial and deep inferior epigastric systems: Doppler ultrasound assessment. *J Plast Reconstr Aesthet Surg* 2009; 62(9):1140-1147.

(292) Bajaj AK, Chevray PM, Chang DW. Comparison of donor-site complications and functional outcomes in free muscle-sparing TRAM flap and free DIEP flap breast reconstruction. *Plast Reconstr Surg* 2006; 117(3):737-746.

(293) Baumann DP, Lin HY, Chevray PM. Perforator number predicts fat necrosis in a prospective analysis of breast reconstruction with free TRAM, DIEP, and SIEA flaps. *Plast Reconstr Surg* 2010; 125(5):1335-1341.

(294) Blondeel N, Vanderstraeten GG, Monstrey SJ, Van Landuyt K, Tonnard P, Lysens R et al. The donor site morbidity of free DIEP flaps and free TRAM flaps for breast reconstruction. *Br J Plast Surg* 1997; 50(5):322-330.

(295) Blondeel PN, Boeckx WD. Refinements in free flap breast reconstruction: the free bilateral deep inferior epigastric perforator flap anastomosed to the internal mammary artery. *Br J Plast Surg* 1994; 47(7):495-501.

(296) Blondeel PN, Beyens G, Verhaeghe R, Van Landuyt K, Tonnard P, Monstrey SJ et al. Doppler flowmetry in the planning of perforator flaps. *Br J Plast Surg* 1998; 51(3):202-209.

(297) Gill PS, Hunt JP, Guerra AB, Dellacroce FJ, Sullivan SK, Boraski J et al. A 10-year retrospective review of 758 DIEP flaps for breast reconstruction. *Plast Reconstr Surg* **2004; 113(4):1153-1160.**

(298) Gusenoff JA, Coon D, De La CC, Rubin JP. Superficial inferior epigastric vessels in the massive weight loss population: implications for breast reconstruction. *Plast Reconstr Surg* **2008; 122(6):1621-1626.**

(299) Kroll SS. Fat necrosis in free transverse rectus abdominis myocutaneous and deep inferior epigastric perforator flaps. *Plast Reconstr Surg* **2000; 106(3):576-583.**

(300) Lejour M, Dome M. Abdominal wall function after rectus abdominis transfer. *Plast Reconstr Surg* **1991; 87(6):1054-1068.**

(301) Lorenzetti F, Suominen S, Tukiainen E, Kuokkanen H, Suominen E, Vuola J et al. Evaluation of blood flow in free microvascular flaps. *J Reconstr Microsurg* **2001; 17(3):163-167.**

(302) Rubino C, Ramakrishnan V, Figus A, Bulla A, Coscia V, Cavazzuti MA. Flap size/flow rate relationship in perforator flaps and its importance in DIEAP flap drainage. *J Plast Reconstr Aesthet Surg* **2009; 62(12):1666-1670.**

(303) Selber JC, Samra F, Bristol M, Sonnad SS, Vega S, Wu L et al. A head-to-head comparison between the muscle-sparing free TRAM and the SIEA flaps: is the rate of flap loss worth the gain in abdominal wall function? *Plast Reconstr Surg* **2008; 122(2):348-355.**

(304) Armitage P, Berry G, Matthews JNS. Statistical Methods in Medical Research. 4th Edition ed. Blackwell Publishing; 1993.

(305) Arnez ZM, Khan U, Pogorelec D, Planinsek F. Rational selection of flaps from the abdomen in breast reconstruction to reduce donor site morbidity. *Br J Plast Surg* **1999; 52(5):351-354.**

(306) Blondeel N, Boeckx WD, Vanderstraeten GG, Lysens R, Van Landuyt K, Tonnard P et al. The fate of the oblique abdominal muscles after free TRAM flap surgery. *Br J Plast Surg* **1997; 50(5):315-321.**

(307) Kroll SS, Sharma S, Koutz C, Langstein HN, Evans GRD, Robb GL et al. Postoperative morphine requirements of free TRAM and DIEP flaps. *Plast Reconstr Surg* **2001; 107(2):338-341.**

(308) Chen CM, Halvorson EG, Disa JJ, McCarthy C, Hu QY, Pusic AL et al. Immediate postoperative complications in DIEP versus free/muscle-sparing TRAM flaps. *Plast Reconstr Surg* **2007; 120(6):1477-1482.**

(309) Schaverien MV, Perks AG, McCulley SJ. Comparison of outcomes and donor-site morbidity in unilateral free TRAM versus DIEP flap breast reconstruction. *J Plast Reconstr Aesthet Surg* **2007; 60(11):1219-1224.**

(310) Scheer AS, Novak CB, Neligan PC, Lipa JE. Complications associated with breast reconstruction using a perforator flap compared with a free TRAM flap. *Ann Plast Surg* 2006; 56(4):355-358.

(311) Man LX, Selber JC, Serletti JM. Abdominal wall following free TRAM or DIEP flap reconstruction: a meta-analysis and critical review. *Plast Reconstr Surg* 2009; 124(3):752-764.

(312) Bonde CT, Christensen DE, Elberg JJ. Ten years' experience of free flaps for breast reconstruction in a Danish microsurgical centre: an audit. *Scandinavian Journal of Plastic & Reconstructive Surgery & Hand Surgery 40(1):8-12*, 2006.

(313) Selber JC, Nelson J, Fosnot J, Goldstein J, Bergey M, Sonnad SS et al. A prospective study comparing the functional impact of SIEA, DIEP, and muscle-sparing free TRAM flaps on the abdominal wall: part I. unilateral reconstruction. *Plast Reconstr Surg* 2010; 126(4):1142-1153.

(314) Mathes S.J., Nahai F. Reconstructive surgery. Principles, Anatomy, & Technique. Churchill Livingston; 1997.

(315) Selber JC, Fosnot J, Nelson J, Goldstein J, Bergey M, Sonnad S et al. A prospective study comparing the functional impact of SIEA, DIEP, and muscle-sparing free TRAM flaps on the abdominal wall: Part II. Bilateral reconstruction. *Plast Reconstr Surg* 2010; 126(5):1438-1453.

(316) Wu LC, Bajaj A, Chang DW, Chevray PM. Comparison of donor-site morbidity of SIEA, DIEP, and muscle-sparing TRAM flaps for breast reconstruction. *Plast Reconstr Surg* 2008; 122(3):702-709.

(317) Hester TR, Jr., Nahai F, Beegle PE, Bostwick J, III. Blood supply of the abdomen revisited, with emphasis on the superficial inferior epigastric artery. *Plast Reconstr Surg* 1984; 74(5):657-670.

(318) Fukaya E, Kuwatsuru R, Iimura H, Ihara K, Sakurai H. Imaging of the superficial inferior epigastric vascular anatomy and preoperative planning for the SIEA flap using MDCTA. *J Plast Reconstr Aesthet Surg* 2011; 64(1):63-68.

(319) Feller AM. Free TRAM. Results and abdominal wall function. *Clin Plast Surg* 1994; 21(2):223-232.

(320) Dupin CL, Allen RJ, Glass CA, Bunch R. The internal mammary artery and vein as a recipient site for free-flap breast reconstruction: a report of 110 consecutive cases. *Plast Reconstr Surg* 1996; 98(4):685-689.

(321) Wolfram D, Schoeller T, Hussl H, Wechselberger G. The superficial inferior epigastric artery (SIEA) flap: indications for breast reconstruction. *Ann Plast Surg* 2006; 57(6):593-596.

(322) Vandevoort M, Vranckx JJ, Fabre G. Perforator topography of the deep inferior epigastric perforator flap in 100 cases of breast reconstruction. *Plast Reconstr Surg* 2002; 109(6):1912-1918.

(323) Schaverien MV, McCulley SJ. Reply: Relationship between Venous Congestion and Intraflap Venous Anatomy in DIEP Flaps Using Contrast-Enhanced Magnetic Resonance Angiography. *Plast Reconstr Surg* 2011; 127(5):2128-2129.

(324) Munhoz AM, Ishida LH, Sturtz GP, Cunha MS, Montag E, Saito FL et al. Importance of lateral row perforator vessels in deep inferior epigastric perforator flap harvesting. *Plast Reconstr Surg* 2004; 113(2):517-524.

(325) Smit JM, Klein S, Werker PM. An overview of methods for vascular mapping in the planning of free flaps. *J Plast Reconstr Aesthet Surg* 2010; 63(9):e674-e682.

(326) Mihara M, Nakanishi M, Nakashima M, Narushima M, Koshima I. Utility and anatomical examination of the DIEP flap's three-dimensional image with multidetector computed tomography. *Plast Reconstr Surg* 2008; 122(1):40e-41e.

(327) Ghattaura A, Henton J, Jallali N, Rajapakse Y, Savidge C, Allen S et al. One hundred cases of abdominal-based free flaps in breast reconstruction. The impact of preoperative computed tomographic angiography. *J Plast Reconstr Aesthet Surg* 2010; 63(10):1597-1601.

(328) Uppal RS, Casaer B, Van Landuyt K, Blondeel P. The efficacy of preoperative mapping of perforators in reducing operative times and complications in perforator flap breast reconstruction. *J Plast Reconstr Aesthet Surg* 2009; 62(7):859-864.

(329) Masia J, Clavero JA, Larranaga JR, Alomar X, Pons G, Serret P. Multidetector-row computed tomography in the planning of abdominal perforator flaps. *J Plast Reconstr Aesthet Surg* 2006; 59(6):594-599.

(330) Rozen WM, Garcia-Tutor E, Alonso-Burgos A, Acosta R, Stillaert F, Zubieta JL et al. Planning and optimising DIEP flaps with virtual surgery: the Navarra experience. *J Plast Reconstr Aesthet Surg* 2010; 63(2):289-297.

(331) Rozen WM, Phillips TJ, Ashton MW, Stella DL, Gibson RN, Taylor GI. Preoperative imaging for DIEA perforator flaps: a comparative study of computed tomographic angiography and doppler ultrasound. *Plast Reconstr Surg* 2008; 121(1 Suppl):1-8.

(332) Casey WJ, III, Chew RT, Rebecca AM, Smith AA, Collins JM, Pockaj BA. Advantages of preoperative computed tomography in deep inferior epigastric artery perforator flap breast reconstruction. *Plast Reconstr Surg* 2009; 123(4):1148-1155.

(333) Alonso-Burgos A, Garcia-Tutor E, Bastarrika G, Cano D, Martinez-Cuesta A, Pina LJ. Preoperative planning of deep inferior epigastric

artery perforator flap reconstruction with multislice-CT angiography: imaging findings and initial experience. *J Plast Reconstr Aesthet Surg* **2006; 59(6):585-593.**

(334) Rozen WM, Ashton MW, Stella DL, Phillips TJ, Taylor GI. The accuracy of computed tomographic angiography for mapping the perforators of the DIEA: a cadaveric study. *Plast Reconstr Surg* **2008; 122(2):363-369.**

(335) Whitaker IS, Smit JM, Rozen W, Dimopoulou A, Acosta R. Pre operative computed tomographic angiography (CTA): a valuable lesson in planning DIEP flaps. *J Plast Reconstr Aesthet Surg* **2009; 62(4):551.**

(336) Lasso JM, Sancho M, Campo V, Jimenez E, Perez CR. Epiperitoneal vessels: more resources to perform DIEP flaps. *J Plast Reconstr Aesthet Surg* **2008; 61(7):826-829.**

(337) Rozen WM, Ashton MW, Stella DL, Phillips TJ, Taylor GI. Magnetic resonance angiography and computed tomographic angiography for free fibular flap transfer. *J Reconstr Microsurg* **2008; 24(6):457-458.**

(338) Rozen WM, Stella DL, Bowden J, Taylor GI, Ashton MW. Advances in the pre-operative planning of deep inferior epigastric artery perforator flaps: magnetic resonance angiography. *Microsurgery* **2009; 29(2):119-123.**

(339) Patel SA, Keller A. A theoretical model describing arterial flow in the DIEP flap related to number and size of perforator vessels. *J Plast Reconstr Aesthet Surg* **2008; 61(11):1316-1320.**

(340) Lorenzetti F, Kuokkanen H, von Smitten K, Asko-Seljavaara S. Intraoperative evaluation of blood flow in the internal mammary or thoracodorsal artery as a recipient vessel for a free TRAM flap. *Ann Plast Surg* **2001; 46(6):590-593.**

(341) Schaverien MV, Ludman CN, Neil-Dwyer J, Perks AG, Raurell A, Rasheed T et al. Relationship between venous congestion and intraflap venous anatomy in DIEP flaps using contrast-enhanced magnetic resonance angiography. *Plast Reconstr Surg* **2010; 126(2):385-392.**

(342) Ali R, Bernier C, Lin YT, Ching WC, Rodriguez EP, Cardenas-Mejia A et al. Surgical strategies to salvage the venous compromised deep inferior epigastric perforator flap. *Ann Plast Surg* **2010; 65(4):398-406.**

(343) Niranjan NS, Khandwala AR, Mackenzie DM. Venous augmentation of the free TRAM flap. *Br J Plast Surg* **2001; 54(4):335-337.**

(344) Niranjan NS. Venous augmentation of the free TRAM flap. *Br J Plast Surg* **2002; 55(4):363.**

(345) Sojitra NM, Vandevoort M, Ghali S, Fabre G. Two new techniques for correcting venous congestion in the free DIEP flap for breast

reconstruction: an analysis of venous augmentation in 581 DIEP flaps. *Plast Reconstr Surg* **2010; 125(2):72e-74e.**

(346) Liu TS, Ashjian P, Festekjian J. Salvage of congested deep inferior epigastric perforator flap with a reverse flow venous anastomosis. *Annals of Plastic Surgery 59(2):214-7*, **2007.**

(347) Tran NV, Buchel EW, Convery PA. Microvascular complications of DIEP flaps. *Plast Reconstr Surg* **2007; 119(5):1397-1405.**

(348) Hallock GG, Rice DC. Efficacy of venous supercharging of the deep inferior epigastric perforator flap in a rat model. *Plast Reconstr Surg* **2005; 116(2):551-555.**

(349) Watterson PA, Bostwick J, III, Hester TR, Jr., Bried JT, Taylor GI. TRAM flap anatomy correlated with a 10-year clinical experience with 556 patients. *Plast Reconstr Surg* **1995; 95(7):1185-1194.**

(350) Guerra AB, Metzinger SE, Bidros RS, Rizzuto RP, Gill PS, Nguyen AH et al. Bilateral breast reconstruction with the deep inferior epigastric perforator (DIEP) flap: an experience with 280 flaps. *Ann Plast Surg* **2004; 52(3):246-252.**

(351) Rogers NE, Allen RJ. Radiation effects on breast reconstruction with the deep inferior epigastric perforator flap. *Plast Reconstr Surg* **2002; 109(6):1919-1924.**

(352) Bozikov K, Arnez T, Hertl K, Arnez ZM. Fat necrosis in free DIEAP flaps: incidence, risk, and predictor factors. *Ann Plast Surg* **2009; 63(2):138-142.**

(353) Cheng MH, Robles JA, Ulusal BG, Wei FC. Reliability of zone IV in the deep inferior epigastric perforator flap: a single center's experience with 74 cases. *Breast* **2006; 15(2):158-166.**

(354) Garvey PB, Buchel EW, Pockaj BA, Casey WJ, III, Gray RJ, Hernandez JL et al. DIEP and pedicled TRAM flaps: a comparison of outcomes. *Plast Reconstr Surg* **2006; 117(6):1711-1719.**

(355) Peeters WJ, Nanhekhan L, Van Ongeval C, Fabre G, Vandevoort M. Fat necrosis in deep inferior epigastric perforator flaps: an ultrasound-based review of 202 cases. *Plast Reconstr Surg* **2009; 124(6):1754-1758.**

(356) Keller A. The deep inferior epigastric perforator free flap for breast reconstruction. *Annals of Plastic Surgery 46(5):474-9; discussion 479-80*, **2001.**

(357) Garvey PB, Buchel EW, Pockaj BA, Gray RJ, Samson TD. The deep inferior epigastric perforator flap for breast reconstruction in overweight and obese patients. *Plast Reconstr Surg* **2005; 115(2):447-457.**

(358) Rozen WM, Ashton MW, Murray AC, Taylor GI. Avoiding denervation of rectus abdominis in DIEP flap harvest: the importance of medial row perforators. *Plast Reconstr Surg* **2008; 122(3):710-716.**

(359) Shoaib T, Marucci D. Adjacent angiosomes instead of zones II and III: reply to "Perfusion zones of the DIEP flap revisited--a clinical study". *Plast Reconstr Surg* 2006; 118(3):817-818.

(360) Henry SL, Cheng MH. A call for clarity in TRAM/DIEP zones. *Plast Reconstr Surg* 2010; 125(5):210e-211e.

(361) Tregaskiss AP, Goodwin AN, Acland RD. The cutaneous arteries of the anterior abdominal wall: a three-dimensional study. *Plast Reconstr Surg* 2007; 120(2):442-450.

(362) Ohjimi H, Era K, Fujita T, Tanaka T, Yabuuchi R. Analyzing the vascular architecture of the free TRAM flap using intraoperative ex vivo angiography. *Plast Reconstr Surg* 2005; 116(1):106-113.

(363) Wong C, Saint-Cyr M, Mojallal A, Schaub T, Bailey SH, Myers S et al. Perforasomes of the DIEP flap: vascular anatomy of the lateral versus medial row perforators and clinical implications. *Plast Reconstr Surg* 2010; 125(3):772-782.

(364) Rozen WM, Ashton MW, Le Roux CM, Pan WR, Corlett RJ. The perforator angiosome: a new concept in the design of deep inferior epigastric artery perforator flaps for breast reconstruction. *Microsurgery* 2010; 30(1):1-7.

(365) Hallock GG. Perforasomes, Venosomes, and Perfusion Zones of the DIEAP Flap. *Plast Reconstr Surg* 2010; 126(6):2282-2284.

(366) Allen RJ. Breast reconstruction with superficial inferior epigastric artery flaps: a prospective comparison with TRAM and DIEP flaps. *Plastic & Reconstructive Surgery 114(5):1084 discussion* 2004.

(367) Taylor GI, Gianoutsos MP, Morris SF. The neurovascular territories of the skin and muscles: anatomic study and clinical implications. *Plastic & Reconstructive Surgery 94(1):1-36*, 1994.

(368) Taylor GI, Pan WR. Angiosomes of the leg: anatomic study and clinical implications. *Plast Reconstr Surg* 1998; 102(3):599-616.

(369) Santoni-Rugiu P, Sykes PJ. A History of Plastic Surgery. Springer-Verlag; 2007.

(370) Gozu A, Poda M, Taskin EI, Turgut H, Erginel-Unaltuna N, Dogruman H et al. Pretreatment with octreotide modulates iNOS gene expression, mimics surgical delay, and improves flap survival. *Annals of Plastic Surgery 65(2):245-9*, 2010.

(371) Acikel C, Kenkel JM, Nojima K, Hoopman JE, Saboorian MH, Brown SA. Evaluation of flashlamp-pumped pulsed-dye laser (585 nm) in nonsurgical delay of dorsal rat cutaneous flaps. *Plastic & Reconstructive Surgery 115(7):2032-41*, 2005.

(372) Odland RM, Poole DV, Rice RD, Jr., Koobs DH. Use of the tunable dye laser to delay McFarlane skin flaps. *Arch Otolaryngol Head Neck Surg* 1995; 121(10):1158-1161.

(373) Reichner DR, Scholz T, Vanderkam VM, Gutierrez S, Steward E, Evans GR. Laser flap delay: comparison of Erbium:YAG and CO2 lasers. *Am Surg* 2003; 69(1):69-72.

(374) Lonnroth P, Smith U. Microdialysis--a novel technique for clinical investigations. *J Intern Med* 1990; 227(5):295-300.

(375) Eliasson B, Smith U, Lonnroth P. No acute effects of smoking and nicotine nasal spray on lipolysis measured by subcutaneous microdialysis. *Eur J Clin Invest* 1997; 27(6):503-509.

(376) Lonnroth P. Microdialysis--a new and promising method in clinical medicine. *J Intern Med* 1991; 230(4):363-364.

(377) Lonnroth P. Microdialysis in adipose tissue and skeletal muscle. *Horm Metab Res* 1997; 29(7):344-346.

(378) Hamani C, Luer MS, Dujovny M. Microdialysis in the human brain: review of its applications. *Neurol Res* 1997; 19(3):281-288.

(379) Mantovani V, Kennergren C, Goiny M, Ungerstedt U, Lonnroth P, Sala A et al. Microdialysis for myocardial metabolic surveillance: developing a clinical technique. *Clin Physiol Funct Imaging* 2006; 26(4):224-231.

(380) Hillman J, Aneman O, Anderson C, Sjogren F, Saberg C, Mellergard P. A microdialysis technique for routine measurement of macromolecules in the injured human brain. *Neurosurgery* 2005; 56(6):1264-1268.

(381) Hillman J, Milos P, Yu ZQ, Sjogren F, Anderson C, Mellergard P. Intracerebral microdialysis in neurosurgical intensive care patients utilising catheters with different molecular cut-off (20 and 100 kD). *Acta Neurochir (Wien)* 2006; 148(3):319-324.

(382) Ambrozy E, Waczulikova I, Willfort-Ehringer A, Ehringer H, Koppensteiner R, Gschwandtner ME. Microcirculation in mixed arterial/venous ulcers and the surrounding skin: clinical study using a laser Doppler perfusion imager and capillary microscopy. *Wound Repair Regen* 2009; 17(1):19-24.

(383) Luettig B, Decker T, Lohmann-Matthes ML. Evidence for the existence of two forms of membrane tumor necrosis factor: an integral protein and a molecule attached to its receptor. *J Immunol* 1989; 143(12):4034-4038.

(384) Rudloff HE, Schmalstieg FC, Jr., Palkowetz KH, Paszkiewicz EJ, Goldman AS. Interleukin-6 in human milk. *J Reprod Immunol* 1993; 23(1):13-20.

(385) Helle M, Boeije L, de Groot E, de Vos A, Aarden L. Sensitive ELISA for interleukin-6. Detection of IL-6 in biological fluids: synovial fluids and sera. *J Immunol Methods* 1991; 138(1):47-56.

(386) Florkiewicz RZ, Ahluwalia A, Sandor Z, Szabo S, Tarnawski AS. Gastric mucosal injury activates bFGF gene expression and triggers

preferential translation of high molecular weight bFGF isoforms through CUG-initiated, non-canonical codons. *Biochemical & Biophysical Research Communications 409(3):494-9*, **2011.**

(387) Ribuffo D, Muratori L, Antoniadou K, Fanini F, Martelli E, Marini M et al. A hemodynamic approach to clinical results in the TRAM flap after selective delay. *Plast Reconstr Surg* **1997; 99(6):1706-1714.**

(388) Restifo RJ, Ward BA, Scoutt LM, Brown JM, Taylor KJ. Timing, magnitude, and utility of surgical delay in the TRAM flap: II. Clinical studies. *Plast Reconstr Surg* **1997; 99(5):1217-1223.**

(389) Restifo RJ, Ahmed SS, Isenberg JS, Thomson JG. Timing, magnitude, and utility of surgical delay in the TRAM flap: I. Animal studies. *Plast Reconstr Surg* **1997; 99(5):1211-1216.**

(390) Scheufler O, Andresen R, Kirsch A, Banzer D, Vaubel E. Clinical results of TRAM flap delay by selective embolization of the deep inferior epigastric arteries. *Plast Reconstr Surg* **2000; 105(4):1320-1329.**

(391) Ghali S, Butler PE, Tepper OM, Gurtner GC. Vascular delay revisited. *Plast Reconstr Surg* **2007; 119(6):1735-1744.**

(392) Bond S, Ferder M, Grossman L, Strauch B. The effect of epigastric vessel ligation on the vascular territories of the pig rectus muscle. *Plast Reconstr Surg* **1996; 97(3):616-620.**

(393) Pang CY, Forrest CR, Neligan PC, Lindsay WK. Augmentation of blood flow in delayed random skin flaps in the pig: effect of length of delay period and angiogenesis. *Plast Reconstr Surg* **1986; 78(1):68-74.**

(394) Williams BA, Currie RW, Morris SF. Impact of arteriogenesis in plastic surgery: choke vessel growth proceeds via arteriogenic mechanisms in the rat dorsal island skin flap. *Microcirculation 16(3):235-50*, **2009.**

(395) Sloan GM, Reinisch JF. Flap physiology and the prediction of flap viability. *Hand Clin* **1985; 1(4):609-619.**

(396) Rohrich RJ, Cherry GW, Spira M. Enhancement of skin-flap survival using nitroglycerin ointment. *Plastic & Reconstructive Surgery 73(6):943-8*, **1984.**

(397) Morain WD, Pettit RJ, Rothkopf DM, Coombs DW. Augmentation of surviving flap area by intraarterial vasodilators administered through implantable pumps. *Ann Plast Surg* **1983; 11(1):46-52.**

(398) Murphy RC, Lawrence WT, Robson MC, Heggers JP. Surgical delay and arachidonic acid metabolites: evidence for an inflammatory mechanism: an experimental study in rats. *Br J Plast Surg* **1985; 38(2):272-277.**

(399) Goertz O, Ring A, Buschhaus B, Hirsch T, Daigeler A, Steinstraesser L et al. Influence of anti-inflammatory and vasoactive drugs on

microcirculation and angiogenesis after burn in mice. *Burns* 2011; 37(4):656-664.

(400) Carroll SM, Heilman SJ, Stremel RW, Tobin GR, Barker JH. Vascular delay improves latissimus dorsi muscle perfusion and muscle function for use in cardiomyoplasty. *Plast Reconstr Surg* 1997; 99(5):1329-1337.

(401) Edstrom LE, Balkovich M, Slotman GJ. Effect of ischemic skin flap elevation on tissue and plasma thromboxane A2 and prostacyclin production: modification by thromboxane synthetase inhibition. *Ann Plast Surg* 1988; 20(2):106-111.

(402) Wu G, Calamel PM, Shedd DP. THe hazards of injecting local anesthetic solutions with epinephrine into flaps: experimental study. *Plastic & Reconstructive Surgery 62(3):396-403*, 1978.

(403) Hendel PM, Lilien DL, Buncke HJ. A study of the pharmacologic control of blood flow to delayed skin flaps using xenon washout. Part II. *Plast Reconstr Surg* 1983; 71(3):399-407.

(404) Kharbanda RK, Peters M, Walton B, Kattenhorn M, Mullen M, Klein N et al. Ischemic preconditioning prevents endothelial injury and systemic neutrophil activation during ischemia-reperfusion in humans in vivo. *Circulation 103(12):1624-30*, 2001.

(405) Wang WZ, Anderson G, Fleming JT, Peter FW, Franken RJ, Acland RD et al. Lack of nitric oxide contributes to vasospasm during ischemia/reperfusion injury. *Plast Reconstr Surg* 1997; 99(4):1099-1108.

(406) Presta M, Moscatelli D, Joseph-Silverstein J, Rifkin DB. Purification from a human hepatoma cell line of a basic fibroblast growth factor-like molecule that stimulates capillary endothelial cell plasminogen activator production, DNA synthesis, and migration. *Mol Cell Biol* 1986; 6(11):4060-4066.

(407) Mignatti P, Tsuboi R, Robbins E, Rifkin DB. In vitro angiogenesis on the human amniotic membrane: requirement for basic fibroblast growth factor-induced proteinases. *J Cell Biol* 1989; 108(2):671-682.

(408) Folkman J, Klagsbrun M. Angiogenic factors. *Science* 1987; 235(4787):442-447.

(409) Most D, Hoyt J, Sibley RK, Press BH. Parenchymal cytokine expression precedes clinically observed ischemia in dorsal flaps in the rat. *Plast Reconstr Surg* 1996; 98(5):856-861.

(410) Wong MS, Erdmann D, Sweis R, Pollmann C, Farrar M, Georgiade GS et al. Basic fibroblast growth factor expression following surgical delay of rat transverse rectus abdominis myocutaneous flaps. *Plastic & Reconstructive Surgery 113(7):2030-6*, 2004.

(411) Lineaweaver WC, Lei MP, Mustain W, Oswald TM, Cui D, Zhang F. Vascular endothelium growth factor, surgical delay, and skin flap survival. *Annals of Surgery 239(6):866-73; discussion 873-5,* **2004.**

(412) Zhang F, Hu EC, Gerzenshtein J, Lei MP, Lineaweaver WC. The expression of proinflammatory cytokines in the rat muscle flap with ischemia-reperfusion injury. *Ann Plast Surg* **2005; 54(3):313-317.**

(413) Schmidt A, Bengtsson A, Tylman M, Blomqvist L. Pro-inflammatory cytokines in elective flap surgery. *Journal of Surgical Research 137(1):117-21,* **2007.**

(414) Erdmann D, Sweis R, Wong MS, Niklason LE, du Laney TV, Levin LS et al. Vascular endothelial growth factor expression in pig latissimus dorsi myocutaneous flaps after ischemia reperfusion injury. *Plastic & Reconstructive Surgery 111(2):775-80,* **2003.**

(415) Hom DB, Baker SR, Graham LM, McClatchey KD. Utilizing angiogenic agents to expedite the neovascularization process in skin flaps. *Laryngoscope 98(5):521-6,* **1988.**

(416) Hom DB, Assefa G. Effects of endothelial cell growth factor on vascular compromised skin flaps. *Archives of Otolaryngology -- Head & Neck Surgery 118(6):624-8,* **1992.**

(417) Ishiguro N, Yabe Y, Shimizu T, Iwata H, Miura T. Basic fibroblast growth factor has a beneficial effect on the viability of random skin flaps in rats. *Annals of Plastic Surgery 32(4):356-60,* **1994.**

(418) Nall AV, Brownlee RE, Colvin CP, Schultz G, Fein D, Cassisi NJ et al. Transforming growth factor beta 1 improves wound healing and random flap survival in normal and irradiated rats. *Archives of Otolaryngology -- Head & Neck Surgery 122(2):171-7,* **1996.**

(419) Yang LW, Zhang JX, Zeng L, Xu JJ, Du FT, Luo W et al. Vascular endothelial growth factor gene therapy with intramuscular injections of plasmid DNA enhances the survival of random pattern flaps in a rat model. *Br J Plast Surg* **2005; 58(3):339-347.**

(420) Hayward PG, Alison WE, Jr., Carp SS, Hui PS, Robson MC. Local infiltration of an angiogenic growth factor does not stimulate the delay phenomenon. *British Journal of Plastic Surgery 44(7):526-9,* **1991.**

(421) Yanagisawa-Miwa A, Uchida Y, Nakamura F, Tomaru T, Kido H, Kamijo T et al. Salvage of infarcted myocardium by angiogenic action of basic fibroblast growth factor. *Science 257(5075):1401-3,* **1992.**

(422) Stavri GT, Zachary IC, Baskerville PA, Martin JF, Erusalimsky JD. Basic fibroblast growth factor upregulates the expression of vascular endothelial growth factor in vascular smooth muscle cells. Synergistic interaction with hypoxia. *Circulation 92(1):11-4,* **1995.**

(423) Carroll CM, Carroll SM, Schuschke DA, Barker JH. Augmentation of skeletal muscle flap survival using platelet derived growth factor. *Plastic & Reconstructive Surgery 102(2):407-15*, 1998.

(424) Pang Y, Lineaweaver WC, Lei MP, Oswald T, Shamburger S, Cai Z et al. Evaluation of the mechanism of vascular endothelial growth factor improvement of ischemic flap survival in rats. *Plastic & Reconstructive Surgery 112(2):556-64*, 2003.

(425) Holzbach T, Neshkova I, Vlaskou D, Konerding MA, Gansbacher B, Biemer E et al. Searching for the right timing of surgical delay: angiogenesis, vascular endothelial growth factor and perfusion changes in a skin-flap model. *J Plast Reconstr Aesthet Surg* 2009; 62(11):1534-1542.